Structural and physical processes in accretionary complexes: the role of fluids in convergent margin development

Brown, K.M.

STRUCTURAL AND PHYSICAL PROCESSES IN ACCRETIONARY COMPLEXES: THE ROLE OF FLUIDS IN CONVERGENT MARGIN DEVELOPMENT

BY

K. M. BROWN

Thesis submitted to the University of Durham for the degree of Doctor of Philosophy

March 1987

ABSTRACT

0.1 ABSTRACT

Accretionary complexes that form at subduction zones develop a spectrum of styles of deformation that range between coherent forms in which the processes of thrusting predominate and incoherent forms in which melanges, formed by such processes as mud diapirism, are the dominant constituent. This thesis examines processes that control the development of these accretionary styles by comparing geophysical observations of the modern Barbados Ridge accretionary complex, with ancient subaerially exposed examples in Sabah, N. Borneo and W. Timor.

A structural and lineament map of the offshore regions of the Barbados Ridge complex has been constructed using GLORIA, Seabeam and seismic data. It reveales marked changes in the surface structure of the accretionary wedge, particularly where basement ridges associated with oceanic fracture zones underthrust it. It also documents the presence of large numbers of mud diapirs in its southern regions. The mud diapirs appear to be associated with the accretion of thick sequences of turbidites and their distribution is proposed to relate to the subcretion or underplating of underconsolidated

material to the base of the complex.

Fieldwork in Sabah and Timor concentrated on describing features associated with currently active mud diapirs, and potential ancient examples. A classification of the various forms of diapiric activity has been erected as part of a general discussion on the importance, genesis and emplacement of mud diapirs. In addition, the general structural development of the accretionary complex in W. Sabah was found to broadly resemble that of the frontal regions of a particularly thin part of the Barbados Ridge complex studied during DSDP Leg 78A and ODP Leg 110.

A series of principal controls or boundary factors appear to control the general development of accretionary complexes. During the course of this study the importance of the sedimentary input, critical taper (or balance between boundary stresses and gravitational body forces) and subducting basement topography has been made particularly clear.

0 INTRODUCTION

This study focuses on a number of modern and ancient subduction zones in which significant sedimentary input has led to the consequent development of large accretionary complexes. In the past, the study of the structure of modern convergent margins and associated active subduction zones has been hindered by seismic reflection techniques not being able to easily image complex subsurface structures and steeply dipping beds. Detailed comparisons with ancient accretionary complexes and the subaerially exposed parts of modern accretionary complexes have not, therefore, been possible. This situation has recently changed with the advent of improved data acquisition and seismic processing techiniques and seafloor mapping systems such as the Seabeam Bathymetric (Biju-Duval et al. 1982) and the GLORIA long-range sidescan sonar systems (Laughton 1981). The Deep Sea Drilling Program and Ocean Drilling Program have also shed further light onto structural development and physical processes occurring within modern accretionary complexes.

This thesis combines information gained from recent advances in the geophysical study of modern submarine accretionary complexes with observations from fieldwork in ancient accretionary terranes. Observations made through geophysical means and in the field are often on very *different scales of magnitude. Geophysical observations (i.e. seismic reflection studies) most readily image large features with dimensions of several hundreds of metres to kilometres or more. Geological field observations are often restricted to an outcrop scale often less than a few 10's m. Interpolation between the two sets of observations should, therefore, give a clearer picture of the processes involved in forming an accretionary complex than would otherwise be possible. As most detailed seismic reflection observations are still limited to the upper 1-5 km of modern accretionary complexes such as the Barbados Ridge, the comparisons made with ancient accretionary complexes in this study have been limited primarily to non-metamorphic examples, such as those found on the island of Barbados, Sabah (N. Borneo) and the collision complex of Timor.*

0.2 REVIEW OF PREVIOUS AND CURRENT IDEAS ON ACCRETIONARY COMPLEX DEVELOPMENT

The examples chosen for detailed study cover most of the spectrum of accretionary complex types (see below). At one end of the spectrum, an accretionary complex may have undergone a complex structural development but, by and large, consist of a series of folded and imbricated thrust packets like the Crocker Formation in Sabah and much of the Barbados Ridge complex (see Chapters 1 & 3 respectively). These complexes are considered in this thesis to have an essentially coherent structural form. At the other end of the spectrum are complexes like that in Timor (Chapter 4), and the Franciscan complex (Cowan 1985, Aalto 1981). These *contain very large bodies of melange and are considered to have an incoherent structural style. The term melange is used in this thesis to mean a mappable, internally fragmented and mixed rock body usually containing a variety of blocks, commonly in a pervasively deformed argillaceous matrix. Broken formations are similar to melanges in many of their characteristics but can usually be related to disruption occurring around fault zones, with the blocks in the matrix being relatable to the formations in the hanging wall and footwall.*

Early ideas, associated with the development of coherent accretionary complexes, with specific regard to modern and ancient accretionary complexes like the Southern Uplands (Karig & Sharman 1975, Dickinson and Seely 1979, Leggett 1979, 1980 & Leggett et al. 1982), stressed the relationship between the diachronôus sedimentation and deformation that must occur in subduction zones (Fig. 0.1), and proposed simple models for the structural thickening of complexes that largely relied on the back rotation of frontally accreted packets. In part these early models were correct. Back rotation of frontally imbricated thrust slices is observed in examples like the Makran (White & Louden 1982). However, as accretionary complexes can be of the order of 20km thick and thrust spacings are generally considerably less than this (even in the Makran where they are especially wide, i.e some 7km), other thickening processes must occur. Moore et al. (1982) pointed out that structures developed in the complex off western Mexico were carried, without much apparent modification, from the trench up into the inner parts of the

FIGURE 0.1 - The general model proposed for the relationship between sedimentation and structural development at subduction zones. The sediments inside each offscraped packet young towards the arc but syntectonic sedimentation means that the packets themselves get older towards the arc.

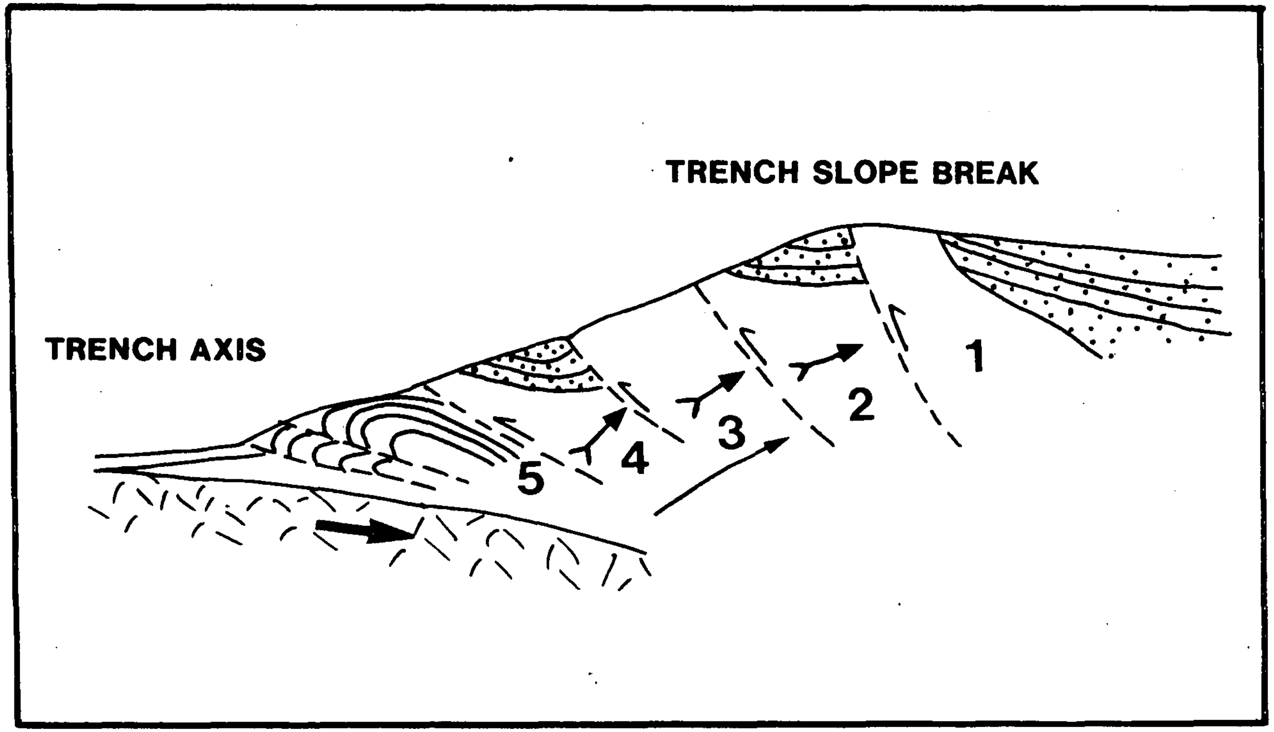
TRENCH SLOPE BREAK
TRENCH AXIS
1
2
3
4
5

complex. They proposed that some sort of 'underplating' mechanism accounted for this. The underthrusting of the leading edge of accretionary complexes by the lower parts of the incoming sedimentary section is a common phenomenon (cf. Peter & Westrook 1976, Westbrook et al. 1982, von Huene 1985, Lu & McMillen 1982, McCarthy & Scholl 1985). It has been proposed by a number of workers (Westbrook & Smith 1983, Leggett et al. 1984, Silver et al. 1985, Sample & Fisher 1986, Platt et al. 1985, Byrne 1986) that these underthrust sediments may be accreted to the base of the complex by a process that is essentially the same as duplex formation in foreland thrust belts (cf. Boyer and Elliot 1982). The duplexes jack up the overlying frontal imbricate section, which tends to passively ride on a complexly evolving interior until out-of-sequence thrusts cut through the imbricate sequence and induce further deformation.

Incoherent accretionary complexes, which are predominantly composed of melanges like the Franciscan (Cowan 1985) and W. Timor (Audley-Charles 1965, Rosidi et al. 1981, Barber et al. 1986), do not appear to have behaved in quite the same manner as the coherent ones. Cowan (1985) & Moore et al. (1985) summarise the melange types in the western Cordillera of N. America and attempt to relate the type of melange to its process of origin. There are three principal processes that may account for large scale melange development; tectonic disruption, sedimentary slumping or olistostromes, and mud diapirism. Theoretical models, proposed by Cowan & Silling (1978) and Cloos (1982), to generate melanges by the basal shear driven viscous flowage of large portions of the accretionary complexes, may be applicable to to incoherent accretionary complexes. However, this project focuses upon mud diapirism as a more likely, commonly observed modern day process that can readily form such melange bodies within a convergent margin setting (See Chapter 4).

Certain processes and factors control the development of either style of accretionary complex. The gross stability of accretionary complexes have been modelled with some success whether they are treated as wedges of Coulomb material (Davis et al. 1983), plastic media (Chapple 1978, Stockmal 1983) or viscoelastic materials (Park 1981). All these models apply the general ideas of balance between gravitational spreading forces and shear stresses on the base to produce tectonic stresses in the wedge. One particular theoretical model by Davis et al. (1983) will be used to illustrate the general form of the critical taper concept. Davis et al. (1983) make the assumption that the rheology of deformation wedges can be modelled using a Coulomb fracture criterion modified for the effects of pore-fluid pressure. The "critical taper" of the deformation wedge is the angle between the surface and basal slope of any particular segment of the complex (Fig. 0.2) when it is in a state of yield throughout, such that the compressive and gravitational forces just balance the resistance to sliding on the base of the wedge (see equation 1, Fig 0.2). The force balance in the wedge, in terms of stresses, is made up of the basal shear stress (τb) which is balanced by two terms on the right hand side of equation 1. The first is a glacier sliding term which expresses the action of gravity on the sloping top surface and corresponds

FIGURE 0.2 - Schematic diagram of an accretionary complex subject to horizontal compression and on the verge of Coulomb faliure throughout. A segment of length dx and height H is subject to a body force W, to a basal traction rb.dx, and to a longitude deviatoric push force σx. Equation 1 is taken from Davis (1984) and indicates the relationship between the resistance to frictional sliding and two terms on the right. The first is a glacier sliding term and the second is a wedge-taper-dependent resistance to horizontal compression term. Equation 2, is the critical taper equation taken from Dahlen et al. 1984. Equation 3 relates the thickess of the complex in which cohesion is significant, to the value of cohesion (Dahlen et al. 1984).

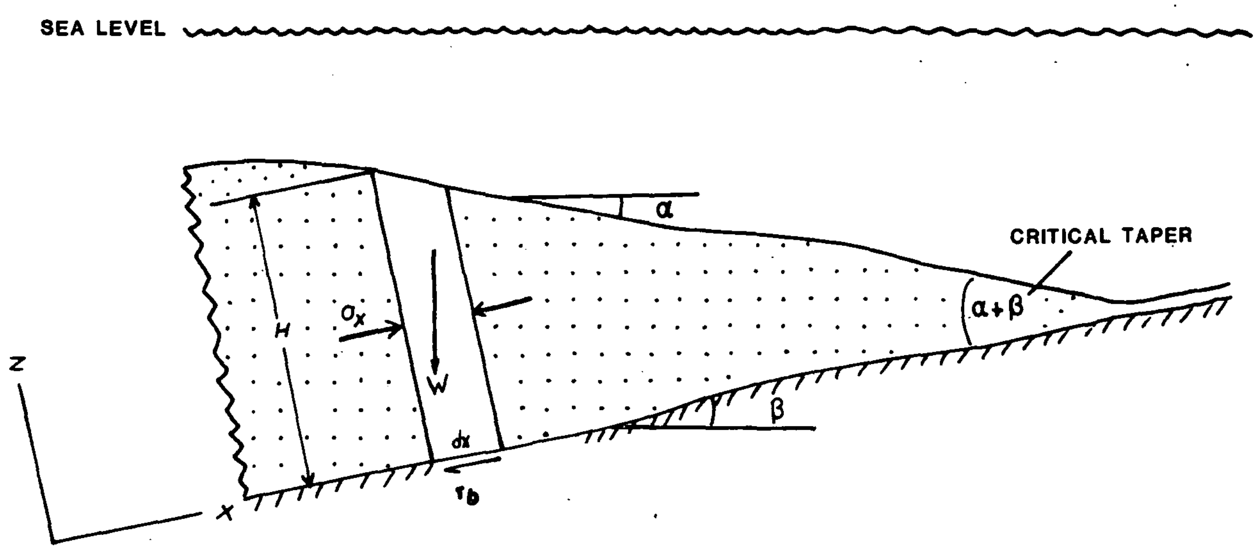

$$\tau_b = (\rho - \rho_w) g H \alpha + (1 - \lambda_b) K \rho g H (\alpha + \beta) \qquad (1$$

$$\alpha + \beta = \frac{(1 - \rho_w/\rho)\beta + (1 - \lambda_b)\mu_B - Q(S_0/\rho g r)\cot\phi}{(1 - \rho_w/\rho) + (1 - \lambda)K} \qquad (2$$

$$h = S_0/[\mu(1 - \lambda)\rho g] \qquad (3$$

- τ_b — SHEAR STRESS
- ρ — BULK DENSITY OF WEDGE SEGMENT
- H — LOCAL THICKNESS OF WEDGE
- ρ_w — DENSITY OF WATER
- g — ACCELERATION DUE TO GRAVITY
- α — LOCAL DIP OF WEDGE SURFACE
- β — LOCAL DIP OF WEDGE BASE
- λ_b — RATIO OF FLUID PRESSUE CHANGE TO NET INCREASE IN LITHOSTATIC OVER BURDEN AT THE BASE OF THE WEDGE
- K, Q — CONSTANTS RELATED TO THE INTERNAL STRENGTH OF THE WEDGE AND THE COEFFICIENT OF FRICTION OF THE BASE OF THE WEDGE
- μ_B — BASAL COEFFICIENT OF FRICTION
- S_o — COHESION
- ϕ — FRICTION ANGLE ALONG THE BASAL DECOLLEMENT
- h — THE THICKNESS OF WEDGE IN WHICH COHESION IS SIGNIFICANT

to a force that tends to produce sliding in the direction of the surface slope. The second term is a wedge-taper-dependent resistance to horizontal stresses, related to material properties of the wedge.

Davis (1984) applied the basic critical taper theory to the Barbados Ridge Complex. In the southern regions the critical taper decreases westwards and the surface topography becomes sub-horizontal. He proposed that the flattening was related in part to the steepening of the basal detachment. He also proposed that as the depth to the basal contact of the complex increases towards the arc it may reach tempreatures that put it below the brittle-ductile transition. Any weakening of the base of the complex as a result of this would correspond to a reduction in the basal shear stresss and consequently the critical taper necessary for equilibrium. Dahalen et al. (1984) extended the critical taper concept in order to better assess the effects of cohesion within the complex (Equation 2, Fig. 0.2). In equation 2 in can be seen that a reduction in critical taper will occur with any increase in cohesion. Therefore with increasing consolidation (and consequently cohesion) in the older regions of the complex a reduction in the critical taper might be expected. Dahalen et al. (1984) also observed, however, that as the thickness of the wedge increases the effect of its cohesion grew less. Equation 3 (Fig. 0.2) relates the cohesion to the thickness of the upper layer of the complex in which cohesion is significant. Therfore, cohesion can only become an important factor if the cohesion increases at a suffiently high rate in these *interior regions to counter the similarly increasing thickness of the wedge. Zhao et al. (1986) have proposed that this may well be the case for the Barbados example. They estimate that the necessary increase in cohesion requires the porostiy to decrease from a near toe value of 70% to approximately 30% at a depth of 3km below sea bottom, 60km west of the deformation front.*

Perturbations of the critical taper, occurring as a result of the addition of material to either, or both, its base or front, lead to interesting results (Fig. 0.3). Adding material by frontal accretion, necessitates additional thickening of the interior regions by out-of-sequence or through wedge faults (Westbrook et al. 1982, Moore & Lundberg 1983, Butler and Coward 1984). The need for out-of-sequence thrusting can be counteracted in part by thicknening associated with underplating or subcretion of material to the base of the complex. Conversely if excessive amounts of material are subcreted to the base of the complex extension and gravity spreading of the interior regions of the complex may occur. Platt (1986) proposed such a model to explain some of the features of the development of the Alps.

The angle between the arc basement and the accretionary complex can have a considerable effect upon the overall geometry and development of the both the posterior regions of accretionary complexes and any forearc basins that may form (Fig. 0.4). Silver et al. (1985) point out that many accretionary complexes have low butress or back stop angles (Fig. 0.4c) rather than steep or overhanging ones (Fig. 0.4 a

FIGURE 0.3 - General models of the consequences of critical taper maintenance. a) Frontal accretion, if not balanced by subcretion, will result in out-of-sequence thrusting in order to maintain the critical taper. b & c) Subcretion, if not balanced by frontal accretion, will result in gravitational instability and collapse of the complex.

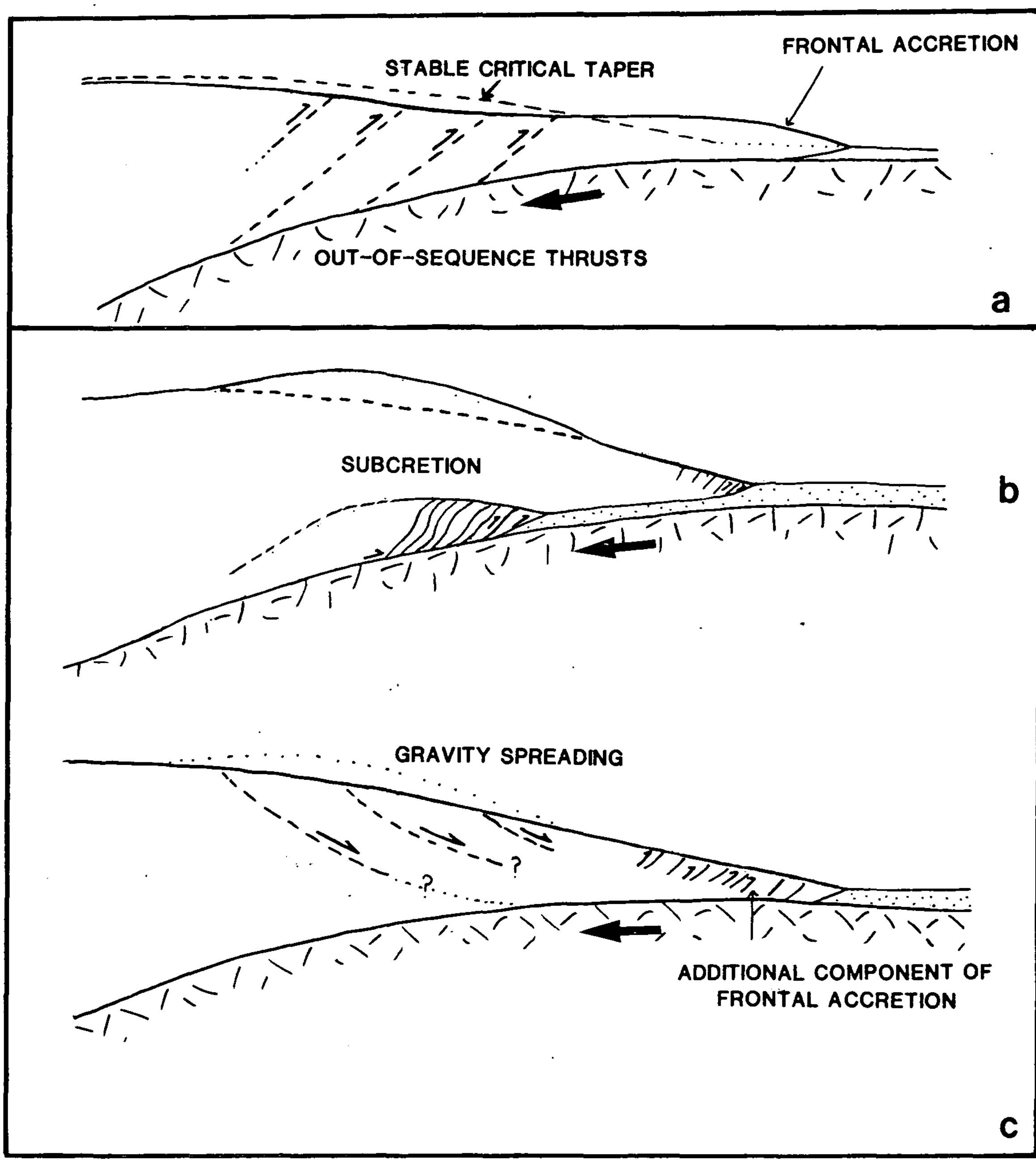

FRONTAL ACCRETION
STABLE CRITICAL TAPER
OUT-OF-SEQUENCE THRUSTS
a
SUBCRETION
b
GRAVITY SPREADING
?
?
ADDITIONAL COMPONENT OF
FRONTAL ACCRETION
c

FIGURE 0.4 - The three possible accretionary complex - arc buttress configurations. a) The underthrust configuration may have been similar to the original configuration in Timor. b) The neutral or steep butress angle will be similar to that developed by strike-slip in Sumatra. c) The obducted configuration is represented by the Barbados Ridge Complex.

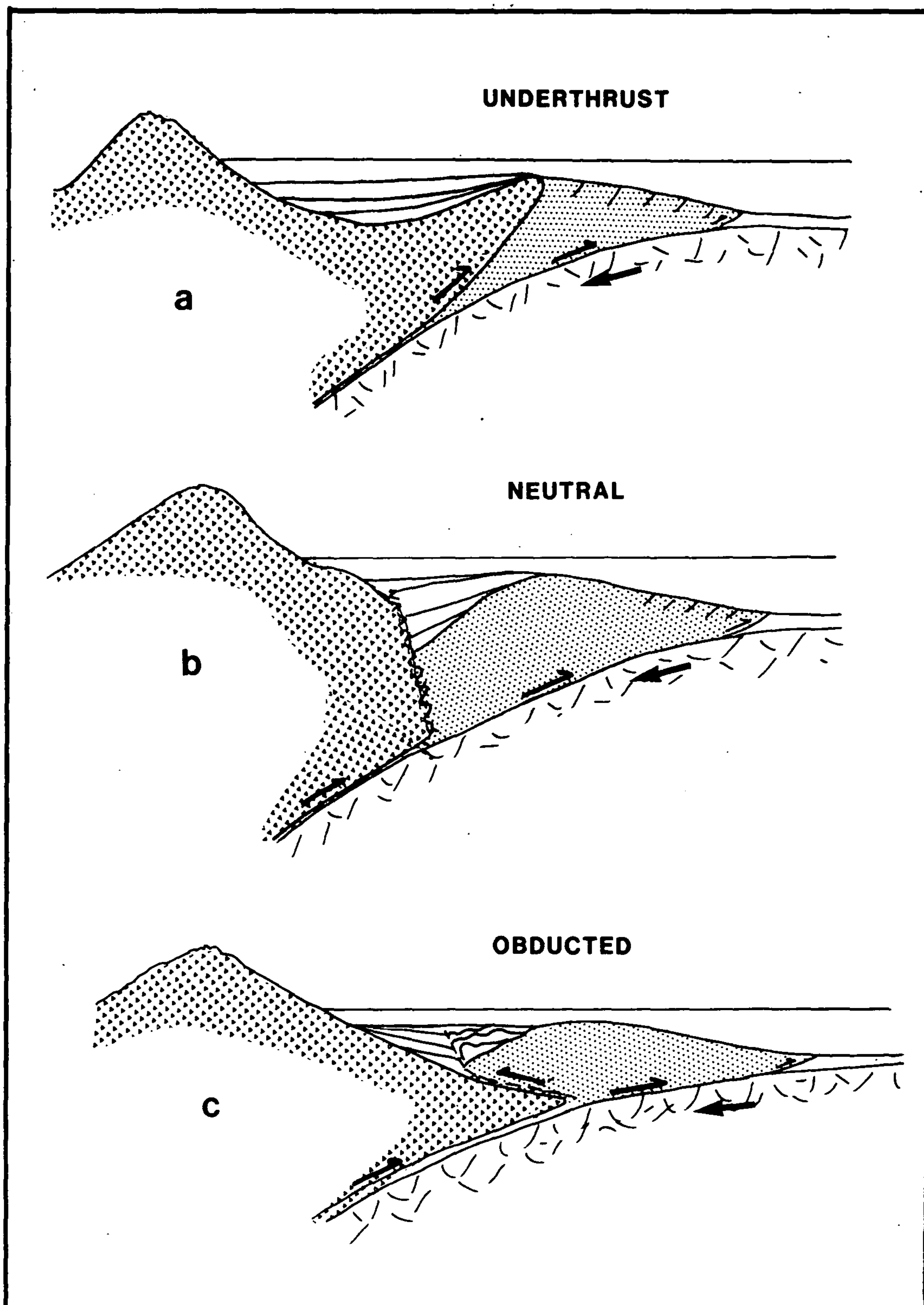
UNDERTHRUST
a
NEUTRAL
b
OBDUCTED
c

& b). This enhances the prospects for obduction of the complex onto the forearc basement, with a consequent accretion of forearc sediments to the inner part of the complex. Such a system has been proposed for the Barbados Ridge Complex (Westbrook 1975). Obduction of the complex loads the forearc basement which undergoes a flexural response in much the same way as would the foreland of a thrust belt.

In recent years, it has come to be realised that high pressure porefluids also exert a profound influence upon the development of accretionary complexes (Westbrook & Smith 1983, Moore et al. 1984, von Huene & Lee 1982). Rapidly deposited sediments like turbidites and hemipelagics may have initial porosities between 60-80% (Moore et al. 1984). Very low permeabilities mean slow compaction rates, with the consequent development of considerable overpressures on the sequence being loaded rapidly during imbrication. The overpressured fluids reduce shear stress along faults and maintain a high degree of underconsolidation within parts of the developing complex that may later be mobilised into mud diapirs. It has also been proposed that fluid pressures within deforming and consolidating sediments affect the mechanism by which they deform. Knipe (1986) discusses the interrelationships between varying states of lithification, strain rates, fluid pressures and the resultant deformation pathways. He proposes the generalised mechanism path diagram illustrated in Figure 0.5, with the following four deformation mechanisms;

a) Independent Particulate Flow, which involves the sliding

FIGURE 0.5 - Generalized deformation mechanism path diagram proposed by Knipe (1986) showing the relative positions of deformation mechanism fields on a strain rate, lithification and fluid pressure plot. IPF - Independent particulate flow, DMT-Diffusion mass transfer, CATA - Cataclastic flow and fracturing.

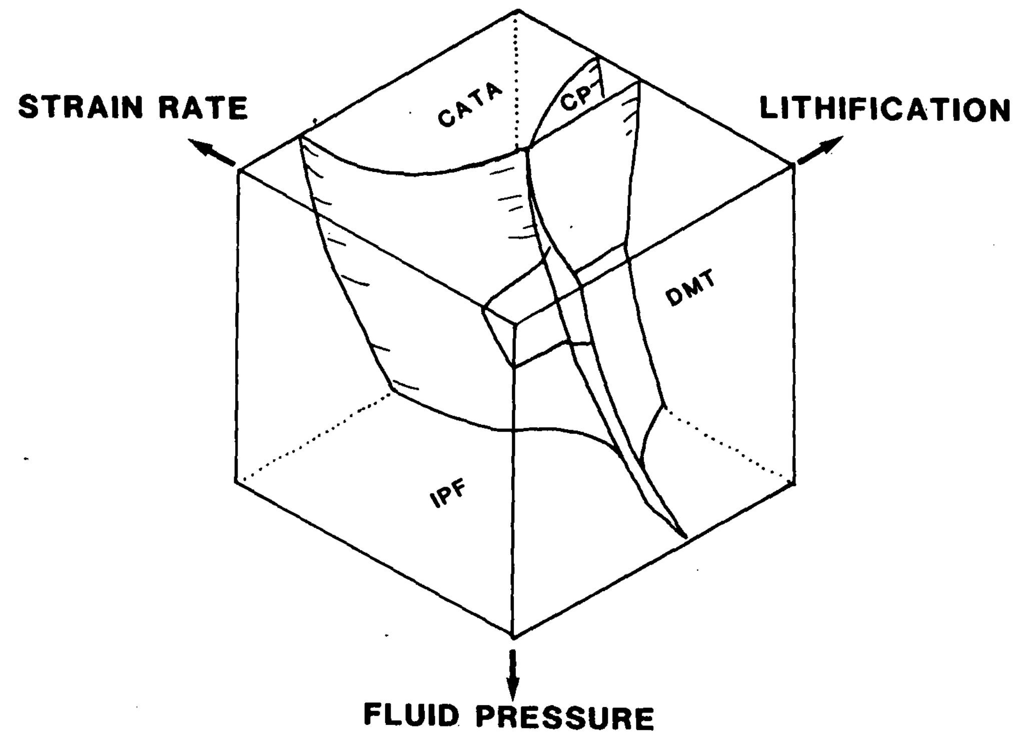
STRAIN RATE
CATA
CP
LITHIFICATION
DMT
IPF
FLUID PRESSURE

of grains past each other without any deformation of the grains. This mechanism is associated with poorly consolidated sediments and high porefluid pressures and is reasonably strain rate independent.

b) Diffusional Mass Transfer, where material is transfered from sites of high stress to sites of low stress via the porefluids (Pressure Solution). This deformation mechanism is favoured by a high degree of lithification, low strain rates and low fluid pressures.

c) Crystal Plasticity, which is an intracrystalline deformation mechanism where strain is accommodated by the movement of defects within crystals. This mechanism occurs in well lithified sediments at low fluid pressures and intermediate strain rates.

d) Cataclastic Flow, which involves a combination of grain boundary sliding, fracture, and volume changes, and predominates in well consolidated sediments at high strain rates and low porefluid pressures.

Head-on convergence does not always occur at subduction zones. The Sumatran subduction system was described by Fitch (1972) and Beck (1983) to be a system in which the lateral tectonic transport of material is driven by oblique accretion. Essentially they advocate a form of strain partitioning, with the oblique convergence vector being taken up by strike slip faulting in a direction subparallel to the magmatic arc, and the convergence vector being taken up by underthrusting (Fig. 0.6). Beck (1983) concluded that strike slip faulting is not apparent in all obliquely converging systems and appears to require a high angle of oblique

FIGURE O.6 - This figure is taken from Beck (1983). Sunda-style plate margin (A) shows conversion of oblique convergence into a subduction-zone transcurrent-fault pair west of Sunda Strait where angle of convergence between the Indian and Asian plates (arrows) becomes markedly oblique. (B) is a cartoon illustrating the geometry of a Sunda-style margin. X and Y are the angle of convergence and the dip of the Benioff-Wadati zone, respectively. (C) is a more geological version of the lower half of (B) and illustrates formation of the transcurrent fault along a thermally-thinned zone coincident with the axis of the magmatic arc.

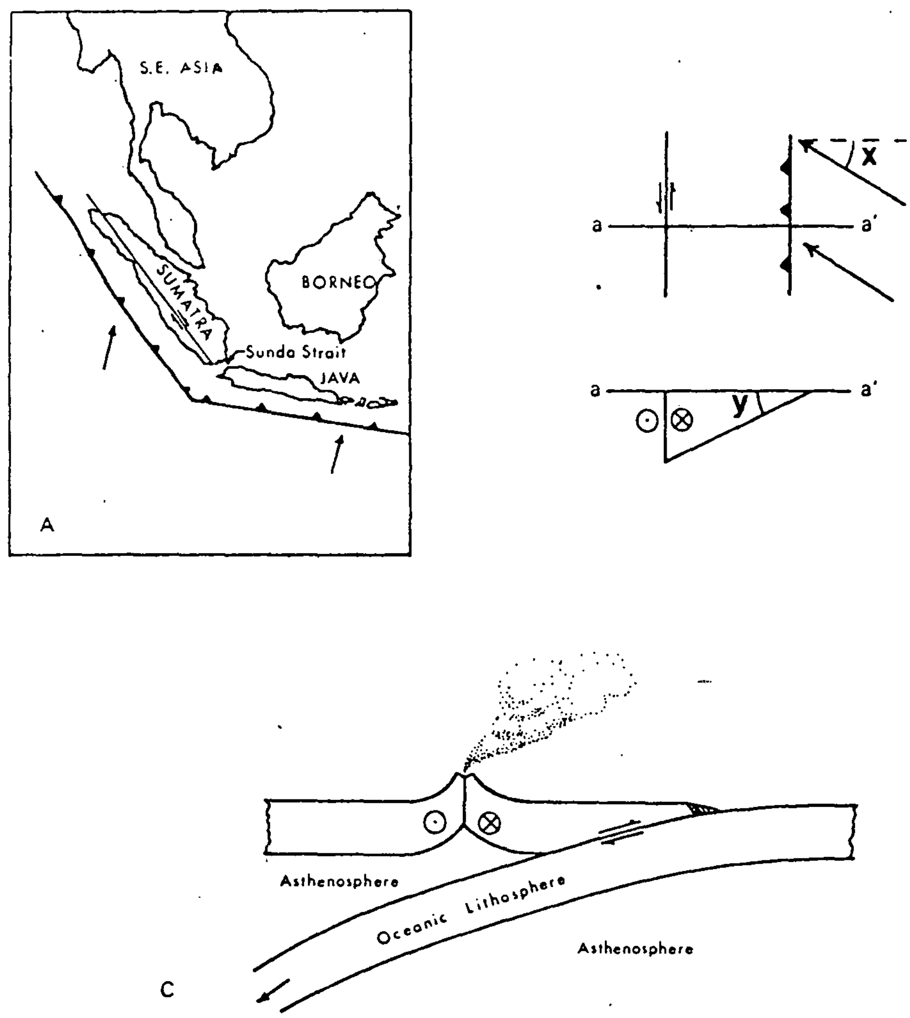
S.E. ASIA
SUMATRA
BORNEO
Sunda Strait
JAVA
A
a
a'
x
y
B
Asthenosphere
Oceanic Lithosphere
Asthenosphere
C

convergence, low angle of subduction and a relative thermal softening of the magmatic arc. The strike-slip fault appears to run down the thermally weakened axis of the arc itself rather than behind the accretionary complex. A system of strain partitioning similar to this is believed to be resposible for the development of the "suspect" terra:nes collage in W. America. The development of a strike slip fault immediately behind the accretionary complex itself might be more likely if the buttress angle was steep, as this would provide a suitably orientated weakness.

The two main aims of this study are to:
1) Identify and describe the various physical and structural processes that can operate within accretionary complexes, including the evolution of thrusting within the complex, mud diapirism and the effects of high porefluid pressure on deformation processes.
2) Define and assesss the principal boundary factors in accretionary systems that control, the occurrence and relative importance of the various physical and structural processes, and ultimately the final overall form of the accretionary complex. Such boundary factors include the sedimentary input, the wedges critical taper, subducting basement topography, obliquity of convergence, and buttress angle.

The active and ancient convergent margin systems chosen for more detailed study show the effects of differing combinations of boundary factors.

The Barbados Ridge Complex was chosen because it is a well-documented example of a modern subduction system where a considerable amount of geophysical data has been collected (cf Speed, Westbrook and others 1984). This has enabled the construction of a lineament and structural map of the offshore regions of the complex which has revealed much of its near surface complexity (see Chapter 1 and Appendix A). The developing accretionary complex was found to vary in response to changes in such boundary factors as subducting oceanic basement topography, thickness and nature of input sediment and and butress angle. In particular, these affected the wavelength and along strike extent of structures developed near the accretionary front, the occurrence and nature of mud diapirism, the development of structures oblique to the strike of the complex and the type of structures affecting the internal regions of the complex.

The Crocker Formation of the ancient N.W. Borneo subduction complex, Sabah, was examined in in the field. The Formation was found to have a complex, but predominantly coherent structural history dominated by sequential thrusting and folding developed in response to the accretion of a thin turbiditic sequence (see Chapter 3). It also contains some bodies of melange that have been interpreted as originating in mud diapirs (Barber et al. 1986). It appears, therefore, to contain many elements that might be expected to occur in a modern accretionary complex such as the Barbados Ridge, in which a sequence of sediments a few hundred meters thick has been accreted.

W. Timor is a recently active accretionary terrane formed during the collision of the Banda forearc with Australia. It includes part of the sedimentary sequence of the northern Australian continental shelf. This collision complex is composed largely of melanges. The melanges appear to be predominantly related to mud diapirs of which Timor contains many active examples (see Chapter 4). Particular attention was paid to the melanges and mud diapirs during the field studies. The processes that operated during the development of this complex must have differed substantially from those governing the construction of the majority of the complexes in Barbados and Sabah and this area provides an informative contrast to them. The sediment thickness controls the wavelength of structures, and the sediment type and consolidation exert an important control on whether the complexes deform predominantly by thrusting and folding, or whether diapiric activity and other processes of melange formation produce an incoherent deformation style.

The subducting basement topography, by controlling the pattern of sedimentation can indirectly influence the style of deformation within the complex. In addition, by causing variations in the orientation of the basal decollement, basement ridges can alter the state of stress within the accretionary complex and directly affect how it deforms. The role and influence of overpressuring in maintaining high states of under-consolidation, the role of mud diapirism and the evolution of the more coherent structural processes of thrust tectonics are also discussed in the thesis.

Constraints of time and opportunity has meant that the work embodied in this thesis has been confined to regional studies in the the Barbados Ridge, Sabah and Timor areas where its possible to make observations on the relationship between the following BOUNDARY FACTORS and physical and structural processes;

1) The gross CRITICAL TAPER of a developing complex and its relationship to the more detailed structural evolution of accretionary complexes. Application of the critical taper concept to actual three dimensional situations in the Barbados Ridge Complex, leads to the observation that as the stress within a deformation wedge is controlled by a number of seperate forces, significant out-of-convergence-plane movements may occur if all the principal forces do not act in that plane (see Chapter 5).

2) The SEDIMENTARY INPUT varies both in its thickness and nature. The thinner the accreted sequence, the shorter wavelengths of structures and the greater the numbers of out-of-sequence structures developed (See Chapter 1, Section 1.5). Variations in the the nature of the incoming section are principally a function of the presence or absence of turbidites in the section and the degree of consolidation of the section. The most obvious example of the control of the nature of the sediments on accretionary processes is on the distribution of mud diapirs in the Barbados Ridge complex (see Chapter 2). It this case they are restricted to the southern regions of the complex where they are associated with the accretion of thick sequences of rapidly deposited *input is proposed to be on whether 'coherent' deformation processes such as thusting and folding are principal constructive agents as in Sabah, (Chapter 3) or whether these become subordinate to 'incoherent' processes, such as mud diapirism, which produce large melange terranes as in W. Timor (Chapter 4). A general trend between increasing volume and degree of underconsolidation of incoming partly-lithified argillaceous dominated sedimentary sections and an increasing likelihood of melange dominated complexes is proposed.*

3) SUBDUCTING BASEMENT TOPOGRAPHY influences the sedimentation pattern on the incoming plate and can produce large variations in both the thickness and nature of the accreted sediments. In the case of the Barbados Ridge they indirectly cause along strike variations in the rate of development of the accretionary complex as consequence of causing relatively rapid changes in the thickness of the accreting sediments, which in turn results in variations in the strike of the accretionary complex and the need to consider three dimensional critical taper effects (see Chapters 1 & 5). The basement topography further influences the structures developed within the complex by causing variations in it's angle of basement detachment, this in turn influences the critical taper needed for stability and can result in reorginizations within the complex. In general, in the Barbados Ridge Complex the ridges are orientated at a relatively small angle to the direction of convergence and produce proportionately narrow discontinuities in the complex.

CHAPTER ONE

DEVELOPMENT OF THE BARBADOS RIDGE COMPLEX

1.1 INTRODUCTION

The Barbados Ridge complex lies on the eastern margin of the Lesser Antilles Island Arc at the eastern margin of the Caribbean plate. Currently the Atlantic oceanic crust is subducting westwards or slightly south of west beneath it at a rate of 20 km-m.y^{-1}. (Minster and Jordan, 1978) to 37km m.y. (Sykes, et al., 1983). Fig. 1.1 is an example of a subduction complex that is extensively developed. A map (Appendix A) of the shallow structure of the accretionary complex and related morphological and sedimentary features has been complied from GLORIA long range side-scan sonar images, Seabeam bathymetry, and seismic reflection profiles. The map shows that within the accretionary complex there are great variations in the style of deformation. These variations arise principally from the changes of the stress regime within different regions of the complex during its development, the along-strike variations in sedimentation both onto and in front of the complex, and the effects of ridges associated with transform faults in the oceanic crust beneath the complex. The positions of the figures in the text are marked on Figure 1.2.

The Barbados Ridge accretionary complex has been subdivided into a series of structural zonations (Fig. 1.1) (Westbrook et al. 1984) that reflect changes in the broad

FIGURE 1.1- The location of the Barbados Ridge Complex East of the Lesser Antilles island arc, with its four main lateral subdivisions. Bathymetric contours are at 1 km intervals.

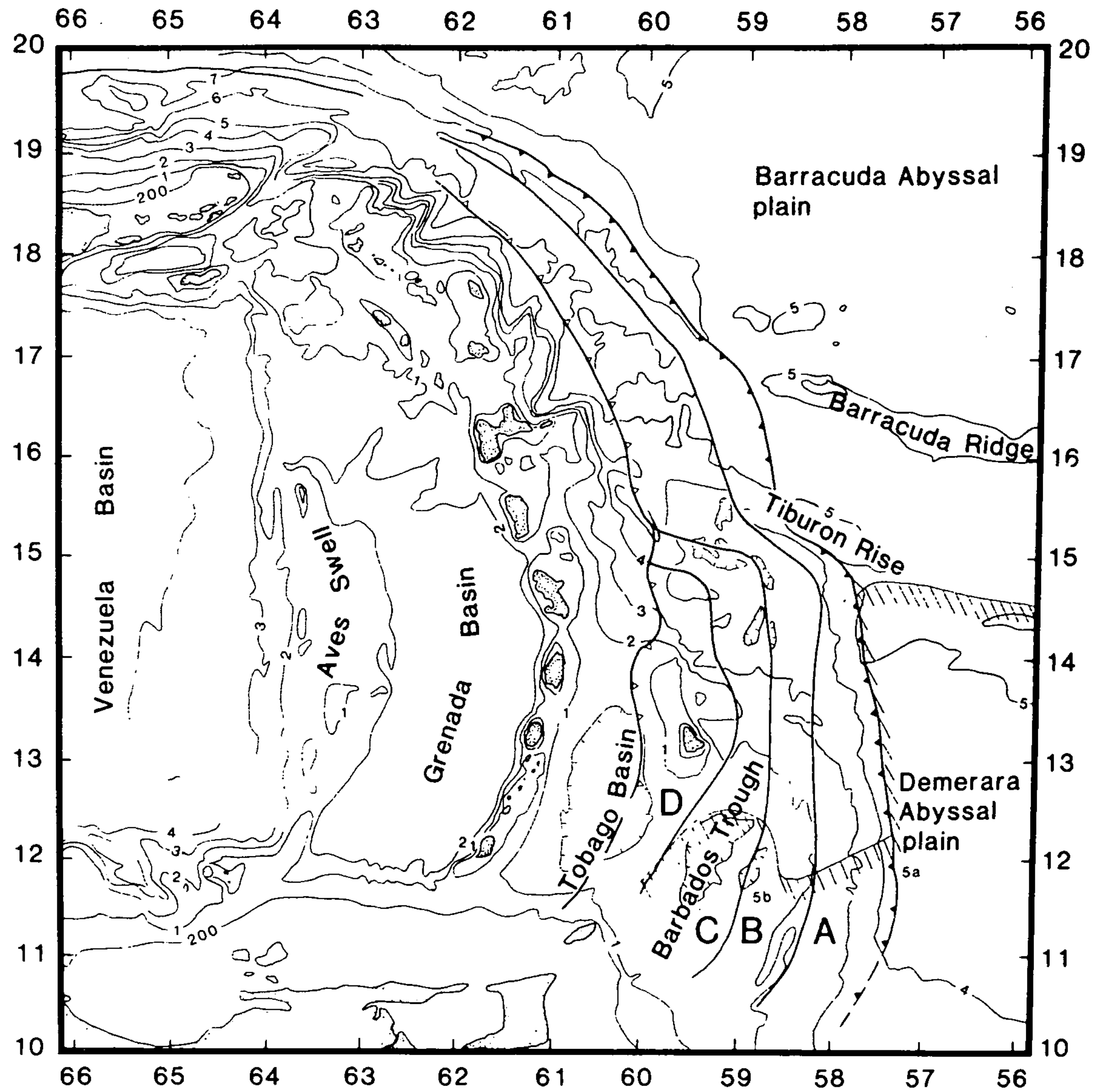

Legend

Outer deformation front

Inner deformation front

Northern limit of Orinoco Turbidite Deposition

A-zone of Initial Accretion

B-zone of Stabilization

C-zone of Supra-Complex Basin

D-Barbados Ridge Uplift

features of the complex's growth; (1) The Zone Of Initial Accretion, where rapid thickening of the complex occurs by frontal imbricate thrusting and further back by subcretion and large scale reimbrication. It characteristically has trenchward facing slopes. (2) The Zone Of Stabilization, where the rate of thickening of the complexes is small. A dynamic equilibrium exists between the gravitational body forces that would cause the complex to spread and the compressional forces that seek to thicken it. The increased strength of the complex, resulting from compaction and lithification, gives it an increased stability in its reaction to stress and reduces the rate of shortening. (3)The Zone of Supra-complex Sedimentary Basins. Well developed south of latitude 13° N. This is a zone where thicknesses of up to 3 km of undeformed sediments lie on top of the accretionary complex in basins caused by the uplift of the parts of the complex that forms their margins. The Barbados Trough is the largest of these basins. (4) The Barbados Ridge Uplift lies just to the east of the inner deformation front and Tobago basin, and west of the main slope basins (and has risen relative to both). The uplift is related to the complex being thrust westwards, up onto the forearc basement. The uplift has recently been most active in the central regions and dies out to the south and north. Forearc sediments of the Tobago basin and other forearc basins are being accreted to the complex along the inner deformation front, which forms the western boundary of the complex.

FIGURE 1.2- Location map of the various figures used in the following text.

The basement ridges that trend at high angles to the strike of the deformation front are associated with fracture zones in the Atlantic crust. The basement ridges pond the Orinoco Fan turbidites, restricting their northward flow to areas south of Tiburon Rise at latitude 15° N. There are pronounced variations in the thickness of sediments between ridge and trough areas (Speed, Westbrook and others 1984) and this effects the wavelength of the frontal accretionary structures. Structures are also induced directly in the complex by the tectonic influence of the ridges.

1.2 *DATA SOURCES AND MAP CONSTRUCTION*

The following data sources were used in the compilation of the structural map (Appendix A, Fig. 1.3) of the offshore regions of the Barbados accretionary complex:

1) A regional, long range side scan sonar (Gloria) survey, undertaken by the Institute of Oceanograph Sciences in 1980 (Stride et al. 1982), plus some additional coverage from a cruise M.T. Farnella in 1982 (See Laughton, 1982 for a description of Gloria).

2) Multichannel seismic reflection lines from RRS Discovery 109 (Westbrook and Smith 1984), from site surveys and the craven project conducted by IFP and CEPM (Biju-Duval et al. 1978, 1982, Valery et al. 1985) from Lamont-Doherty Geological Observatory (Ladd 1984, Maufrett et al. 1984) and from Shell International. Single channel seismic profiles, principally from cruises by Lamont-Doherty Geological

FIGURE 1.3- Map showing the coverage of GLORIA and Seabeam data and multichannel seismic reflection sections used in the compilation of the structural map of Fig. 1.2 & Appendix A.

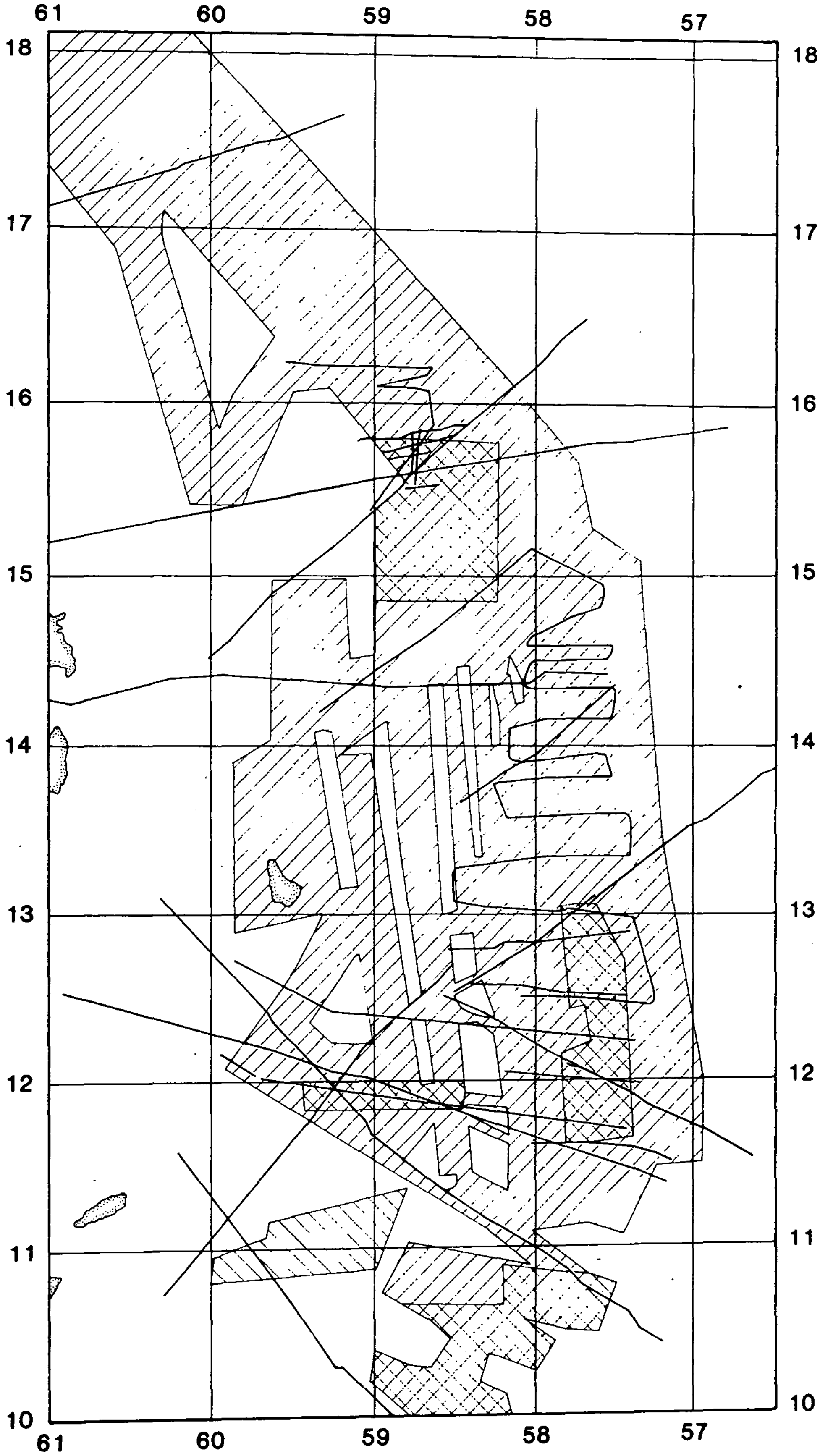
61
60
59
58
57
18
17
16
15
14
13
12
11
10

Observatory and Woods Hole Oceanographic Institute were also found to be of use in some areas.

3) Seabeam bathymetric surveys undertaken in the Carven project were also found to be of great use in the limited areas surveyed (Biju-Duval et al. 1982, Valery et al. 1985).

A lineament map was derived using Gloria data

in the preliminary stages of constructing the structural map. GLORIA records the intensity of the backscatter of sound waves from features on the sea floor against the time taken for sound to return to the transducer. The backscatter intensity is enhanced if the slope of the sea floor is towards the sensor or if it has a small scale surface roughness that might be of a tectonic or sedimentary origin. GLORIA images features that strike roughly parallel to the ships track more readily than those that are highly oblique to it, and the most detailed information comes from regions of the map where the ships track forms a grid pattern. Features appear on the sonographs at a distance from the centre line that is proportional to the travel time of reflected sound waves not true distance (Fig. 1.4). Features were marked on the sonographs and then their positions were corrected for slant range before transcription on to the lineament map. (These data were recorded in analogue form, and sonographs digitally corrected for slant range were not available.)

The lineament map was then interpreted using the structural information gained from the seismic data. Although less able to define smaller structural features, the

FIGURE 1.4- An illustration of the slant-range distortion produced in GLORIA sonographs by the depth of the sea beneath the transducer. This gives a finite offset on the sonograph of the seabed reflection beneath the ship's track. The simple correction does not take into account the depth of the imaged feature; only depths beneath the ships track have been used.

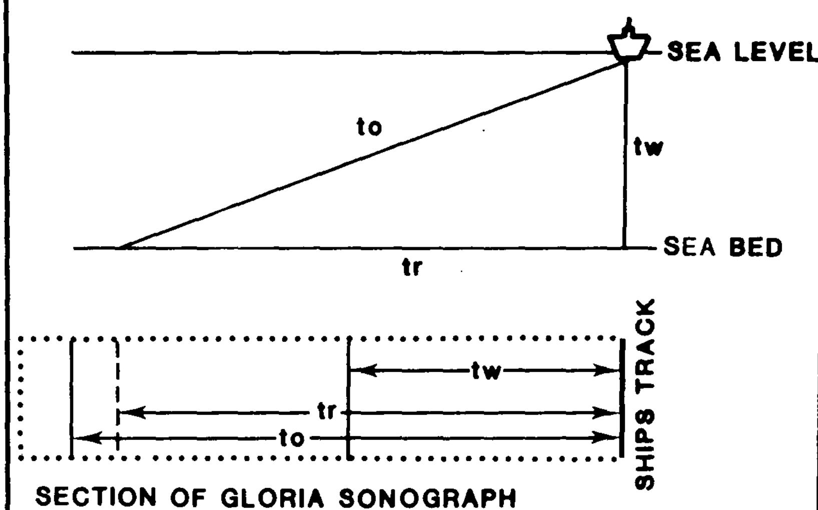

$$tr = \sqrt{to^2 - tw^2}$$

Seabeam bathymetric data was useful in assesssing the true magnitudes of the features imaged by the GLORIA. It was also used in its own right to map more major features. In the southern regions of the map where the wavelength of the structures is large, individual structures can be traced along strike for great distances and the seismic coverage is sufficient for correlation. Further north, where structures are less continuous along strike, direct correlation with seismic sections is not always possible. However, certain features of the sea floor have a characteristic form on the GLORIA sonographs. Ridges, that commonly correspond to anticlines in the hanging wall of thrusts, show up as alternating brighter and darker bands on the sonographs (Fig. 1.5) as the intensity of back scattering changes with the changes of slope across the images. If there is much disruption of the seafloor along surface fault traces, they may show up as narrow bands bright bands. Sinuous channels in the submarine fan at the foot of the complex (Belderson et al. 1984) can have a similar appearance although their relief is much smaller, presumably because of changes in bottom roughness related to variations in sedimentation. So quantitative measurements of bathymetry, even if only along profiles, are important to the correct interpretation of some features on the sonographs. Mud volcanoes on the seafloor form very 'bright' features because of the backscattering from the rough surface of erupted material.

FIGURE 1.5 An example of a GlORIA sonograph. The ship's track lies along the centre of the figure. Either side of it, bilaterally symmetric, the first line is the reflection of the seabed beneath the ship's track from the transducers on each side of the towed sonar vehicle. The sonograph was displayed with automatic gain control to equalise the strength of image from weakly and strongly reflecting areas. This process can produce false shadows in front of brightly reflecting features. Features shown on the sonograph include anticlinal ridges, fault traces and mud volcanoes. (Postion of this Figure is marked on Figure 1.2)

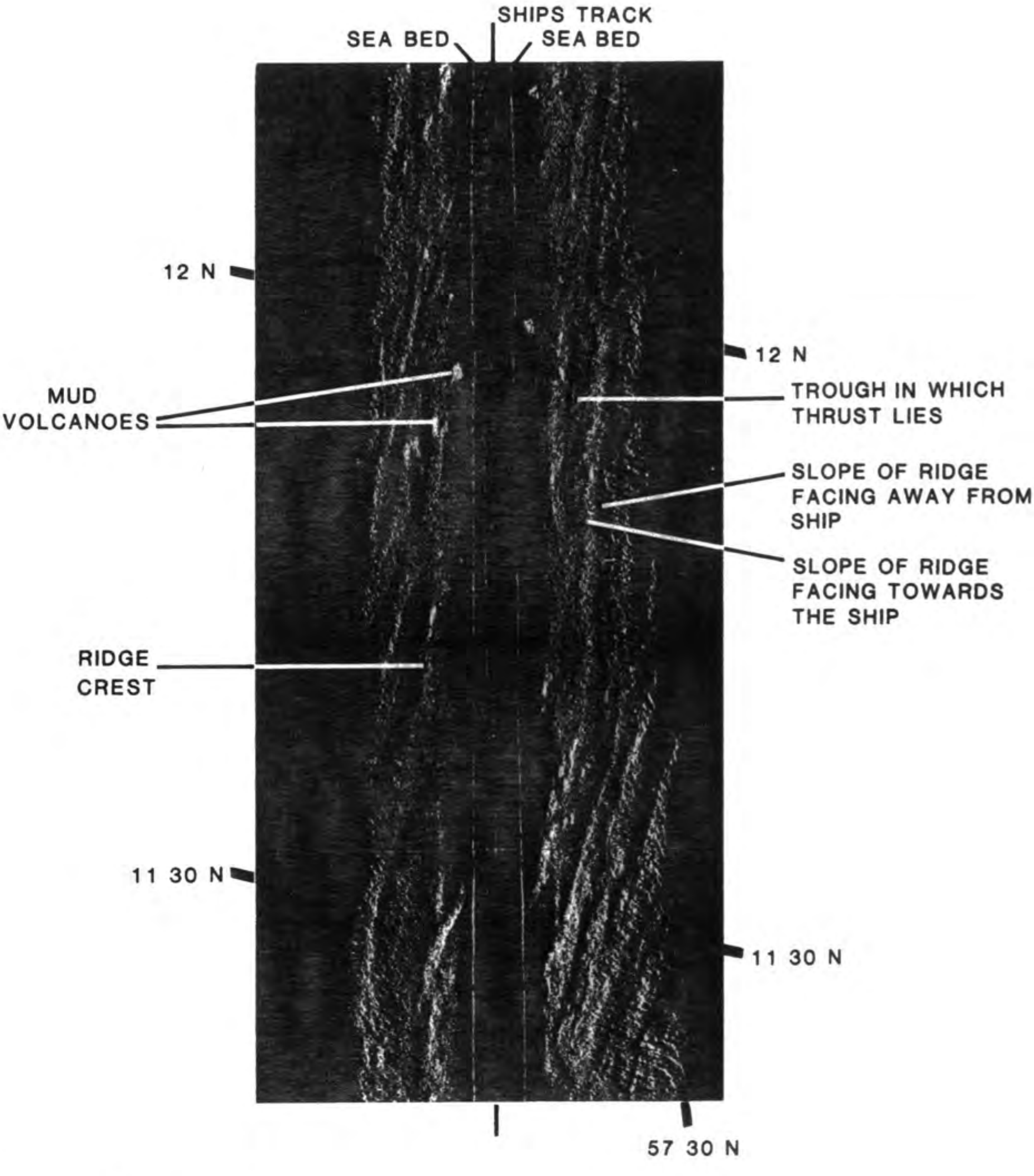
SHIPS TRACK
SEA BED
SEA BED
12 N
12 N
MUD
VOLCANOES
TROUGH IN WHICH
THRUST LIES
SLOPE OF RIDGE
FACING AWAY FROM
SHIP
SLOPE OF RIDGE
FACING TOWARDS
THE SHIP
RIDGE
CREST
11 30 N
11 30 N
57 30 N
25km

1.3 *THE EFFECT OF VARIATIONS IN THE THICKNESS OF SEDIMENTS ON THE SUBDUCTING ATLANTIC CRUST UPON THE GENERAL MORPHOLOGY OF The COMPLEX*

The Barbados Ridge complex varies in width (300-80 km) and maximum thickness (20-10 km) from south to north, reflecting the overall northward thinning of the Orinoco fan turbidites on the Atlantic oceanic floor. Sediment thickness on the incoming Atlantic oceanic crust decreases from about 7 to 5km between latitude 11° N to 12° 20' N (Speed, Westbrook et al. 1984) due to a northward thinning of the turbidites of the submarine fan of the Orinoco. At the base of the sediment sequence a group of horizons of consistant character and high lateral continuity of horizons, interpreted as pelagics, maintain a thickness of approximately 1 km through out these southern regions. North of 12° 20' N, the oceanic basement ridges have dammed the northerly flowing turbidites causing a reduction in the sedimentary thickness across them. This results in slower rates of accretion and pronounced indentations of the outer deformation front. The largest indentation is produced by the Tiburon Rise. North of the Tiburon Rise there are only a few turbidites in the sedimentary sequences.

The overall northward decrease in the elevation of the complex is not uniform. There are a series of northward facing steps in the topography of the complex that lie above the westward extensions of the oceanic basement ridges beneath the complex. These features appear to result from *two effects of the ridges (Westbrook 1982). Due to the indentation of the accretionary front the complex begins to rise at a position further to the east on the south side of a ridge. Therefore, if the eastward slope of the complex remains constant, for a given longitudinal transect the complex has a higher elevation to the south of a ridge. In addition, the obliquity of convergence of the WNW-ESE trending ridges produces an extra southward directed component of compressional stress that steepens the slope of the complex above the southern flank of the ridges.*

The complex undergoes its most pronounced lateral change across the Tiburon Rise (Appendix A) in both its topography and width and also in the type of sediments that are accreted to it. For the ease of description of the features associated with its development the complex can be divided into two regions south and north of the Tiburon Rise.

1.4 *VARIATIONS IN STRUCTURAL STYLE OF THE REGIONS SOUTH OF THE TIBURON RISE*

South of latitude 10° 20′ N the accretionary complex merges with the undeformed Orinoco Fan sequence that extends across the Southern American continental margin and out onto the Atlantic floor (Fig. 1.1 & Appendix A). Parts of the Orinoco fan system extend across the accretionary complex itself, swathing it in a thick syntectonic sequence of turbidites. The southern margin of the complex, lying along the extension of the dextral transpressive margin (Speed 1985) between the South American and Caribbean plates, is one of broad *transition. It is also experiencing a component of dextral shear but the tectonics of the region are complicated by the accretionary complex being partly decoupled from both plates. Extensive mud diapirism adds to this complication. The strike of the accretionary front and frontal structures swings to a NE-SW orientation. One of the two large canyons of the Orinoco turbidite fan, that cut across the accretionary complex in this southern most area, is associated with a cross-fault (Fig. 1.6). There appears to be a NW-SE trending dextral tear fault along the line of the canyon across which a displacement the front of the complex occurs (Fig. 1.7). In addition, a sudden change in the amplitude and wavelength of structures also occurs across it. Structures intersected by the canyon further to the west of the accretionary front are also not matched on the other side and it would appear that the fault continues for at least 40-50 Km into the interior of the complex (Fig. 1.6). The orientation of the tear faults suggests that the sence of movement of the thrust sheets is to the SE in this southern area, rather than to the east as would be suggested by the E-W sense of plate convergence. It is not clear whether the canyon exploited the pre-existing line of weakness along a fault, or whether its incision across the frontal parts of the complex generated a line of weakness that was later used as a tear fault.*

The canyons themselves tend to wind their way down to the front accretionary complex, deflected by the ridges formed by the frontal imbricates (Figs. 1.8 & 1.9). The Orinoco fan turbidites that extend across the complex are primarily

FIGURE 1.6- A closer view of the southern part of the accretionary complex taken from Fig 1.2 & Appendix A. A dextral tear fault lies along the line of the canyon (see Fig. 1.7). The positions of Figures 7-9 are marked.

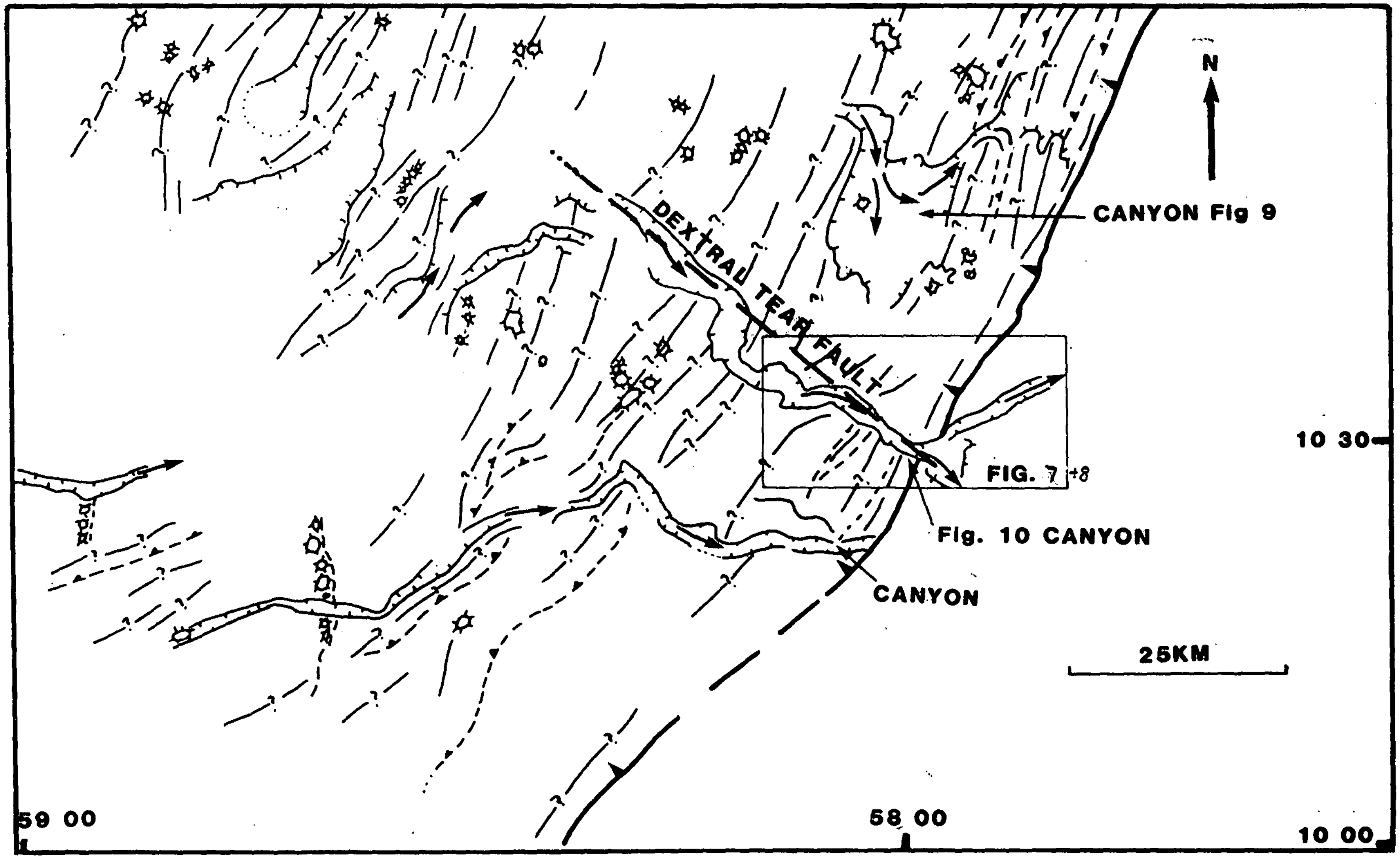
N
CANYON Fig 9
DEXTRAL TEAR FAULT
FIG. 7 +8
Fig. 10 CANYON
CANYON
25KM
10 30
10 00
59 00
58 00

FIGURE 1.7- A Seabeam bathymetric map showing the displacement of the accretionary front, across the canyon, by the dextral tear fault. (Position of this Figure is marked on Figure 1.6)

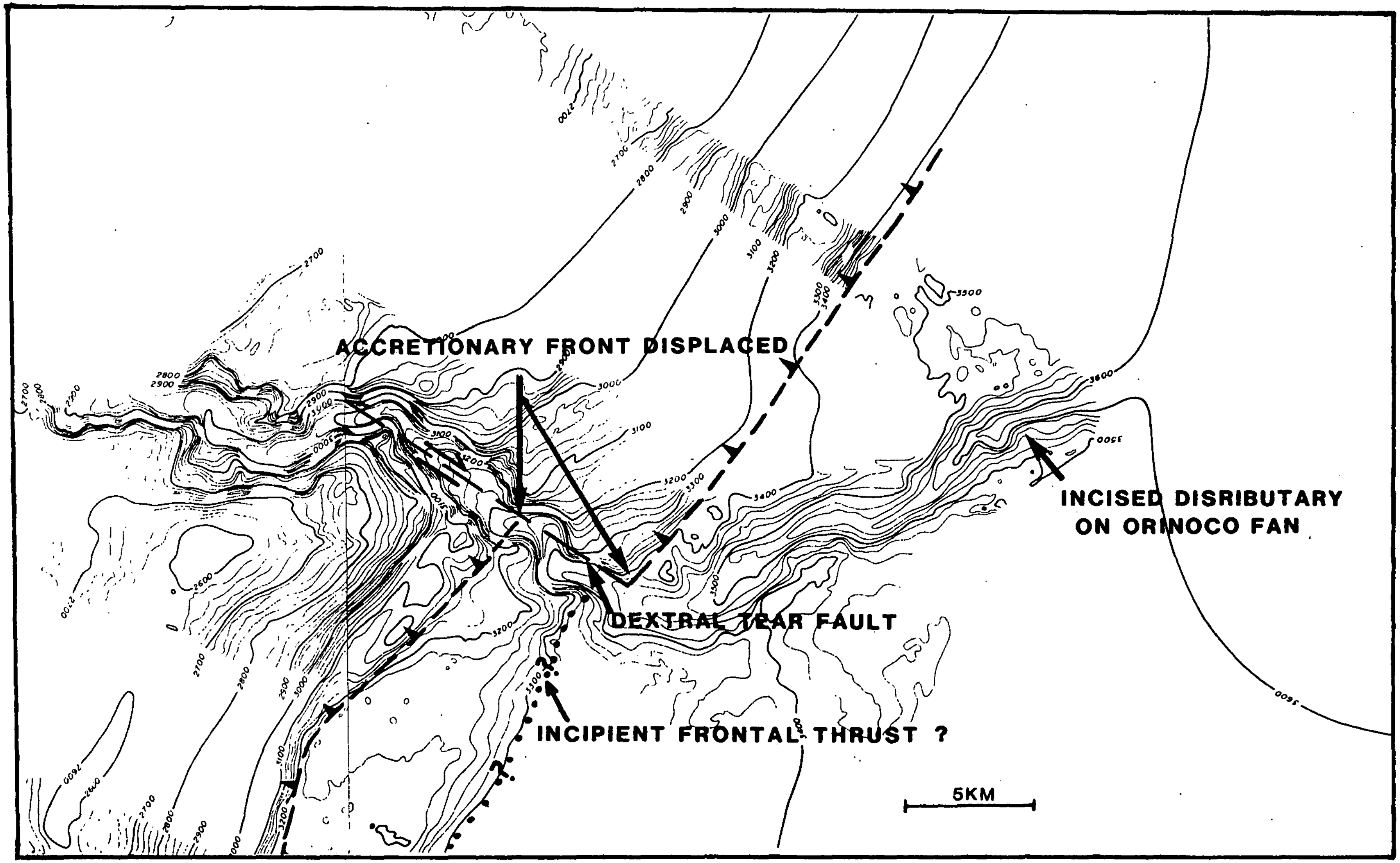
ACCRETIONARY FRONT DISPLACED
DEXTRAL TEAR FAULT
INCIPIENT FRONTAL THRUST ?
INCISED DISRIBUTARY
ON ORINOCO FAN
5KM

FIGURE 1.8- GLORIA sonograph of the canyon system which has developed along the dextral tear fault which must form a line of weakness in the complex. (Position of this Figure is marked on Figure 1.6)

FIGURE 1.9- GLORIA sonograph of a canyon system that cuts down across the anticlinal ridges of the accretionary complex. Inter-ridge troughs are the sites of syntectonic deposition of turbidites and show up brightly on the GLORIA images, ridges are dark on the sonographs as they are sites of little turbidite deposition. (Position of this Figure is marked on Figure 1.6)

restricted to the trough areas in between the anticlinal ridges, and syntectonically infill the synclines. The recently deposited turbidite sequences in the troughs show up as bright bands on the GLORIA sonographs (Fig. 1.8).

A roughly linear zone of complexity occurs in the accretionary complex just to the north of latitude 11 N, running westward from approximately 59 E latitude, to intersect with the along strike continuation of the El Pilar dextral transpressive fault system. The structural grain in this region of complexity has a predominantly E-W to SW-NE orientated and it is the southern boundary to the N-S trending structures of the accretionary complex to the north. The zone of complexity consists of a series of elongate and occasionally arcuate or irregular ridges, mounds and troughs (Fig. 1.10). The elongate ridges are formed above northerly dipping thrusts (Valery et al. 1985). The thrusts are associated with abundant shale diapirism, which form domal structures, and mud volcanoes which form smaller mounds. The zone of complexity is, in all likelihood, a major zone of compressive dextral shear that represents the southern termination of the Barbados Ridge complex.

The style of deformation in the Zone Of Initial Accretion (Figs. 1.1 & Appendix A) south of latitude 12° 20′ N, is relatively unaffected by the basement topography of the subducting Atlantic oceanic crust (Fig. 1.11), which is covered by thick sediments. The structures of the frontally imbricated section are in the form of gently asymmetric folds with amplitudes of approximately 0.5 km and wavelengths of

FIGURE 1.10- Seabeam bathymetric map of the roughly east-west striking zone of complexity that occurs along the southern termination of the accretionary complex, along strike of the eastern termination of the El Pilar Fault system. The zone of complexity is believed to result from the combination of dextral compressive shear and mud diapirism.

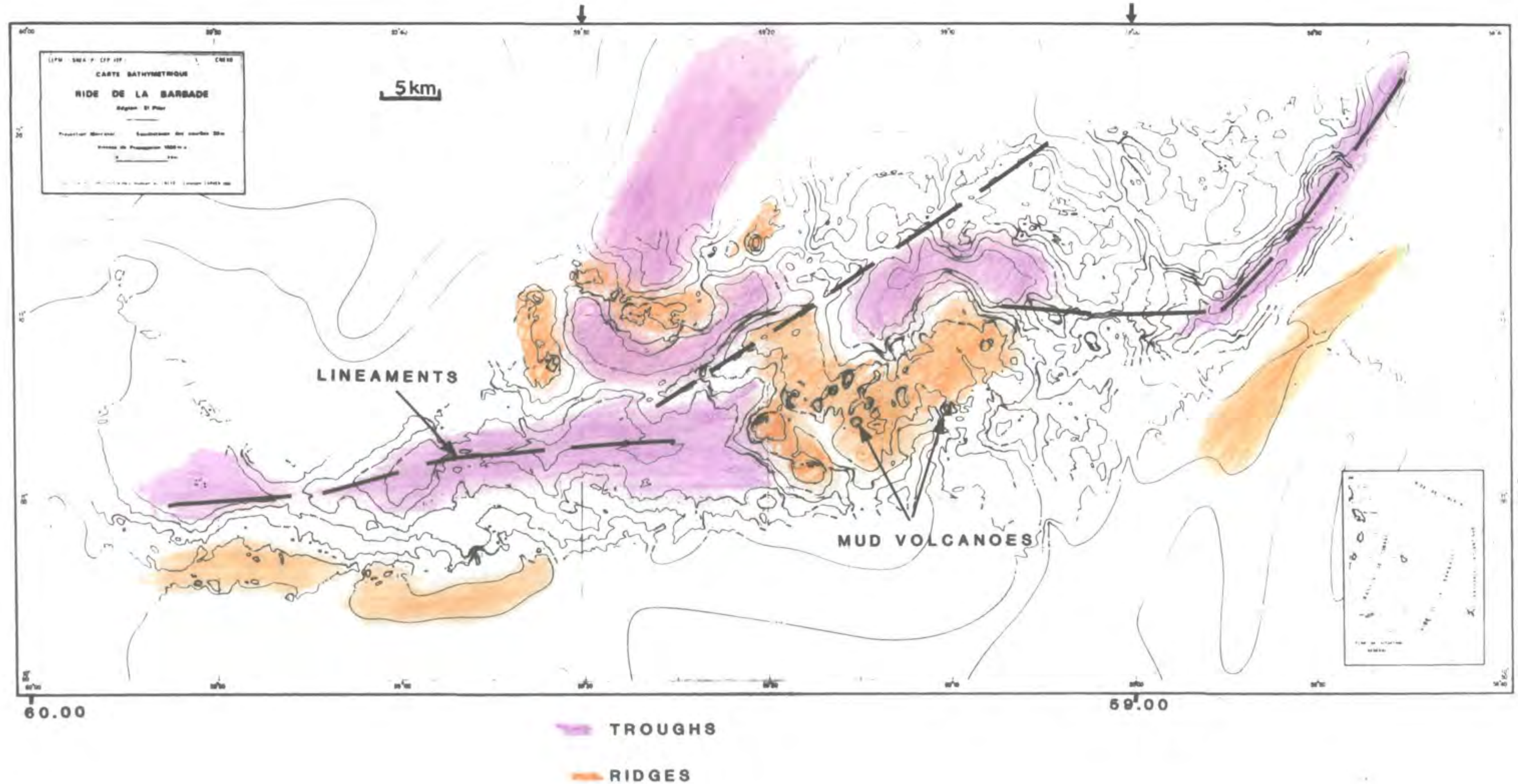
CARTE BATHYMETRIQUE
RIDE DE LA BARBADE
5km
LINEAMENTS
MUD VOLCANOES
11.00
60.00
59.00
TROUGHS
RIDGES

FIGURE 1.11- Map showing the relationship between the principal structural trends of the accretionary complex and the topography of the oceanic igneous basement beneath the complex. (Basement topography from Westbrook and others, 1984). Also shown is the diffuse boundary of the region where slope sediments obscure the structures formed during the accretion of sediment.

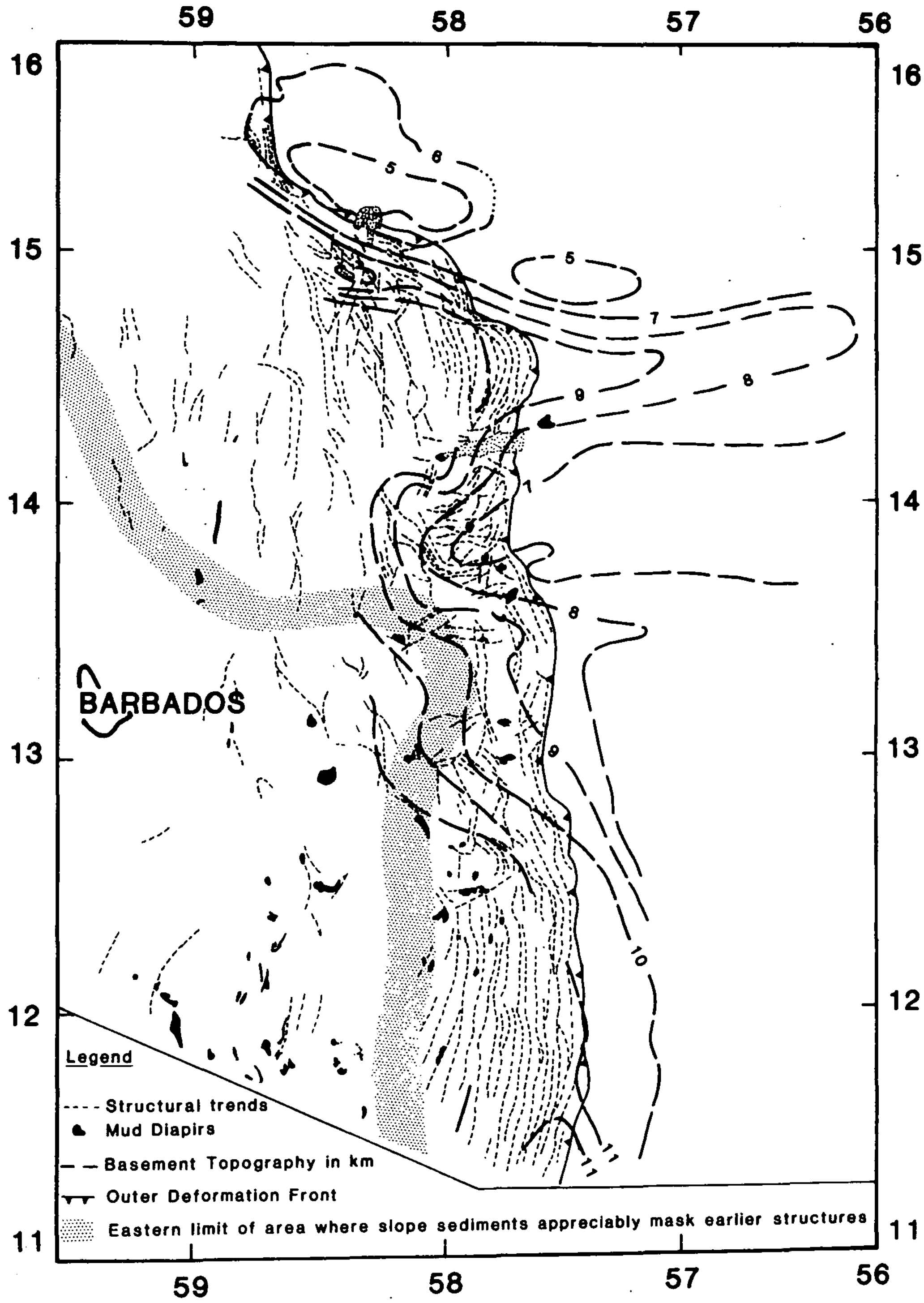

59
58
57
56
16
15
14
13
12
11
BARBADOS
5
6
5
7
8
9
7
8
9
10
Legend
Structural trends
Mud Diapirs
Basement Topography in km
Outer Deformation Front
Eastern limit of area where slope sediments appreciably mask earlier structures

between 8 and 9 km (Fig. 1.12a & Appendix B, Sections 1 & 2). The folds, with an eastward vergence, are developed above thrusts which dip westwards at 20° (Westbrook 1982), rooting into a decollement that lies 2.5-3.5 km beneath the sea floor at the toe of the complex. The relatively long wavelength of the frontal structures is a consequence of the thickness of the deformed layer. The folds form bathymetric ridges, some of which can be traced for over 120 km along strike using GLORIA side-scan sonar (Appendix A) and Multibeam Bathymetric survey data. Fold amplitudes vary gently along strike. A further feature of the Zone Of Initial Accretion in this southern region is the development of slumps resulting from the failure of portions of the steeper, eastward facing slopes of a small number of the ridges formed by the thrust related folds (Fig. 1.13a & Appendix A) . The slump deposits form mounds which can extend up to 1km out from and 20 to 50 km along the foot of the slope.

The thickest, frontally accreted packets in the southern most regions of the complex south of latitude 12° 40' N (Appendix B, section 2) can be seen to remain at or near the surface during subsequent thickening of the complex. Thickening is accomplished by back rotation of the frontally accreted packets and folding during the early stages. Subcretion, continued internal thickening at depth, and occasional out-of-sequence thrusts may play an increasingly important role further back in the Zone Of Initial Accretion in these southern most regions but are not obvious features on seismic reflection sections. Further north, where the incoming section is thinner, the wavelengths of the frontal

FIGURE 1.12- Line drawings of two seismic sections illustrating some of the characteristic features of the southern part of the complex. The positions of the two sections are shown in Fig. 1.2. They come from a multichannel seismic reflection line shown in Biju-Duval et al. (1982).

Section A shows the front of the complex with its seaward verging thrusts and associated ridge-froming anticlines. The steeper seaward slopes of some of the anticlinal ridges has become unstable slumping into the troughs below.

Section B shows the transitional region between the Zone of Stabilization and the Zone of Supra-complex Basins, where the slope cover has been deformed during sedimentation. Some landward verging structures are present and mud diapirism is prevalent.

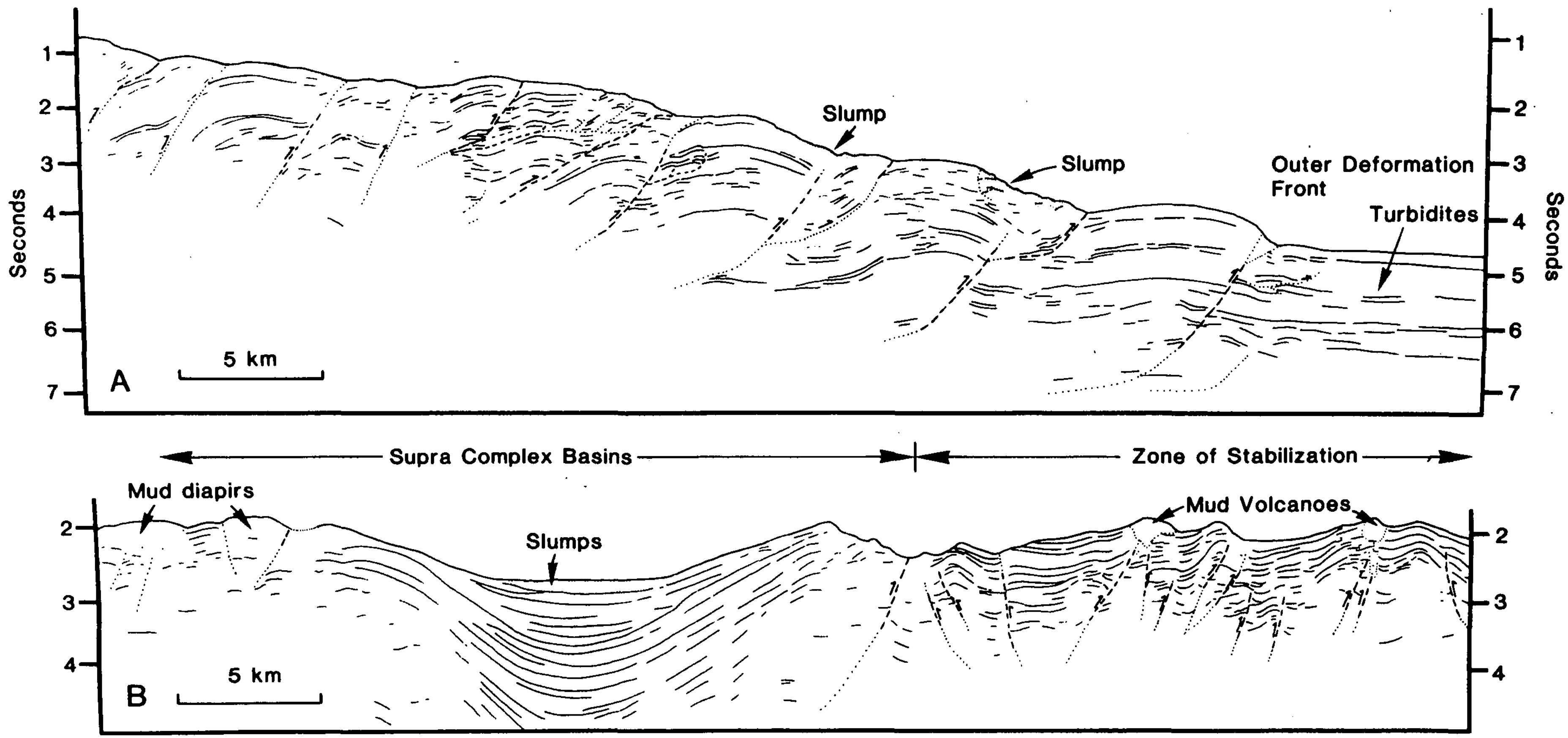

Seconds
1
2
3
4
5
6
7
Slump
Slump
Outer Deformation Front
Turbidites
5 km
A
Supra Complex Basins
Zone of Stabilization
Mud diapirs
Slumps
Mud Volcanoes
5 km
B

FIGURE 1.13- GLORIA sonograph of the abyssal plain in front of the accretionary complex, where a large slump has ponded northerly flowing turbidites. Currently the turbidites are begining to top the slump deposit and it is begining to be progressively obscured. (Position of this Figure is marked on Figure 1.2)

structures gets shorter. The occurrence of structures that have been interpreted to be out-of-sequence thrusts are also more obvious and commonly developed (Appendix B, Section 3). Where major 'late' (or out-of-sequence) thrusts cut the surface of the complex, there is commonly a break in slope, with increased topographic dips above their hanging walls.

North of latitude 12° 20' N the incoming oceanic basement has greater topographic relief with maximum amplitudes of 3 to 4 km between basement ridge crest and adjacent trough (Westbrook et al. 1984) (Fig. 1.11). This results in the imposition of the following additional features on the frontal regions of the complex; (1) Marked variations in the strike and wavelength of structures occur across the ridges. Thrusts and folds tend to to develop subparallel to the deformation front preserving a record of past orientations of the outer deformation front. (2) Wavelengths of structures vary in proportion to the thickness of the thrust slice. The spacing of the thrusts is usually three times the thickness. Consequently thrusts are widely spaced opposite troughs, where the sedimentary section is thicker and the level of the decollement is usually deeper, and closely spaced opposite ridges. (3) The number of crossfaults, striking at high angles to tha accretionary front, greatly increases in the regions of the basement ridges. They are particularly abundantly developed around latitude 14° N. They form discontinuities that have westerly to northwesterly trends across the frontal region of the complex where they are present in large numbers. Many are probably oblique slip transpressional faults resulting from the continued *deformation of the complex by the basement ridges. Some may also be normal faults that might be expected to originate during readjustments of the critical taper of the complex (see Chapter 5). (4) Several slumps or debris flows occur in the area of impinging ridges. The slump occurring off the northward facing slope of the accretionary complex, where the Tiburon Rise impinges on the complex, covers an area of some 100 km. Further south at latitude 14° 20′ N another debris flow appears to have been initiated by a mud volcano (see Chapter 2). The intense deformation and cross-faulting may have destabilised the accretionary complex in these regions. The large area of disturbed sea floor in front of the complex at latitude 13° N appears to be a thin skinned slump that has been subsequently obscured by later sedimentation (Fig. 1.13). The slump extends 20 km out from the present position of the outer deformation front and covers an area of approximately 500 km.*

In the south, the decollement beneath the frontal imbricates initially lies within the turbidites sequence so that the lower part of the turbidite and all the pelagic section passes, undeformed, beneath the leading edge of the accretionary complex. Further to the north around latitudes 13° to 14° N, where sediments are thinner, subcretion of turbidites beneath the frontal imbricate section can be seen (Westbrook & Smith 1983, Westbrook et al. 1984, Speed, Westbrook and others 1984) (Appendix B, Section 3 & Fig. 2.5, Chapter 2). There are considerable numbers of mud diapirs on the Barbados accretionary complex (Stride et al. 1982). It has been proposed that the mud volcanism is sourced from the *subcreted section and are part of the normal processes that allow these regions to dewater (See Chapter 2).*

The ***Zone Of Stabilization*** *lies to the West of the Zone Of Initial Accretion and is characterised by an undulating plateau region (Figs. 1.1 & Appendix A). In the south its earlier structural fabric is masked by slope cover which increases in thickness westwards (Fig. 1.11 & 1.14). The slope sediments were mostly deposited during a period when active deformation of the Zone of Stabilization was at a minimum and they gently onlap and drape previous topographical features. In the north the slope sediments are thin and many of the original deformational features are still visible. The style of the recent phase of deformation of the Zone of Stabilization is most visible in the south where it deforms the slope sediments. A similar pattern of deformation may occur in the north, but it is hard to delineate between this and earlier features. The recent phase of deformation is thought to have begun in upper Pliocene times (Hill, 1983) and is characterised by N-S trending reverse faults and associated folds that verge both to the east and west, deforming the slope sediments quite strongly in places (Fig. 1.12b & Fig. 14 Section A). The deformation becomes more intense westwards, towards the Zone of Supra-Complex basins. Two sets of cross-faults structures with NW-SE and NE-SW orientations are also developed (Appendix A). Biju-Duval et al. (1982) mapped one NW-SE trending feature, using Seabeam, and proposed that it was a transcurrent fault on finding that reverse faults terminated at it. A recent syn-tectonic sedimentary sequence of*

FIGURE 1.14- A line drawing of a seismic reflection section across the whole accretionary complex showing the major near surface structures. It comes from a multichannel seismic reflection line shown in Biju-Duval et al. (1982). (Position of this Figure is marked on Figure 1.2)

probable turbiditic origin causes thickness changes across the reverse faults, with progressive thickening in the synclinal troughs and offlap and subsequent overstep on to the flanks of the anticlines. There has been some erosion of steep slopes and fault scarps.

Mud volcanoes and shale diapirs (see Chapters 2 & 4) are the most prominent features observed on Gloria sonographs in the Zone Of Stabilization. The mud volcanoes are concentrated in the areas where the current phase of deformation is most intense and some are interpreted, on seismic evidence, as having intruded up the reverse faults (Fig. 1.12b) (Biju-Duval et al. 1982), others appear to be associated with the cross-faults.

The Zone Of Supra-complex Basins lies to the west of the Zone Of Stabilization. It appears that before the present phase of deformation the southern regions of the complex were dominated by a single very large basin which tended to subside relative to the Zone of Stabilization and Barbados Ridge Uplift (Fig. 1.1), but which is now divided into sub-basins by the tectonic uplift and deformation of sediments, associated with westward verging thrusts, to form intervening ridges. At present it is filled with approximately 2 to 3km of sediment (Speed, Westbrook and others, 1984). The Barbados Trough is its largest sub-basin. The thrusts have a horizontal spacing of approximately 10-15 km (Fig. 14 sections C & D, Appendix A) and their associated folds form ridges that rise 500 to 600 m above the intervening troughs. Some of the troughs are in fact *synclines that are tightening as the present phase of deformation proceeds (Fig. 14 section B. They contain a syntectonic sedimentary infilling of turbidites and slump deposits, the latter having originated from their over-steepened margins (Biju-Duval et al. 1982).*

Considerable numbers of mud diapirs are concentrated along the ridge crests and thrust faults. GLORIA sonographs show that some of the shale diapirs are up to 17km long and 1 km wide. From the number and size of the diapirs associated with them, it would appear that large portions of some of the ridges may be of diapiric material (see Chapter 2).

The Barbados Ridge Uplift is the most westerly structural zone of the Barbados accretionary complex (Fig. 1.1, Fig. 14 section E). The central part of the ridge has been uplifted by at least 3 km relative to the Tobago Trough which lies on its western margin (Westbrook et.al.1984). The uplift is currently greatest in its central regions and dies out to the north and south. The uplift is a result of the westwards obduction of the complex up onto the forearc basement. The inner deformation front is the western limit of the accretionary complex and is made up of an few wide spaced but large westward verging thrusts which are currently deforming and incorporating the sediments of the Tobago forearc basin into the accretionary complex, except in the area south of 12° N. The thrust spacing is approximately 15-20 km, which would correspond to a depth of about 5-7 km for the decollement they root into. This matches the estimated, 7km or slightly greater, thickness of sediments that lie above acoustic *basement in the Tobago Trough near the inner deformation front (Speed and Westbrook and others 1984), and suggests that the main detachment is at, or near, the base of the sedimentary pile.*

The Barbados Ridge Uplift rises above sea level to form the island of Barbados, on which the accreted material of the complex is exposed as the Eocene Scotland Formation. This is tectonically overlain by the Eocene to Miocene pelagic rocks of the Oceanic Formation, Bissex Hill Formation and Consett Marl, which are interpreted to be part of the forearc basin sequence (see Section 1.6.1).

The ridge crest is generally covered by Plio-Pleistocene sediments except in areas where these have been eroded. These areas of outcropping older terrigenous or pelagic rocks correspond, in general, to areas of rough brightly reflecting sea floor on Gloria sonographs (Fig. 1.15).

Few mud diapirs have been positively identified on the Barbados Ridge Uplift except on its eastern flank. However, mud diapirs have been identified on the island of Barbados, as intrusions into the Basal complex and Oceanic Formation (Larue and Speed 1984, Torrini et al. 1985). To the north of 12° 20′ N a number of canyons and slumps occur of the sides of the uplift.

FIGURE 1.15- GLORIA sonograph showing the sea foor morphology of part of the Barbados Ridge Uplift. The bright area on the western side of the ships track is a steep eastfacing slope, undergoing mass wasting, and down which cannyons are incised. The basement outcrop at the southern margin of the sonograph is part of a larger outcrop on top of the ridge itself. (Postion of this Figure is marked on Figure 1.3)

1.5 *VARIATIONS IN STRUCTURAL STYLE OF THE REGIONS NORTH OF THE TIBURON RISE*

North of the Tiburon Rise, very little turbiditic deposition has occurred on the incoming plate and the Zone of Supra-complex basins and the Barbados Ridge Uplift die out. There is also little or no mud diapirism in the complex. Near the crest of the Tiburon Rise, where DSDP sites 541 and 542 were drilled into the leading edge of the complex, an approximately 200m thick veneer of predominantly hemipelagic section is frontally accreted (Moore & Biju-Duval et al. 1984). The wavelength of accretionary structures as revealed on GLORIA is therefore correspondingly short, being between 0.5 and 1Km (Fig. 1.16, Appendix A). Individual ridges can be followed along strike for up to 12 km and are approximately 10 m high within the vicinity of the DSDP site (Belderson et al. 1984). Seismic reflection reveals that the Pelagic section is thrust, undeformed, at least 70 km beneath the accretionary complex in the region between the Tiburon and Barracuda ridges (Westbrook et. al, 1982). The thickening of the accretionary wedge near the frontal regions of the complex is therefore almost exclusively accomplished by extensive reworking of the frontally accreted section (Appendix B, Section 4). The recent ODP Leg 110 re-investigation of the region of the first Leg 78a cruse, revealed that within 17 km of the accretionary front (Leg 110, Site 674, Moore and Mascle et al., 1987, in press.) much of the section is dipping at more than 60°, it is intensely deformed, with the abundant development of scaly clay fabrics

FIGURE 1.16- GLORIA sonograph of the DSDP Leg 78A & ODP Leg 110 areas. The fine grain of the structural fabric near the accretionary front occurs as a result of the thinness of the sediment offscraped on top of the Tiburon Rise which inpinges on to the complex at this point. (Postion of this Figure is marked on Figure 1.3)

and the occurrence of tight to isoclinal folds and numerous stratigraphic repetitions occurring across steeply dipping thrusts (Moore and Mascle et al., 1987, in press.). The early thrusts, across which bio-stratigraphic repitions occur, have down-hole spacings of less than a few 10's m, with much unbiostratigraphically defined faulting on a smaller scale. These predominantly steeply dipping structures are cut across by closely spaced low angled out-of-sequence thrusts (with dips under 5°degrees) that have recorded down-hole spacings of between 150-250m (ODP, Leg 110, Site 674 report in progress). Structural fabrics in cores from Sites 674 and 673 (Fig. 1.17c for position) include well-developed scaly fabric, stratal disruption, cataclastic shear zones, thick intervals of overturned section, and calcite veins that are folded and disrupted locally (Moore and Mascle et al., 1987). Stratigraphic horizons that presently occur below the decollement horizon are within the complex at Site 674 indicating that at some time in the past the basal decollement was lower in the stratigraphic sequence.

DSDP Leg 78A revealed, during an inadvertent packer experiment, that near lithostatic fluid pressures may occur near the basal decollement of the complex, implying that friction on the basal decollement may be substantially reduced (Moore & Biju-Duval et al. 1984). Much greater than expected temperature gradients were also recorded in the complex, which Davis & Hussong (1984) attributed to upward migration of warm fluids out of the overpressured deeper regions of the complex. The recent ODP Leg 110 results

FIGURE 1.17- Figures taken from More & Mascle (in Press.). Sections A & B are schematic representations of the features seen during ODP Leg 110. Section C is a line drawing (no vert. exag.) through roughly the same section.

A) Generalised schematics proposed for the structural development of regions near the accretionary front above the northern flank of the Tiburon Rise. Closley spaced frontal imbricate faulting is closely followed by out-of-sequence faulting. The latter begins to become important within 10km of the accretionary front.

B) Fluid migration paths out of the frontal areas of the Barbados Ridge Complex. Thermogenic methane appears to be restricted to the basal decollement, frontal thrusts and the deep sand layer. The thermogenic methane was also encountered in the reference site, some distance in front of the complex.

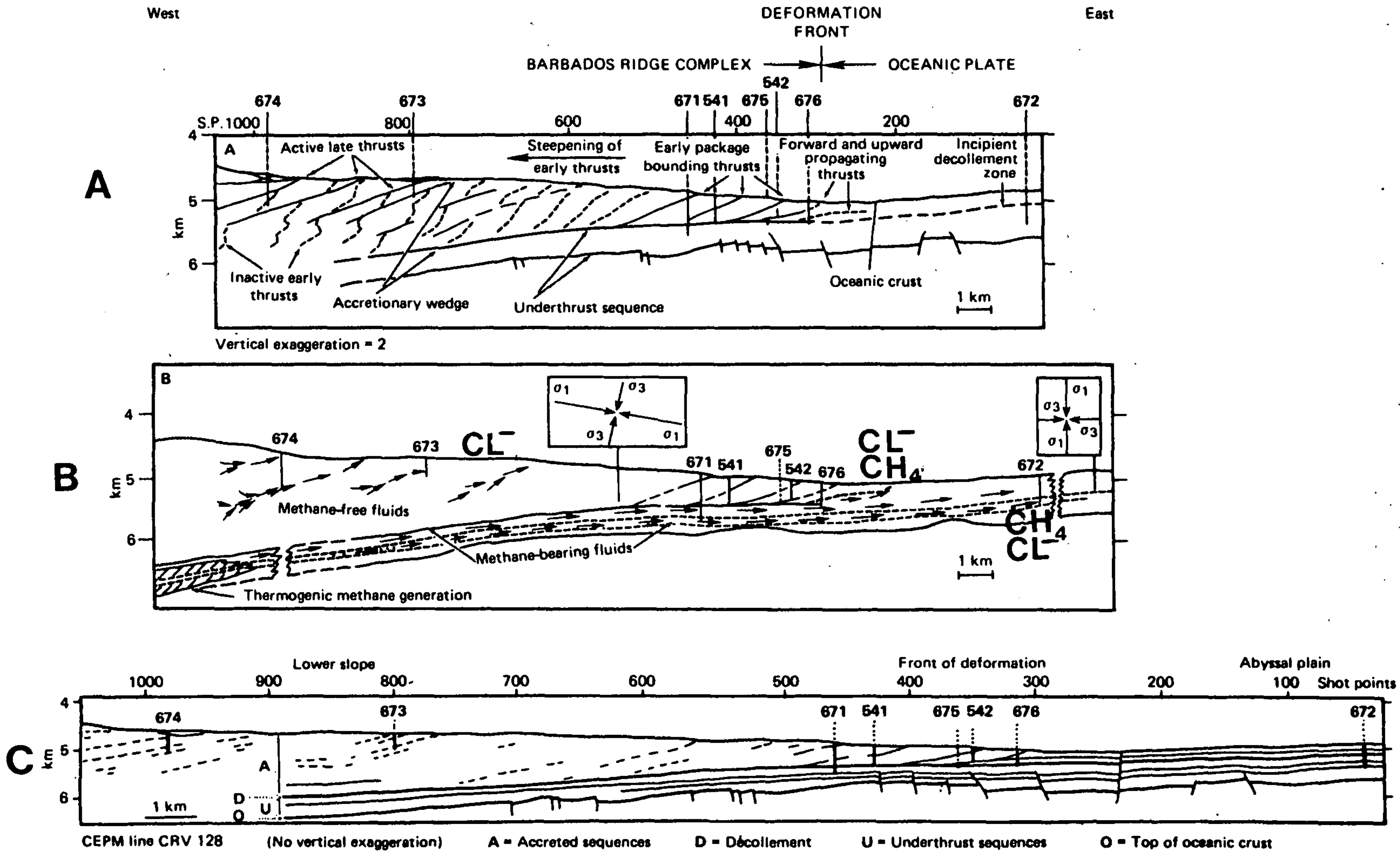
West
DEFORMATION FRONT
East
BARBADOS RIDGE COMPLEX
OCEANIC PLATE
A
S.P. 1000
800
600
400
200
674
673
671
541
675
542
676
672
Active late thrusts
Steepening of early thrusts
Early package bounding thrusts
Forward and upward propagating thrusts
Incipient decollement zone
Inactive early thrusts
Accretionary wedge
Underthrust sequence
Oceanic crust
1 km
km
Vertical exaggeration = 2
B
CL⁻
CL⁻ CH₄
CH₄ CL⁻
σ1
σ3
Methane-free fluids
Methane-bearing fluids
Thermogenic methane generation
C
Lower slope
Front of deformation
Abyssal plain
Shot points
1000
900
800
700
600
500
400
300
200
100
A
D
U
O
CEPM line CRV 128
(No vertical exaggeration)
A = Accreted sequences
D = Décollement
U = Underthrust sequences
O = Top of oceanic crust

(Moore & Mascle et al., 1987, in press.) show that thermogenic methane generated in the hotter deeper parts of the complex is expeled along the basal decollement and continues out into the undeformed sediment pile along the proto-decollement horizon (Fig. 1.17B). Thus, the basal decollement horizon appears to be predetermined by fluid migration paths. The fluids are expeled despite the low permeability of the section. In order to be present in the sediments in front of the complex the laterally expeled fluids must migrate at a velocity faster than the advance of the accretionary front. The rate of advancement is not known with any accuracy but is most probably in the order of a few cm-a-year, corresponding to a plate convergence rate of 2 cm a year. This would seem to indicate the presence of some sort of horizontal fracture permeability within the argillaceous section. Such fluid filled fractures would make an ideal locus for later shearing and basal decollement development.

Further westwards and to the North of latitude 16° 20' N the structural grain increases in wavelength to approximately 2 km, reflecting an increase in the thickness of section offscraped in the frontal imbricates (Appendix A). The wavelengths of structures vary only a small amount on either side of the basement ridges. Apparently, there are only slight variations in the thickness of the frontally accreted layer either side of the ridges in this northern area. The ridges, however, do cause variations in the strike of the structural grain of the complex. The Barracuda Ridge impinges on the accretionary complex at latitude 17° N and

FIGURE 1.18- GLORIA sonograph of part the frontal areas of the accretionary complex to the north of the Tiburon Rise. Basement features such as ridges, steps and hummocks cause, discontinuites to be imposed on the structure of the complex.

results in the imposition of a major discontinuity on the complex (Appendix A). The discontinuity is mostly inactive west of the Zone of Initial Accretion. Other smaller basement features are associated with similar smaller discontinuities (Fig. 1.18). The trend of the deformation front and resulting structures progressively swing to NW-SE orientation, becoming more oblique to the convergence direction as the Puerto Rico Trench is approached.

1.6 <u>THE ACCRETIONARY COMPLEX EXPOSED ON THE ISLAND OF BARBADOS</u>

1.6.1 <u>General Geology Of The Island</u>

The rocks exposed on the Island of Barbados (Fig. 1.19) are divisible into three lithostructural units (Speed and Larue 1982, Speed 1983, Larue and Speed 1984) namely: A) The Basal Complex consisting of material offscraped from the Atlantic Crust. B) The Oceanic Series, interpreted to be forearc basin sediments. C) The Pleistocene reef cap that mantles most of the island.

A) The Basal Complex

The Basal complex is constructed from a series of imbricated and folded thrust packets, composed of turbidites and radiolarite hemipelagic rocks, and possible diapiric melanges (Speed and Larue 1982, Speed 1983, Larue and Speed 1984, Torrini et al. 1985). The turbidites are thought to have been derived from the S. American Continent (Baldwin et al. 1985). It is not clear that they were axial trench fill results in the imposition of a major discontinuity on the complex (Appendix A). The discontinuity is mostly inactive west of the Zone of Initial Accretion. Other smaller basement features are associated with similar smaller discontinuities (Fig. 1.18). The trend of the deformation front and resulting structures progressively swing to NW-SE orientation, becoming more oblique to the convergence direction as the Puerto Rico Trench is approached.

1.6 THE ACCRETIONARY COMPLEX EXPOSED ON THE ISLAND OF BARBADOS

1.6.1 General Geology Of The Island

The rocks exposed on the Island of Barbados (Fig. 1.19) are divisible into three lithostructural units (Speed and Larue 1982, Speed 1983, Larue and Speed 1984) namely: A) The Basal Complex consisting of material offscraped from the Atlantic Crust. B) The Oceanic Series, interpreted to be forearc basin sediments. C) The Pleistocene reef cap that mantles most of the island.

A) The Basal Complex

The Basal complex is constructed from a series of imbricated and folded thrust packets, composed of turbidites and radiolarite hemipelagic rocks, and possible diapiric melanges (Speed and Larue 1982, Speed 1983, Larue and Speed 1984, Torrini et al. 1985). The turbidites are thought to have been derived from the S. American Continent (Baldwin et al. 1985). It is not clear that they were axial trench fill

FIGURE 1.19- Map of the island of Barbados showing the distribution of the three main units on the island namely; the Basal Complex, Oceanic Nappes and Pleistocene reef cap.

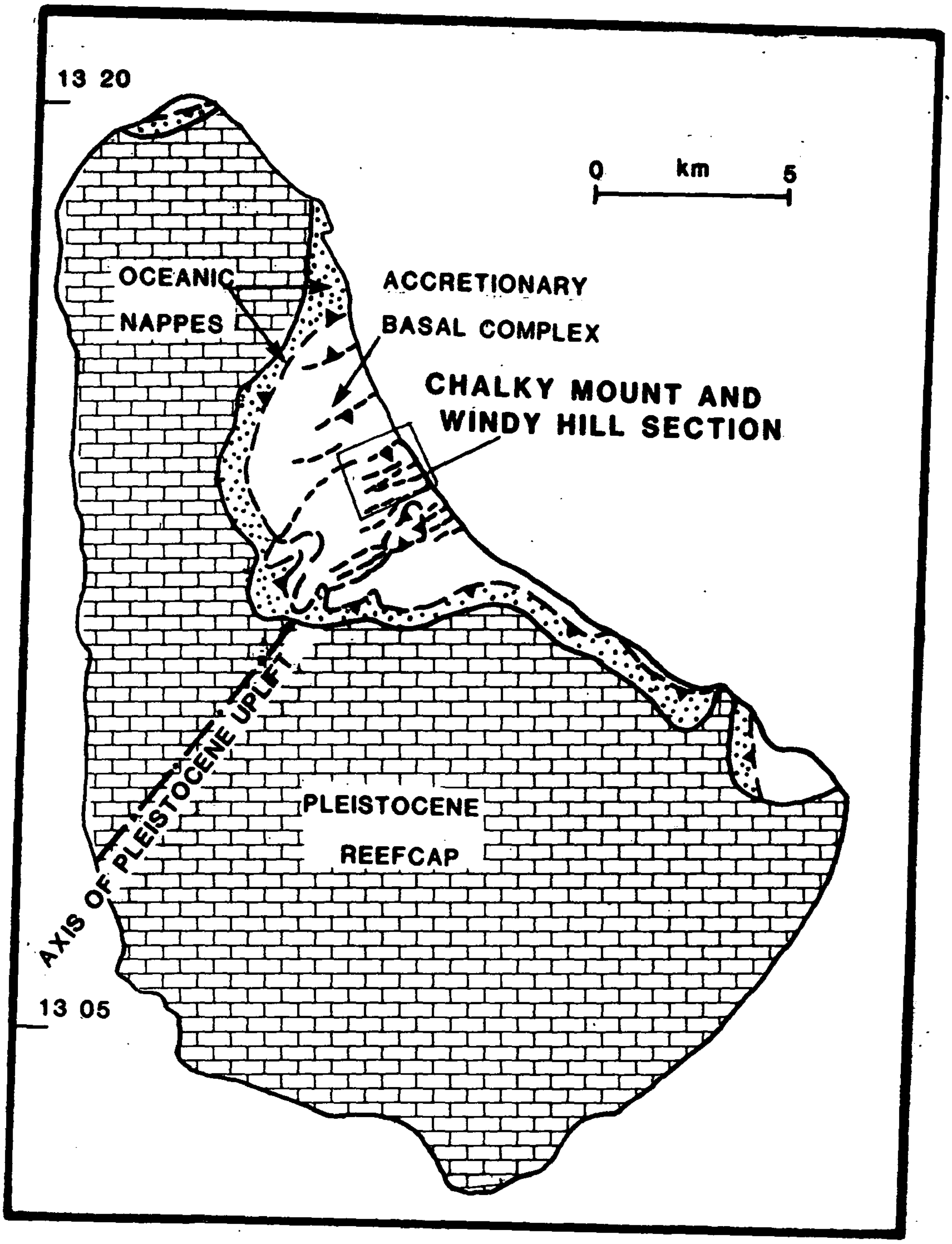

13 20
0 km 5
OCEANIC
NAPPES
ACCRETIONARY
BASAL COMPLEX
CHALKY MOUNT AND
WINDY HILL SECTION
AXIS OF PLEISTOCENE UPLIFT
PLEISTOCENE
REEFCAP
13 05

deposits, as parts of the section appear to have originated in a radial fan system with dominant north to east directions of transport relative to the present coordinates (Larue & Speed 1983). Larue and Speed concluded that either they were deposits off the northern margin of a S. American passive continental margin that were later displaced northwards and incorporated into the complex or the trench system in which they were deposited had a topographically irregular course which promoted the formation of local depositional lobes. Recent petrographic studies by Kasper & Larue indicate that the deep sea fans were probably deposited north of the Araya peninsula, S. America, during and shortly after the late middle Eocene. The turbidites occur as massive units and in interbedded sequences with mudstones and facies associations indicating Upper, Middle and Lower fan depositional environments (Speed 1983, Larue and Speed 1983, Larue and Speed 1984). Sparse palynomorph dates indicate that the turbidites are of Paleocene to Eocene age (Larue and Speed 1984).

The hemipelagics are composed of siliceous muds and oozes, noncalcareous muds and minor, but conspicuous, quartz sand. The hemipelagics were deposited in the early and middle Eocene. The hemipelagics either represent abyssal plane deposits tectonically juxtaposed with the turbidites or, represent lulls in turbidite deposition during which they covered the fan deposits (Speed 1983, Larue and Speed 1984).

The melanges were originally called the Joes River Formation (Senn 1940). Larue and Speed (1984), describe the *melange as being composed of blocks of mudstone and sandstone in a foliated mudstone matrix and a layered breccia of scattered poorly to well orientated blocks of sandstone, radiolarite, and calcareous pelagic rocks. A rough lower Eocene to Paleocene age has been derived for the matrix from pollen studies. Either the younger blocks in the matrix were diapirically stoped, or reworking of the pollen occurred.*

B) The Oceanic Series

The Oceanic Series are from middle Eocene to middle Miocene in age and are composed of pelagic chalks, volcanogenic beds and radiolarian mudstones. Some volcanogenic beds have indications of a turbiditic origin, others are interpreted to be air fall deposits (Torrini et al. 1985). Deposition of the Oceanic Series occurred synchronously with parts of the Basal Complex. Their totally different facies characteristics, and the existence of a thrust contact between them and the basal Complex, led Speed and Larue (1982) to propose that the Oceanic Formation was composed of forearc basin sediments that were thrust eastwards over the top of the accreted turbidites. The Paleogene-lower Miocene Oceanic strata were deposited at depths between 2-4.8 km whilst, the middle Miocene Oceanic beds accumulated at Shallower depths (1-1.5 km), suggesting that the inception of the thrusting was of late Eocene age Torrini et al. (1985). There is a certain amount of imbrication of the lower parts of the Oceanics with biostratigraphic inversions being recorded at Bath (Torrini et al. 1985). There is however, little evidence of large *scale imbrication of the Basal Complex and Oceanic Series and so either the thrust contact remained localised on their boundary for a considerable distance, or movement on it was fairly limited.*

Pleistocene Reef Cap

The raised reef terraces form a SW. trending arch that results from uplift and emergence of the island since 0.7 my. ago. Taking individual reef tracts as isochronous, the axis of maximum differential uplift trends in a SW-NE direction across the island (Bender et al. 1979). The Joes River melanges, around the Bissex Hill nappe area (Torrini et al. 1985), lie on this axis and it is conceivable that diapirism was responsible for the doming.

1.6.2 Accretionary Tectonics As Revealed In The Basal Complex

Detailed geological mapping of the basal complex by Speed (1983), Larue and Speed (1984) and Torrini et al. (1985) gives a good idea of the general form of its structural development. The following questions need to be asked;

A) Is the section revealed in the Basal Complex subcreted or frontally accreted, and what was the probable thickness of the original sedimentary section before imbrication ?

B) The pelagic section that should lie beneath the turbidites and hemipelagics is missing, why is this so?

C) What was the state of consolidation of the sediments during their initial deformation phases and what effect has this had on the style of deformation?

D) What is revealed about the behaviour of the diapiric melanges.

E) Can the recently accreted sections of the Barbados Ridge Complex be used as a modern analogue that explains the anomqlous east-west strike of the structures, the presence of strike parallel, sub-vertical sinistral strike slip faults and the fan-like depositional pattern of the turbidites in the basal complex of Barbados?

A) Frontal Accretion Or Subcretion?

A number of general features can be used to assesss the relative likelihood of formation of this sequence by frontal accretion or subcretion. Clay mineralogy and vitrinite reflectance studies were used, along with other independant indicators, by Larue et al. (1985) to obtain maximum burial depths for the Basal complex. It was found that the maximum temperature attained during diagenesis was below 80°C. Using a geothermal gradient of 15°C (which may be a little high) and a sediment-water interface temperature of 10°C, they estimated that maximum burial depths of the Basal Complex were between 2-5 km, with a possible minimum burial depth of below 1km. A position, such as this, near the surface of the complex favours frontal accretion.

The intensity of the deformation affecting the frontally accreted sections in the offshore regions of the Barbados Ridge Complex depends largely on the thickness of the accreted section (see Section 1.4 this Chapter). The thinner the accreted section the more intense the deformation it *suffers. As will be seen below, the deformation history of the basal complex is complicated and would seem to correspond to a fairly thin accreted section. The maximum observed thickness of sediments in any individual packet in the Basal Complex is in the order of 250-300m (the packet includes the massive sandstones of Chalky Mount (Speed 1983)), implying that the paleo-thrust spacing may have been in the order of 750-900m.*

B) The Missing Pelagic Section

No pelagics or spilites, corresponding to the abyssal plain or upper parts of the oceanic crust, have been identified in the basal complex on Barbados. Unless the turbidites were deposited directly on to igneous oceanic crust and then cleanly offscraped, a missing pelagic section has to be accounted for. At present the pelagic section sitting on the subducting oceanic crust is about 1-1.5km thick (see Section 1.3, this Chapter).

In short either the pelagics were subducted with the oceanic crust, or they were subcreted at much greater depths and lie at present deep within the complex beneath Barbados. If they are there, they must be at depths exceeding 4.5km (borehole data, Baadsgaard 1960).

B) Effect Of State Of Consolidation On Deformation Style

The Windy Hill area is a particularly well exposed section through a series of imbricated packets of turbiditic sediments (see Figs. 1.19 & 1.20 for location). Sections 1 & 2 (Fig. 1.21) run through Chalky Mount and Windy Hill. Section 2 (Fig. 1.22) is a detailed representation of the structures in Windy Hill itself. The rather complex looking structure of Windy Hill can be divided into a series of packets (A-G), separated by major fault zones (Fig. 1.21).

Packet A consists of a broken formation derived from disrupted sandstones and shales and has Thrust 1 as its basal contact. The blocks often contain tight to isoclinal folds with thickened hinges (Plate 1.1) and lie in a variably sheared scaly clay matrix. Folding of the more coherent sequence of Packet B below has deformed Thrust 1 and affected the orientation of structures near the base of Packet A but has little or no effect on them in the higher regions. Hinges of the minor disrupted folds in the broken formation have orientations that lie between $280^\circ/20^\circ$ and $238^\circ/10^\circ$ (Fig. 1.23). The vergence of these minor folds indicates that movement of Packet A was to the north or northwest. Thrust 1 ramps up through the Packet B sequence at the southern end of the section (Section 2, Figs. 1.21 & 1.22) and deforms the footwall sequence (see below).

Packet B contains a fairly coherent sequence of interbedded turbiditic sandstones and muds which are folded into a series of fairly large wavelength folds (in the order of 40-60m). The most southern of these, is a ramp anticline that sits on Thrust 2. Axial planes of these folds are generally inclined towards the south at moderate angles and have strikes that vary between the southeast and east. The

FIGURE 1.20- A geological map of the Chalky Mount Windy Hill Area adapted from Speed (1983). The major sinistral fold pair plunge at approximately 50-60 degrees to the north and are also proposed to relate to sinistral shearing along the Chalky Mount Fault Zone along with the second folds.

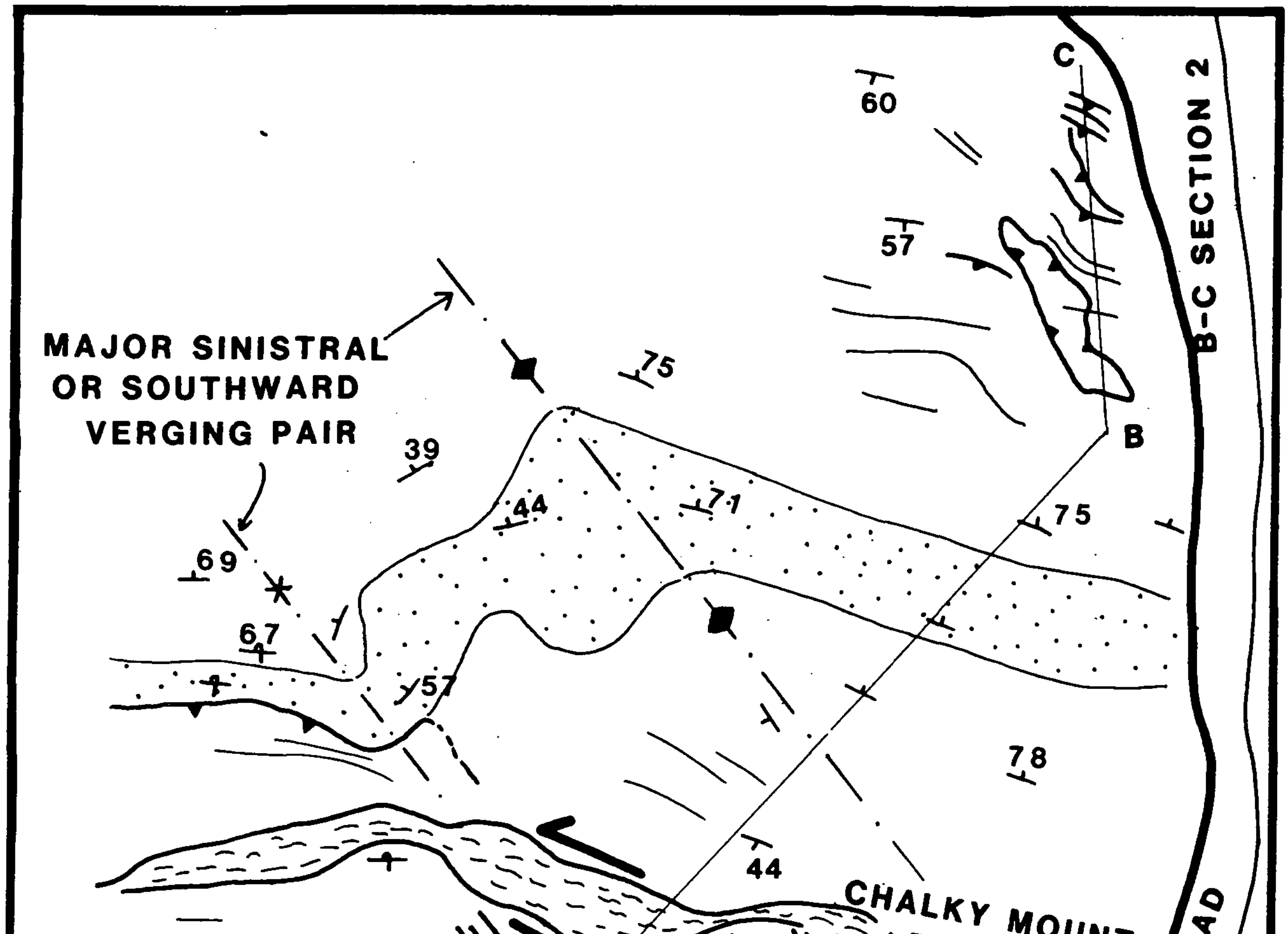
MAJOR SINISTRAL OR SOUTHWARD VERGING PAIR
CHALKY MOUNT FAULT ZONE
B-C SECTION 2
A-C SECTION 1
COSTAL ROAD
JOES RIVER MELANGE
A
B
C
N
1st FOLDS
2nd FOLDS
500M
60
57
75
39
44
71
75
69
67
57
78
44
36
57
55
78
45

FIGURE 1.21- Sections across the Chalky Mount (Section 1 A-B) and Windy Hill (Section 2, B-C) (see Fig. 1.20 for location). Section 2 is represented in greater detail in Fig. 1.22.

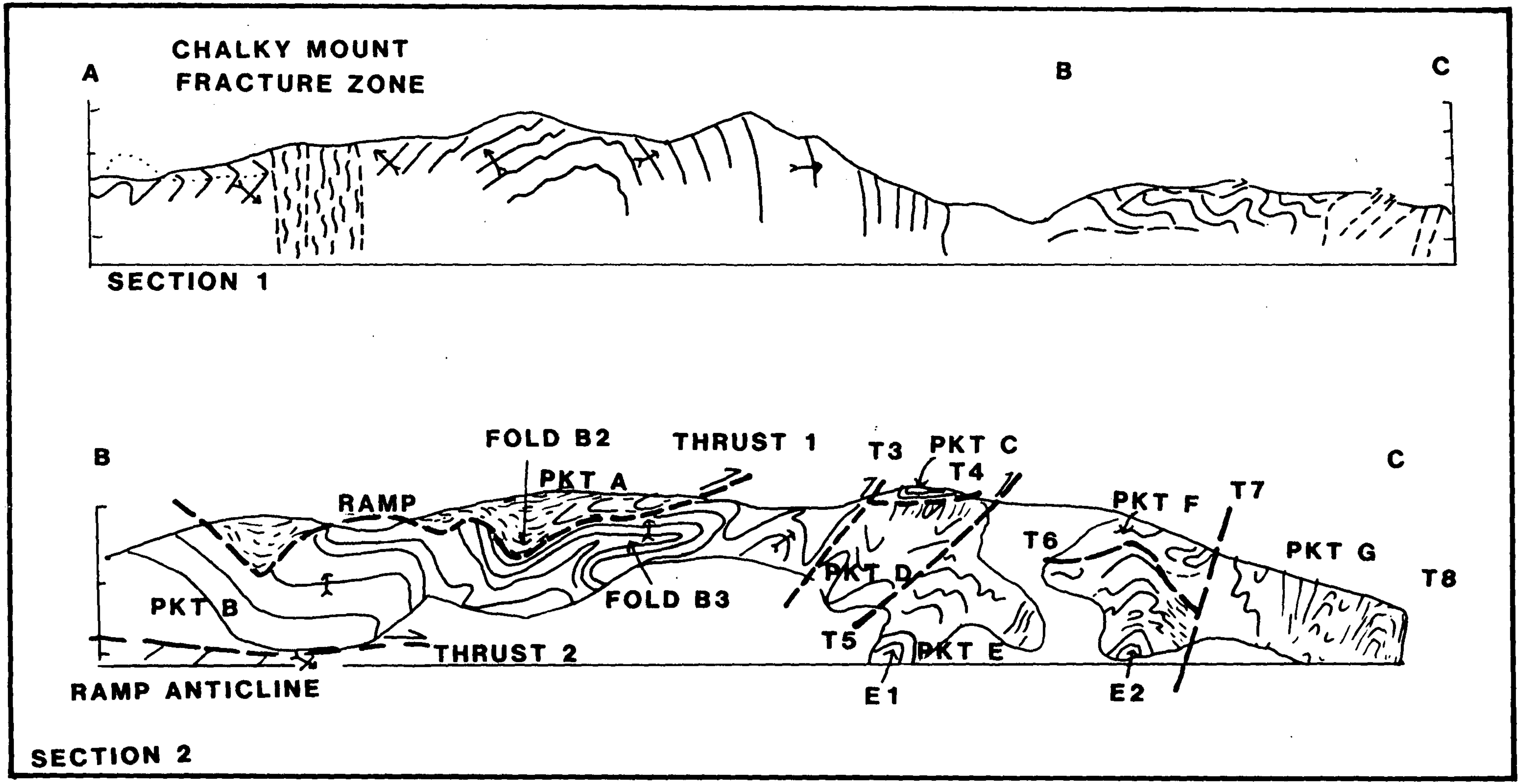
CHALKY MOUNT
FRACTURE ZONE
A
B
C
SECTION 1
B
C
FOLD B2
THRUST 1
T3
PKT C
T4
PKT A
RAMP
PKT F
T7
T6
PKT G
T8
PKT D
PKT B
FOLD B3
T5
PKT E
THRUST 2
RAMP ANTICLINE
E1
E2
SECTION 2

FIGURE 1.22- Detailed cross section (Section 2) through Windy Hill see Fig. 1.20 for location). The positions of Plates 1.1-1.5 are marked.

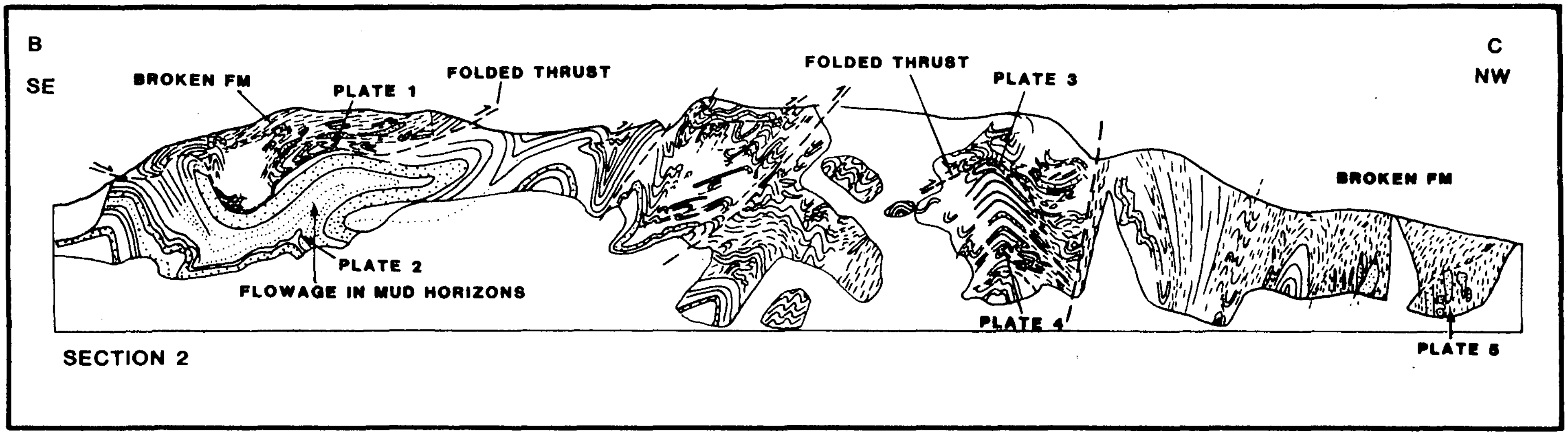

B
SE
BROKEN FM
PLATE 1
FOLDED THRUST
FOLDED THRUST
PLATE 3
C
NW
BROKEN FM
PLATE 2
FLOWAGE IN MUD HORIZONS
PLATE 4
PLATE 5
SECTION 2

FIGURE 1.23- Equal area stereogram illustrating the distributions of hinges of minor folds in the broken formations associated with the major low angle thrust zones a the later more upright fold round which they are folded coaxially.

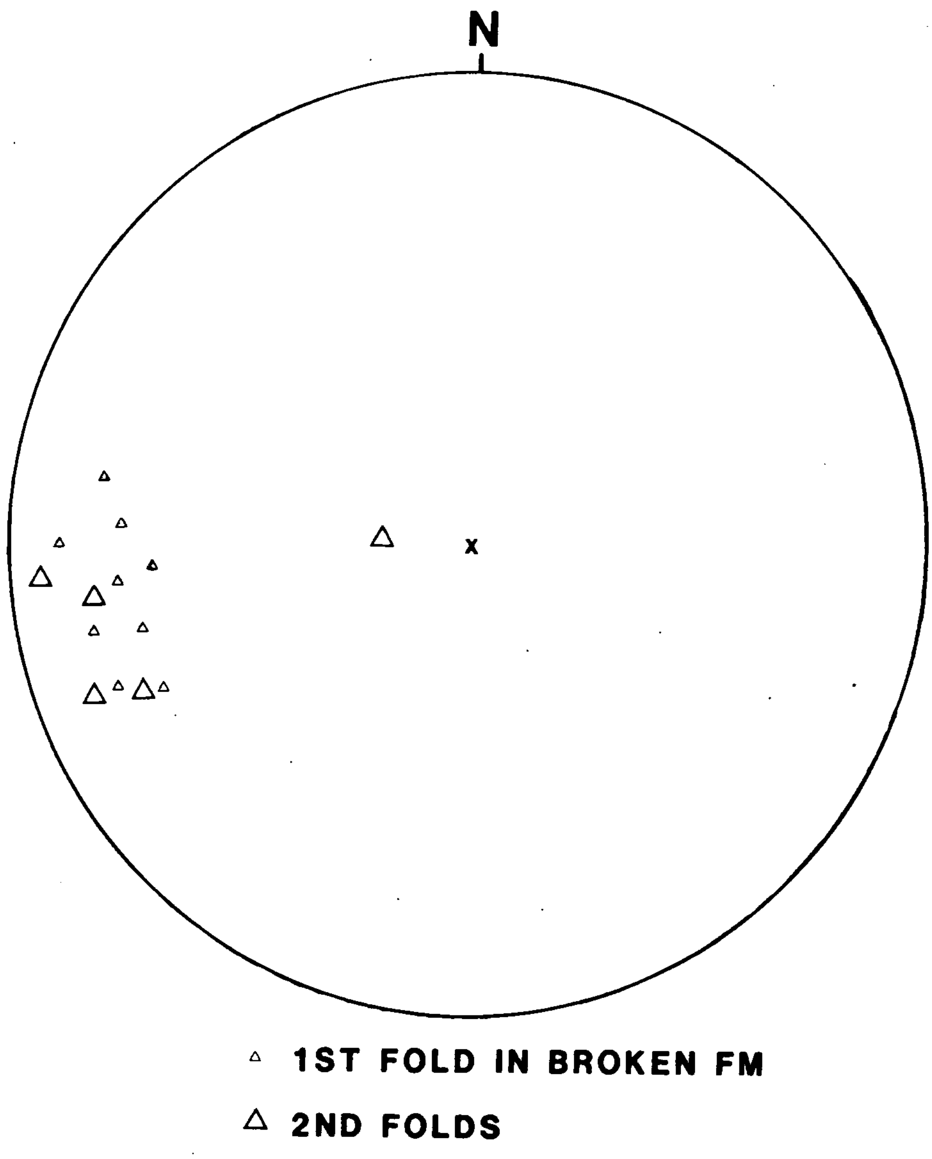
N
1ST FOLD IN BROKEN FM
2ND FOLDS

PLATE 1.1- Isoclinal fold in the broken formation of Packet A. The limbs are sheared out and the tightness of folding is accomodated by flowage of the muds that are interbedded with the sandstones. Some thickneing of the sandstones in the hinge regions also occurs. (North to the right, hammer for scale, see Fig. 1.28 for location)

PLATE 1.2- A part of the disharmonic anticline (B3) in which a large ammount of flowage of the muds has occured. A scaly clay fabric is developed in places in the muds. (see Fig. 1.28 for location)

folds are highly disharmonic, with the anticlines increasing in amplitude dramatically up through the section (i.e. Anticline B3, Section 2, Fig. 1.22). Their disharmonic nature is accommodated by considerable viscous flowage of the muds, in which scaly clay fabrics are not usually developed, and which consequently must have been very unconsolidated (Plate 1.2). The folds increase in amplitude up towards Thrust 1 and its proposed that they originated on the "ductile collapse" of the ramps footwall suffering drag beneath a major overthrust, of which the broken formation of Packet A only represents the disrupted basal portions (Fig. 1.24). Thrust 2 (Fig. 1.21) is proposed by Speed (1983) to only have a minor displacement on it. However, poor exposure prohibits any real evaluation of the size of the displacement on the structure and it could be quite large.

West of Packets A & B lie a series of minor Packets (C-G) seperated by a series of low and high angled thrusts (Fig. 1.21 & 1.22). Three general features predominate;

a) The low angled thrusts (Thrusts T4-T6) lie roughly subparallel to bedding and are associated with tight to isoclinal subrecumbant folds and broken formations. Some folds have a soft sediment look to them with flowage of the mud in the hinges, again suggesting that the section was not well consolidated during this phase of deformation.

b) Both the low angled thrusts and folds are refolded around more upright open folds (Folds D1, E1 & E2 Fig. 1.21, Plates 1.3 & 1.4, Fig. 22).

c) The later upright structures flatten against late steep faults Faults T3, T5 & T7) that cut across the earlier thrust

FIGURE 1.24- The sequential development of structures in part of Windy Hill illustrating how the 'ductile' collapse of the ramp and subsequent formation of the drag folds beneath Thrust 1 is proposed to have occurred.

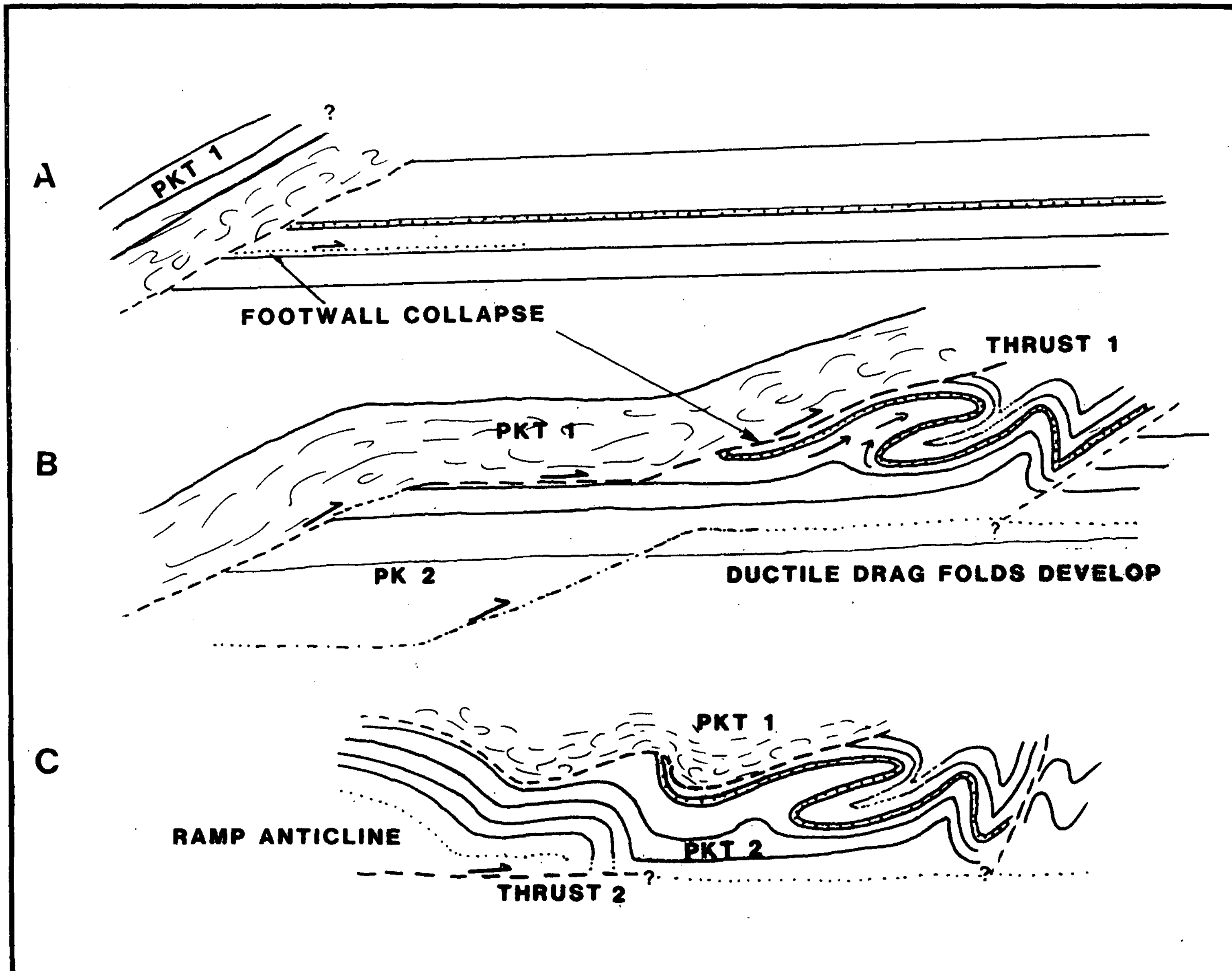
A
PKT 1
?
FOOTWALL COLLAPSE
B
THRUST 1
PKT 1
PK 2
?
DUCTILE DRAG FOLDS DEVELOP
C
PKT 1
RAMP ANTICLINE
PKT 2
?
THRUST 2
?

PLATE 1.3- Refolded syncline. (North is to the right, see Fig. 1.28 for location)

PLATE 1.4- Coaxially refolding of a north verging early fold pair. (North is to the right, rucksack of the left for scale, see Fig. 1.28 for location)

PLATE 1.5- Part of the broken formation at the northern end of Section 2. (North is to the right, field of view approx. 5m, see Fig. 1.28 for location)

systems. At least some of these late structures have demonstrable north verging reverse movements on them. The broken formation of Packet G, at the northern end of the cross section, becomes steadily more disrupted northwards and is probably the southern margin of a very large steep fault zone (T8). In the less disrupted areas, north verging isoclinal fold pairs can still be made out.

The early subrecumbant folds in the broken Fm. have been coaxially refolded around the later more upright folds, suggesting that they may have formed at different times during the same overall deformation phase (Speed 1983) (Fig. 1.23). Both sets of folds exhibit features that indicate that they formed in unconsolidated sediments and are most likely to be examples of primary frontal accretion structures. The distinctive disharmonic fold structures that are developed in Packet B related to the ductile collapse of the ramp and drag beneath Thrust 1. Their 'ductile form' originates as a consequence of the ability of the unconsolidated muds to undergo viscous flow.

It is not immediately clear why the steep faults should cut the earlier low angled thrusts. Most models of frontal accretion predict that early thrusts should back rotate and then potentially be cut by low angled out-of-sequence thrusts rather than be dissected by steep structures (see Introduction). A possible model that does explain these features and the general development of Barbados is proposed below (see section E).

D) Origin And Emplacement Of Joes River And Associated Diapiric Melanges

The Joes River melange in the Bissex Hill area of Barbados (Larue & Speed 1984) consists of massive, sandy pebbly mudstone containing blocks of sandstone and turbiditic sequences, or massive green muds containing asphaltic sandstones and pebble breccias, and blocks of radiolarite interbedded with quartz sandstone and mudstone up to 100m in length. The matrix of melanges is of variable composition. Some parts have a muddy sand for a matrix others have an argillaceous matrix in which a pervasive scaly clay fabric is developed, reflecting folding and bulk flattening in response to N-S or NW-SE compression. The melange laps northwards over the southern portions of the Bissex Hill nappe and cuts through parts of the sequence (Larue & Speed 1984). Its emplacement therefore continued at least partly after early Miocene times when the forearc strata were thrust eastwards over the complex. In the Bath area of Barbados the diapiric melanges are also interpreted to have cut the oceanic nappes (Torrini et al. 1985). Diapiric activity therefore occurred in the complex under radically different stress conditions. The axis of antiformal uplift of the Pleistocene reefs runs through the melanges and may indicate that movement at depth may have continued episodically during their deposition i.e that diapiric activity may have been active in the island of Barbados over a period of 10-15 my or since the late middle Miocene.

Larue & Speed (1984) interpret the genesis of the melanges as being gravity flow or olistrostromal deposits that have be reactivated diapirically after accretion. However, as will be discussed in Chapters 3 & 4 such mixing of lithologies can be produced during the diapiric phase alone, without recourse to an earlier phase of disruption.

E) Origin Of Basal Complex on the Island of Barbados

The basic early accretionary story of the Basal Complex has been discussed above. However, it is not clear in exactly what environment or geometry of accretionary complex it originated. The present major packet bounding faults and early accretionary structures strike, E-W to SE-NW, approximately at right angles to the majority of structures in the Neogene to recent regions of the accretionary complex (Appendix A). Furthermore, the direction of early overthrusting on the majority of the packet bounding thrusts is to the north or northwest, in contrast to the current eastward overthrusting along much of the frontal area of the complex. Late rigid rotation of Barbados has been proposed as a possible solution (Speed 1982), but no real proof has been put forward. The proposals of large scale rearrangements of the arc configuration (Speed 1985) also appear to conflict with the current observation of a geometrically simple configuration for all, but the southern most part lateral trailing edge of the Lesser Antilles Arc System. This is currently undergoing oblique collision with the South American continental margin (Speed 1985).

Another possible explanation for the origin of Barbados is that it represents a portion of the complex that was accreted along an approximately east-west striking margin, such as the big bend at latitude 15°N. The exposures in Barbados could fit into the oblique striking domain many times over.

1.7 *SUMMARY AND CONCLUSIONS*

A considerable amount of data from the Barbados accretionary complex have been condensed into the form of a single structural map. A number of major aspects of the structure are apparent from the map and on shore data of which the following are the most significant:

1) As a result of variations in the stresses within the complex there is an east-west change in the dominant direction of vergence of currently active structures across the southern areas of the complex. Thrust vergence changes from being to the east at the outer deformation front, to being both to the east and west in central regions of the complex and then finally to the west in the western regions of the complex. Through the development of the complex a body of material may move from one region to another over a period of time.

2) As a result of the interaction of the fracture zones and the pattern of sedimentation, the complex undergoes marked *north to south changes in strike, type of sediment accreted and style of structures developed at its front. In particular a series of E-W to NW-SE trending discontinuities are imposed on the complex. The effects of the ridges are two fold, by damming the northerly flowing turbidites they cause abrupt changes in the type and thickness of sediments being accreted to the complex. The initial sedimentary thickness controls the intensity and spacing of both the initial frontal thrusts and the later through wedge out-of sequence structures (see below). The nature of the accreted section also determines whether such processes as mud diapirism will operate in the complex (see Chapter 2).*

3) The thickness of the accreted sedimentary section controls the spacing of the initial frontal thrusts and the later out-of-of sequence structures. The thinner the section, the narrower the spacing of the frontal thrusts and out-of sequence structures will be. The onset of out-of–sequence faulting also occurs nearer the accretionary front.

4) Mud diapirism only occurs, and in great abundance, in the regions of the complex south of the Tiburon Rise, where rapidly sedimented terrigenous sediments have been accreted.

5) There are a number of slumps developed in different parts of the complex. In the south they are associated with the failure of the steep slopes of the folds associated with the frontal thrusts and with the oversteepening of the margins of the slope basins. In the north slumps have tended to occur in areas affected by the impinging ridges, where discernible, *thicknesses of slumps are less than a few hundreds of metres.*

6) The basal complex on the Island of Barbados most probably corresponds to a thin frontally accreted section that was only partly consolidated during the early phases of it deformation.

CHAPTER TWO

MUD DIAPIRISM AND SUBCRETION IN THE BARBADOS RIDGE ACCRETIONARY COMPLEX: THE ROLE OF FLUIDS IN ACCRETIONARY PROCESSES

2.1 INTRODUCTION

The widespread occurrence of mud volcanoes in the Barbados Ridge complex was first reported by Stride et al. (1982), who detected them using long-range side scan sonar. Examples of mud volcanoes and diapirs imaged by Seabeam bathymetry and multichannel seismic reflection were also given by Biju-Duval et al. (1982). In this chapter the range in the form of occurrence of the mud diapirs and their relationship to the structural and sedimentary processes active in the Barbados Ridge Complex is examined. The mud diapirs are important in themselves but can also be used to indirectly study the effects of overpressuring on accretionary processes. The principal types of data analysed in the study have been sonographs from GLORIA long-range side scan sonar, multichannel seismic reflection sections, and Seabeam bathymetry.

High pore fluid pressures in accretionary complexes are generally attributed to low permeabilities that inhibit the progressive compaction of the accreted sediments by the stresses developed during the building the wedge. This results in a major part of the overburden and tectonic stresses being transmitted to the pore fluids which become overpressured as a result. The existence of high-pore fluid *pressures in accretionary complexes associated with subduction zones is indicated by several lines of evidence:*

A) Analysis of the wedge shape of an accretionary complex in terms of its overall rheology and stresses acting upon it (see Introduction), lead to the conclusion that the stresses applied to its base are very low. The most likely cause of low shear stresses is the reduction of the normal stresses on fault surfaces by water pressure (Chapple, 1978; Park, 1981; Westbrook et al., 1982; Davis at al., 1983). The predicted water pressures are generally in excess of 70% of the lithostatic load and for many accretionary complexes they are generally greater than 90% of the lithostatic load (Davis et al., 1983).

B) High pore fluid pressures have been identified in such studies as Leg 78A of the Deep Sea Drilling Project, in which pore fluid pressures very close to lithostatic were inferred in hole 541 near the base of the Barbados Ridge Complex as a result of an inadverted packer experiment (Moore et al., 1982). Similarly high pressures were inferred in the accretionary wedge offshore from Guatemala during DSDP Leg 84 (von Huene 1985).

C) A study of the porosity and velocity data like that undertaken in the accretionary complex of the Nankai Trough by Bray and Karig (1978), indicates that 10km from the front of the wedge there is a 5% reduction in porosity at a depth of of 1km.

D) Other features that have been attributed to high porefluid pressures are mud volcanoes and mud diapirs which are known to occur in accretionary complexes far back from the accretionary front in the Aleutians (von Huene, 1972), Oregon (Snavely et al., 1977), Washington (Rau and Grocock, 1974) and British Colombia (Shouldice, 1971). The outflow of water, attributed to overpressuring and compaction at depth, causes features such as the warm water vents recently discovered off Oregon (Kulm et al., 1986).

The layer of sediments thrust beneath the leading part of an accretionary complex below the basal decollement, is proposed to also become subject to overpressuring. This is principally the consequence of increased overburden pressures arising from the thickening wedge above it. The lateral pressure gradient that is produced by this drives fluids out towards the front of the accretionary complex and beyond, producing mud volcanism. This phemomenon has been observed off the Barbados Ridge complex (Westbrook and Smith, 1983), Sumba, Indonesia (Breen et al., 1986) and Oregon (Kulm et al., 1986). The unfractured sediments in the layer beneath the complex's basal decollement may also not compact as readily as those in the wedge as they should have less of a fracture permeability.

Concepts of processes of underplating or subcretion by which material is added to the base of an accretionary complex have been prevalent for several years (Shipley et al., 1979; Westbrook and Smith 1983, Silver et al., 1985). Silver et al. (1985) show evidence of underplating, or *subcretion, by duplex formation during the footwall collapse of a ramp linking the basal decollement between two different stratigraphic horizons. Successive duplex structures transfer material into the complex, from the layer beneath, as the decollement steps down. (That part of an accretionary complex that has been formed in this way will be referred to as the subcreted section). It is proposed that the disruption of the subcreated sediments during the subcretion process is thought to release more fluids into the accretionary complex with possible consequent effects on fluid pressure and mud diapirism.*

Mud diapirism in the Barbados accretionary complex is associated with the accretion of turbidites. Turbidites from the Orinoco flow northwards axially along the accretionary front forming a large fan (Fig. 2.1) (Belderson et al. 1984). The sequence thins northward from a thickness of 7km near the source at latitude 10°N. Only a few individual turbidites are present in the sedimentary section north of the Tiburon Rise at latitude 15°N. The rate of sedimentation in the south is approximately 1km per million years, rapid enough for the section to be very underconsolidated.

The transverse ridges in the oceanic basement pond the turbidites and produce lateral changes in sediment thickness of the order of a few kilometres, affecting the thickness of the accreted section and wavelengths of the initial accretionary structures. The Tiburon Rise forms a significant barrier with little turbidite deposition to the north (Wright, 1984) and forms the northern limit to the

FIGURE 2.1 - Location map of eastern Caribbean showing some of the main elements of the Barbados Ridge Complex. Note: 1) The region of greatest diapir density narrows northwards. 2) The relationship between the distribution of the mud diapirism in the accretionary complex and the area in which Orinoco fan turbidites are being deposited on the subducting plate.

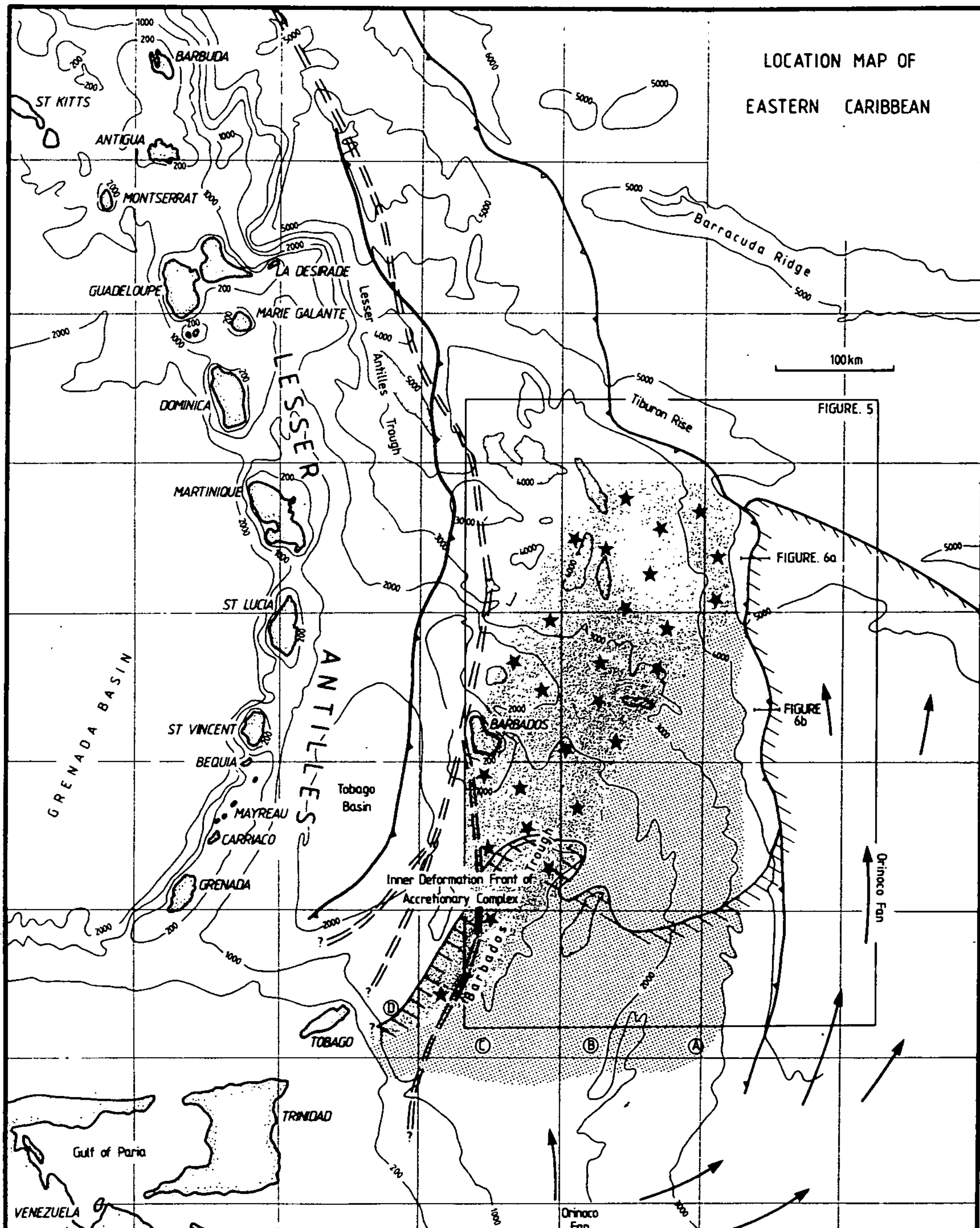

LEGEND

NORTHERN LIMIT OF ORINOCO FAN TURBIDITES

OUTER DEFORMATION FRONT

INNER DEFORMATION FRONT

★ SCATTERED DIAPIRS

ABUNDANT DIAPIRS

occurrences of mud diapirism (Stride et al., 1982) and gas hydrate patches. The ridges have an approximately WNW-ESE orientation and therefore underthrust the complex obliquely putting the complex into more compression on their southern side (Westbrook, 1982). The ridges initiate structures that strike transversly across the complex (Fig. 1.2, Appendix A) and locally influence the diapir and gas hydrate distributions. The ridges also destabilize the frontal accretionary slope, causing slumping of accreted material.

2.2 THE SURFACE MANIFESTATION OF MUD DIAPIRISM

Based on their morphology the surface manifestations of mud diapirism in the Barbados Ridge Complex can be split into three groups:

2.2.1 Mud Volcanoes

Figures 2.2 & 2.3 illustrate some of the expressions of structures that are considered to be mud volcanoes that are visible in seismic reflection sections and GLORIA. Mud volcanoes are only sporadically imaged on seismic lines so that it was necessary to predominantly map them using the GLORIA system. In general, the fluid mud spreads out from the conduit to produce circular edifices. The local topography of the sea floor can however channel the mud flows in certain preferred directions, and ovoid to irregular shapes can sometimes be produced. The low viscosity mud rises through a conduit with a much smaller diameter than the edifice, as the mud spreads out widely on the seabed. On the

FIGURE 2.2 - A line drawing (left) through a mud volcano with an interpretation of some of the internal features. To the right is the original uninterpreted reflection section, taken from Biju-Duval et al, (1982). The curvature of the lower parts of the slope sediment section down into the area of the conduit, results from the mud volcano having intruded up through a syncline. The deeper form of the conduit is not clearly visible and may be out of the plane of section. Unbedded material, imaged as chaotic reflectors on the seismic sections, appears to form lense-like bodies in the sediments around the mud volcano. They have been interpreted to represent sill-like intrusions of diapiric material in this figure. Conversely they may be a series of mud flows interbedded with slope sediments. This would imply that the mud volcano has had a prolonged history of activity. (see Fig. 2.8 for position)

Mud Volcano

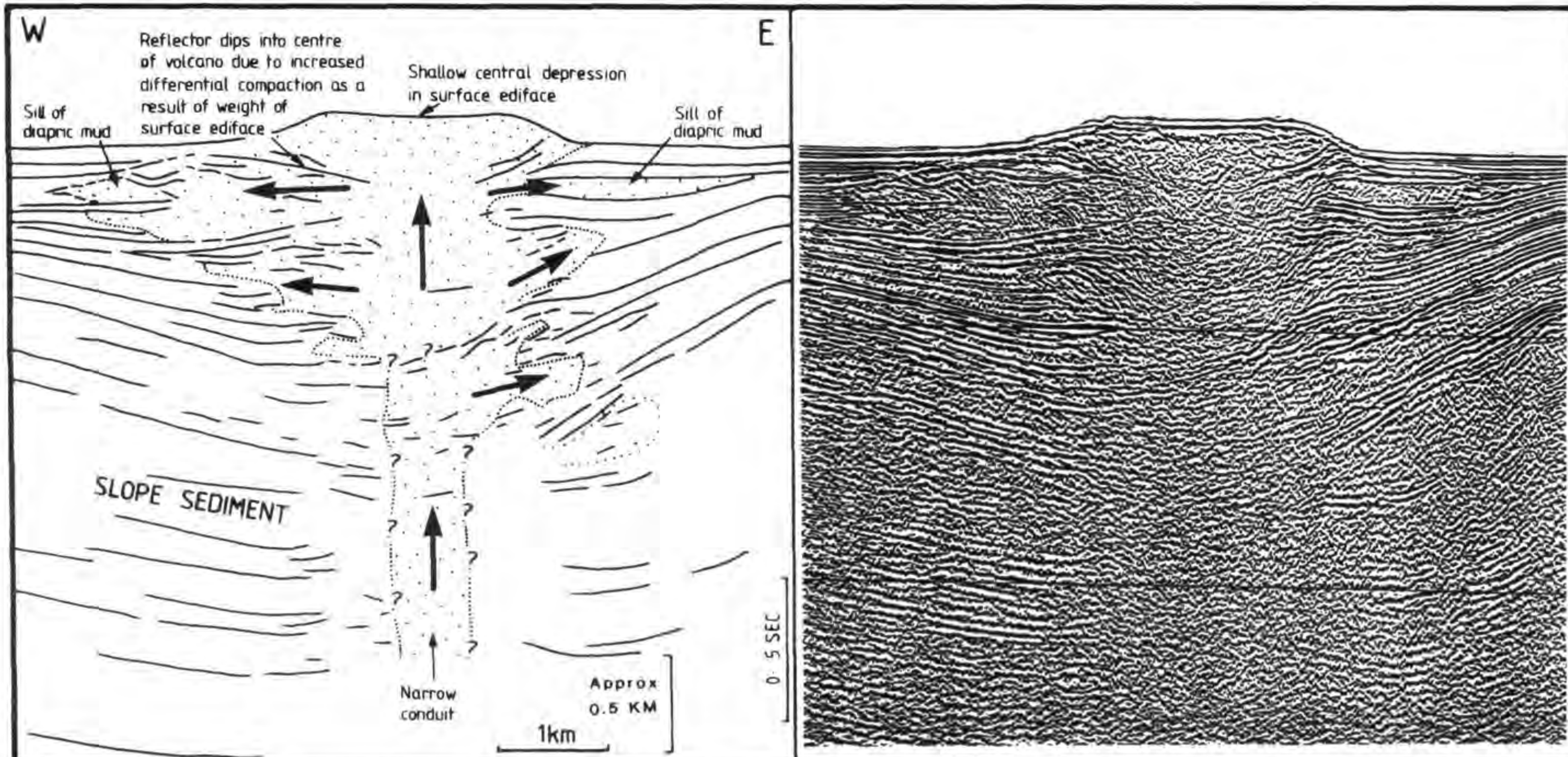
W
E
Reflector dips into centre of volcano due to increased differential compaction as a result of weight of surface ediface
Shallow central depression in surface ediface
Sill of diapric mud
Sill of diapric mud
SLOPE SEDIMENT
Narrow conduit
Approx 0.5 KM
1km
0.5 SEC

FIGURE 2.3 - Gloria sono-graph image of a group of bright sub-circular features that are interpreted to represent mud volcanoes. The mud volcanoes sometimes form linear chains or, if they coalesce, elongate bulbous features. The mud volcanoes in this image appear to intrude along a cross fault that strikes obliquly across the main structural grain. (see Fig. 2.8 for position)

Barbados Ridge Complex the widths of edifices can exceed 6 km, typically they are between 1-3 km. The smallest mud volcano diameter easily resolvable by GLORIA is in the order of 300-500m, so that there may be many smaller unidentified extrusions. Sub-aerial extrusions dewater more rapidly so that maximum edifice diameters are usually less than 1-2 km. Figure 2.2 is a line drawing and seismic section through what is thought to be a fairly typical mud volcano. Diapiric material appears to have intruded as sills into the horizons around the conduit so that the subsurface geometry of the intrusion is complex. Further example of mud volcanoes in the southern most regions of the Barbados Ridge complex are illustrated in Valery et al. (1985), and from regions in front of the complex by Westbrook & Smith (1983).

2.2.2 Mud Ridges

Developed in the interior regions of the complex are long sinuous ridges that appear to relate to material that has been exuded from fault lines. Mud ridges are particularly well developed around the slope basins (Fig. 2.4) extruding from large thrust faults. Individual ridges may be up to 18km long and 1km wide. Snead (1964), describes the occurrence of long ridges of viscous mud that have been exuded like toothpaste from major faults in the Baluchistan area of Pakistan. One ridge is 20 miles long and has slopes of 40-70°. The diapir came up as a continuous mass that did not spread out much at the surface. This behaviour is very different from that of the material forming mud volcanoes which would extrude to form a linear chain of subcircular

FIGURE 2.4 - Gloria sonograph image of a series of long sinuous bright reflectors that correspond to major fault line on seismic images. These have been interpreted to be ridges of mud exuded from the major late thrust faults which bound the small slope basin (Sub-basin A, See Figs. 2.7 & 2.8).

edifices.

2.2.3 *Gas Blow-Out Structures*

Only one probable example as been identified, occurring just in front of the accretionary complex at latitude 14°N. Visible on Gloria as a very bright irregular area some 15km long and 5km wide (Fig. 2.5) this feature is picked up on a nearby seismic reflection section as a small depression (less that 10m or so in depth) in which the seafloor topography is rough (Fig 2.6). Sedimentary relectors are undisturbed a few 10's of meter below the sea floor and it appears to be a relatively near surface phemenon. Similar "pock marks" have been identified in the seafloor of the North Sea and Scotian Shelf and have been attributed to violent gas escape (Hovland et al. 1984).

2.3 *THE RELATIONSHIP OF THE DISTRIBUTION AND NATURE OF DIAPIRISM AND THE OTHER STRUCTURAL COMPONENTS OF THE BARBADOS ACCRETIONARY COMPLEX*

More than 450 diapirs are observed in the Barbados Ridge accretionary complex with their products covering about 730 Km of its surface area (Figs. 2.7 & 2.8). Two mud volcanoes and a possible gas blow-out structure are also developed in front of the complex (Westbrook and Smith, 1983; Langsett et al., 1986). There are a number of factors that appear to control the distribution and nature of mud diapirism on the Barbados Ridge Complex.

FIGURE 2.5 - GLORIA sonograph of an irregular highly reflective feature occuring just in front of the accretionary complex. Its reflective character is different from that normally associated with slumps or mud volcanoes.
A gas blow out structure appears to be the best explanation for the feature. The presence of abundant gas hydrate in the accretionary complex does indicate that large quantites of methane is present. (see Fig. 2.8 for position)

FIGURE 2.6 - A Seismic reflection line that runs along the edge of the possible gas blow out structure. The depression could be formed by a down warping of the sedimentary section and may not directly relate to the gas blow-out. It may be due to basement faulting or sagging due to compaction on the release of gas. (see Fig. 2.8 for position)

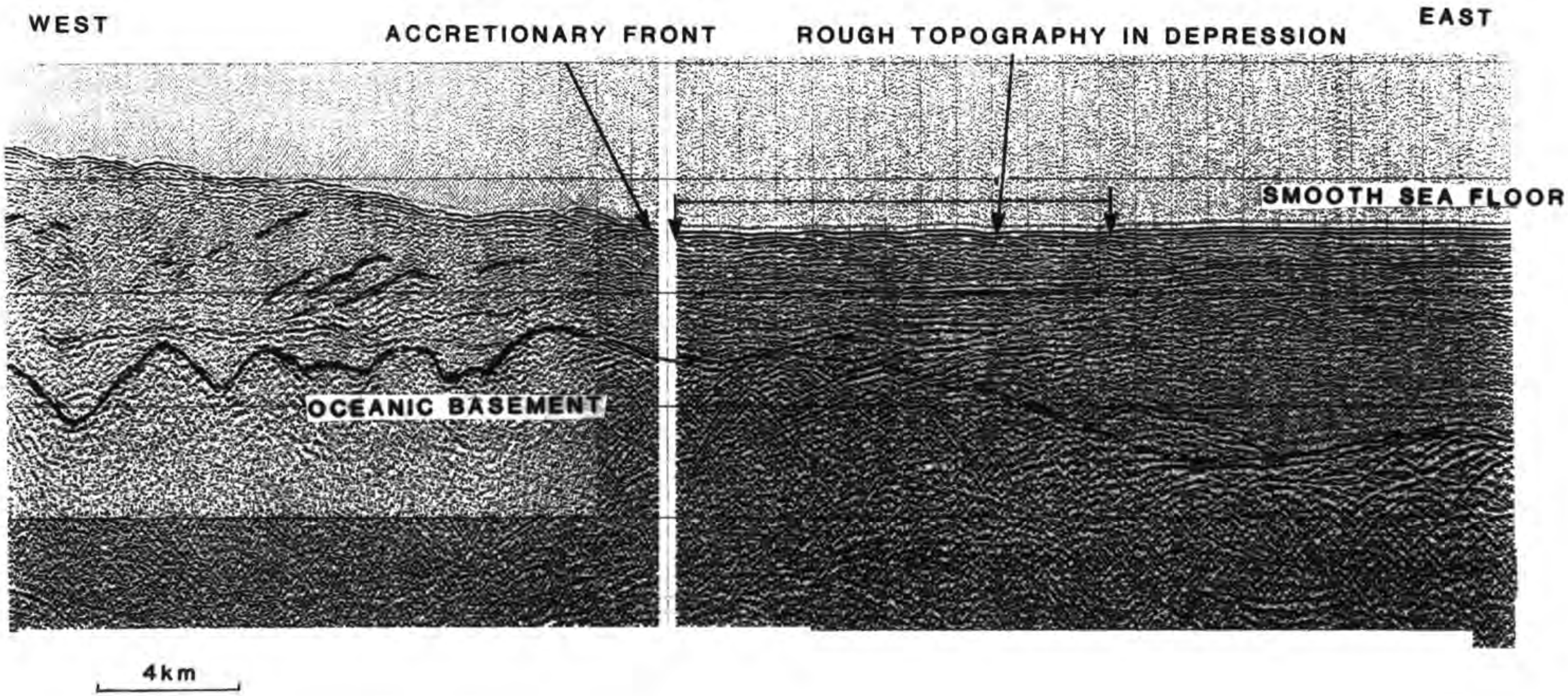
WEST
ACCRETIONARY FRONT
ROUGH TOPOGRAPHY IN DEPRESSION
EAST
SMOOTH SEA FLOOR
OCEANIC BASEMENT
4km

2.3.1 *The Control Of Sediment Facies On The Presence Of Mud Diapirism*

Diapirism only occurs in the Barbados Ridge south of latitude 15 N (Stride et al., 1982) (Fig. 2.1 & 1.2 & Appendix A). Currently a thin sequence of hemipelagic and pelagic sediments is being accreted in the north and a thick sequence of rapidly deposited turbidites is being accreted in the south. Mud diapirism is associated with the accretion of the turbidites.

The accretionary complex is relatively much thinner and narrower north of latitude 15° N than the complex in the south. It would appear that the past sedimentation pattern has been broadly similar to the present one for a substantial period of the complex's development.

2.3.2 *The Eastern Diapiric Front*

Perhaps unexpectedly, mud volcanoes are not associated with the early stages of imbrication, rapid thickening and associated dewatering all along the southern regions of the accretionary complex. Indeed at latitude 11° 30′ N the first occurrence of mud volcanism is not until 40 km west of the deformation front (Fig. 2.7). The eastern limit of diapirism (or diapiric front) approaches the outer deformation front northwards until it is within 10 km by latitude 13° 30′ N.

FIGURE 2.7 - A map showing the distribution of mud volcanoes, mud ridges (MR), and gas hydrate occurences. NOTE that the eastern limit of mud diapirism and the initiation of subcretion are approximately coincident where the latter is observable on seismic reflection sections. Mud diapirs associated with obliquely striking cross-faults are marked (CF).

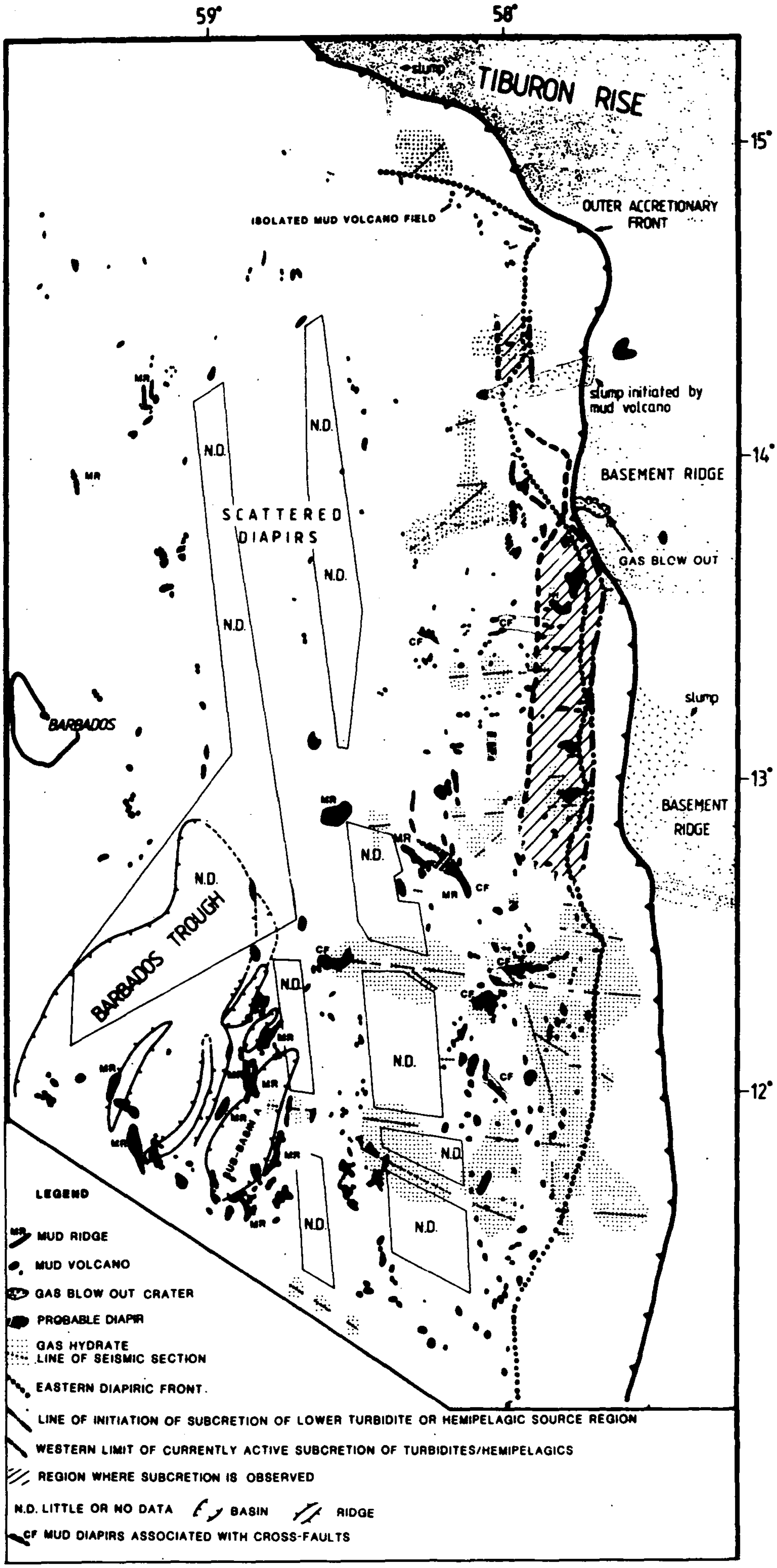

59°
58°
15°
14°
13°
12°
TIBURON RISE
slump
OUTER ACCRETIONARY FRONT
ISOLATED MUD VOLCANO FIELD
slump initiated by mud volcano
BASEMENT RIDGE
GAS BLOW OUT
slump
BASEMENT RIDGE
SCATTERED DIAPIRS
N.D.
BARBADOS
BARBADOS TROUGH
MR
CF
SUB-BASIN
LEGEND
MUD RIDGE
MUD VOLCANO
GAS BLOW OUT CRATER
PROBABLE DIAPIR
GAS HYDRATE
LINE OF SEISMIC SECTION
EASTERN DIAPIRIC FRONT.
LINE OF INITIATION OF SUBCRETION OF LOWER TURBIDITE OR HEMIPELAGIC SOURCE REGION
WESTERN LIMIT OF CURRENTLY ACTIVE SUBCRETION OF TURBIDITES/HEMIPELAGICS
REGION WHERE SUBCRETION IS OBSERVED
N.D. LITTLE OR NO DATA
BASIN
RIDGE
CF MUD DIAPIRS ASSOCIATED WITH CROSS-FAULTS

On closer examination the diapiric front appears to correlate closely with the initiation of subcretion of the lower most portion of the turbidite section or hemipelagic sequence for some 150 km between latitudes 13° N and 14° 30' N (Fig. 2.7, 2.9 & 2.11). Figure 2.9 is one of several seismic reflection lines that cross this region of the complex (see also Appendix B, section 3). South of this area, the complex is too thick for the basal decollement to be imaged in detail by existing seismic reflection lines and so in this region a correlation between the two processes can only be inferred.

2.3.3 Diapirism Associated With Southern Termination Of the Complex

South of 11° N latitude the eastern diapiric front swings eastwards towards the accretionary front (Fig. 2.8). This area is the most proximal part of the Orinoco Fan and perhaps the accreting sedimentary section is so underconsolidated that any disturbance of the section initiates mud volcanism. Large canyon systems also deposit further turdidites directly onto the complex. The stress distribution within this southern part of the complex is also complicated by a possible additional component of gravity spreading (see Chapter 5) which may play a role in the initiation of diapirism. The zone of dextral compressive shear (Fig. 1.10) along strike of the El Pilar fault system, that marks the southern termination of the complex, is associated with abundant mud volcanoes and possible diapiric domes above shale diapirs (the diapir field at latitude 11 20 N, longitude 50° 30' W). These are closely related to

FIGURE 2.8 - A map of the Barbados Ridge Complex showing the distribution of the various figures used in the chapter.

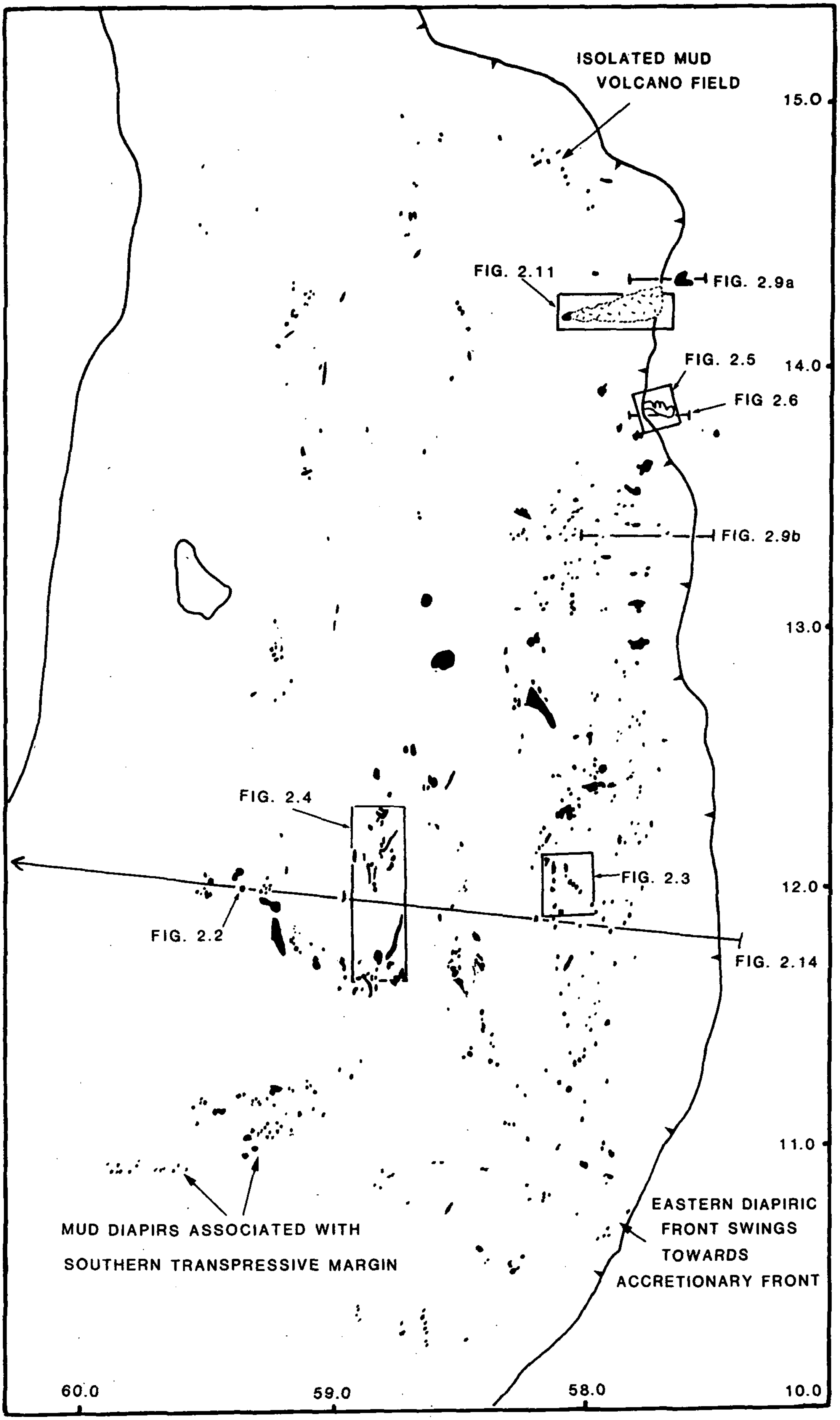

ISOLATED MUD
VOLCANO FIELD
15.0
FIG. 2.11
FIG. 2.9a
FIG. 2.5
14.0
FIG 2.6
FIG. 2.9b
13.0
FIG. 2.4
FIG. 2.3
12.0
FIG. 2.2
FIG. 2.14
11.0
EASTERN DIAPIRIC
FRONT SWINGS
TOWARDS
ACCRETIONARY FRONT
MUD DIAPIRS ASSOCIATED WITH
SOUTHERN TRANSPRESSIVE MARGIN
60.0
59.0
58.0
10.0

FIGURE 2.9 - a) Line drawing of a seismic reflection section across a mud volcano in front of the complex at latitude 14 20 N. NOTE that the basal decollement of the frontal imbricates lies at the top of the source region of the mud volcano, resulting in the overpressured section being thrust beneath the complex.

- b) Line drawing of a seismic reflection section at latitude 13 20 N that images the subcretion of a series of turbidite (X & Y) sequences. If the distribution of overpressured horizon and decollement is similar to that occuring in Fig. 2.9a either, or both horizons X and Y may contribute to the mud volcanism that is initiated above the subcreted section. The along-strike trace of the eastern diapiric front is marked on the section. Horizon Z is roughly equivalent to the distal turbidite or hemipelagic section that sources the mud volcano in Fig. 2.9a. (see Fig. 2.8 for position)

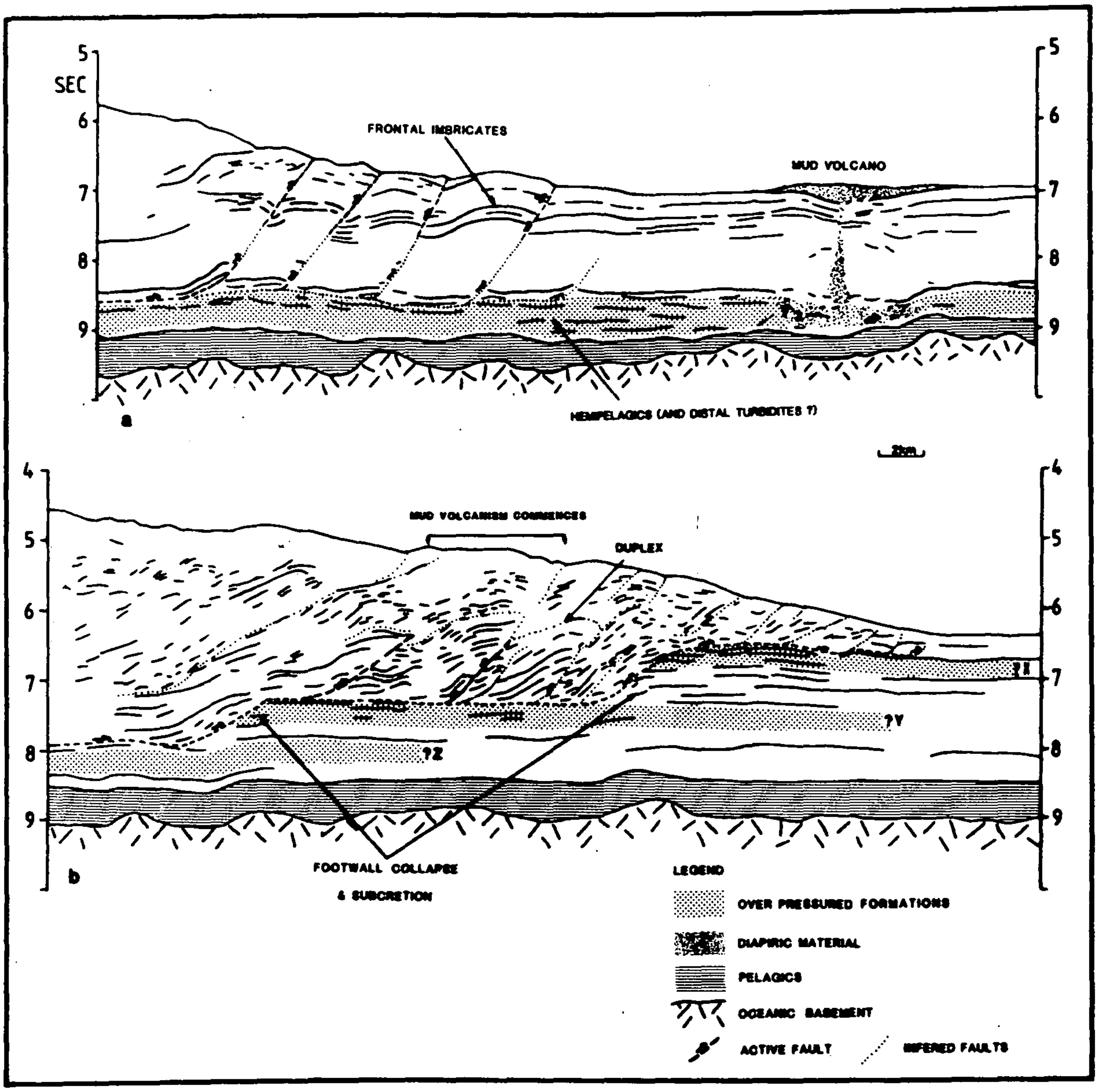

SEC
FRONTAL IMBRICATES
MUD VOLCANO
HEMIPELAGICS (AND DISTAL TURBIDITES ?)
a
MUD VOLCANISM COMMENCES
DUPLEX
?X
?Y
?Z
FOOTWALL COLLAPSE
& SUBCRETION
b
LEGEND
OVER PRESSURED FORMATIONS
DIAPIRIC MATERIAL
PELAGICS
OCEANIC BASEMENT
ACTIVE FAULT
INFERED FAULTS

predominantly southerly verging thrusts and positive flower structures (Valery et al. 1985).

2.3.4 *The Variation In The Abundance And Nature Of Mud Diapirism Across The Accretionary Complex*

The approximate area of greatest concentration of diapirs is pear shaped, narrowing northwards (Fig. 2.1). To the west and north of this (but south of latitude 15°N) only scattered groups of diapirs occur.

Superimposed on the variation in abundance is a gradation in the morphology of the diapirs which is believed to be related to their physical properties. This gradation is most readily observed in the southern regions of the complex, south of latitude 12°20′N (Fig. 2.7). Apart from those eastern areas of the complex where mud diapirism is conspicuous by its absence, the diapirism near the front of the accretionary complex (Figs. Appendix A, & 2.7) as imaged on GLORIA, is characterised by round-oval to slightly irregular edifices in plan, which are usually about 1-3 km wide although they are occasionally as much as 6km in diameter. They have a random distribution by and large although some appear to be associated with the crestal regions of the anticlinal ridges. These diapirs are thought to be almost exclusively of the mud volcano variety.

Further towards the interior regions of the complex 'crossfaults' also occur. These structures strike NW-SE to WSW-ENE, at high angles to the initial imbricate thrusts and *are can be associated with linear chains or clusters of mud volcanoes (Appendix A, Fig. 1.5 & 2.3 & 2.7). Similar crossfault patterns occur in the Eastern Mediterranean accretionary complex (Stride et al., 1977). When the mud volcanoes coalesce they form complex bulbous shapes.*

Progressing westwards the complex is increasingly covered by an appreciable thickness of sedimentary slope cover, up to 1.5 km thick in the south, which masks the initial accretionary fabric and earlier evidence of diapirism. In the south, the high slope sedimentation rate would have rapidly covered any ancient edifices. The present-day surface distribution of diapirs is therefore the result of fairly recent activity and the numbers of diapirs observed are an underestimate of the numbers actually present.

A recent phase of deformation affects the slope cover. The deformation takes the form of both easterly and westerly dipping reverse faults, and associated folds (see Chapter 1). Seismic reflection profiles indicate that diapiric material intrudes these faults (Fig. 1.4 section 4, see also Biju-Duval et al. 1982).

The form of diapirism among the slope basins is well illustrated by the small basin (sub-basin A, Fig. 2.7) which is partly rimmed by mud volcanoes and mud ridges. This basin also features in in Figures 2.4, 1.14 section B. Predominantly westward verging reverse faults have inverted the eastern margin of a previous broad basin. These have uplifted portions into hanging wall anticlines that form *ridges that are 3-12Km wide and up to 700m high. These ridges now define boundaries to the present basins. Many of the mud volcanoes and mud ridges are associated with the thrusts or the faulted ridge crests (Fig. 1.14). One particular mud ridge on the eastern side of the basin is 17 km long, 1 km wide and has intruded along a westward dipping thrust fault. Mud volcanoes lie along the continuation of this thrust and may have their source regions in the continuation of the same shale diapir at depth. The mud volcanoes are generally smaller, less elongate and more irregular in form. Several elongate sub-parallel mud ridges are associated with the western uplifted edge of this basin. It would appear that a sizeable percentage of the ridge's volume may be of diapiric material. The syntectonic onlap of the recent sedimentary section on to the ridges and slumping of material off them into the basin, testifies to their continuing uplift (Biju-Duval et al., 1982).*

The larger Barbados Trough at present contains recently deposited relatively undeformed sediments that unconformably overlie folded slope sediments. The few mud ridges and mud volcanoes (Fig. 2.2) in the basin have their source regions either in the lowest parts of the basin fill (at a depth of more than 3km) or more probably from deep beneath it, in the accreted section.

Diapirism is abundant in the south eastern areas of the slope basins. Further to the north the pattern is of scattered groups of diapirs of both kinds occurring in only locally favourable positions (Fig. 2.7).

In the most western areas of the basins only occasional scattered mud ridges and mud volcanoes occur. Subaerially exposed intrusive parts of mud diapirs have been identified in the island of Barbados as the Joes' River Formation (Larue and Speed, 1985) and at Bath (Torrini et al., 1985) (See Chapter 1).

2.3.5 The Effect Of The Impinging Oceanic Basement Ridges On The Diapir Distribution

North of latitude $12^\circ 30' N$ the pattern of diapirism is affected by the slightly oblique underthrusting of the complex by oceanic basement ridges (Fig. 1.10). The general morphology and variation in thickness of the complex across the Tiburon Rise indicates that the turbidites must have been stopped from flowing northwards by a ridge in roughly the present position of the Tiburon Rise, relative to the complex, for an extensive period of time. If this indentation is caused by an extension of the Tiburon Rise itself, it cannot have an orientation that differs widely from the plate convergence vector.

Diapirs are rare north of latitude $14^\circ 20' N$ and the impinging Tiburon Rise appears to have enhanced the development of mud volcanoes to its south, forming the isolated diapir field at latitude $14^\circ 50' N$ (Fig. 2.7). These mud volcanoes are small, usually less than 1km in diameter. In the area affected by the ridges, lateral changes occur in the level of the basal decollement in the sedimentary section

FIGURE 2.10 - Map of the Barbados accretionary complex relating the nature and thickness of undeformed sediments below the basal decollement to the oceanic basement topography of the underthrusting plate. All contours are in kilometers. Sediment thicknesses above 1.5 km are thought to have turbidites in the section. The section which is the source of the mud volcanoes in front of the complex lies at the base of the turbidite sequence, it is several 100 meters thick and is presumed to be an overpressured argillaceous horizon. Thicknesses below 1 km are thought to be made up of pelagics only.

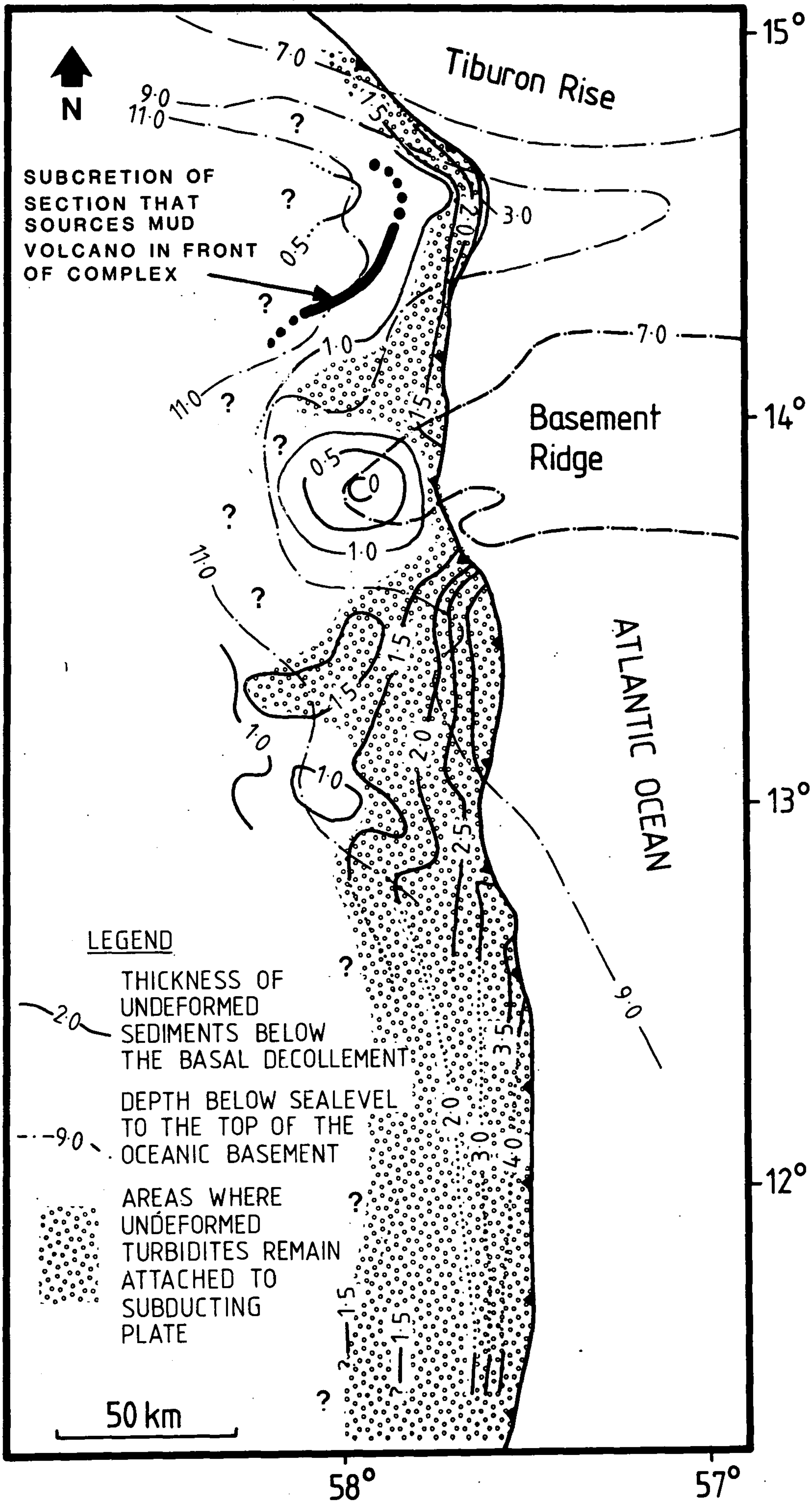

N
Tiburon Rise
SUBCRETION OF SECTION THAT SOURCES MUD VOLCANO IN FRONT OF COMPLEX
Basement Ridge
ATLANTIC OCEAN
LEGEND
THICKNESS OF UNDEFORMED SEDIMENTS BELOW THE BASAL DECOLLEMENT
DEPTH BELOW SEALEVEL TO THE TOP OF THE OCEANIC BASEMENT
AREAS WHERE UNDEFORMED TURBIDITES REMAIN ATTACHED TO SUBDUCTING PLATE
50 km
15°
14°
13°
12°
58°
57°

(Fig 2.10). It can be seen that on the ridge crests, in places, subcretion of the pelagic section has occurred as well. The decrease in diapirism north of the ridge at latitude 14°N corresponds to only a very thin turbidite or hemipelagic sequence being thrust beneath the complex to be later subcreted. The basement ridges have also initiated large slumps off the front of the complex in positions just to the north of the areas underthrust by the ridges. One of these slumps at latitude 14°20'N appears to have been initiated by a mud volcano (Fig. 2.11). Material from deep within the complex will have been strewn across a considerable area of the complex in this instance.

2.4 THE RELATIONSHIP OF METHANE PRODUCTION TO GAS HYDRATE FORMATION AND DIAPIRISM

The gas hydrate is a non-stoichio-metric substance in which small gas molecules are trapped in structural voids in a water-ice lattice. One volume of pure hydrate can yield up to 170 volumes of methane gas on decomposition (Kvenvolden and McMenamin, 1980; Kvenvolden, 1983; Shipley, 1979). In deep water where bottom water temperatures are near 2°C, the gas hydrate is stable within the sediment column down to approximatly 500m sub-bottom. Below the gas hydrate, the pore space is filled with water and methane resulting in a large impedence contrast across the boundary. This is identified on seismic reflection lines as a strong Bottom Simulating Reflector (BSR) that crosscuts any deformed horizons.

FIGURE 2.11 - GLORIA image of a mud volcano that apparently has helped initiate a debris flow down the front of the accretionary complex. (see Fig. 2.8 for position)

On the Barbados Ridge complex the gas hydrate is found in large irregular patches up to 100 km across, most commonly developed in the south and east of the complex. Its overall distribution is very similar and may be related to that of the mud volcanoes (Fig. 2.7). The gas hydrate indicates that large quantities of methane are present in the complex. Furthermore, the volume increase associated with the production of methane from organic material may contribute significantly to overpressuring the complex at depth if the excess volume cannot escape out of the section (Hedberg, 1973).

The organic content of the sediments needs to be above 0.5% (Kvenvolden, 1984) for sufficient methane to be produced to form the gas hydrate. The observed northward decrease in the gas hydrate abundance is therefore likely to either relate to the northward decrease in the percentage organic content of the turbidites away from their terrigenous source or to the decrease in the initial thickness of the turbidites. No definite occurrences of gas hydrate are observed north of latitude 15°N where only pelagic and hemipelagic muds with very low organic contents have been accreted (Moore et al., 1984).

McIver suggested that melting of the gas hydrate may release methane in a catastrophic manner, initiating mud volcanism. The gas hydrates destruction could be initiated by the escape of warm fluids up active faults and by diapirism. DSDP Leg 78A and ODP Leg 110 (Davis & Hussong, 1984, Moore & Mascle et al. 1987) recorded anonamously high *heat flows attributed to the upward migration of warm fluids from deeper within the accretionary complex. These latter two processes do not, however, appear to be important for the mud volcanoes that are generated on the Barbados accretionary complex. The gas hydrate and mud volcano occurrences do correlate on a broad scale (Fig. 2.7) but there are many mud volcano occurrences in areas where there is no gas hydrate. In addition where mud volcanoes are imaged on seismic reflection lines they appear to originate from regions often deeper than 3km (the limit of detailed seismic resolution), which is below the level where the gas hydrate is stable (ie deeper than 0.5 km).*

There are patches of gas hydrate in the areas east of both the diapir field and the zone where subcretion is thought to commence, indicating that upward migration of methane does occur in the early stages of deformation of the frontal imbricates. In summary, although the presence of the gas hydrate is not directly responsible for mud volcanism, it indicates the presence of abundant methane which is proposed to be important for mud volcanism (see Chapter 4).

2.5 MUD DIAPIRISM AND THE PHYSICAL & STRUCTURAL PROCESSES OPERATING DURING ACCRETION

The distribution and nature of mud diapirs in the Barbados Ridge accretionary complex is controlled by processes associated with accretion and deformation. Following the ideas of Hubbert and Rubey (1959), and Rubey and Hubbert

(1959), Westbrook and Smith (1983) introduced a mechanism for generating overpressures and mud volcanoes in front of the accretionary complex. They proposed, that pore fluids could be driven through the undeformed section in advance of the advancing accretionary front, by the lateral pressure gradient generated by the loading of the underthrust sequence by the accretionary wedge.

Figure 2.9a is a line drawing of the seismic line published in Westbrook and Smiths (1983) paper. The basal decollement of the frontal imbricates lies at the top of the lateral extension of the source region of the mud volcano in front of the complex. Consequently, the potential source horizon is carried, apparently as an undefomed layer, for some distance beneath the complex before being subcreted (Fig. 10). If, therefore, this arrangement of basal decollement and overpressured horizon is developed commonly along the accretionary front, the subcretion of such overpressured horizons will be widespread (Fig. 2.9).

The main features to be explained are first; the lack of diapirism associated with the early period of frontal accretion in the southern part of the complex and secondly; the apparent correlation between latitudes 12° 40'N & 14°N, of the line bounding the eastern limit of mud diapirism in the complex and the position where subcretion of the lower turbidite or hemipelagic section commences (Fig. 2.9). In the far south, at the southern termination of the complex, the Eastern Diapiric Front does swing towards the accretionary front.

An absence of mud volcanoes in association with the initial period of frontal accretion (between Latitudes 11°-13° 20′N, Fig. 2.9) is proposed to signify that during the initial stages of rapid deformation and consolidation, the necessarily high degree of underconsolidation and overpressuring required for diapirism are not attained. This may result from the ease with which fluids may escape from the section. Initially high permeabilities might be expected due to the presence of numerous turbiditic sand horizons and fractures generated during accretion. It has been observed in ODP Leg 110 (Moore & Mascle et al. 1987) that fluids may escape to the surface via active frontal faults (Fig. 1.17 & 2.12). The latter provide routes to the surface even from the deeper parts of each thrust packet. Perhaps the situation is analogous to that occurring in the fold and thrust belt of Taiwan (Fig.2.12). Suppe & Wittker (1977), note that in Taiwan in the frontal parts of the complex and advance of the deformation front near hydrostatic pressures occur in the upper parts of the sedimentary section which is composed of interconnected permeable sands. These allow the lateral bleeding off of fluids, inhibiting the formation of overpressures.

In Taiwan the basal decollement is preferentially associated with the deeper overpressured argillaceous units, much like the situation proposed for the Barbados Ridge Complex (Figs. 2.12 & 2.13). Suppe & Wittker (1977) find that the basal decollement actually develops along a similarly overpressured, isolated transgressive sandstone unit within the argillaceous sequence. The decollement is

FIGURE 2.12 - A model explaining the relationship between subcretion and mud volcanism. The basal decollement of the frontal imbricates lies at the upper margin of a particularly overpressured section in the lower turbidites or hemipelagics. The frontal imbricates consolidate rapidly as fluids escape via permeable sandstone horizons and up active faults to the surface. Their permeability does not allow sufficient over pressures to build up for them to originate mud volcanoes. Mud volcanism occurs above the regions where the overpressured section has been subcreted. The disruption associated with the subcretion mobilizes the potential source regions, perhaps allowing fluids to migrate and concentrate. The overpressuring itself may initiate vertical hydro-fractures, or active faults may breach the relatively impermeable section above, resulting in a distructive release of fluid pressure and mud volcanism.

NB- In the case of the Barbados Ridge Complex seismic velocity studies do show that to some extent that the frontal regions of the complex remain underconsolidated.

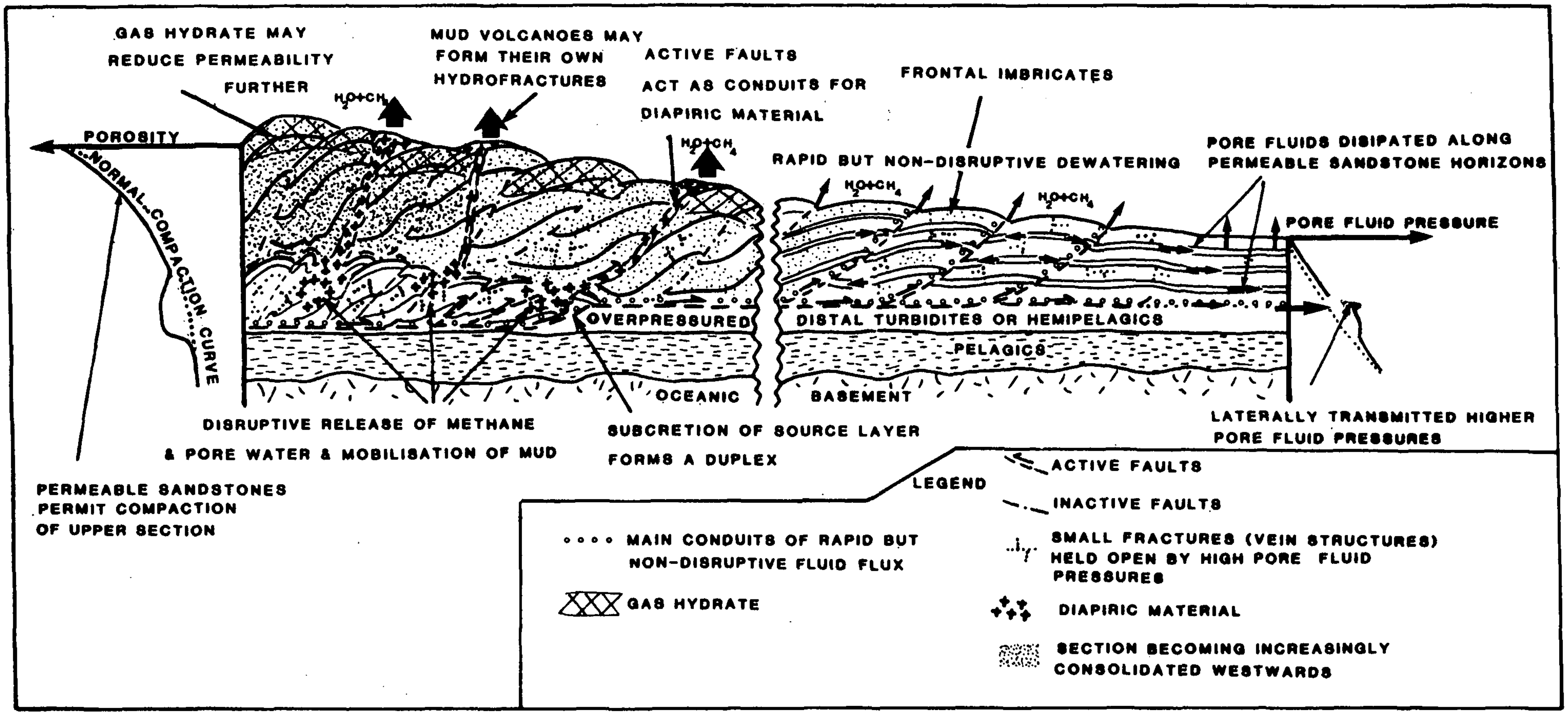

GAS HYDRATE MAY REDUCE PERMEABILITY FURTHER
MUD VOLCANOES MAY FORM THEIR OWN HYDROFRACTURES
ACTIVE FAULTS ACT AS CONDUITS FOR DIAPIRIC MATERIAL
FRONTAL IMBRICATES
RAPID BUT NON-DISRUPTIVE DEWATERING
PORE FLUIDS DISIPATED ALONG PERMEABLE SANDSTONE HORIZONS
H_2O+CH_4
POROSITY
NORMAL COMPACTION CURVE
PORE FLUID PRESSURE
OVERPRESSURED
DISTAL TURBIDITES OR HEMIPELAGICS
PELAGICS
OCEANIC
BASEMENT
DISRUPTIVE RELEASE OF METHANE & PORE WATER & MOBILISATION OF MUD
SUBCRETION OF SOURCE LAYER FORMS A DUPLEX
LATERALLY TRANSMITTED HIGHER PORE FLUID PRESSURES
PERMEABLE SANDSTONES PERMIT COMPACTION OF UPPER SECTION
LEGEND
ACTIVE FAULTS
INACTIVE FAULTS
MAIN CONDUITS OF RAPID BUT NON-DISRUPTIVE FLUID FLUX
SMALL FRACTURES (VEIN STRUCTURES) HELD OPEN BY HIGH PORE FLUID PRESSURES
GAS HYDRATE
DIAPIRIC MATERIAL
SECTION BECOMING INCREASINGLY CONSOLIDATED WESTWARDS

FIGURE 2.13 - Relationship between the fluid-pressure/depth ratio and stratigraphic horizon in the thrust belt of Tiawan. Note that the transition zone between hydrostatic and overpressured horizons is dependent of stratigraphy rather than depth. The permeable interconnected sands in the upper parts of the sequence are at normal hydrostatic pressure, where as overpressuring occurs in the argillaceous horizons at the base of the sequence. Diagram is adapted from Suppe & Wittker (1977), with additions of the lithologies and stratigraphic positions of main decollement horizons. The authors denoted that certain of the decollement horizons were no longer active. Note the relationship between overpressuring and activity on the decollement horizons.

BOREHOLES NOMALISED TO HYDROSTATIC PRESSURE

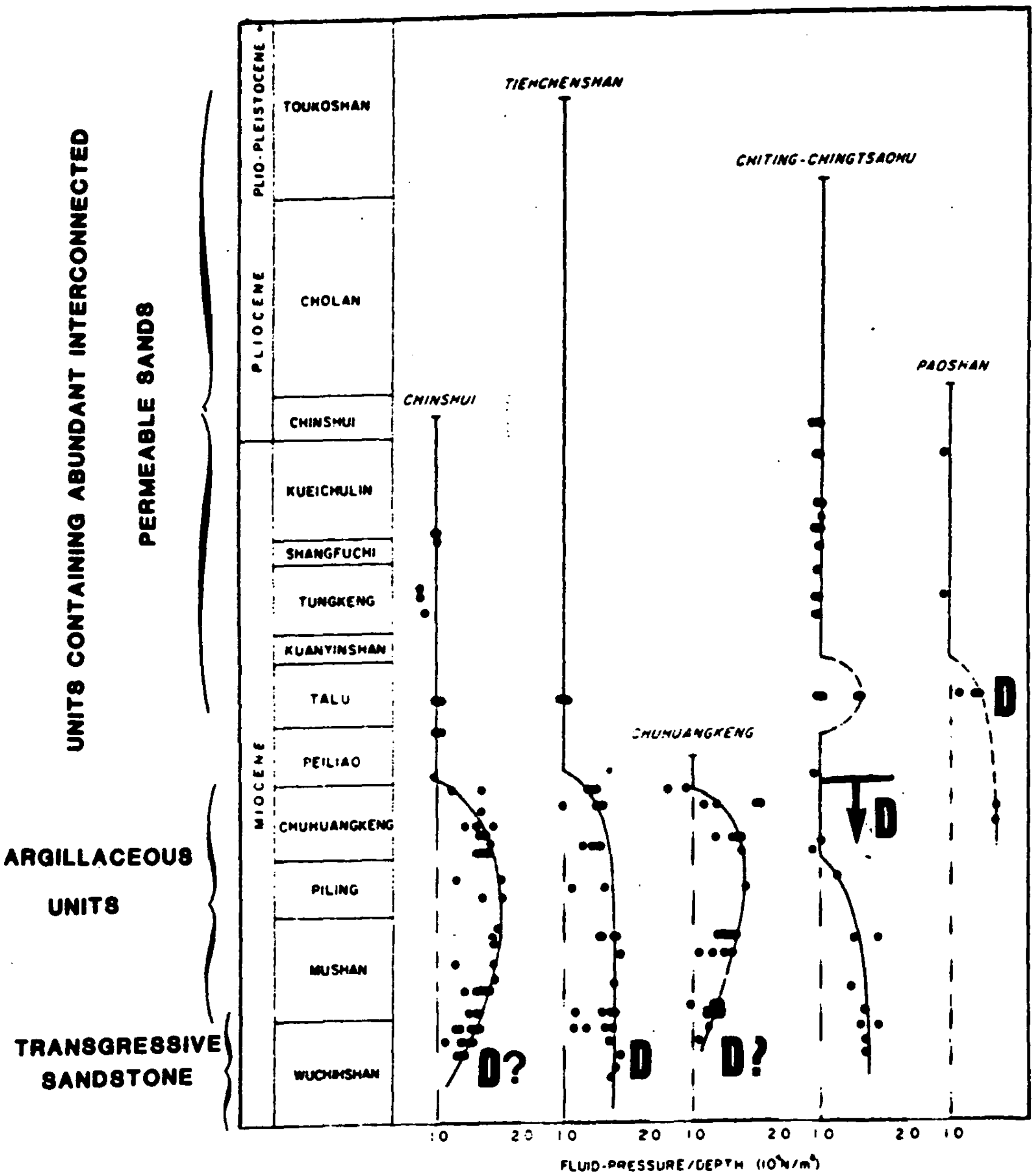

D DECOLLMENT ACTIVE

D? DECOLLMENT NOT THOUGHT TO BE ACTIVE BY AUTHORS perhaps associated with the sandstone unit because it forms an efficient conduit along which further overpressured fluids can be laterally transmitted from deep within the deformation complex, counteracting any losses of fluid from the system. They fail to discuss an interesting feature of the distribution of pore pressures in the thrusted sequence. The currently active thrusts appear to correspond to areas in which the sandstone unit is as equally overpressured as the shales (Fig. 2.13), whereas the thrusts are inactive in the areas where the overpressures are approaching hydrostatic pressures in the sandstone unit. It is not clear whether the thrusting ceased as a result of the confining seal being breached around the sandstones allowing a rapid loss of fluid pressure, or conversely if inactivity led to a subsequent slow loss of fluid pressure and later compaction.

The association of the subcretion of material beneath the complex with mud diapirism is proposed to occur for the following reasons. During the deformation and consolidation of the frontal imbricate section, the overpressured section below the basal decollement (that in places forms the source region of mud volcanoes in front of the complex) appears to remain relatively undeformed. The lack of fracture permeability would inhibit fluid loss, so that the section would become increasingly more overpressured as it is thrust further beneath the complex. On this overpressured section being subcreted, to form a duplex beneath the accretionary wedge, there is a potential for the release of pore fluids. Porewater, methane and fluidised mud that form the diapirs is *expelled from the horses, into the overlying wedge and through fractures to the surface during and following subcretion (Fig. 2.12). The disturbance of beds from their original horizontal orientation also promotes the gravitational driving of diapirism. The residual shear strength of the disrupted argillaceous horizons is also less than the original strength of the undeformed material, thus enhancing its potential mobility (See Chapter 3 , Fig. 3.29) The development of two ramps at sucessivelly deeper levels is shown on a seismic section at latitude 13° 20′ N (Fig. 2.9).*

The occurrence of mud diapirism further back in the western parts of the complex could result from subcretion of sediment at deeper and more western ramps in the basal decollement of the wedge. In addition later deformation in a previously subcreted section may also regenerate sufficient overpressures in regions for them to become unstable and produce further diapirism. Major late or out-of-sequence thrusts that allow the accretionary wedge to maintain its equilibrium profile or critical taper (see Introduction) appear to play a role initiating and acting as pathways for this diapirism (see below).

South of latitude 12° 20′ N, in areas unaffected by impinging basement ridges, the mud volcanoes appear, in the eastern portion of the complex, to have circular surface expressions and a uniform distribution. They are not obviously influenced by frontal imbricate thrust faults although some may be associated with the crestal regions of the anticlinal ridges. Perhaps the frontal faults are *inactive by the time they reach the region of the complex where subcretion starts and the mud volcanoes have initiated their own vertical hydrofractures (Fig. 2.12).*

Later faults, active further back in the complex, are preferentially associated with mud diapirs, presumably because they provide convenient conduits. The development of mud ridges is strongly influenced by the out-of-sequence thrust faulting along the margins of the slope basins. The mud extrudes up [illegible] some of the thrusts to form long diapiric ridges. Indeed, the intrusion of the mud may have been initiated by these large late faults. To the north of latitude 12° N, late cross-faults in the regions affected by the impinging ridges, are quite often sites for diapirism with chains of mud volcanoes developing along them (2.3). These sometimes coalesce to form bulbous-shaped surface expressions.

There is an east-west progression in the number and nature of diapiric forms seen at the surface of the Barbados Ridge Complex. Around latitude 11° 30′ N there are increasing numbers of mud ridges from approximately 120 km westward of the accretionary front (Fig. 2.7). The density of diapirs of either form also decreases westwards. A similar progression in the nature of the diapirism across an accretionary complex is observed in the Makran accretionary complex, with mud volcanoes along the coast and mud ridges further inland away from the accretionary front (Snead, 1964). Morphological variations among extrusive mud diapirs are proposed to result from differences in the viscosity (related to fluid content) *and are likely to be related to the bulk characteristics of the deep seated source regions (Fig. 2.14, also See Chapter 4).*

Where they are observed sub-aerially, mud volcanoes are surface edifices formed by extrusions of mud with a significant methane component. The release of large volumes of methane is a characteristic feature of nearly all the mud volcano eruptions so far documented (i.e. Kugler 1939, Arnold & McCready 1956, Freeman 1967, Hedberg 1974, McIver 1982, Morgan et. al. 1965, Ridd 1970, Higgins & Saunders 1973). There may, therefore, be a genetic relationship between the presence of methane and mud volcanism. The methane may be biogenic or thermogenic, occurring below and above 50°C respectively. As will be discussed further in Chapter 4, fluid contents are high but very variable with the volume of fluids potentially exceeding that of the solids so that their source regions must be correspondingly rich in fluids. The very large quantities of methane that are normally associated with the eruption of mud volcanoes would seem to indicate some sort of previous or concurrent concentration of the methane at depth. Such gas pockets are often recorded as trip gas in drilling operations through overpressured mud bodies (Hedberg, 1974). The mud volcanoes associated with the anticlines may have their source regions in gas rich pockets formed by the migration of methane up into the anticlinal structures.

The elongate and some times sinuous diapiric forms seen in the Barbados Ridge Complex are proposed to be analogous to *the mud ridges like those observed in the sub-aerially exposed regions of the Makran accretionary complex (cf. Snead 1964). These are, in comparison to mud volcanoes, composed of more viscous, methane poor material.*

In short, mud volcanoes and their source regions, have a higher proportion of fluid phases, such as methane and water, than mud ridges. It is proposed that both the westward trend in the nature and abundance of the diapirs suggests that, in general, the deeper seated regions of the complex are becoming depleted in fluids (Fig. 2.14).

The northward narrowing of the area in which the main concentration of diapirs and gas hydrate occurs most probably relates to an overall decrease in the thickness, rate of sedimentation, under-compaction, and organic content of the Orinoco turbidites. This is because going northwards, the subcreted regions are also likely to be volumetrically smaller, better consolidated and contain a lower proportion of organics from which methane can be produced. This means they will exhaust their potential for mud diapirism and methane generation sooner, increasingly restricting the diapirism to eastern areas of the complex.

The absence of any diapirism in the regions to the north of latitude 15°N results from the lack of suitably underconsolidated horizons being subcreted beneath the complex. The hemipelagic section is frontally accreted (Moore et al., 1984) whilst the pelagic section is thrust under the complex for distances exceeding 80 km (Westbrook et

FIGURE 2.14 - a) A crossection through the Barbados Ridge accretionary complex at latitude 11^{o} 40' N (vertical exaggeration x 3). The near surface structure is derived from high resolution multichannel seismic data. The depth to oceanic basement is taken from Speed, Westbrook and others (1984). The deeper parts of the complex are schematicaly represented with some of the major structures, such as the major late back-thrusts, having been extrapolated downwards from near-surface structures. An undeformed pelagic section beneath the basal decollement is shown to underthrust the complex to distances in excess of 80km elsewhere in the accretionary complex. It is suspected that not all (if any) of the pelagic section is eventually subducted and that at least some is subcreted. The physical properties of the deeper parts of the accretionary complex will be very variable in detail and the boundaries between regions will be transitional. Only a generalised representation of them is attempted.

- b) A crossection illustrating where figure 9a lies in respect to the other major components of the accretionary complex.

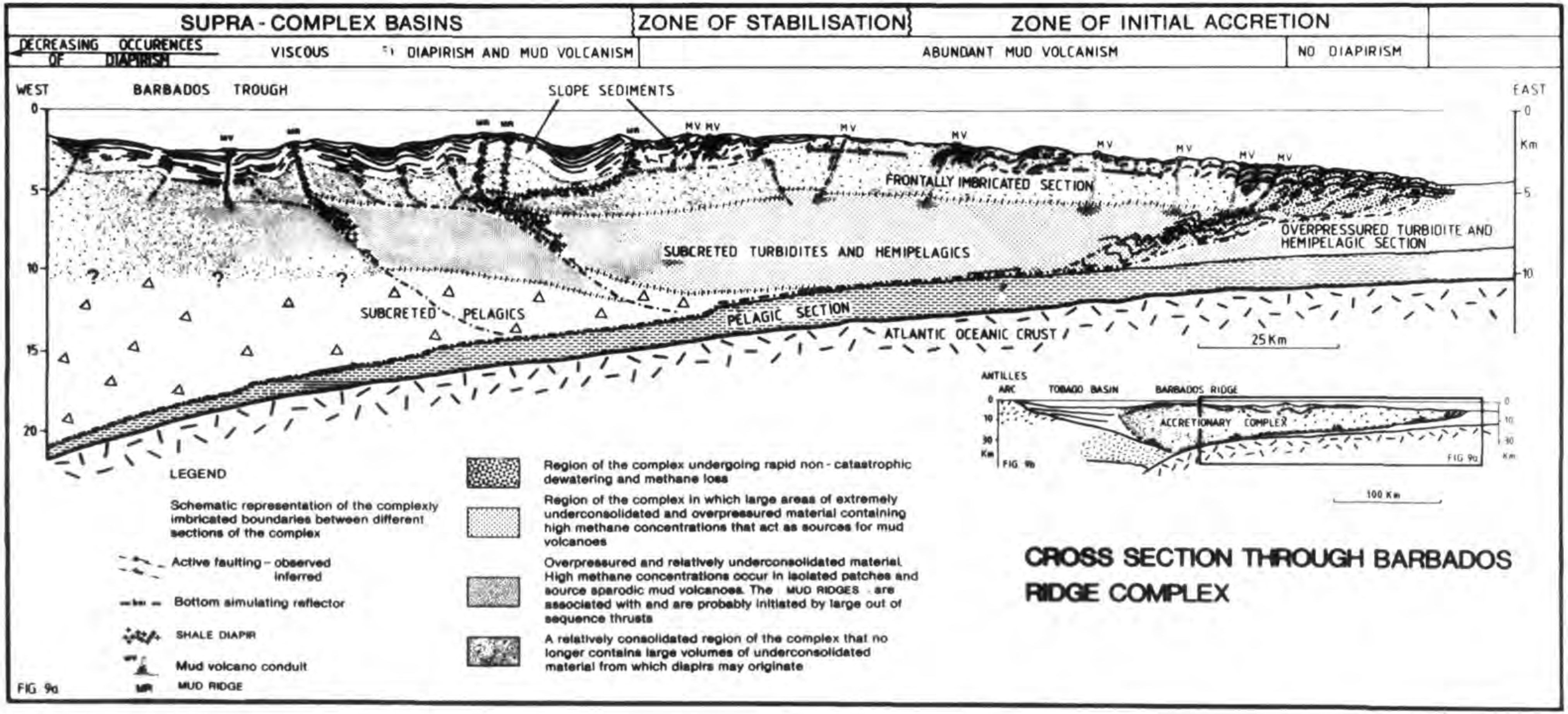

CROSS SECTION THROUGH BARBADOS RIDGE COMPLEX *al., 1982) before becoming too deep to be imaged seismically. If and when the pelagic section is subcreated, its low water and organic content (More et al., 1984) make it an unlikely candidate for diapiric source region in any event. The low organic content is further indicated by the absence of gas hydrate occurrences.*

2.6 CONCLUSIONS

From this study of mud diapirism in the Barbados Ridge accretionary complex the following conclusions can be drawn:

1) The concentration of diapirs in the southern regions of the Barbados accretionary complex south of latitude 15°N is a result of the incorporation of rapidly deposited and underconsolidated Orinoco Fan sediments into the complex since late Eocene to Miocene times.

2) There is a general northward decrease in diapirism in the complex which is due to the "diapiric source potential" of the accreting section becoming poorer. This is inferred to result from a northward decrease in the thickness and underconsolidation of the source rocks and in the amount of organic material available for methane production.

3) The basal decollement of the frontal imbricates initially develops at different stratigraphic levels. Some of these stratigraphic horizons can be observed to be the source of mud diapirs in front of the accretionary complex. These potential source horizons tend to be thrust beneath the *complex and later subcreted.*

4) Diapirism is initiated by the disruption of underconsolidated and overpressured horizons as they are subcreted beneath the complex.

5) The westward and northward decrease in diapiric abundances and the westward increase in diapirs with morphologies that suggest high states of diapiric material consolidation, are proposed to be related to a general increase in the consolidation of the accretionary complex at depth. However, at latitude 11° 30′ N, the accretionary complex must be still sufficiently underconsolidated to generate both abundant mud volcanoes and mud ridges, 120km west of the accretionary front.

6) Although the broad variation in diapirism on the accretionary complex is controlled by the physical properties of the source region, the distribution and form of the surface expression can be strongly influenced by the pattern of near surface faulting. In general, the pattern of diapirism appears to be fairly random. However, the cross-faults and the out-of-sequence thrusts and reverse faults (prominent round the slope basins) are more commonly associated with mud diapirs than the initial frontal imbricate thrusts because they are active later in the complex's development when conditions at depth are more favourable for diapirism.

7) The distribution of the gas hydrate is broadly coincident *with that of the main body of mud volcanoes. This strongly implies that methane is an important, perhaps necessary, element in the generation of mud volcanoes. It is not thought, however, that the gas hydrate directly controls where mud diapirism occurs.*

8)Mud diapirism has affected large areas of the complex, particularly in the south, and a small but significant proportion of the complex is composed of diapiric melange. Recognition of these melange deposits in old exposed accretionary terranes will provide a means of establishing the importance of diapirism in old accretionary complexes.

9) Mud diapirism is an important mechanism for expeling fluids that are brought into the complex by subcretion. The greatest depth from which diapirs may rise may be potentially much deeper than 3-4km, the limit of good seismic resolution over much of the complex.

CHAPTER THREE

THE STRUCTURAL DEVELOPMENT OF THE NORTH BORNEO SUBDUCTION COMPLEX

3.1 *INTRODUCTION*

The development of the NW Borneo Tertiary subduction complex is proposed to be in many ways analogous to that of the modern Barbados Ridge accretionary complex, with the frontal accretion of turbidites and subcretion of argillaceous horizons and pelagics. Similarities extend beyond this, with the sequential development of early and late trenchward verging thrusts, late back thrusts, and the presence of large slumps and mud diapirs. As only the uppermost few km of the Barbados Ridge can be studied in any great detail geophysically this study of the NW Borneo subduction complex provides a complementary study of the outcrop scale structures developed in the deeper but still submetamorphic regions of such accretionary complexes.

3.1.1 *Tectonic Setting*

Borneo can be divided into three main tectonic components, consisting of a basement-magmatic arc complex, accretionary complexes and outer arc basins (Fig. 3.1). The pre-Tertiary basement complex and magmatic arc forms the core of southern

FIGURE 3.1 - The main morphotectonic units of Borneo (Hamilton 1979). The outer arc basins, accretionary complexes and metamorphic and igneous basement complexes, comprise the bulk of the units.

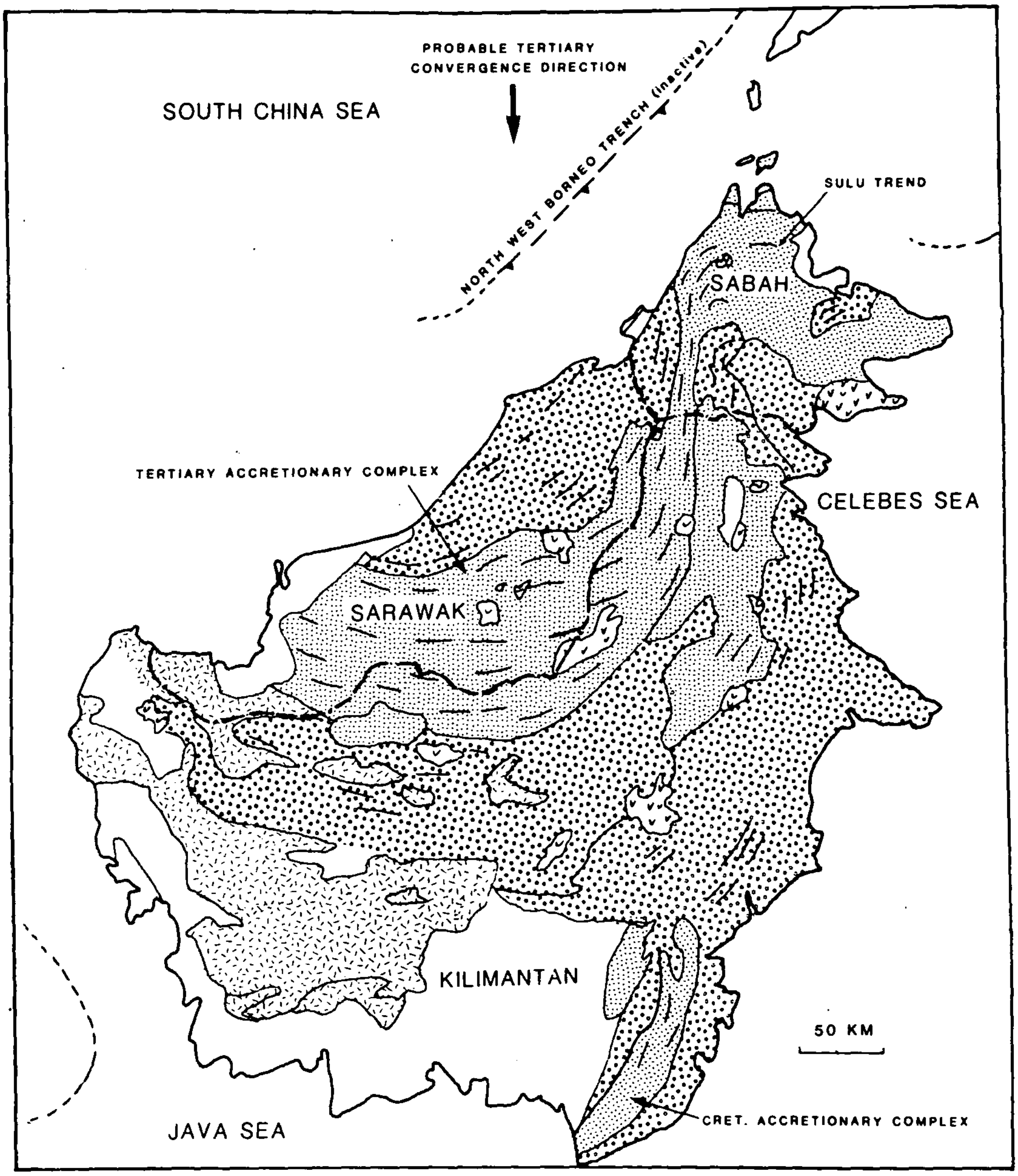

QUATERNA. RY ALLUVIAL DEPOSITS

VOLCANICS (Quat-Tertiary)

FOREARC BASINS (Ter)

ACCRETIONARY COMPLEXES (Ter-Cret)

METAMORPHIC AND IGNEOUS BASEMENT COMPLEXES (pre-Ter)

Borneo. It is an extension of Sutherland, a collage of accreted terrains that stabilized towards the end of the Mesozoic (Hutchinson 1973). In Sabah, N. Borneo, smaller areas of basement complex that outcrop in eastern areas are composed of amphibolites, gneisses, schists, calc-silicates, meta-tuffs and meta-volcanic rocks (Lee 1979). These metamorphics have been intruded by granodiorite, tonalite, ultramafic and mafic bodies. The ultramafic bodies, in particular, are aligned sub-parallel to the strong east-west trending foliation in the metamorphics. The basement complex has been variously interpreted as obducted oceanic crust (Hutchinson 1975), or as a metamorphic belt formed in the basal regions of a volcanic arc (Coleman 1977). Very probably, it may be best explained by a combination of both mechanisms, and is in fact an obducted volcanic arc.

The accretionary complexes have been assembled around this core (Fig. 3.1) and range from late Cretaceous to middle Tertiary in age (Lee 1979). Cretaceous to Eocene complexes, adjacent to the core complex in NW & SE Borneo, are composed of two formations. The Sapulut Fm., consists of mainly argillaceous strata with minor limestones, cherts, conglomerates and sandstones and is interpreted to have formed in a marine but not necessarily oceanic trough. The Chert-Spilite Fm. contains limestones, cherts, sandstones, spilite, pillow basalt, dolerite and keratophyre, the typical assemblage of an ophiolite bearing accretionary complex (Lee 1979, Tan 1982, Wilson and Wong 1964).

Eocene to Middle Tertiary accretionary complexes occur further out from the core, as nested crescentic belts that extend through Sarawak Northwest Kalimantan and Southwestern Sabah (Fig. 3.1). To the south, the complex stretches through central and eastern Sarawak and adjacent Kalimantan, to the north, it abruptly swings to the east in the North Sulu Trend. The Sulu Trend developed in the Oligocene as a result of the progressive collision,in a southeasterly direction, of the lateral extension of the Sulu Arc with Borneo. The Crocker and Trusmadi Formations represent the continuation of these belts in Sabah (Fig. 3.2a). The exterior western sections are dominated by the Crocker Fm. (see below), composed of turbidites, argillites and occasional limestones. The more interior or central regions contain the Trusmadi Fm. composed of slates, phyllites, quartzites, limestones, cherts and tuff (Lee 1979, Wilford 1967, Staffer 1967).

Neogene arc volcanics extend unconformably out onto the Eocene accretionary complex of central Sarawak and upon various terranes in Northern Kilimantan. Oligocene to Quaternary volcanic arc rocks occur extensively in central and southeastern Sabah.

In SW Sarawak and adjacent Kalimantan and running northwards up into south-central Sabah a Paleogene outer-arc basin lies, in the south, on pre-Eocene granitic and metamorphic basement and, in the north, on an accretionary complex of probable Cretaceous age. Middle Tertiary forearc basins occur on top of the Eocene subduction complex exposed *in Northwest Borneo. Neogene forearc basins occur offshore in Western and Northeastern Sabah on middle Tertiary accretionary complex (Bol & Hoorn 1980).*

The general configuration of the subduction zones in which the early Cretaceous to Eocene accretionary complexes originated is not clear. At present the strike of the dominant structures in them are in an approximately E-W direction (Tjia 1974, Lee 1980, Collenette 1958 (memoirs)). However, the Tertiary Crocker Fm. was probably accreted in a trench with a similar configuration to the present NE-SW trending, NW Borneo trench. Subduction of "proto-South China Sea oceanic crust" occurred during the Paleogene, as a result of the opening of the south China Sea basin. Magnetic lineaments in the South China Sea indicated the opening occurred in a N-S direction (Khain & Levin 1980) and there may have been a component of oblique (left lateral) convergence along the N. Borneo subduction system. Subduction ceased along the western margin of Borneo in late Miocene times with the collision of a small microcontinental fragment with the trench. Since then the NW Borneo region has under gone dextral shearing (Bol & Hoorn 1980) with the generation of a series of N-S and NE-SW trending structures (Fig. 3.3b).

3.1.2 <u>The Crocker Formation</u>

The Crocker Formation in Western Sabah forms part of the crescent of the Eocene and middle Tertiary subduction complex

(Fig. 3.2a). It predominantly consists of turbidites with occasional occurrences of pelagics and spilites. They are imbricated to form a extensive accretionary complex. Together with bodies of melange that have been interpreted to be of diapiric origin (Barber et al. 1986) the Crocker Formation has the appearance of being a sutiable sub-aerial analog for the deeper regions of parts of the Barbados Ridge Complex. A series of cross sections through the better exposed portions of the Formation in the environs of Kota Kinabalu were undertaken in order to assess its general structure and to look at the fabrics developed in broken formations associated with fault zones; chaotic deposits formed by slumping, and melanges that are thought to be associated with mud diapirs.

The term Crocker Formation was introduced by Collenette (1957) for the sedimentary rocks that form the Crocker Range. Bowen and Wright (1957) subdivided the sequence into the East and West Crocker Formations (Fig. 3.2). The East Crocker Formation consists predominantly of flysch-type sediments, composed of mudstones and turbiditic sandstones and occasional conglomerates and marls, with the argillaceous components make up about half the formation. Marls barren of foraminifera are a distinguishing feature, along with a distinctive association of basic pyroclastic rocks and massive limestone breccias that occur at or near its base. The degree of metamorphism varies, increasing towards the east, until phyllites occur on its eastern margin. The nature of its eastern contact with the phyllites of the Trusmadi Formation is unknown but is suspected to be a major

FIGURE 3.2 a - A geological map of W. Sabah (adapted from Winford 1967). The approximate positions of Study Areas 1 & 2 are marked. The most important units in the areas studied are the West Crocker Fm., the East Crocker Fm. and the Sapulut Fm. b - Lineament map of W. Sabah derived from Landsat images (adapted from Lee 1979). Important late faults are named. They appear to be dominantly transcurrent in nature (See Fig 3) and cut across the early accretionary fabric which has a dominant N to NE orientation over most of the map.

FIGURE 3.3 - Summary diagram of major structures in Sabah (compliation by Lee 1980) taken from Toluyama (a), Leong (b), & McManus (c). The Kadmaian fault and Crocker linearment best match previously infered faults. The sinistral faults of Toluyama, also appear to be represented by strong NW-SE trending linearments in the Landsat images (See Fig. 2b).

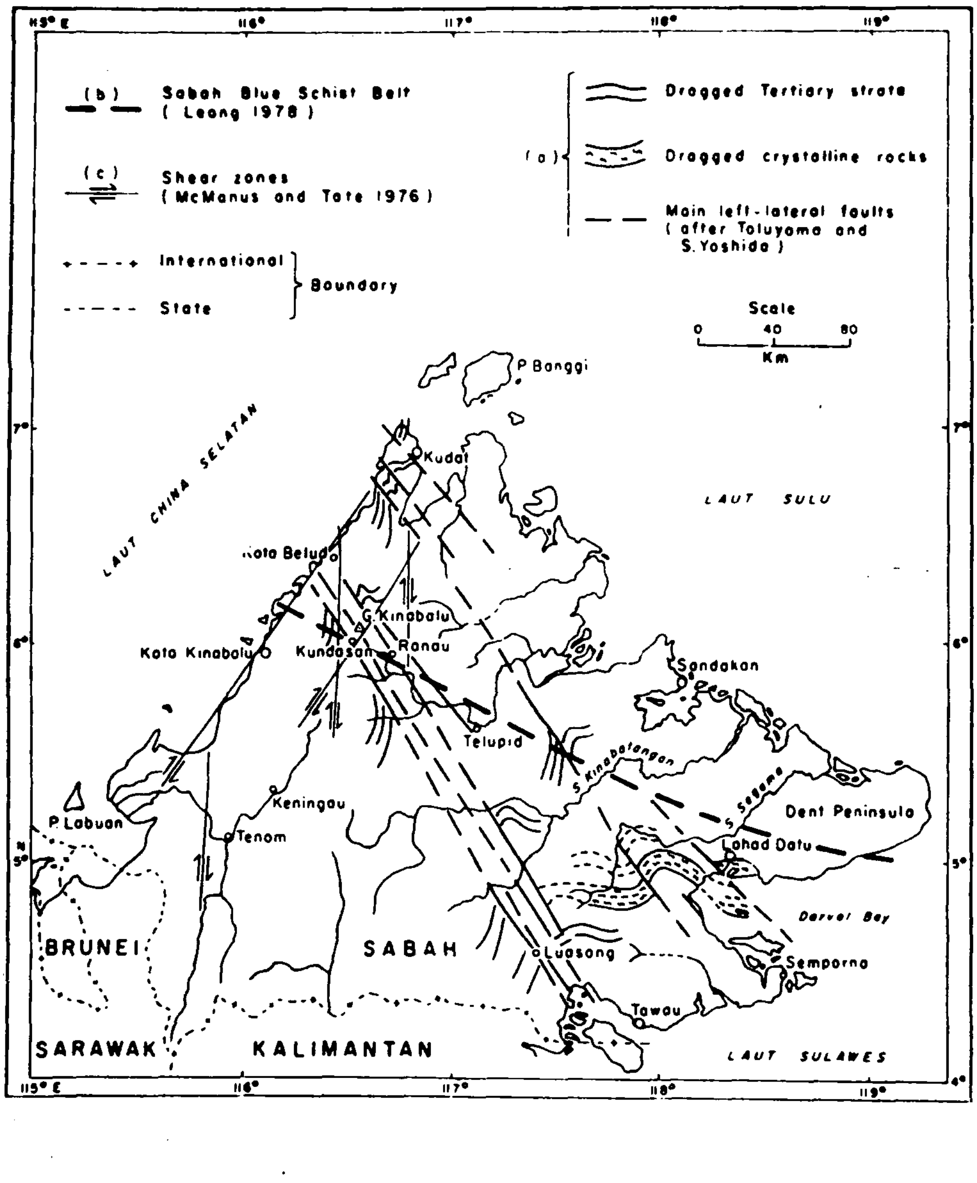

(b) Sabah Blue Schist Belt (Leong 1978)
(c) Shear zones (McManus and Tate 1976)
International Boundary
State Boundary
(a) Dragged Tertiary strata
Dragged crystalline rocks
Main left-lateral faults (after Toluyama and S. Yoshida)
Scale
0 40 80
Km
115° E
116°
117°
118°
119°
7°
6°
5°
4°
P Banggi
Kudat
LAUT CHINA SELATAN
LAUT SULU
Kota Belud
G. Kinabalu
Kota Kinabalu
Kundasan
Ranau
Sandakan
Telupid
S. Kinabatangan
S. Segama
Dent Peninsula
Keningau
P. Labuan
Tenom
Lahad Datu
Darvel Bay
BRUNEI
SABAH
Luasong
Semporna
Tawau
SARAWAK
KALIMANTAN
LAUT SULAWES

thrust. This eastern contact separates the recumbently folded Trusmadi Fromation from the steeply dipping and imbricated East Crocker Fromation. The age range, from of Paleocene to Eocene, is about the same for the two formations.

The East and West Crocker Formations boundary is transitional mainly defined on the lack of the barren marls and pyroclastics in the lower part of the West Crocker Formation. Stauffer (1967) described the West Crocker Formation as being composed of turbidites, laminites, grey, red and green shales and slump deposits, with turbiditic sandstones predominating. The western parts of the East Crocker and the West Crocker Fromation as a whole are not metamorphosed and cleavage is only sporadically development in western areas.

Two areas in the Crocker Fm. were studied. The first area was in the West Crocker Fm. in the environs of Kota Kinabalu (Fig. 3. 2a), where extensive land-clearance, quarrying and general land development has resulted in the complete stripping of thick lateritic soils in many areas. The second study area is situated inland and consists of a series of road sections along the Kota Kinabalu to Ranu road.

3.2 STUDY AREA I: THE KOTA KINABALU AREA

3.2.1 Local Stratigraphy

The Crocker Formation in the Kota Kinabalu area consist entirely of flysch deposits in which a distinctive local stratigraphy has been identified, and which is repeated many times by imbricate thrusting. A summary of the the main features of the stratigraphy is shown in Figure 3.4. The stratigraphic sequence as a whole is in the order of 140-180m thick, internal imbrication makes a more accurate estimation difficult. The sequence has been subdivided into a series of units.

Basal Grey Shale Unit

At the base of the stratigraphic sequence are grey shales rhythmically interbedded with thin grey fine-sand and siltstones. The siltstone and sandstone beds occasionally have graded bases, laminated centres and rippled tops and have been interpreted as distal turbidites (Tongkul 1985). The siltstones rarely get above 30cm in thickness (and are usually under 10 cm in thickness) and make up some 20-40% of the sequence. The thickness of the unit is unknown (but is above 10m) as its base is always a thrust fault. In many imbricate packets this unit cut out altogether (see below).

Sandstone unit

FIGURE 3.4 - Local stratigraphy of Kota Kinabalu area (Study Area 1). The posibility of unidentified structural thickening means that the stratigraphic thickness are only approximate.

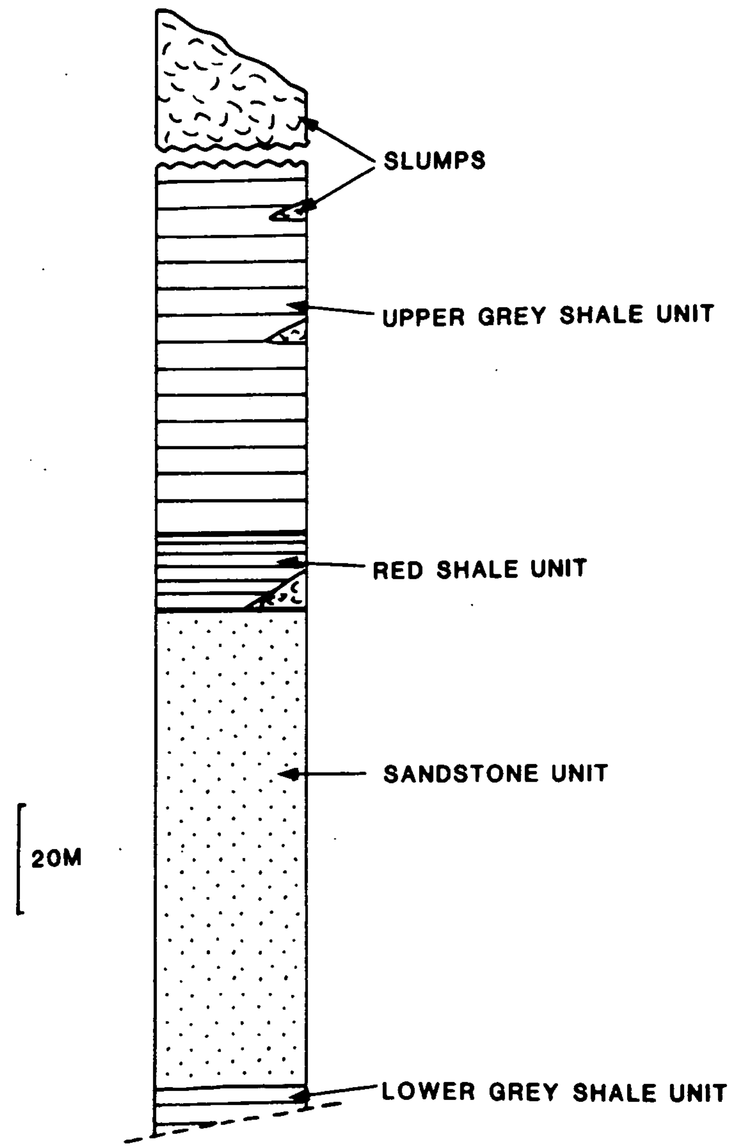

LOCAL STRATIGRAPHY IN KOTA KINABALU AREA

A thick sequence of sandstones (with subordinate grey shales and slits) approximately 70-90m thick overlies the Basal Grey Shale Unit. The contact between the two units is transitional, with an increase in the proportion and thickness of the sandstones in comparison with the shales. As a whole the Sandstone Unit has a thickening and coarsening-up sequence into its central sequences with a fining-up seqence at its top.

The basal parts of the Sandstone Unit commonly have the sandstone to shale ratio of about unity. The sandstone beds range between 30-150cm in thickness and are medium to coarse grained. Their bases commonly display sole markings and load structures (Plate 3.1). The full a, b, c, d, e, Bouma sequence is rarely displayed in any beds. They commonly have a graded 'a' division (with grading being more apparent near its top) and a cross-laminated or convoluted 'c' division. Only occasional beds show the parallel laminated 'b' division and even less often the 'd'&'e' divisions.

The middle sequences of the Sandstone Unit are characterised by massive medium to very coarse sandstones between 5-15m thick (Plate 3.2). Channelised bases are sometimes seen on outcrop scale. Internally, the sandstones are usually homogeneous ('a' division), although some show grading and crude laminations. Rip-up clasts are common near their bases. Amalgamated sequences,and erosive contacts between sandstone beds are common. Thin shale and silt partings are rare and form less than 2-3% of the sequence. The sequences of very massive sandstones are interspersed

PLATE 3.1 - Flute and grove casts on the base of turbiditic sandstone beds in the Sandstone Unit. (Pencil at middle bottom for scale, looking south, right of picture is W.)

PLATE 3.2 - Thick turbiditic sandstones in the Sandstone Unit. (looking south, right of picture is W.)

PLATE 3.3 - Interbedded thin sandstones and grey shales in the Upper Grey Shale Unit. (looking south, right of picture is W.)

with interbedded sequences of thick sandstones (30-300cm) and shales the latter making up only 5-15% of the sequence. These thinner interbedded sandstones often have homogeneous bases ('a' division) with grading being more evident at their tops, which may be laminated ('b' division). Their bases can be irregular, due to the presense of scour and groove marks. Sandstone dykes and other dewatering structures are sometimes found in this sequence. The upper sequences of the Sandstone Unit shows an overall upward fining and thinning sequence and exhibits many of the characteristics described for the basal sequences of the Sandstone Unit.

Red Mudstone Unit

A distinctive Red Mudstone Unit is found above the Sandstone Unit. The contact between the Red Shale and Sandstone Units is a rapid transition between interbedded thin sandstones and grey shale of the unit below and the red mudstones with only very occasional thin silts or fine sandstones above. The thickness of the Red Mudstone Unit is variable, as it is often the site of shearing and thrusting. The maximum undisturbed thickness recorded was in the order of 10-15m. The unsheared red mudstone exhibits a blocky fracture pattern and is massive. In one outcrop (Locality 1, see below) it would appear to have slumped. The contacts with the grey shale above and below are often the sites of reduction with the development of green shales. Similarly the margins of sandstone dykes in the slumped locality also often have green shale halos.

Upper Grey Shale Unit

The Upper Grey Shale Unit is similar in character to the Basal Grey Shale unit, being composed of interbedded grey silty shales and fine sand or siltstones with the grey shales generally predominating (Plate 3.3). The units thickness is in the order of 50-70m. The light grey sandstones are often graded with homogeneous ('a' division) or occasionally rippled (some are climbing ripples, 'c' division) bases, and silty parallel laminated tops ('d' division) which grade into the shales ('e' division). In some parts of the sequence the slity tops have a reddish colour. Present in the sequence are minor coarsening and thickening-up cycles, maximum bed thicknesses rarely exceed 70cm and are on average between 10-20cm thick. Slumped horizons a few meters thick also occur within the sequence.

Chaotic Unit (or Units)

The origin and possible stratgraphic position (if any) of these units is not clear. They consists of a chaotic mixture of sandstone and shales that are very similar to those of the other units in the stratigraphic sequence. The proportion of the different constituents is very variable and changes from exposure to exposure. It may be dominated by components derived from the Sandstone or Grey Shale Units. However, Red Shale Unit fragments have not been identified in them and it is not certain that the materials are derived from the stratigraphic section that is described below.

The distinctive feature of the unit is that the sandstones were not all consolidated at the time of its formation. Sandstone dykes are present and some sandstone blocks exhibit rounded or wispy terminations and pinch and swell structures. Complex, irregular, refolded folds are also seen. Occasionally sandstone blocks up to 10m in diameter occur, these are similar to the massive facies that characterizes the central regions of the Sandstone Unit. However, most blocks are under a few meters thick.

The matrix is unfoliated unless it has been later tectonised and can vary from being argillaceous through to being composed of muddy dark grey to black silt or even sand. The dark muddy silts are the most common constituent of the matrix. In the cases where the matrix is composed of bodies of sand and argillaceous material they often mixed in complex swirling patterns, suggesting that they were behaving as fluids during the main phase of disruption of the enclosed blocks. In other areas of melange intrusive relationships between matrix and enclosed blocks indicates that disruption may have occurred under high formational pressures.

3.2.2 Depositional Environment

The sedimentary sequence of the Crocker Formation in the Kota Kinabalu area is made almost entirely up of turbidites. No pelagic sediments have been identified. Northerly palaeocurrent directions, subparallel to the strike of the complex (Tongkul 1985; Stauffer 1967), are consistant with the interpretation that the turbidites were confined to a northerly trending trench in front of the accretionary complex.

Tongkul (1985), proposed that the Basal Grey Shale Unit is composed of distal turbidites. deposited below the carbonate compensation depth. Into this area a depositional lobe and channel system of a turbidite fan prograded, depositing the Sandstone Unit. The depositional lobe deposited the bedded sandstones at the base and top of the unit, whilst the massive amalgamated sandstones in the central portion are interpreted to be channel sequences. Eventually, the system migrated laterally or was abandoned and conditions returned to distal turbidite deposition which laid down the Upper Grey Shale Unit.

The association of the Red Shale Unit with the turbidites above and below would suggest that it is probably not a pelagic red shale deposit. Red shales are also interbedded with turbiditic sandstones in the East Crocker Fm. and it is much more likely that the red shale horizon represents a change in provenance of the incoming terriginous sediments.

The Chaotic Units are essentially melanges. Some exposures show abundant evidence of soft sediment deformation which are, in this study, generally interpreted to be slump deposits (see below, Localities 4 & 5). Other exposures, in which the matrix appears to have been mobile and intrusive in relation to blocks within it and wall rocks of the melange body, are better interpreted as diapiric in origin (see *below, Localities 8, 9 & 10).*

The stratigraphic position of the slump or slumps is not clear, but is thought to be high up in the Upper Grey Shale Unit. This is based on three lines of evidence:
1) The Upper Grey Shale Unit has a number of thin slumped horizons within it. Slumps are rare in other parts of the stratigraphic section.
2)The Chaotic Unit contains blocks that could easily have come from the Sandstone and Grey shale units.
3) The Chaotic Unit is commonly found just below the basal thrust of the imbricate packets i.e. commonly just below the Sandstone Unit.

3.2.3 *Description of Localities*

Good aerial photographic coverage of the environs of Kota Kinabalu and a large difference in topographic expression between the Sandstone Unit (Prominent Ridges) and Shale Units (valleys) has enabled structures to be extrapolated along strike relatively easily (Fig. 3.5). In the following text, structures described as "trenchward verging" are formed by overthrusting to the west or northwest and "arcward verging" structures by overthrusting to the east. The following descriptions are only of well exposed localities in which varying structural styles are developed. In each, part of the complex history of thrusting, folding and fabric development is revealed and taken toge. ther give a reasonable picture of the general structural development.

FIGURE 3.5 a - A geological map of Study Area 1 showing the distribution of the main lithostratigraphic units, general bed dips and identified and postulated thrust faults. Beds are in general steeply dipping (›65) and predominantly young to the east. The positions of the various sections/localities described are marked.

b - Photo lineament map compiled from air photos. Sandstones form NE trending ridges, whilst shales form valleys.

FIGURE 3.6 - Section 1 through Locality 1 showing a major westward verging fold pair whose central limb has been imbricated by a series of eastward verging thrusts (see Fig. 5 for position).

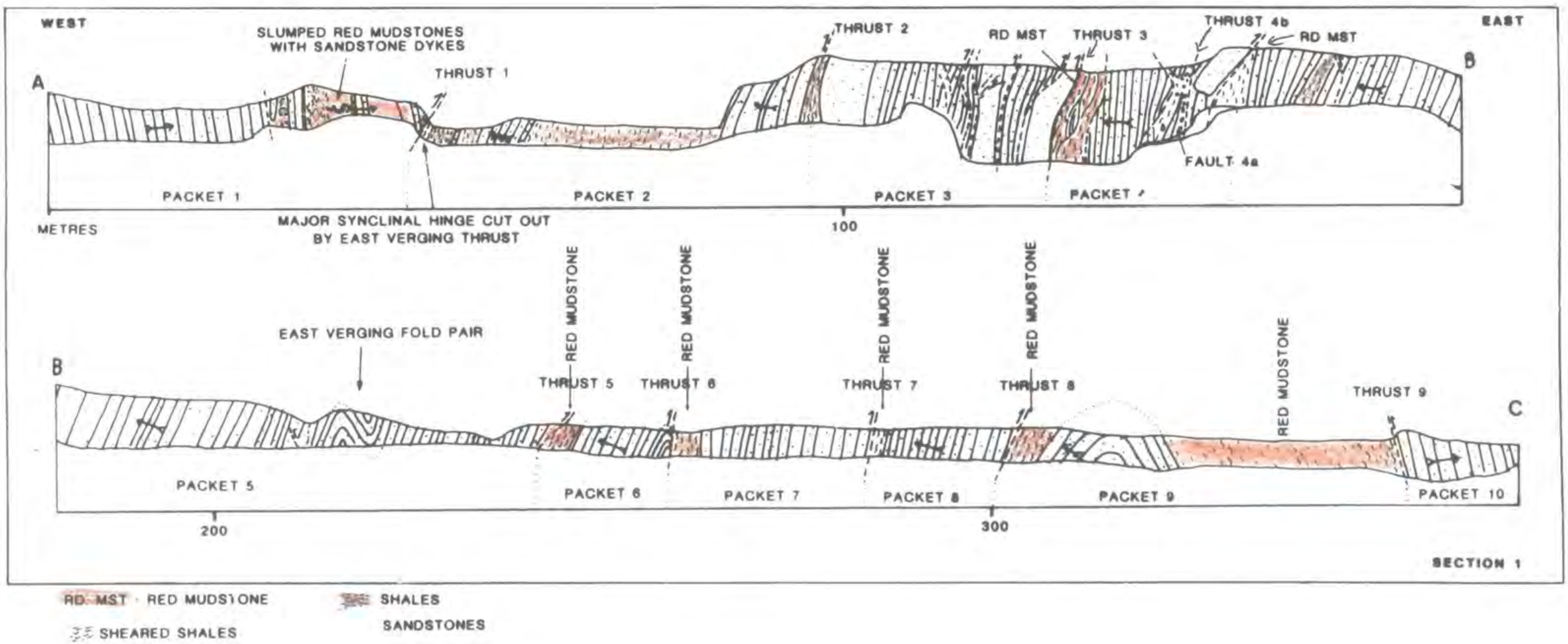
WEST
EAST
SLUMPED RED MUDSTONES WITH SANDSTONE DYKES
THRUST 1
THRUST 2
RD MST
THRUST 3
THRUST 4b
RD MST
FAULT 4a
A
B
PACKET 1
PACKET 2
PACKET 3
PACKET 4
METRES
MAJOR SYNCLINAL HINGE CUT OUT BY EAST VERGING THRUST
100
EAST VERGING FOLD PAIR
RED MUDSTONE
RED MUDSTONE
RED MUDSTONE
RED MUDSTONE
RED MUDSTONE
THRUST 5
THRUST 6
THRUST 7
THRUST 8
THRUST 9
B
C
PACKET 5
PACKET 6
PACKET 7
PACKET 8
PACKET 9
PACKET 10
200
300
SECTION 1
RD MST · RED MUDSTONE
SHEARED SHALES
SHALES
SANDSTONES

PLATE 3.4 - Sandstone dyke cutting through a slumped Red Mudstone sequence. Note blocky fracture pattern in the unsheared mudstones and the green reduction halo around the sandstone dyke. (looking south, right of picture is W., lense cap bottom centre for scale)

PLATE 3.5 - Intense scaly clay development and minor disrupted folds in the Red Mudstones along Thrust 1. Green reduced areas in the shales, on the right of the picture, are also sheared. (Looking South, right of picture is W.)

PLATE 3.6 - Intensely sheared red and green scaly clays along Thrust 3. Minor folds in scaly clays indicate an eastward direction of overthrusting. (Looking south, right of picture is W.)

fracture pattern with the green alteration forming irregular patches in them.

The red mudstones are cut-out by a Thrust 1 which dips to the west (Fig. 3.6). Thrust 1 also cuts out the hinge of a major syncline, as indicated by a younging reverse. The fault zone is characterised by the development of intense scaly clay fabrics over a 5m band (Plate 3.5). The scaly clays are affected, in places, by minor eastward verging folds.

Packet 2 (45-85m, Fig. 3.6) consists of grey shales and occasional sandstone beds. The sandstones young to the west. The grey shales are sheared in places, with the development of scaly fabrics, and are thought to be internally imbricated. From 85m eastwards, sandstones become with some imbrication along their contact. Minor imbrication and folding in the scaly clay fabrics in the grey shales along Thrust 2 suggest that over-thrusting was the to the east. S-C fabrics (see Loc 2) are developed in the most intensely sheared regions of the fault zone.

The sandstones in packet 3 (95-125m) are internally imbricated with the minor thrusts having eastwards senses of over-thrusting. Thrust "3", lies in intensely sheared red and green shales (Plates 3.6 & 3.7). Included in the intense scaly clays of the fault zone are phacoidal sandstone blocks, disrupted and extended along brittle shears (Plate 3.7).

PLATE 3.7 - Close up of the intensely deformed interior regions of the fault zone of Thrust 3. Distrupted phacoidal sandstone blocks and folded scaly clays are common in the hanging wall regions of the fault zone. (Looking south, right of picture is W.)

Packet 4 sandstones (125-145m) are affected by a distinctive fault zone (Fault 4a). The sandstone blocks in the fault zone do not have the usual phacoidal shapes, but are instead more rounded in shape (Plates 3.8 & 3.9). Closer examination of the blocks reveals that the blocks are disaggregating along their margins, with sandstone fragments spalling off into the mud matrix. The process was proceeded by the injection of the block's margins by the argillaceous matrix, which consequently must have behaved as a fluid and been fairly mobile at that time. The matrix is now composed of scaly clays, indicating that there has been post injection/disruption shearing of the matrix. Thrust 4b at 145m, is thought to be the main packet bounding fault. It consists of a 3-4m thick zone of sheared red and green shales in which scaly clay fabrics are well developed.

Packet 5 (150m-240m) contains an eastward verging fold pair (at 220m), that has a sense of overthrusting that is consistant with the eastward verging thrusts. Packets 6,7 & 8 (Fig. 3.6), are roughly the same thickness (15-20m) and appear to be minor imbricates of the upper parts of the Sandstone Unit and Red Mudstone Unit. The sheared red mudstones are proposed as the sites of the packet bounding thrust faults (Thrusts 5 to 8).

Packet 9 (Fig. 3.6) contains a shallowly plunging, up-right, major anticlinal fold (Fig. 3.7), which duplicates the red mudstones. The red mudstones on its eastern limb are much thicker than those on its imbricated western limb (described previously) and the latter are considered to be

FIGURE 3.7 - Plunges of the major west verging fold pair and later superimposed minor east verging fold pair that is associated with the eastward directed thrusts.

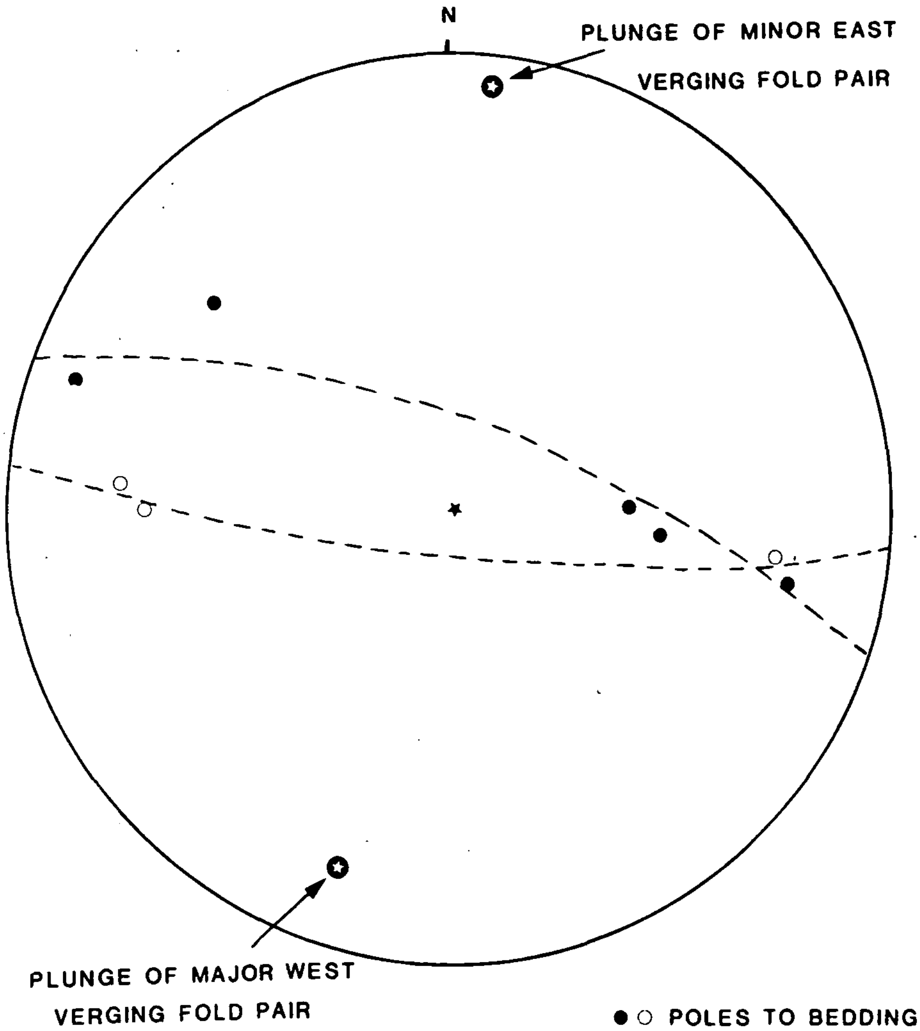
N
PLUNGE OF MINOR EAST VERGING FOLD PAIR
PLUNGE OF MAJOR WEST VERGING FOLD PAIR
● ○ POLES TO BEDDING

PLATE 3.8 - Distinctive rounded ends to elongate sandstone blocks and rounded smaller blocks in Fault zone 4a. (Looking south, right of picture is W.)

PLATE 3.9 - Close up of rounded blocks in Fault Zone 4a in which the intrusion of argillaceous material into the exterior regions of the sandstone block has contributed to its disruption and rounded shape. (Looking south, right of picture is W.)

structurally thinned. Sandstones outcrop above the red shales on the eastern limb of the anticline (eastwards of 345m, Fig. 3.6) and it is necessary to propose that a thrust contact exists between them.

Interpretation of structures- *The main structural elements developed at this locality appear to be a westward (trenchward) verging major fold pair, and the eastward (arcward) verging minor fold pair and thrusts that have eastward sences of over-thrusting. The eastward verging thrusts are interpreted to imbricate and, therefore, postdate the main fold pair, shortening its central limb, faulting out the hing of the syncline and repeating the Red Mudstone Unit (Fig. 3.8). The half-wavelength of the main fold pair is at present some 280m, and was probably considerably longer before shortening of the central limb took place, perhaps in the order of 500m or more. Such a long wavelength fold would require a considerably thicker stratigraphic section than is available (140-180m). Therefore, prior to the formation of the main fold pair, structural thickening of the 140-180m stratigraphic section by thrusting is proposed to have occurred (Fig. 3.9). The postulated early imbrication and subsequent folding into a trenchward verging fold pair may have occurred relatively soon after accretion. The back-thrusting potentially occurred much later. Back-thrusts in the Barbados accretionary complex (see Chapter 1) develop well back in the accretionary complex, in the Zones of Stabilization, and Supra-Complex basins. The back-thrusting may be preferentially associated with the central limb of the fold-pair as a result of its previous rotation into a low*

FIGURE 3.8 - Sketch cross section illustrating a likely configuration for the deeper regions of the back thrust system. There is no vertical exageration.

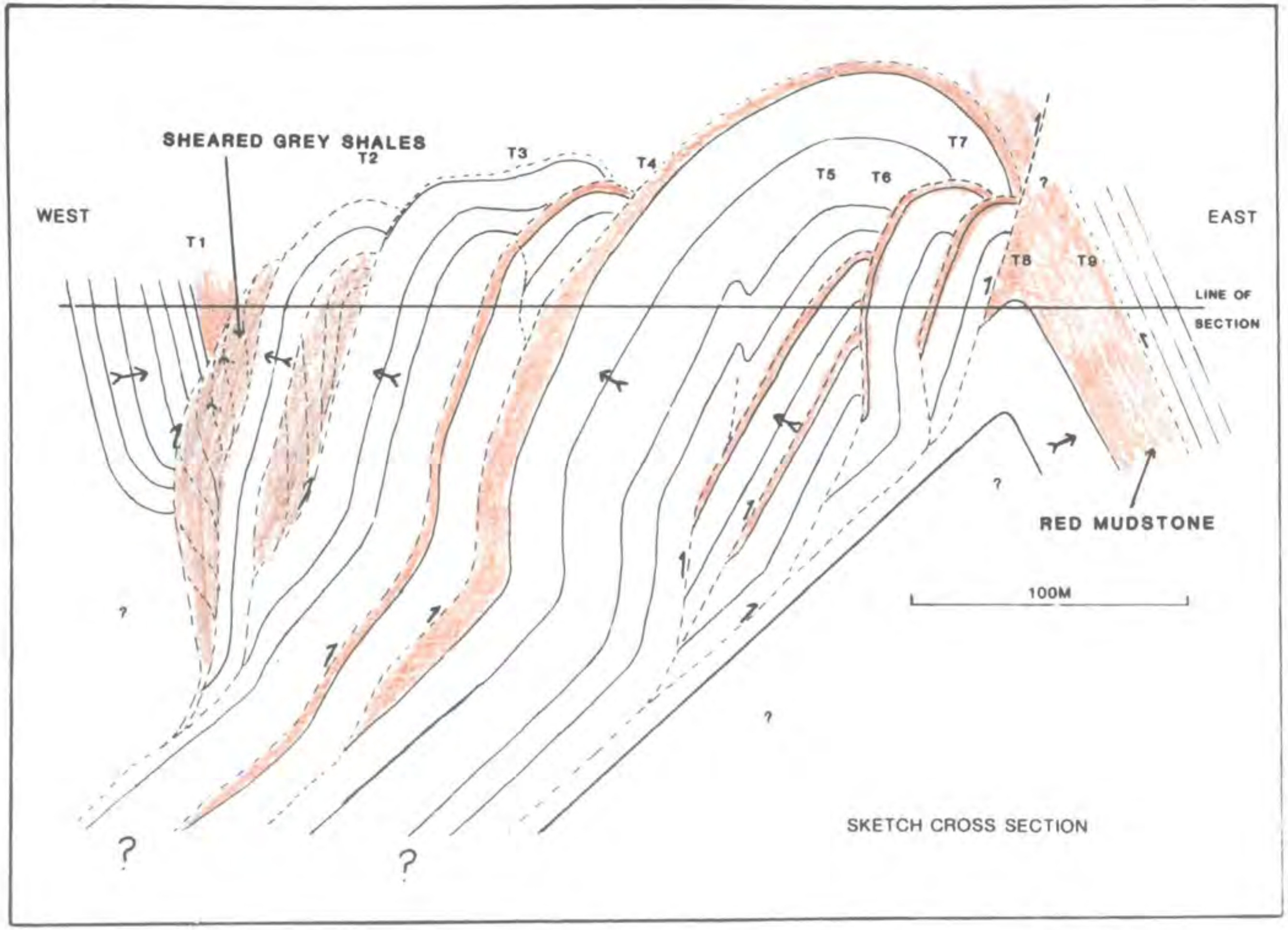
SHEARED GREY SHALES
WEST
EAST
T1
T2
T3
T4
T5
T6
T7
T8
T9
LINE OF SECTION
RED MUDSTONE
100M
SKETCH CROSS SECTION

FIGURE 3.9 - Possible previous configuration of the early major west verging fold pair before the back thrust system imbricated its central limb. The probable original long wavelength of the fold pair suggests that it affected an sequence already thickened by thrusting.

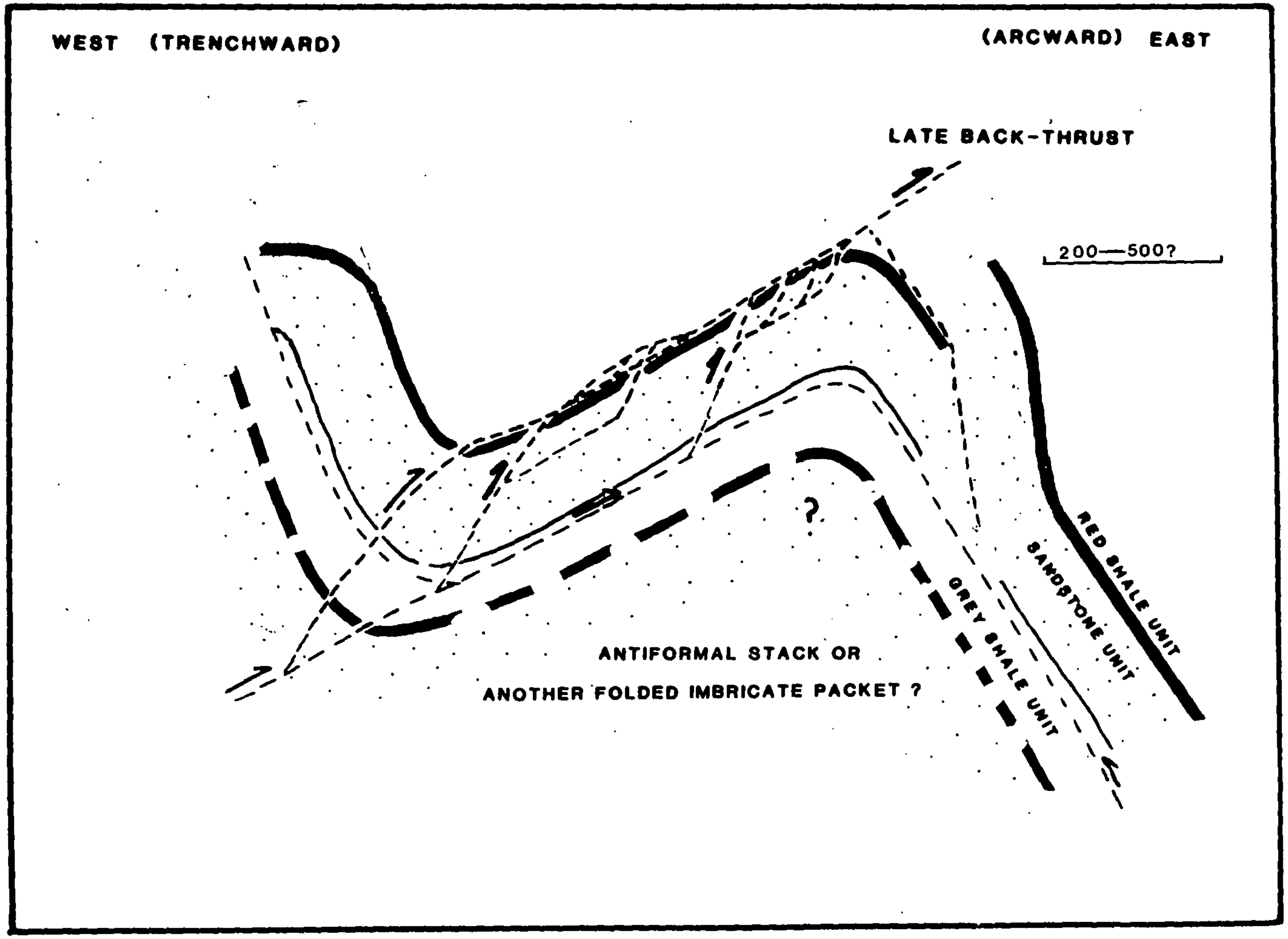
WEST (TRENCHWARD)
(ARCWARD) EAST
LATE BACK-THRUST
200—500?
?
RED SHALE UNIT
SANDSTONE UNIT
GREY SHALE UNIT
ANTIFORMAL STACK OR
ANOTHER FOLDED IMBRICATE PACKET ?

angled orientation, enhancing the prospects for thrust development.

Location 2

Locality 2 is a section through a thrusted sequence of steeply dipping grey shales and sandstones (Sections 2a & 2b respectively, Figs. 3.10 & 3.11). The exposures are a result of quarrying and trenching during the construction of a housing estate.

The grey shales (Section 2a, Fig. 3.11) are interleaved with thin slivers of the red mudstones and have subsequently been in part dismembered by abundant conjugate faults. The conjugate faults strike in a northerly direction and indicate east-west compression and vertical extension. The western 20m of Section 2a is moderately to intensely deformed with a considerable amount of bedding parallel faulting and disruption. Parts of the section have suffered soft sediment deformation with irregular bulbous folds and sandstone dyking and it would appear that slumped horizons have been caught up in the fault zone. The red mudstone unit marks the eastern edge of this zone of deformation, which is interpreted to be a major fault zone. Minor folds and a larger dismembered west verging fold pair indicate that it has a westward sense of overthrusting. Apart from minor reversals across folds, beds dominantly young towards the east.

Section 2b (Figs. 3.10 & 3.11) is a cross section through a sandstone ridge in which there is a major, well exposed 45m

FIGURE 3.10 - Sketch section across area of Locality 2 showing relationship of detailed Sections 2a and 2b to other nearby structures. (see Fig 3.5 for position)

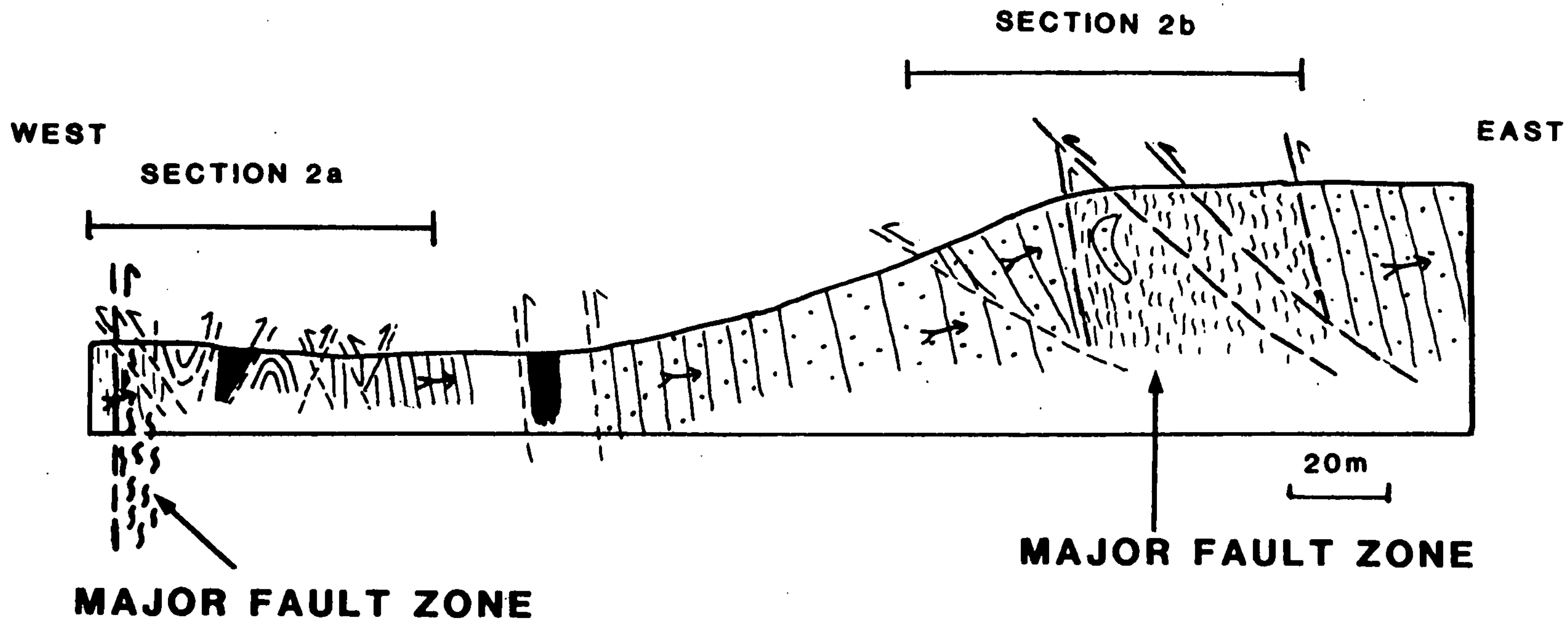
SECTION 2b
WEST
EAST
SECTION 2a
20m
MAJOR FAULT ZONE
MAJOR FAULT ZONE

FIGURE 3.11 - Detailed sections through a Grey Shale Unit (Section 2 a) and a major fault zone (Section 2b) at Locality 2. Insets a, b & c (Section 2b) show the detailed fabric relationships in key areas of the fault zone.

wide fault zone. The bounding surfaces of the fault zone strike and dip at 55°-65°/200° E and the sandstones on either side of the fault zone young to the east. The fault zone is confined to a grey shale lithology, shearing and chloritic mineral growth has given it a metamorphic resemblence. Occurring within the fault zone are a complex, but well developed, set of fabrics that document the varying response of material in the fault zone to a prolonged history of movement. The fabric development can be divided into three stages (Fig. 3.12).

Stage 1, fabrics are preserved at the western margin of the fault zone (Plate. 3.10). They consist of layer parallel intense scaly clay fabrics and the layer parallel extension and disruption of thin sandstone beds within the grey shales. Where later fabrics have not rotated the larger disrupted bodies, the orientation of their long axes is subparallel to the margins of the fault zone. Associated with this phase are a series of disrupted tight to isoclinal folds, of which only the hinge areas now remain. At the eastern end of the section the scaly clays appear to have been replaced by a more uniform set of fabrics (see below).

Stage 2, is the formation of two, more planar spaced fabrics near the eastern margin of the fault zone (inset a, Section 2b Fig. 3.11). Almost ubiquitously developed is an intense closely spaced sub-planar fabric, striking sub-parallel to the fault zone but with an oblique vertical, or slightly westward dip. This fabric is orienatated nearly sub-parallel, or with a clock-wise transection (up to 20°-30°

PLATE 3.10- Moderately well developed scaly clay fabrics near the footwall of the fault zone. Scaly clay fabrics and long axes of sandstone fragments in the scaly clays are roughly subparallel. (Looking north, right of picture is E.)

PLATE 3.11 - Proposed SC fabric development next to block shown in inset b on section 2b. S fabrics have sub-vertical orientations whist the shear planes of the C fabric dip from left to right. The block has suffered shearing across a zone in which the C fabrics are particularly strong. This picture is from the point where the shear zone deflects the block so that it is orientated sub-parallel to the C fabric. (Looking north, right of picture is E.)

degrees) in relation to the long axes of the sandstone blocks (Plates 3.11 & 3.12). Similar mixed relationships are seen with folds developed with in the zone, with the development of axial planar to slightly clock-wise transecting cleavages, (Fig. 3.11, insets b & c). This early fabric (or cleavage) and blocks are cut and displaced by closely spaced shear zones, that dip at 60° degrees, sub-parallel to the fault zone margins (Plate 3.11). The latter are most intensely developed within certain narrow zones (see Section 2b, Fig. 3.11).

Stage 3 consists of moderately low angled (between 38°-45° degrees) thrusts and associated shear zones that have a westward sense of overthrusting. The thrusts and shear zones cut across the blocks and earlier fabrics alike causing them to deflect into the higher strain zones (Fig. 3.11, inset c & area marked as containing third stage fabrics). The thrust zones and related shear zones 25m from the eastern end of Section 2b, are the best developed of these late lower-angled features (Plate 3.13).

<u>Interpretation of structures-</u> The Stage 1 & 2 fabrics are thought to have formed in a shear zone corresponding to an originally much lower angled thrust (Fig. 3.12 a & b). The dismembered folds and irregular scaly clay fabrics associated with the Stage 1 disruption are only preserved near the footwall of the fault zone and appear to be similar to those developed in the thrusts of other localities, with extension of the blocks occurring parallel to the fault zone margins. The Stage 2 fabrics are rather different. Cleavage is rarely

PLATE 3.12 - Proposed S- C fabric development nearer the hanging wall of the fault zone. S fabrics are closly spaced and have near vertical dips cutting at high angles across the long axes of the blocks. The C fabrics are spaced some 1-5mm appart and dip at lower angles and are sub parallel to the margins of the larger blocks. (Looking north, right of picture is E.)

PLATE 3.13 - Crude S-C fabric development along a late low angled thrust zone approx 60m east of western end of section 2b.

FIGURE 3.12 - Proposed stages in the evolution of the fault zone fabrics. a) Early scaly clay development. b) Later development of ductile shear fabrics (S & C Fabrics) as the material in the fault zone consolidates. Lastly, (c) either the development of late extensional crenulation clevages 3ECC) as a continued response to ductile shearing or (d) Extensional shear bands developed in response to a later low angled phase of thrusting after back rotation of the fault zone.

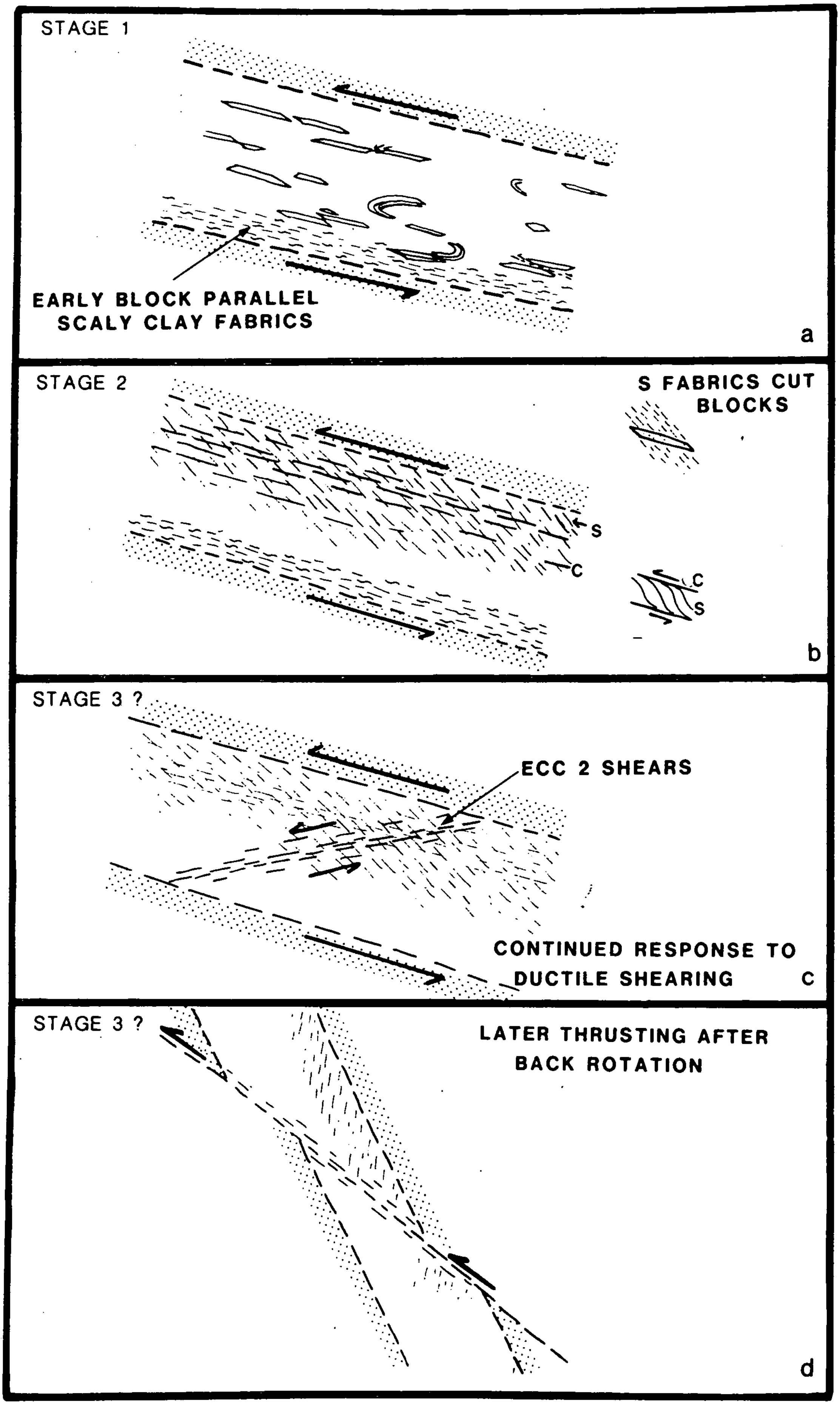

STAGE 1
EARLY BLOCK PARALLEL
SCALY CLAY FABRICS
a
STAGE 2
S FABRICS CUT
BLOCKS
S
C
C
S
b
STAGE 3 ?
ECC 2 SHEARS
CONTINUED RESPONSE TO
DUCTILE SHEARING
c
STAGE 3 ?
LATER THRUSTING AFTER
BACK ROTATION
d

developed in these western regions of the Crocker Fm., the association of a particularly well developed cleavage in this fault zone suggests that its occurrence is in some way related to the kinematics of faulting. The now sub-vertical fabric appears to have resulted from flattening of the fault zone material, with the folds and blocks having been at least partly rotated into the flattening plane. It may, therefore, correspond to a type of "S-fabric" in a ductile shear zone (cf. Platt 1984, Fig. 3.13). S or shape fabrics are interpreted to develop in response to flattening strains and correspond to the XY plane of the finite strain ellipsoid (Ramsay & Graham 1970). In this case flattening during simple shearing is thought to have caused the compaction of the argillaceous material of the fault zone with the possible development of a pressure solution cleavage. The shear zones that dip sub-parallel to the fault zone margins may then correspond to "C-fabrics" (after Ponce de Leon & Choukroune 1980). They are not very strongly developed and appear to correspond to only relatively minor amounts of post flattening (post S fabric) displacement.

The Stage three thrusts and shear zones may be accounted for by two different mechanisms. A third set of fabrics, termed extensional crenulation cleavages (ecc), may develop in ductile shear zones (Fig. 3.13 & Fig. 3.12 c) and the orientation and sense of shear on the stage 3 fabrics are consistant with their origin by such a mechanism. It is thought more likely, however, that Stage 3 results from a quite unrelated episode of later thrusting, affected the zone after it was rotated to high angles (Fig. 3.12 d). The

FIGURE 3.13 - Development of shear fabrics (S-Fabrics, C-fabrics & extensional crennulations (EEC)) in ductile shear zones (Platt 1986).

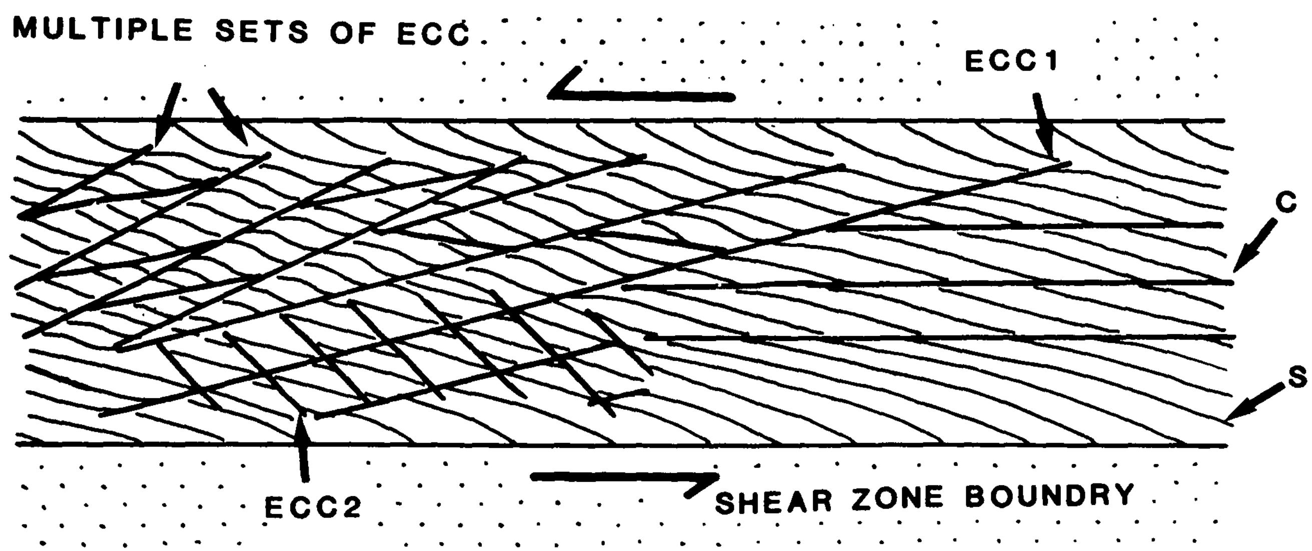
MULTIPLE SETS OF ECC
ECC1
C
S
ECC2
SHEAR ZONE BOUNDRY

thrust, 5-10m from the western end of the Section 2b (Fig. 3.11) that verges to the west, cutting down section through the sandstones (i.e. with a lag geometry), is a neighbouring example of this late out-of-sequnce thrusting.

Locality 3

Locality 3 is a series of sections through a Grey Shale Unit and its thrusted contact with a structurally higher Sandstone Unit package (Fig. 3.14). Sections 3a & 3b are through the Grey Shale Unit which consists of interbedded gray shales (40-70% of section), and thin sand and siltstone beds a few centimetres to 50cm in thickness (dominant thickness 4-20cm). The beds are dominantly steeply bedded ($\gg 60^{\circ}$ degrees) and strike to the NE (between 210°-225° N).

The western end of the cross section (Section 3a, Figs. 3.14 & 3.15) is through homoclinally bedded strata cut by occasional west and east verging reverse faults that dip at between 25-80 degrees (~~Plate 3.14~~). The westward verging reverse faults cut down section and are more obviously late structures. The eastward verging faults show variable cross cutting relationships with the west verging set and are interpreted to have formed at the same time. Larger faults (displacements > 1m) commonly have red calcite veins running along them. Figure 3.16, is a stereoplot of poles to reverse fault planes and illustrates the conformity in the NW strike, but spread in dips of the the faults. They are interpreted to be conjugate fault systems formed in a NW-SE compressional field, with vertical extension. The variation in dips may reflect complex variations in local stress conditions.

In the central areas of the cross section (Section 3b, Figs. 3.14 & 3.15) the intensity of faulting increases, and west verging fold pairs become common (~~Plate 3.15~~). The

FIGURE 3.14 - Detailed Sections (3a , 3b & 3c) through a grey shale unit and a m ajor thrust contact with a structurally overl ying sandstone unit. (See Fig. 3.5 for position)

FIGURE 3.15 - Summary section showing the main features of Section 3a, b & c.

FIGURE 3.16 - Equal area stereoplot of poles to reverse c onjugate fault plains. A NW- SE principal axis of compression is indicated by the pattern.

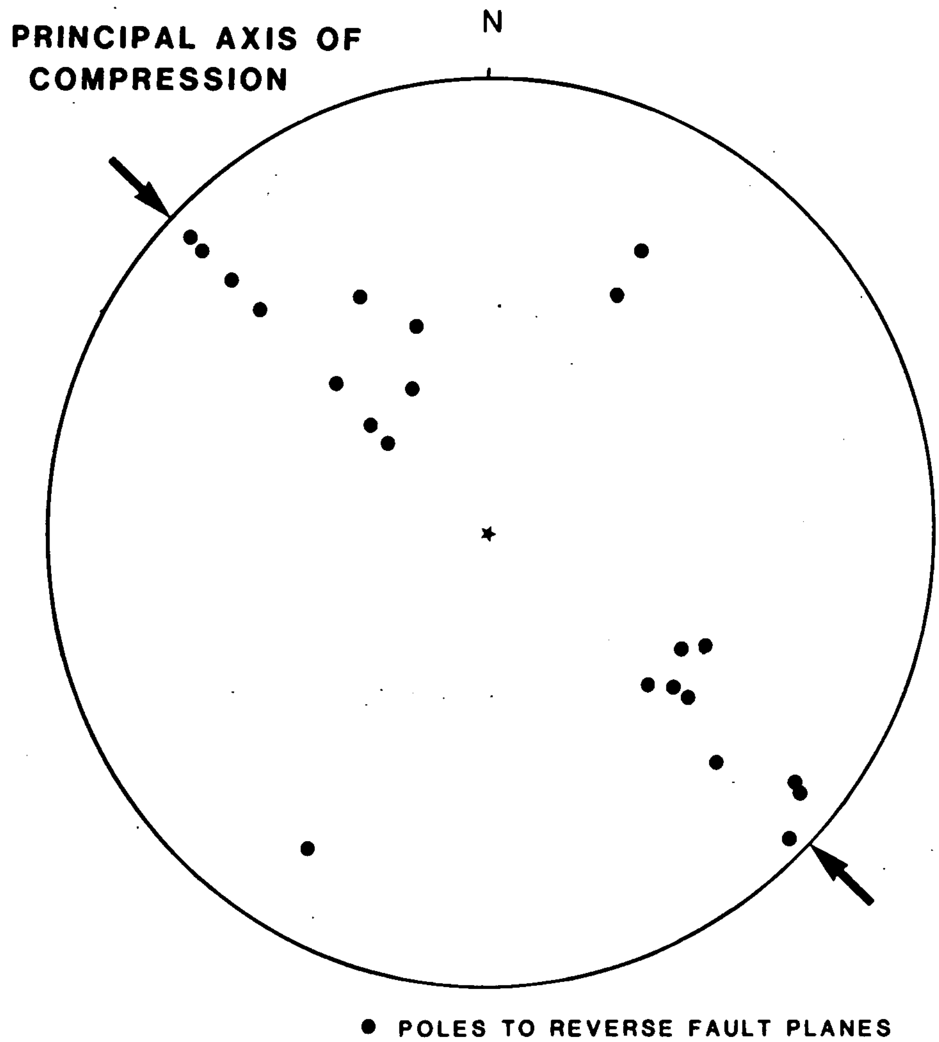
PRINCIPAL AXIS OF
COMPRESSION
N
● POLES TO REVERSE FAULT PLANES

folds trend NE and are generally upright with sub-horizontal hinges. The folds are cut-by, and predate, the conjugate fault systems.

The major fault zone between the Sandstone and Grey Shale Units (Section 3c, Fig. 3.14) is a 15-20m wide zone of intense stratal disruption situated in the uppermost part of the Gray Shale Unit. The evolution of the zone has been complicated by the possible effects of two periods of movement on it. Early deformation in the zone is characterised by layer parallel shearing and extension of thin sandstone beds with a mild scaly clay fabric (individual chips 0.25-0.5cm in length) running sub-parallel to the long axes of the blocks (Plate 3.16). Part of the western contact of the deformed zone is preserved and fabrics dip vertically, sub-parallel to bedding and it is thought that early displacement occurred parallel to bedding so that the fault zone reflects a 'flat' of a ramp and flat thrust geometry. The disrupted, foliated material has than been folded into a series of west verging folds in the central regions of the fault zone. The folds are asymmetrical, with axial planes that dip at approximately 60° degrees (Plate 3.17). It is possible that the folds formed, after initial layer parallel disruption had occurred, but during the same phase of movement on the fault zone. However, the shear zones associated with the folds appear to continue as more discrete fault zones cutting, down section, into the footwall of the fault zone, displacing the western margin of the fault zone and dismembering an early isoclinal fold.(Section 3c, Fig. 3.14). The eastern margin of the fault zone cuts obliquely

PLATE 3.16 - Early extensional fabrics in the major thrust zone beneath the Sandstone Unit. Thin sandstone beds are cut by extensional shears that root into the scaly clays around them. (Looking north, right of picture is E.)

PLATE 3.17 - West verging folds deform the scaly clays and early extensional fabrics. (Looking north, right of picture is E., field-of-view approx. 15m)

across the base of the hanging wall sequence, also suggesting that at least some movement on the fault zone occurred after rotation of the beds to steep orientations, relatively late in the areas structural development.

Location 4

Location 4 is a cross section through an area of melange, of uncertain origin, that occurs along the thrusted contact between the red mudstone and gray shale lithologies (Fig. 3.17, Section 4). The eastern margin , and probable hanging wall, of the zone of disruption, youngs to the west and is, from reconaissance mapping, the western limb of a large (›› 200m wavelength) anticline (see Fig. 3.19 below). The contact between the relatively undeformed hanging wall sequence and the melange is complex and very irregular (Plate 3.20). In part, this is the result of its displacement by later faulting but an intrusive relationship is possible.

The earliest deformation features of the melange are soft sediment structures such as bulbous or necked sandstone beds, irregular wispy and rootless folds, and irregular or rounded to sub-circular block shapes (insets a, b & c Fig. 3.17, Plates 3.18 & 3.19). Some of the rounded blocks appear to have become further disrupted insitu, by a process that gives them an exfoliated appearance (Plate 3.19). In the areas where a random block orientation is preserved there may be little or no scaly clay development. In the region where exfoliation of the blocks appears to be occurring, the fabric wraps itself round the blocks. Early tight to isoclinal

FIGURE 3.17 - Section 4 runs through an area of melange along a thrust contact. The melange exibits early soft sediment features (insets a, b, c, d) that have been subsequently overprinted by shearing, scaly clay formation and conjugate reverse faulting. The later phase of shearing is probably of tectonic origin and has produced a series of west verging and downward facing folds and refolds (inset e). The early soft sediment features may be a product of slumping.

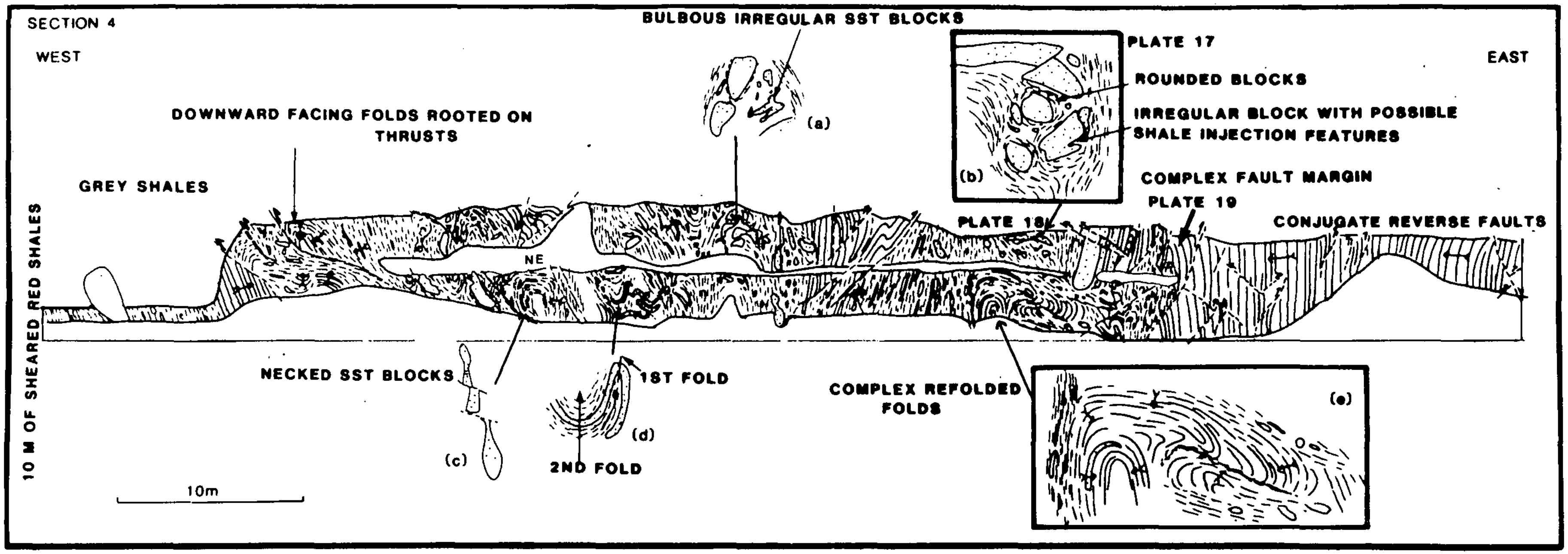

SECTION 4
WEST
EAST
BULBOUS IRREGULAR SST BLOCKS
(a)
PLATE 17
ROUNDED BLOCKS
IRREGULAR BLOCK WITH POSSIBLE SHALE INJECTION FEATURES
(b)
COMPLEX FAULT MARGIN
PLATE 19
PLATE 18
CONJUGATE REVERSE FAULTS
DOWNWARD FACING FOLDS ROOTED ON THRUSTS
GREY SHALES
NE
10 M OF SHEARED RED SHALES
NECKED SST BLOCKS
(c)
1ST FOLD
2ND FOLD
(d)
COMPLEX REFOLDED FOLDS
(e)
10m

PLATE 3.18 - Mild scaly clay fabrics wrapping rounded sandstone blocks. (Looking north, right of picture is E.)

PLATE 3.19 - Chaotically oriented sandstone blocks in the less sheared areas of the melange. Note exfoliated appearance of some of the blocks. (Looking north, right of picture is E.)

PLATE 3.20 - Irregular eastern contact of the melange body. Note late reverse faults that cut and displace the contact between deformed and undeformed areas. (Looking north, right of picture is E., field-of-view is approx 10m)

folds may have a fabric developed parallel to their axial planes (inset d, Fig. 3.17).

The majority of the scaly clay fabrics are thought to have been imposed on an already disrupted sequence, modifying block shapes and aligning them with the foliation. Early folds and disrupted blocks and fabrics alike have been folded round a series of later structures. Near the western end of Section 4 the later folds can be seen to be rooted on shear or thrust zones that verge to the west. Complex patterns of disharmonic refolding are developed in places (inset e, Fig. 3.17) and where younging directions of blocks in the melange can be identified the later folds are commonly downward facing. Late brittle east and west verging reverse conjugate faults sets cross-cut melange and wall rocks alike they are best seen at the eastern end of the section (Plate 3.20).

<u>Interpretation of structures-</u> The simplest explanation for the origins of the melange body is that it is a slumped sequence that has been caught up along a thrust zone with the imposition of tectonic fabrics like the scaly clays. However, there is the possibility that the eastern contact is an intrusive one and this favours a diapiric emplacement mechanism.

Location 5

Location 5 is a quarry exposure, situated in an area of melange approximately along strike of the similar, or, equivalent, body of melange at Location 4 (Fig. 3.5). Both, *early soft sediment deformation features, and intrusive relationships are seen in Locality 5 and the mode of its origin is not immediately apparent.*

Soft sediment deformation textures include, irregular sandstone blocks with wispy terminations and sandstone dykes preserved in less deformed regions of the outcrop (Plates 3.21 & 3.22). The matrix of the melange is a dark gray silty and sandy mudstone in which only a crude, spaced scaly foliation is developed over much of the outcrop. The overall foliation and minor block orientation is highly irregular in the upper parts of the outcrop forming swirling patterns that suggests a high degree of mobility during its formation.

Another important feature of Section 5 (Fig. 3.18) is a block containing a currently recumbent and partially disrupted syncline composed of thick bedded sandstones (30-80cm) of the Sandstone Unit. This has been disrupted by the matrix which appears to have flowed up round, and detached part of it (Plate 3.23; inset b, Fig. 3.18). Near the eastern edge of the exposure, intrusive looking configurations between the bodies of sandstone and melange occur (Plate 3.24).

Interpretation of structures- *The intrusive configurations and apparent disruption of the synclinal block by the matrix (Inset b. Fig. 3.18) suggest a diapiric origin for the melange, whilst the soft sediment textures indicate it may be part of a very large slump sequence. Tectonism along a fault zone has been ruled out as a likely cause, as structures and textures are much too irregular to have formed in simple zone of shearing.*

FIGURE 3.18 - Location 5, a quarry exposure through part of a body of melange in which soft sediment features occur. The argillaceous matrix appears also to be flowing up round the large sandstone blocks (Inset b) developing intrusive relationships in places.

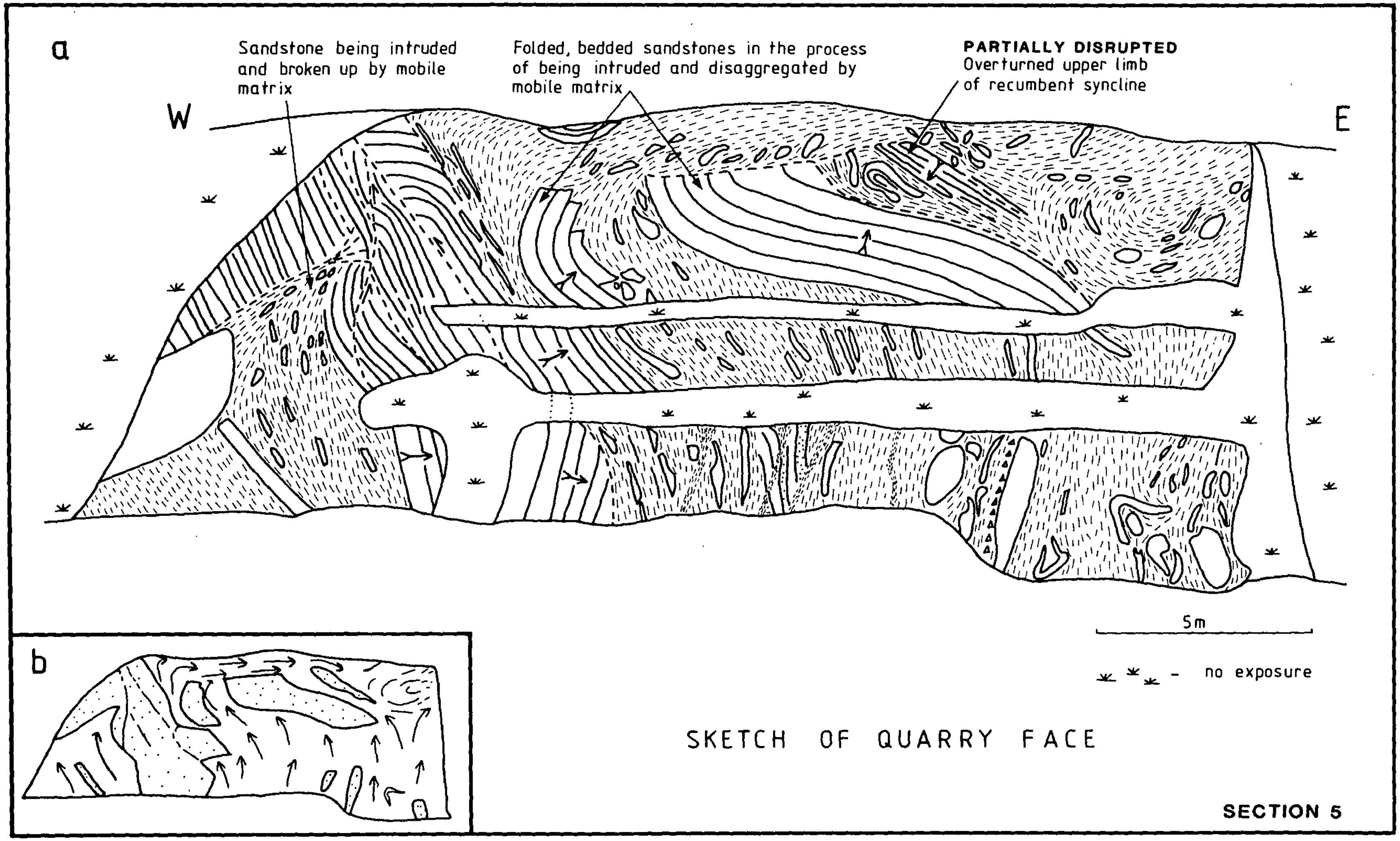

SKETCH OF QUARRY FACE

SECTION 5

PLATE 3.21 - Irregular wispy terminations to sandst one blocks (Looking north, right of picture is E.)

PLATE 3.22 - Sandstone dykes and other rounded sandstone bodies. (Looking north, right of picture is E.)

PLATE 3.23 - General shot of locality 5 showing the dark grey mudstone matrix intruding up round a large sandstone block (Looking north, right of picture is E.)

Location 6

Location 6 consists of two transects through areas of poor exposure east of Locations 4 & 5 (Sections 6a & 6b, Fig. 3.19). Section 6a continues westward of Location 5 for 900 m and reveals the existence of several important younging reversals that appear to indicate the existence of large folds (approx. 150m half-wavelength) with slightly overturned, west younging limbs. A synclinal hinge is thrust out in the centre of the section and there is a strong possibility of similar thrusts elsewhere in the section. The major fault zone (Loc 6a, Section 6a, Fig. 3.19) on the western margin of the sandstone ridge runs through an zone of melange (or broken formation) which appears to be primarily tectonic in origin. However, occasional large subrounded blocks do occur within the zone (Plate 3.24). They appear to have formed as mega-boudins and suggest that the sandstones were not well consolidated before they were tectonised. Sense of shear indicators such as minor folds indicate overthrusting to the west. The central portions of Section 6a run across a ridge of higher land, indicating that they are composed mainly of sandstones.

The melanges (Loc 6b), at the eastern end of Section 6a are over 40m thick and exhibit a wide range of features that suggest they were not consolidated before they were deformed (Section 6c, Fig. 3.20) In particular, parts of the melange have a matrix consisting of sandstones, complexly interfingered with unfoliated muds, indicating that the matrix was completely fluid during the main phase of

FIGURE 3.19 - Two transects through areas of relatively poor exposure (Section 6a & 6b). The sections run through Localites 4 & 5 and reveal that several important younging changes occur, indicating the existance of 150 - 200 half wavelength folds. (See Fig. 3.5 for position)

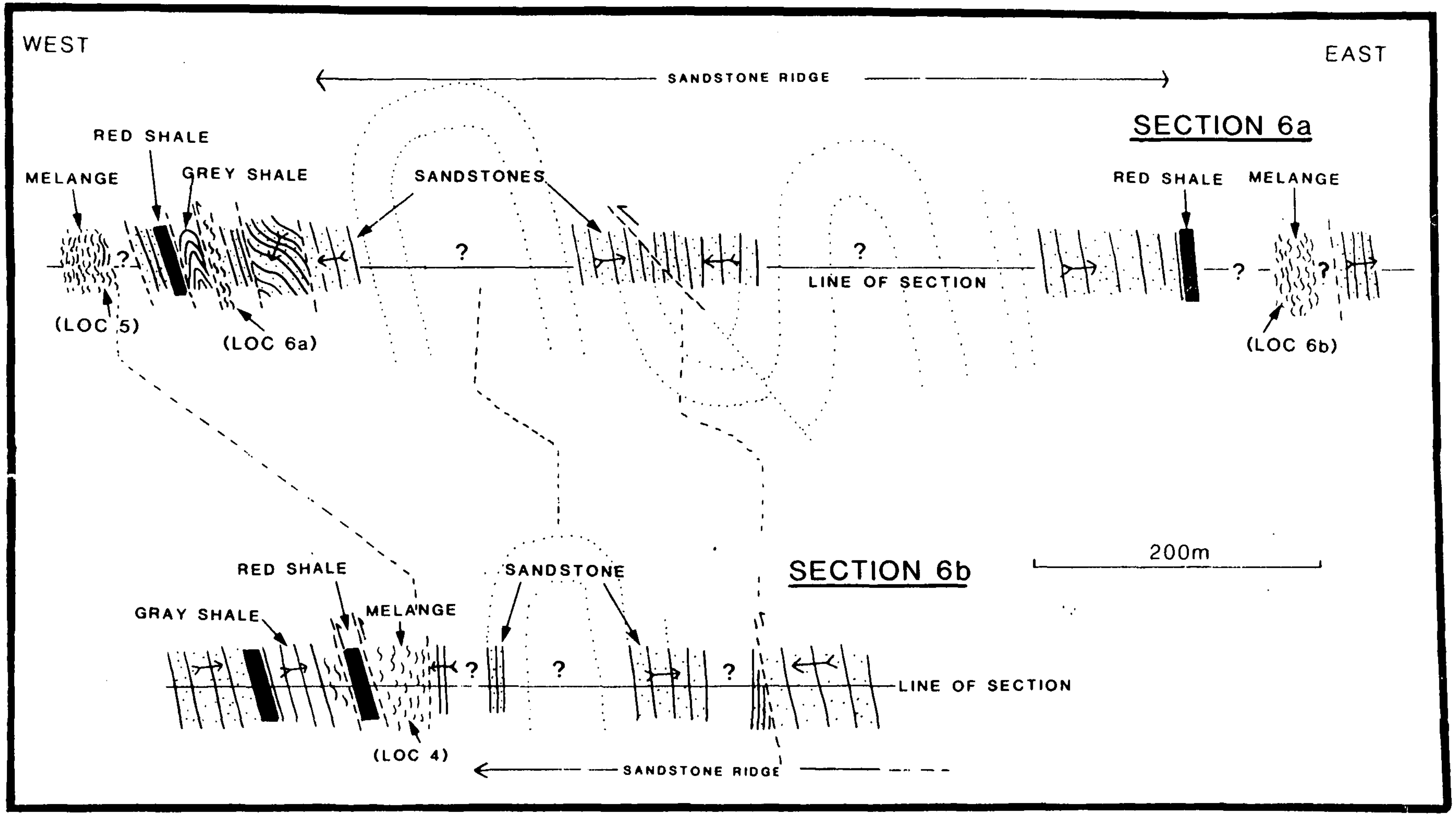
WEST
EAST
SANDSTONE RIDGE
SECTION 6a
RED SHALE
MELANGE
GREY SHALE
SANDSTONES
?
RED SHALE
MELANGE
LINE OF SECTION
(LOC 5)
(LOC 6a)
(LOC 6b)
SECTION 6b
200m
RED SHALE
SANDSTONE
GRAY SHALE
MELANGE
LINE OF SECTION
(LOC 4)
SANDSTONE RIDGE

FIGURE 3.20 - Location 6b (see section 6a Fig. 3.19 for position) runs through part of a melange body that is interpreted to be a slump deposit.

SECTION 6c

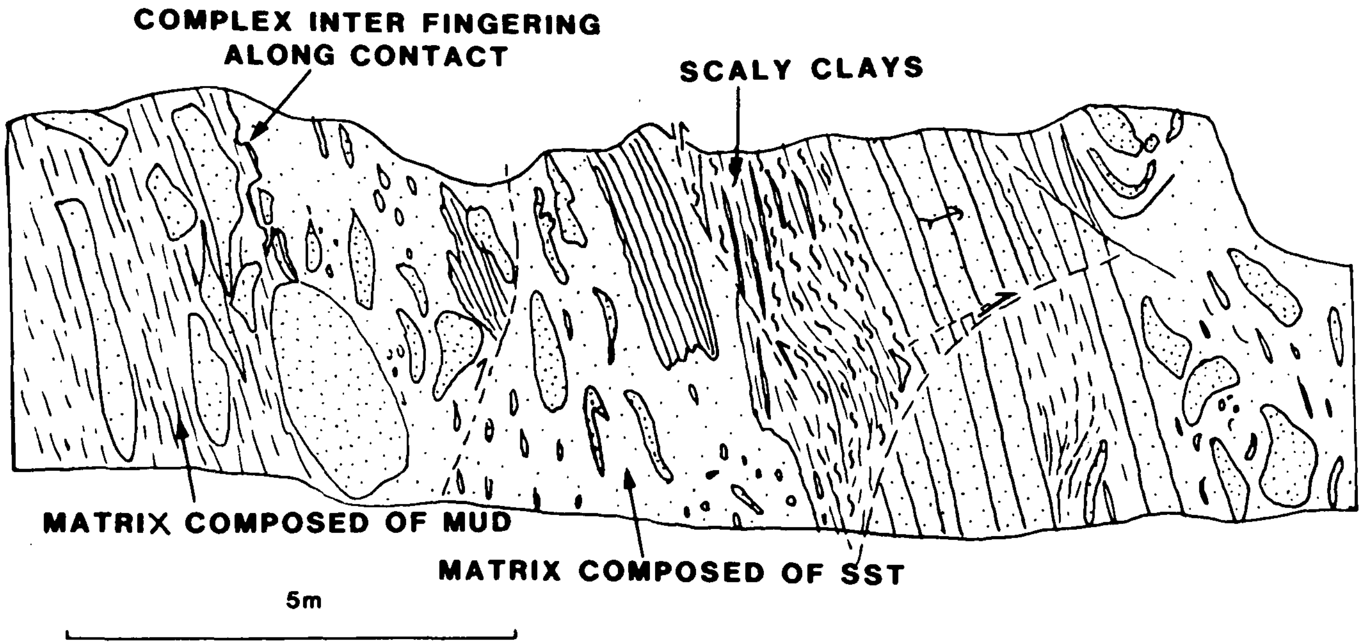

LOCATION 6b

PLATE 3.24 - Rounded block in a area of broken formation (Loc. 6a). (Looking north, right of picture is E., red box is 40cm long)

disruption. These melanges are interpreted to have formed in slumps.

Section 6b (Fig. 3.19) runs through the melanges of Locality 4. Younging reversals indicate the existence of large folds in the section and there appears to be some along strike consistancy in the structure of the sandstone ridge between Section 6a and 6b, a distance of approximately 1.3 km (Fig. 3.5a).

Location 7

Location 7 is a cross section through a sandstone ridge and up through the Sandstone Red Mudstone Upper Grey Shale contacts (Section 7, Fig. 21). The main structural feature of the locality is a downward facing anticline at the western end of the section which is situated in a section of grey shales. The closure of the synformal anticline has been complicated by later westerly verging thrusts (Figs. 21 & 22). It may be a major structure (half wavelength > 100m), as the sandstones young to the west for more than 100m beyond the end of Section 7 (see below).

The westward verging fold pair 30-40m from the western end of the section are upward facing and the anticline folds a previous bedding parallel scaly clay fabric in the grey shales. Associated with the fold is a faint second axial planar cleavage that transects bedding on the limbs of the fold (inset a, Fig. 3.21). For the next 90m to the east of the fold pair, the section youngs consistently to the west

FIGURE 3.21 - Section 7 (Location 7) running through a sandstone ridge. A potentially major synformal anticline occurs at the western end of the section. Early faults exibit soft sediment (pseudo-ductile) deformation features such a boudinage & necking.

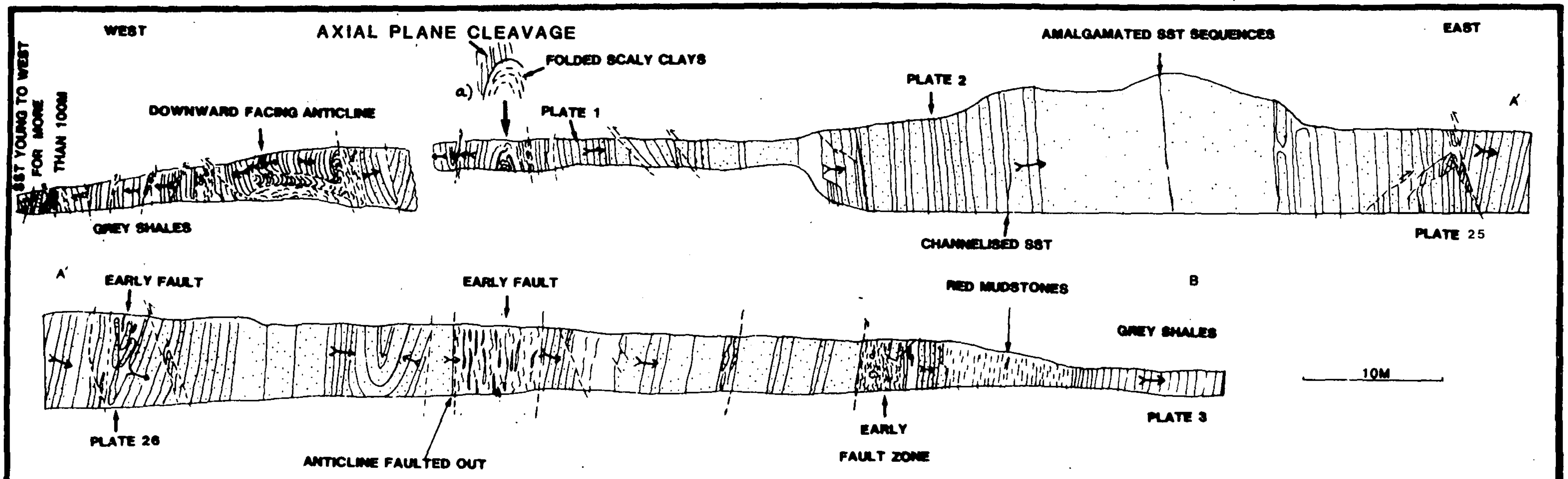

WEST
AXIAL PLANE CLEAVAGE
AMALGAMATED SST SEQUENCES
EAST
FOLDED SCALY CLAYS
a)
PLATE 2
SST YOUNG TO WEST FOR MORE THAN 100M
DOWNWARD FACING ANTICLINE
PLATE 1
A'
GREY SHALES
CHANNELISED SST
PLATE 25
A'
EARLY FAULT
EARLY FAULT
RED MUDSTONES
B
GREY SHALES
10M
PLATE 3
PLATE 26
EARLY
FAULT ZONE
ANTICLINE FAULTED OUT

SECTION 7

and is dominated by the thick beds of the turbiditic sandstone lithology with well developed flute and grove casts on the bases of some of the beds (Plates 3.1 & 3.2). Channelised bases and amalgamated sequences occur around the two very thick (8-9m) sandstone units, 80m from the western end of the section. Late conjugate reverse faults, with a dominant westerly verging set, are common throughout the section; a well developed pair is shown at 100m from the western end (Plate 3.25).

The fault zones that occur at 110m and 130m contain lenticular wispy blocks of sandstones that are boudinaged and necked (Plates 3.26). These are thought to be 'early fault zones' that formed in only partly consolidated sediments. Such structures were probably active within the initial stages of frontal accretion and may be the sites of large imbricate faults that thicken the sandstone sequence. The fault zone at 130m has cut out the anticline of the westward verging fold pair and is also thought to be westward verging. Unfortunately, at this locality another 'early looking' fault zone also separates the Red Mudstone lithology from the top of the main sandstone sequence but its transition up into the Upper Grey Shale Unit (Plate 3.3) is preserved.

Interpretation of structure- The downward facing anticline at the western end of the section may have been produced during the early phases of deformation as a result of coaxial refolding within the same deformation sequence (Fig. 3.23). Such coaxially refolded folds are similarly developed in other accretionary complexes, such as the small scale

FIGURE 3.22 - Hinge area of the synformal anticline that occurs at the western end of Section 7.

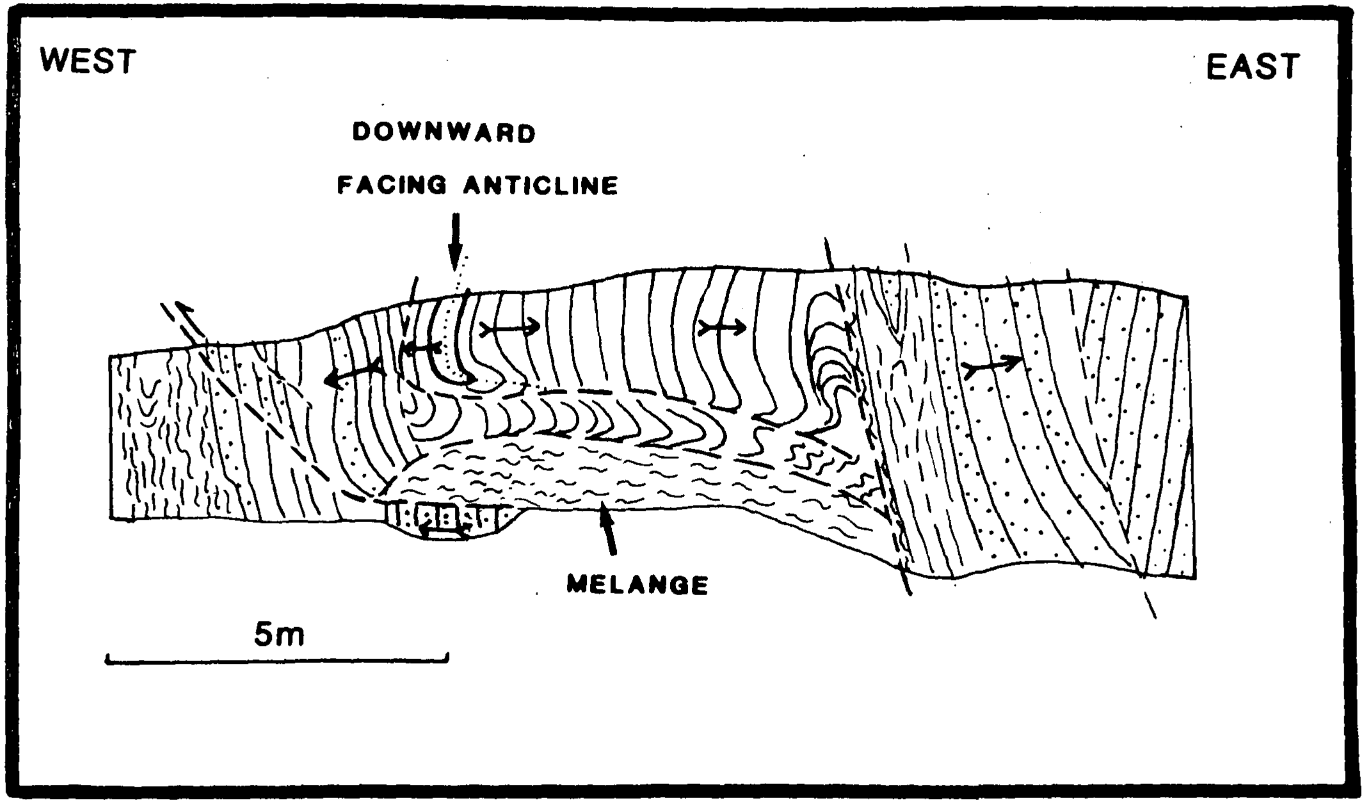
WEST
EAST
DOWNWARD
FACING ANTICLINE
MELANGE
5m

FIGURE 3.23 - Generation of downward facing structures by coaxial refolding during the same overall deformation phase.

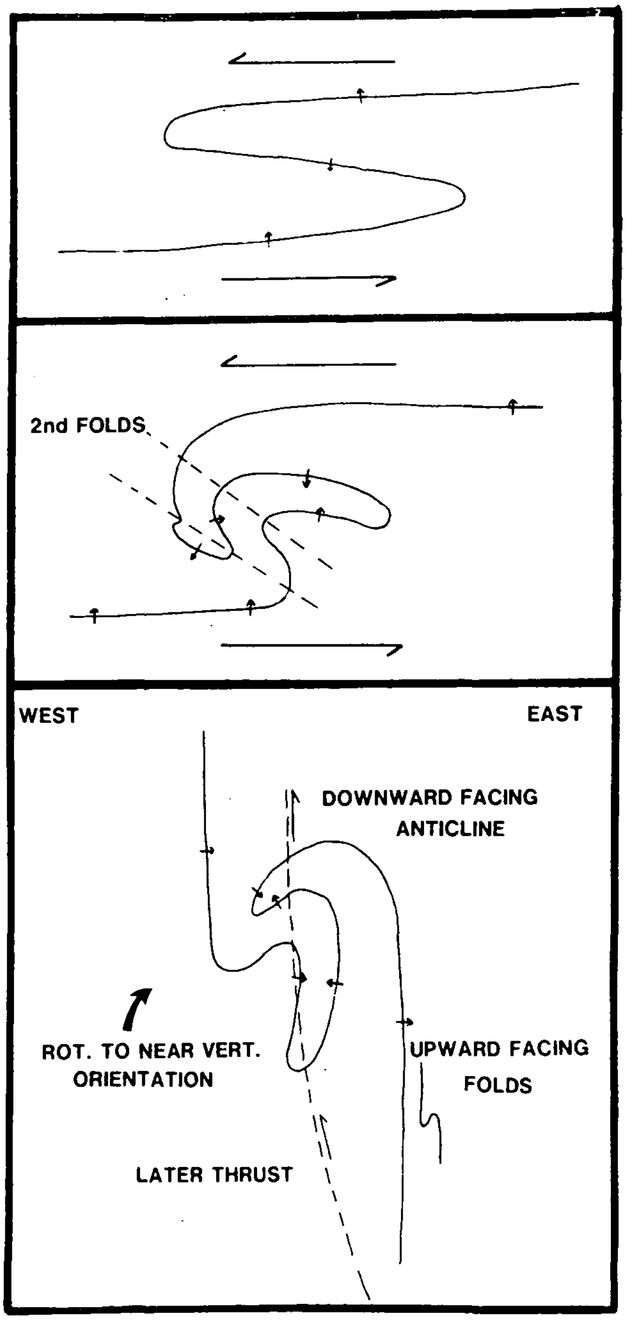

2nd FOLDS
WEST
EAST
DOWNWARD FACING
ANTICLINE
ROT. TO NEAR VERT.
ORIENTATION
UPWARD FACING
FOLDS
LATER THRUST

FIGURE 3.24 - alternative model for the generation of a more localised downward facing structure on the lower limb of a large upward facing anticline that is cut by a later thrust.

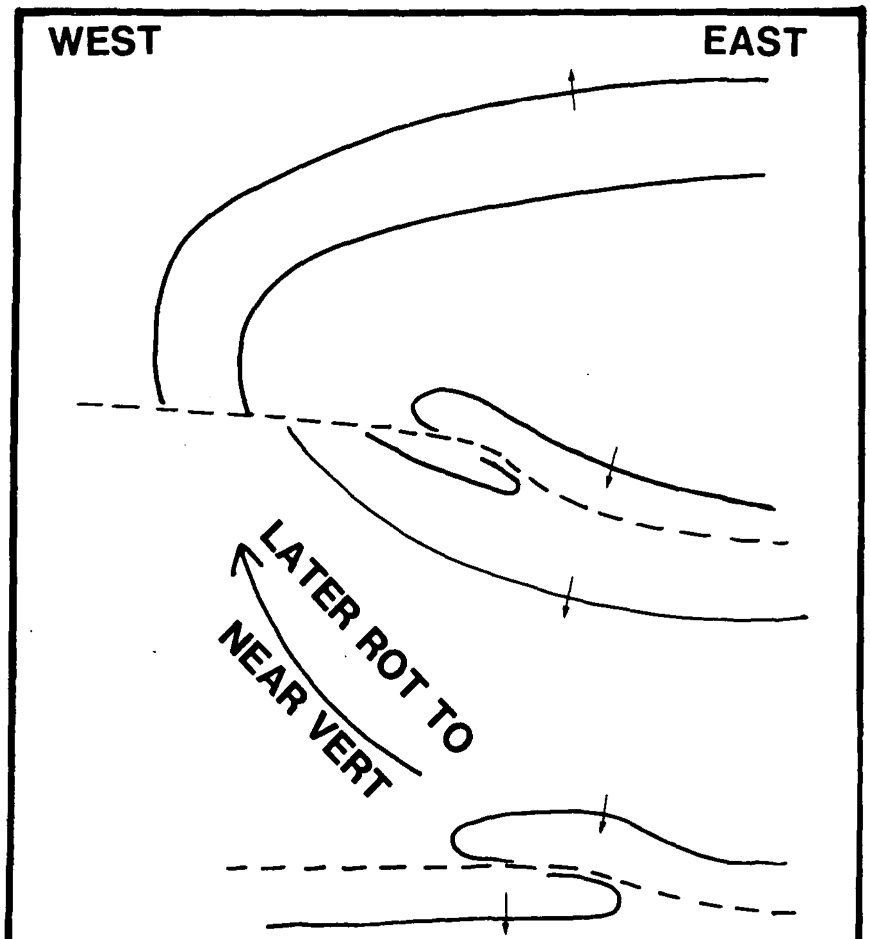

DOWNWARD FACING ANTICLINE

PLATE 3.25 - Late conjugate faults, west verging set is dominant. (Looking south, right of picture is W.)

PLATE 3.26 - Necked and boudinaged sandstones in a fault zone that affected only partialy consolidated sediments. (Looking south, right of picture is W.)

examples in the Windy Ridge sequence of Barbados (see Chapter 1). Subsequent thrusting may have then cut out part of the structure emplacing the eastern sequence, containing the upright folds, next to the anticline hinge. The early and now downward facing structure formed by the above mechanism would have to be large (half wavelength $>$ 100m). A more local downward facing structure could be formed as a result of drag along a thrust fault that cuts through the lower limb of a major inclined or recumbent up or sideways facing anticline (Fig. 3.24). This latter possibility is favoured as it requires a less complex sequence of events and produces only a minor downward facing structure.

Location 8

Location 8 (Manantanga quarry) is an area of melange (Fig. 3.25) containing a series of sandstone blocks, the largest of which being over 20m in diameter. Figure 3.26, is a line drawing of Plate 3.28 and illustrates the main features of the location. The dismembered sandstone blocks lie in a mildly sheared grey, scaly clay matrix and commonly have irregular shapes (Plates 3.28 & 3.29). The wispy, irregular terminations of some blocks and boudinage of others (Plate 3.29) suggest that they were not all well consolidated at the time of their disruption. Intrusion of the blocks by the argillaceous matrix also occurs. The fabric in the melange is highly irregular in its orientation (Fig. 3.25 a), wrapping around the large sandstone block in the centre of the quarry, and is unlikely to have originated primarily as a result of shearing along a fault zone.

FIGURE 3.25 - a) Location 8, plan view of quarry showing that the foliation in the melanges wrap around the large sandstone block in the centre of the outcrop.

- b) Section X-Y through the quarry with an interpretation of the lines of flowage of the melange material, up around the block.

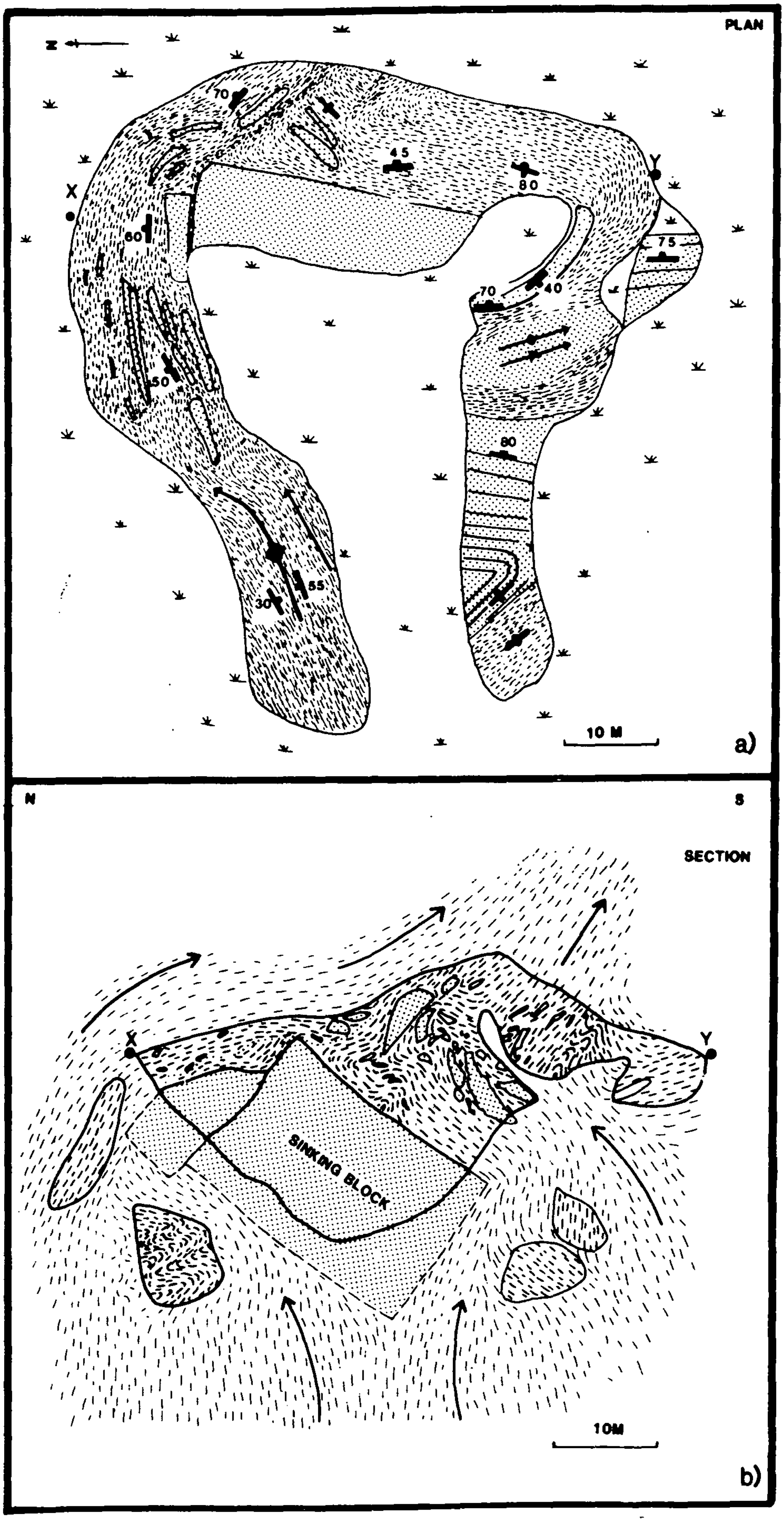

PLAN
N
X
Y
70
45
80
60
75
70
40
50
80
55
30
10 M
a)
N
S
SECTION
X
Y
SINKING BLOCK
10M
b)

PLATE 3.28 - Quarry face in which large irregular shaped sandstone blocks are exposed in an area of melange. The large block appears to be subsiding in the melanges, which are flowing up round it as a consequence. (Looking east, right of picture is south, field-of-view approx. 40m)

PLATE 3.29 - Irregular shapes of the sandstone blocks in the melange. Note wispy terminations to some of the blocks.

Structural interpretation- The favoured explanation for the orientation pattern round the large sandstone block is that the melange flowed up round it as it sank, carrying the small sandstone blocks up with it (Fig. 3.25 b). The melange may therefore be diapiric.

3.3 *STUDY AREA II: KOTA KINABALU TO RANU ROAD*

The road from Kota Kinabalu to Ranu provides an interesting transect across the more interior areas of the Crocker Range. Constant upgrading of the road provides a number of relatively fresh exposures in parts of the East Crocker Formation with large structures, such as the isoclinal fold in Plate 3.30, being visible in the road cut exposures. The majority of the exposures are of relatively steeply dipping turbiditic sandstone and shale sequences and occasional red shales. The red shales are sometimes interbedded with the sandstones and the local stratigraphy, established for the West Crocker Formation in the Kota Kinabalu area (Study Area I), cannot be used east of approximately 10 km inland from the coast. Two particular localities will be discussed in detail, as they include melanges of probable diapiric origin.

PLATE 3.30 - Major isoclinal synclinal fold in thick turbidite sequeces, E. Crocker Fm. (Looking south west)

3.3.1 *Description of Localites*

Locality 9

Locality 9 is a road cut approximately 3 Km east of Church Kapar. In contrast with the steep dips common elsewhere in the Crocker Fm. this structure appears to have maintained its original low angle dip (Section 9, Fig. 3.27). Revealed in the section is a major westward verging thrust system with a large antiformal stack at the eastern end of the section, a series of ramps and flats in the centre, and a large melange body at the western end of the section.

The ramp anticline (Plate 3.31) has, in fact, a more complex origin than a simple emplacement of a hanging wall ramp sequence onto a flat. The disharmonically folded thinly bedded sequence in the mid regions of the anticline appears to be an imbricate packet, detached from a collapsed footwall sequence whilst, the thick sandstone bed appears to be a flat of the original hanging wall sequence (Fig. 3.28). The 'flat' beneath the ramp anticline appears to cut across an already folded, steeply dipping sequence of rocks and therefore may be an out-of-sequence structure. Within this fault zone, intense scaly clays are developed with a phacoidal shapes predominating in the included small (< 5cm diameter) disrupted sandstone blocks.

FIGURE 3.27 - Section 9 (Location 9), runs through a relatively flat lying, thrusted sequence of turbidites and a large body of melange that continues for at least another 30m beyond the western end of the section.

PLATE 3.31 - General shot of Locality 9 showing the culmination or antiformal stack at the eastern end of the section and the isolated block of the thick sandstone unit at the western end of the section. (looking south, field-of-view approx. 15m)

PLATE 3.32 - Diapiric upwelling of fault zone material behind extended block. (looking south, red box 40cm long, see section 9 for position)

The complexities in the region of the ramp, at approximately 60m from the eastern end of the section, are not readily explainable by normal thrust ramp geometries. Part of the thick sandstone bed has been detached and separated from the rest of the bed. The void created has been filled by the collapse of the sequence above along a series of normal faults. Furthermore, material from the fault zone below also appears to have welled up diapirically and filled part of the void (Plates 3.31 & 3.32). The normal faulting appears to have occurred at some point before the arrival of this part of the section at the ramp (Fig. 3.28). A later layer-parallel thrust has removed the upper part of the normally faulted sequence. It must have been active before the formation of the antiformal stack at the eastern end of the section. The diapiric intrusion most probably occurred on the arrival of this part of the sequence at the ramp.

The minor reverse fault (80m from the eastern end of the section) appears to have been active during movement on the main thrust ramp and minor folding and adjustments of the ramp geometry have occurred around the area of interference, with the general upward migration of the main thrust surface.

A major fault zone is thought to occur in the large body of melange which continues for at least another 30m beyond the western end of Section 9 (Plate 3.33). It exhibits a number of features that suggest that the argillaceous matrix was very mobile during the main phase of block disruption. Intrusion of the matrix into sandstone blocks is common

FIGURE 3.28 - Proposed sequence of development for the structures at the eastern end of of Section 9. a) Plucking of part of the large sandstone unit beneath the thrust initiates the collapse of the hanging wall and the development of a normal fault system. b) Later movement on a thrusts situated above the thick sst bed shears off the upper parts of the normal fault system. The collapse of a ramp associated with a lower thrust eventually generates the antiformal stack. c) Continued later normal extension initiates the small diapiric upwelling.

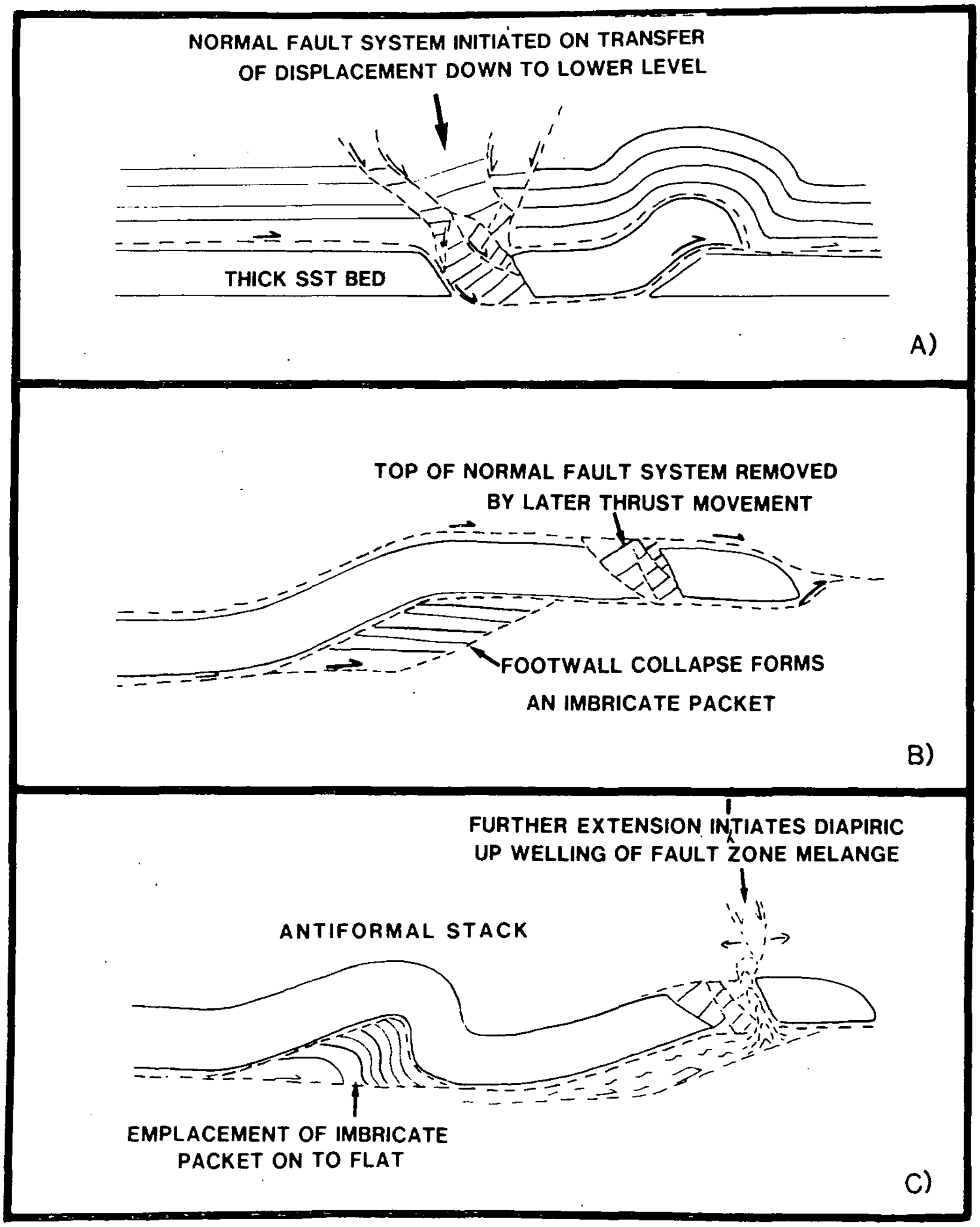

NORMAL FAULT SYSTEM INITIATED ON TRANSFER
OF DISPLACEMENT DOWN TO LOWER LEVEL
THICK SST BED
A)
TOP OF NORMAL FAULT SYSTEM REMOVED
BY LATER THRUST MOVEMENT
FOOTWALL COLLAPSE FORMS
AN IMBRICATE PACKET
B)
FURTHER EXTENSION INTIATES DIAPIRIC
UP WELLING OF FAULT ZONE MELANGE
ANTIFORMAL STACK
EMPLACEMENT OF IMBRICATE
PACKET ON TO FLAT
C)

FIGURE 3.29 - The relationship between the shear strength of argillaceous material and strain. After the peak strength is over come the argillaceous material has a lower residual strength and deformes at at lower shear stresses (Craig 1983, Smith 1975).

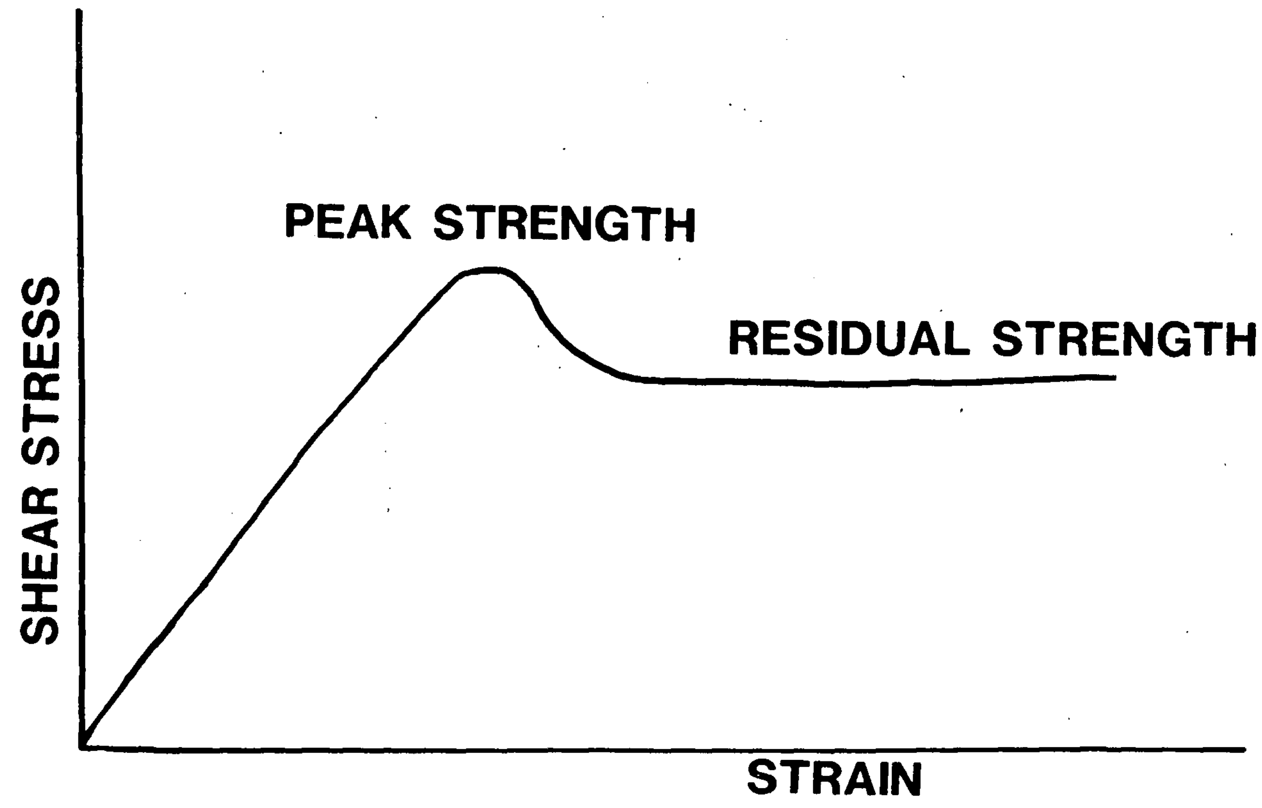
PEAK STRENGTH
RESIDUAL STRENGTH
SHEAR STRESS
STRAIN

PLATE 3.33 - General shot of major melange body at the western end of Section 9 (Looking south, field-of-view approx. 15m)

PLATE 3.34 - Red shale rafts and large blocks of sandstone in the melanges. Plate 3.35 is of a shale injection feature into the laregest sandstone block in this view. (Looking south, field-of-view approx. 7m)

PLATE 3.35 - Shale injection structure, note the scaly clay fabric development in the intruded flame. The argillaceous material may have been consolidated enough to sustain shearing during its intrusion. (Looking south)

PLATE 3.36 - Highly irregular terminations of some sandstone blocks in the melange may be the product of disaggregation in a previously fluid medium or form as a result of plucking during shearing. (Looking south)

PLATE 3.37 - Soft rounded terminations to some of the less sheared shale rafts suggest the they were originally only partly consolidated during at least their initial disruption.

Plate 3.38 - Intrusion of mud into sandstone block near the pencil. In the fault zone out side the block the muds have undergone shearing and intense scaly clay fabric development. The argillaceous material in the block has also developed a mild scaly clay fabric. (Looking south)

(Plates 3.34 & 3.35) and many blocks have highly irregular shapes that may be the product their disaggregation in an originally fluid medium (Plate 3.36). Red shale rafts, occasionally preserved with 'soft' blurred irregular terminations, are also suggestive of a fluid ductile matrix (Plate 3.37). A later intense scaly clay fabric is imposed on parts of the melange zone, strongly modifying the earlier features of the melange (Plates 3.38).

This locality is an example of the inter-relationships between thrusts and mobile and potentially diapiric melanges and is considered to be a good small-scale model for the large diapiric melange terranes such as those in Timor and the Barbados Ridge Accretionary Complex, considered in Chapter 4. This follows on from the observation that the shear strength of muds decrease after their peak strength has been exceeded (Fig. 3.29, Craig 1983, Smith 1975). The argillaceous matrix of the fault zone has its mobility enhanced as a consequence of its disruption and therefore becomes a potential diapiric source region.

Location 10

Location 10 consists of a series of road cut exposures around the entrance to the Mount Kinabalu National Park. The exposures are through a body of melange that has an east-west diameter of well over 1km and a north-south width of 200m or more. The locality is in a geologically complex area and is situated close to a major regional structure called the Kadamaian fault (Tjia 1974). Figure 3.30, is a geological

FIGURE 3.30 - Structural map of the Ranu-Tenomok area, taken from Tija (1974).

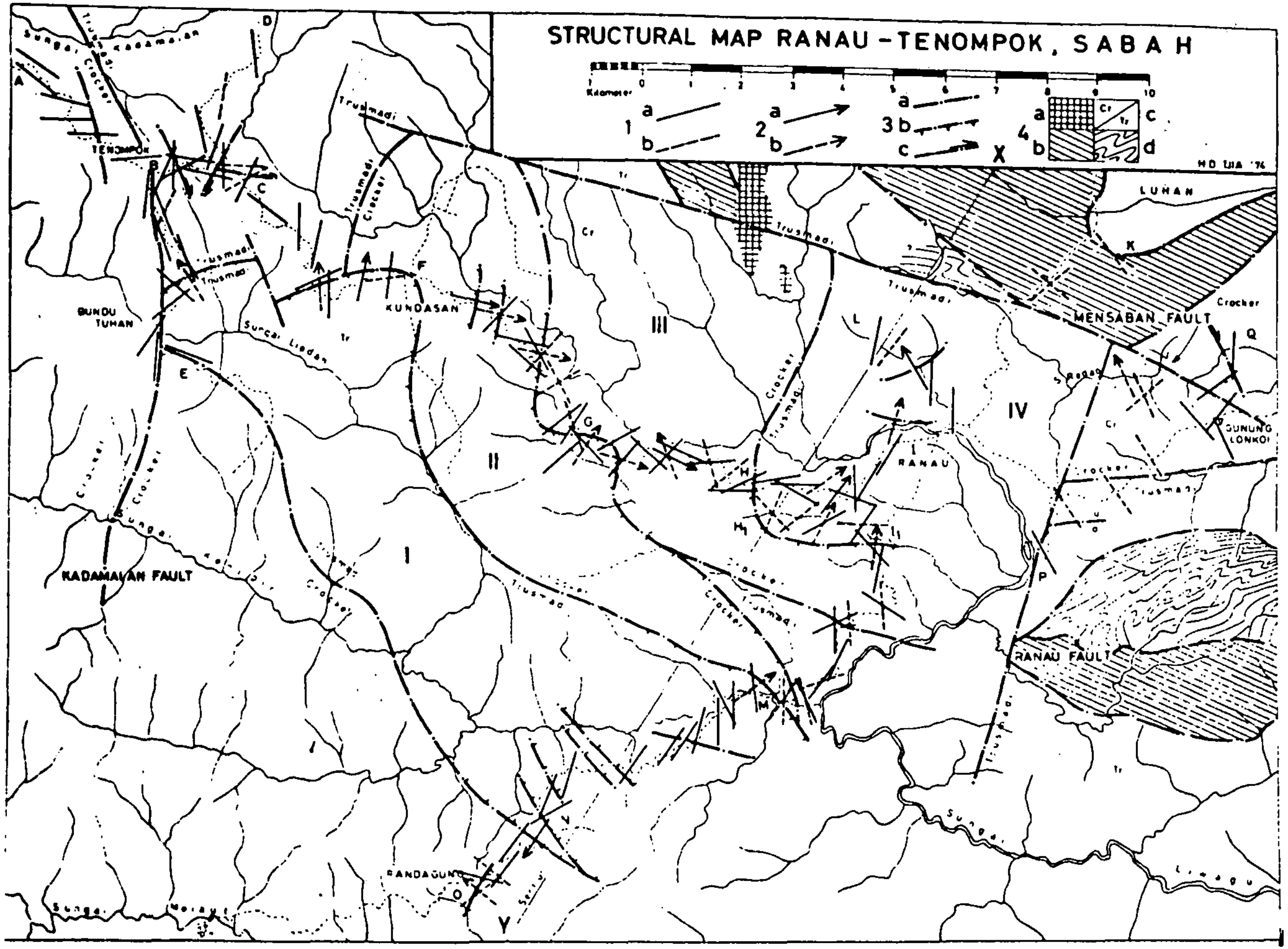

Key: 1(a) = direction of horizontal compression determined by visual inspection of S-planes (bedding and foliation) for particular sections along a traverse.
1(b) = ditto, but determined from stereoplot of structural elements along a particular section.
2(a) = like 1(a) but indicating sense of low-angle reverse faulting or overthrusting.
2(b) = like 1(b) but indicating sense of low-angle reverse faulting or overthrusting.
3(a) = trace of fault zone.
3(b) = trace of moderately to subhorizontally dipping fault zone; barbs are on the upper fault plate.
4(a) = adamellite (porphyritic).
4(b) = ultrabasic rock.
4(c) = Cr: Crocker Formation, Tr: Trusmadi Formation.
4(d) = crystalline schist.
Thin dashed lines indicate roads.
Letters A through Q denote traverse segments.
X–Y = cross section shown on figure 23.

map of the area adapted from Tjia (1974). Present in the area are: (1) Crystalline basement schists or metabasites, Jurassic or older in age. (2) Ultra-basic rocks (Serpentinized), emplaced probably in Tertiary times. (3) The Tertiary Trusmadi Formation (dominantly dark argillaceous rocks + occasional thin arenaceous beds metamorphosed to low greenschist facies). (4) The Tertiary Crocker Formation (argillaceous sediments and thicker more abundant arenaceous beds). (5) Pleistocene to Recent tilloid and alluvial sediments.

Three major periods of deformation have been recognised in the Mt. Kinabalu-Ranu area. The Crystalline metamorphic basement rocks are of pre-Jurassic age, whilst the Tertiary and Metabasite rocks were deformed in mid Miocene times. The Mount Kinabalu pluton was intruded at or after the end of this phase. A Quaternary deformation phase has raised the area to heights of 2000m, with the Mt. Kinabalu pluton being affected by predominantly strike-slip and normal faulting (Collenette 1958, Jacobson 1970).

The Kadamaian fault strikes north to north-west, large bodies of melange occur to the east of it, termed flaser beds by Tjia (1974), and squeezed strata or Chert Spilite Formation by Collenette (1958). There is a widespread occurrence of chaotic bodies of melange along the line of the Kadamaian fault and ophiolitic material in the Trusmadi Formation in this area. The fault was interpreted to be some sort of depositional fault or hinge zone along which olistostromes occurred (Liechti 1960). Such a hypothesis cannot be correct as the region has suffered intense deformation, the fault appears to be a syn- or post orogenic feature, cutting across and dividing structures in the Crocker Range into two domains. To the west of the fault the main structures strike in a north to northeast direction and the sense of overthrusting is to the west or north-west. To the east the structures strike approximately east-west and the dominant sense of overthrusting is to the north (Tjia 1974). A strike slip origin is proposed for the fault. A large amount of both dextral and sinistral strike slip faulting has been indentified in the central regions of Sabah. McManus and Tate (1976) propose the existence of major dextral faults in central and western Sabah trending in a northerly and northeasterly direction whilst, Tokuyama and Yoshida (1974) propose to existence of northwesterly trending sinistral faults that cut across the whole of Sabah (Fig. 3.3). It is not certain that these different fault systems were active at the same time but, if they were, they form a conjugate fault set corresponding to an approximately east-west principal axis of compression. Landsat images of the region (Lee & Choi 1980) clearly pick out the Kadamaian fault as a series of subparallel lineaments (Fig. 3.2b) and it might be better to term it a fault zone, rather than an individual fault. Landsat images also pickout another major lineament, that intersects with the Kadamaian Fault in the region of locality 10, termed the Crocker Linearment. Lee & Choi (1980), propose that it it is a large major overthrust. It appears to be cut by the strike slip faults and therefore predates them.

The melanges of locality 10 lie just to the east of the Kadamaian Fault and may be part of the supposed associated "olistostromal deposits" (Liechti 1960). The actual strike of the foliation superimposed on the melanges can very widely but generally trends roughly in an East-West direction and the melanges are, therefore, interpreted to be part of the structural domain, east of the fault.

Evidence of the early origins of the melanges are preserved in areas where the later superimposed east-west foliation is not too intense. Re-entrant angles of and pressure shadows behind large blocks have been found to be the best places to study the early fabrics developed within the argillaceous matrix. Plates 3.39 to 3.42 are of an irregular but roughly equi-dimensioned sandstone block with a shape that is typical of these melanges. In the re-entrant angles the argillaceous matrix is unfoliated and highly heterogeneous (Plate 3.30b). In particular, it can be seen that the argillaceous material was made up of a variety of units, with very varied degrees of competency. Some behaved in a brittle manner, forming angular fragments while others were less competent forming fragments with more irregular wispy shapes. The fragments are of different shades of grey, with the actual intrusive argillaceous material being very dark grey to black in colour. In the areas furthest away from the surrounding scaly clays, the shapes of the included blocks of sandstone and other argillaceous lithologies are sub-rounded or very irregular, but do not appear to have been flattened or sheared. They become steadily more lenticular and sheared nearer the scaly clays, until all evidence of the

PLATE 3.39 - a) An example of a relatively common sandstone block shape which is roughly equidimensional, and subrounded to subangular. Within re-entrant angles of the block the early form of the fabrics in the argillaceous matrix and the relationships of the blocks and matrix can be seen (see below).

- b) The unfoliated heterogenious nature of the argillaceous matrix is preserved near the block but becomes steadily more sheared towards the scaly clays until all the original relationships become overprinted. Note subrounded shapes to many of the sandstone bodies some also have highly irregular diffuse edges. Argillaceous material fills a net work of hydrofractures in the body of the large block to the right of the picture.

- c) Irregular & subrounded sandstone blocks are intruded by argillaceous material. In detail their margins are fretted and, in places, diffuse, These relationships are overprinted in the areas where scaly clays are developed.

early heterogenious and chaotic nature is overprinted. Red shale rafts also occur occasionally in the melanges.

The dark grey to black fluid argillaceous matrix intrudes into the sandstone blocks (Plate 3.40) and can be found as pods up to 20 cm in diameter in the centre of the main block. The interior regions of large and small blocks alike are intensely fractured (Plate 3.41). Some are filled with thin films of argillaceous material and form an anastomosing network. They are interpreted to be hydrofractures formed during, and assisting in, the disruption of the blocks. They often delineate irregular shapes that are thought to be the precursors to the isolated blocks in the melange. The large block (Plate 3.42) appears to have been veined by quartz after disruption but before movement of the melange had ceased.

Elsewhere in the melanges, rounded or irregular equi-dimensional block shapes are abundant (Plates 3.42 & 3.44). Many of the blocks show evidence of having been intruded by the argillaceous matrix. The argillaceous material weathers out to reveal deep fissures into the interior of the blocks. Some of the fissures are also filled with calcite (Plate 3.45). The calcite veined filled fissures in particular appear to be orientated perpendicular to the foliation plane and may have developed in response to later flattening and lateral extension (see below).

Roughly east-west trending shear zones, dipping at between 50°-80° to the north and south, cut across the melanges. The

PLATE 3.40 - A pod of argillaceous diapiric matrix intruded into the interior regions of the sandstone block in Plate 39 along a fracture subsequently used by a quartz vein.

PLATE 3.41 - Anastomosing hydrofractures filled with a thin seam of argillaceous material.

PLATE 42 - Quartz veins that die out towards the centre of the block are cut by the scaly clays of the sheared melange matrix.

PLATE 43 - Contact between a large (<20m diameter) block of recumbantly folded interbedded thin sandstones and shales (right) and the dark matrix of the melange (left). Note the rounded or angular eqidimensional block shapes.

PLATE 3.44 - a & b) Common sandstone block shapes, note the rounded or angular eqidimensional forms.

PLATE 3.45 - Close up of an individual sandstone block with a fissured exterior that has been intruded by the argillaceous matrix.

PLATE 3.46 - Flattening of argillaceous material causes the formation of pressure shadows behind sandstone blocks.

PLATE 3.47 - Close up of a pressure shadow behind a block in which early fabrics are preserved. The lack of scaly fabric suggests that the argillaceous matrix must have been behaving as a fluid during the main early phase of disruption. The blocks in the argillaceous material are drawn out parallel to the maximum extension direction and perhaps the flattening stresses were imposed before the argillaceous material was fully lithified.

shear zones are marked by an intensification of the scaly clay fabrics and commonly have a reverse sense of shear. Blocks caught up along the shear zones have their long axes rotated into the vertical plane. Pressure shadows, in which the early unfoliated fabrics are partially preserved, indicate considerable north-south flattening across the shear zones, with a vertical maximum extension (Plates 3.46 & 3.47). Larger blocks of bedded material contain structures such as recumbent isoclinal folds. The axes of the folds are orientated east-west parallel to the strike of the foliation. The foliation is also folded in places into recumbent folds with recorded hinges striking to 120° N. The steep shear zones appear to cross cut and post date the recumbent folds. The isoclinal and recumbent folds in the melanges may be related to the mid-Miocene deformation phase that produced the recumbent folds and thrusts with north to northeasterly senses of overthrusting in the surrounding coherent units (Tjia 1974). The melanges appear, therefore, to have originated at some point before or during the early stages of orogenesis and have been substantially modified by north-south flattening and folding during the later phases. This has imparted a preferred orientation and a degree of structural coherency to what was originally a completely chaotic melange body. In summary, there are six main features of the melanges at Locality 10:

1) Early disruption took place in a largely unfoliated argillaceous matrix that behaved as a fluid.

2) Disruption took place under highly overpressured conditions with the formation of mud injection features and calcite and quartz veining.

3) The disruptive process created an intially completely chaotic deposit with no prefered orientations of blocks or fabrics.

4) Distinctive rounded to irregular/angular, but roughly equant sandstone block shapes were produced by the disruptive process.

5) The argillaceous matrix of the melange originated from a variety of units with widly differing degrees of competency.

6) Scaly clay fabrics were superimposed on the melange after the principal disruptive period had occurred. The fabrics modified the earlier-formed block shapes and imparted a degree of structural coherence to the melanges that otherwise may not have existed.

3.4 DISCUSSION

To gain an understanding of some of the general processes going on within this well developed accretionary complex, it is first necessary to assesss the significance of the general distribution of rock types within the complex. The Tertiary accretionary complex of northern Borneo, by and large, consists of an imbricated series of turbidites and argillaceous sediments. It is structurally complex but has a development predominantly controlled by the 'coherent' processes of thrusting and folding. Melanges form a minor proportion of the volume of the western areas of the complex (Study Area I), but become increasingly more important in the interior eastern regions (Study Area II). Four important points or questions spring to mind from this examination of the structural development of the complex.

1) There is an absence of pelagic sediments in either of the Study Areas. Presuming the turbidites were not deposited directly onto oceanic crust, there must have been a detachment between them and a missing lower pelagic section. The pelagics may have been thrust further beneath the accretionary complex and subcreted at much greater depths. Along strike equivalents to the missing pelagic section in the study areas may, therefore, give additional information on what sort of processes have occurred in these deeper regions.

2) Can the structural evolution of the areas studied be related to specific environments in a developing accretionary complex ?

3) Do the turbidites represent a frontally accreted or subcreted section?

4) What is the origin of the melanges in Study Areas I & II ?

3.4.1 Lateral equivalents of the missing pelagic section in the Kota Kinabalu area

There are a number of formations in Sabah and Sarawak that contain pelagic rocks. Figure 3.31 (adapted from Tan 1980) shows the distribution of chert (often accompanied by pelagic limestones and spilites) that may be part of the pelagic section offscraped from the subducting plate. The main contenders for the missing pelagic section in western Sabah are the Wariu Formation (Sabah) and the Lubok Antu melange (W. Sarawak) which are of Paleocene to Miocene age. These

FIGURE 3.31 - The cherts in N. Borneo form part of the Pelagic section, [illegible] *(Tan 1980).*

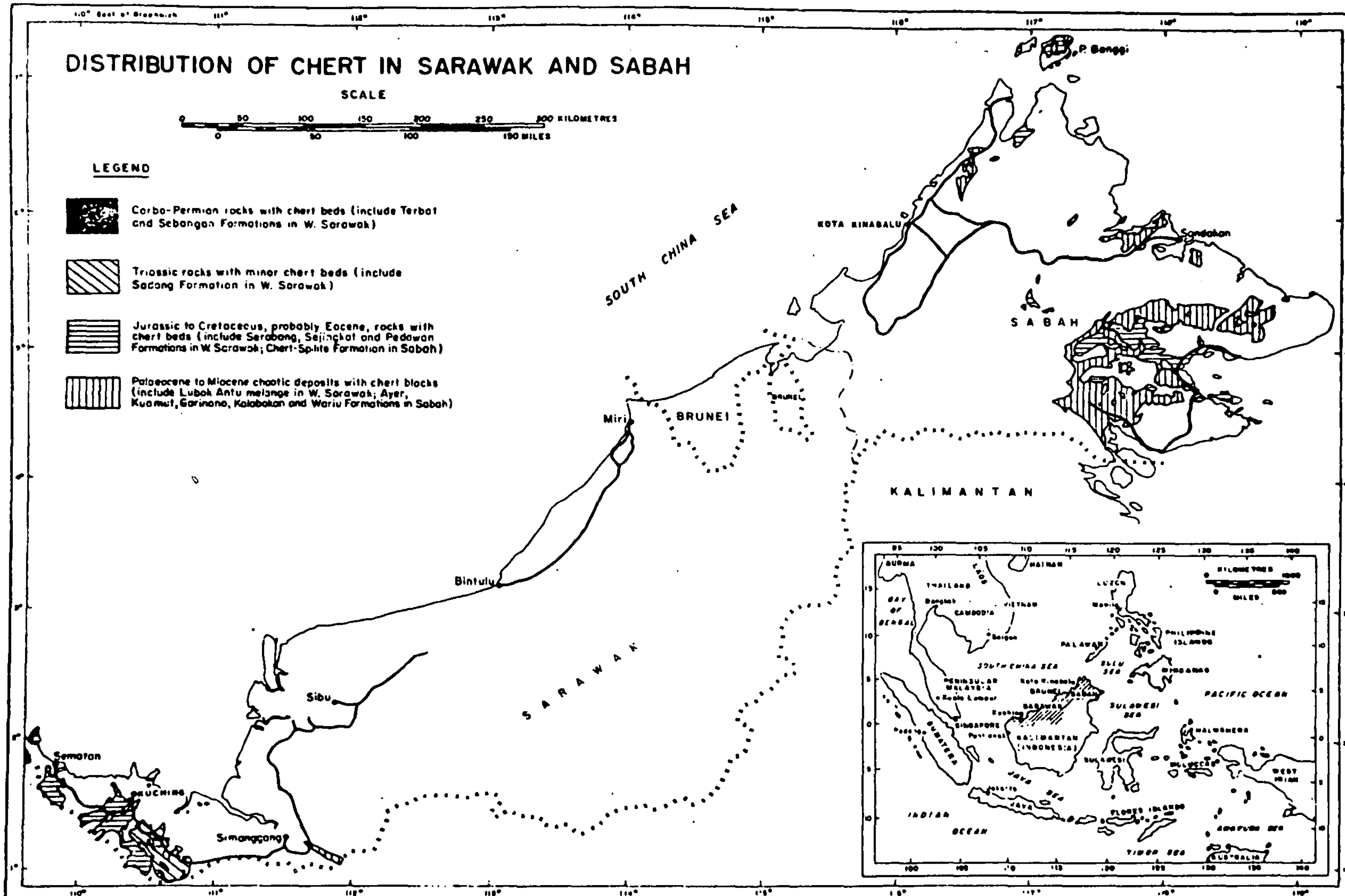
DISTRIBUTION OF CHERT IN SARAWAK AND SABAH
SCALE
0 50 100 150 200 250 300 KILOMETRES
0 50 100 150 MILES
LEGEND
Carbo-Permian rocks with chert beds (include Terbat and Sebangan Formations in W. Sarawak)
Triassic rocks with minor chert beds (include Sadong Formation in W. Sarawak)
Jurassic to Cretaceous, probably Eocene, rocks with chert beds (include Serabang, Sejingkat and Pedawan Formations in W Sarawak; Chert-Spilite Formation in Sabah)
Palaeocene to Miocene chaotic deposits with chert blocks (include Lubok Antu melange in W. Sarawak; Ayer, Kuamut, Garinono, Kalabakan and Wariu Formations in Sabah)
SOUTH CHINA SEA
P. Banggi
KOTA KINABALU
Sandakan
S A B A H
BRUNEI
Miri
K A L I M A N T A N
Bintulu
S A R A W A K
Sibu
Sematan
KUCHING
Simanggang
SOUTH CHINA SEA
PACIFIC OCEAN
INDIAN OCEAN
SULAWESI SEA
PHILIPPINE ISLANDS

are described below. There are also Jurassic to Cretaceous aged pelagics present as the Chert-Spilite Formation on Banggi Island, NW Sabah, and as the Serabang, Sejingkat and Pedawan Formations in W. Sarawak.

The Wariu Formation, just to the north of Study Area 1, is a melange deposit, containing blocks of sandstone, phyllitic shale, radiolarian chert, spilite, and ultrabasic rocks in a pelitic matrix (Tan 1980). Tan proposed that it is an olistostromal deposit derived from the Chert-Spilite Formation.

The Lubok Antu Melange is composed of mudstone, sandstone, shale, hornfels, radiolarian chert, conglomerate, limestone, basalt, gabbro , ultrabasics (serpentinized) and their metamorphic equivalents, in a cleaved, chloritized and highly sheared scaly clay matrix (Tan 1982). The matrix has been dated as being Eocene in age, although there is a possible Paleocene to Miocene range. Blocks of chert and oceanic basement material up to 2-5.5 km in length and up to 500m wide are found in the melange. Tan (1982) describes the melange as containing metamorphic blocks derived from the surrounding Formations (which include part of a dismembered ophiolite sequence) which have been regionally metamorphosed to greenschist facies. The matrix, and other exotic blocks that do not have equivalents in the surrounding formations are, on the other hand, not metamorphosed. Tan proposed that the melange originated as a result of shearing in an accretionary complex possibly in a manner similar to the viscous flow models postulated by Cloos (1982). The melange *is, however, related to a relatively late strike slip fault called the Lupar fault (Tan 1982), and its present disposition may not be directly related to the primary accretion event.*

Another possible interpretation this melange deposit, is that it formed in mud diapirs that originated deep within the complex. The diapirs could have incorporated the metamorphic blocks during its intrusion through overlying formations by stoping them from the roof and walls. Thrusting could have been responsible for the original juxtaposition of the metamorphic and ophiolite sequences above the underconsolidated sequences that later formed the mud diapirs. The strike slip faulting may have initiated diapirism by providing steep planes of weakness through the thrust sheets. The behaviour and origin of these melanges may be similar to the diapiric melanges in W. Timor, discussed in Chapter 4 (see below).

A dismembered pelagic section is therefore present in the complex. However, there is a strong possibility that it has been raised to the present structural level via mud diapirs and that considerably larger volumes may be present at depth within the complex. It appears to be almost exclusively present as melanges suggesting that the environment under which it was accreted favoured bulk deformation by one mechanism or another (see section 3.4.4).

3.4.2 Structural Evolution

It is possible to distinguish an evolutionary progression in the form of the structures developed in Study Area I. The distinctive local stratigraphy enables the delineation of levels with in the stratigraphy that are commonly used as the sites of detachment. The top and bottom of the Sandstone Unit, where the contrast in shear strengths of the different units are greatest, appears to be the prime sites for localising the main detachment levels.

The dominant sense of overthrusting is to the east with a few notable exceptions such as the westward directed thrusts at locality 1. Some of the large fault zones and numerous smaller ones have lag geometries, that is, they cut down through the sequence and appear to extend it (i.e. Localities 2 & 3). At localities 2 & 3 a general geometrical progression can be seen. These fault zones initially appear to have developed parallel to bedding as flats. Later in their development (or as a result of other cross cutting thrusts) the footwall and hanging wall flats appear to be breached to form the lag geometries. Figure 3.32 is a schematic model that explains this general geometrical progression. The period of initial imbrication and back rotation of the sequence (and flats) during the construction of a duplex or imbricate fan is thought to be followed by the development of lower angle out-of-sequence thrusts as the strata and faults become rotated to orientations that are too steep for further effective movement (Fig.3.32). The general anisotropy of the dipping bedding may encourage the

FIGURE 3.32 - a) Simplified model depicting the lag geometry of an out-of-sequence thrust that cuts stratigraphically down through a series of back-rotated frontal imbricate thrusts. The preexisting structure may be considerably more complex than is shown.

-b) The out-of-sequence thrust may have a stepped topography as a result of the competency contrasts between the sedimentary units.

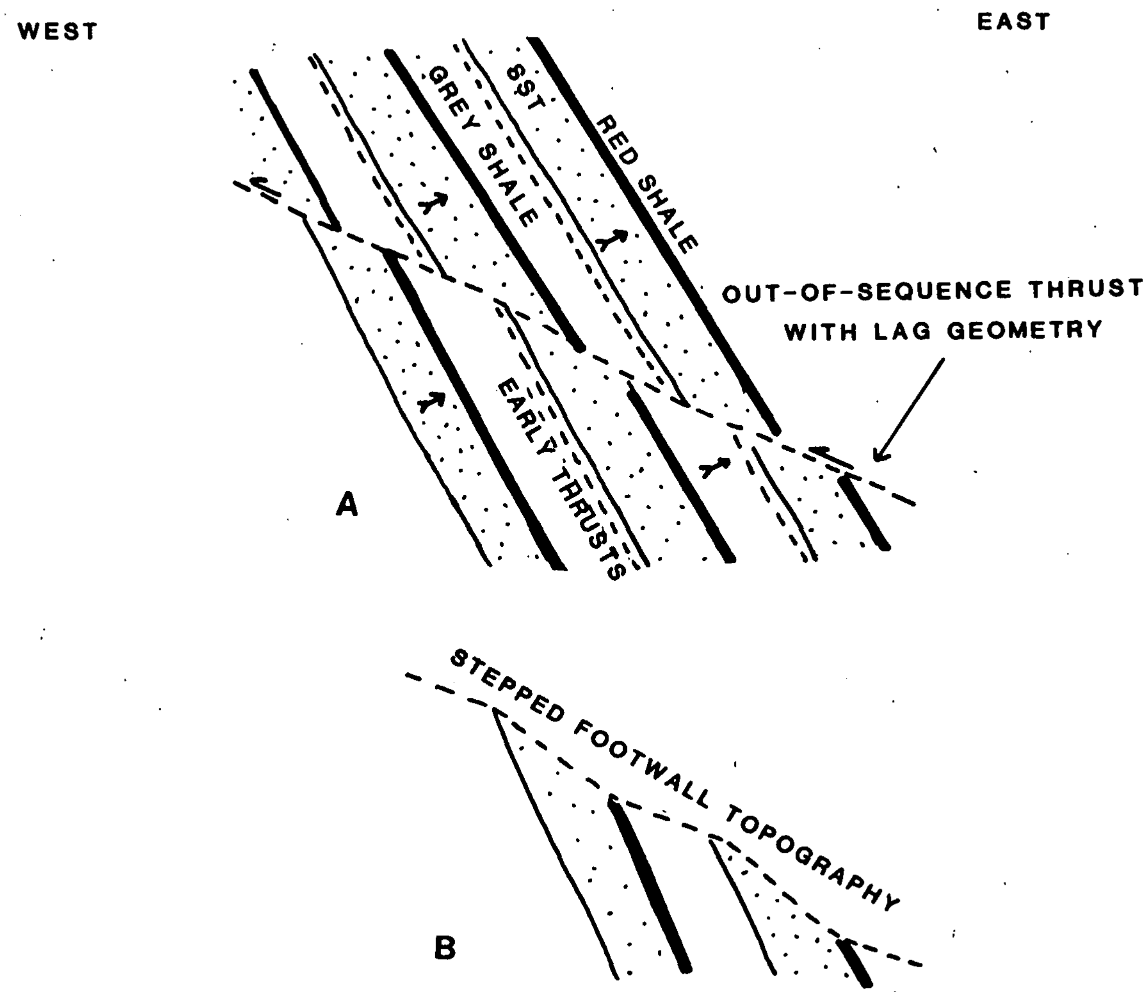
WEST
EAST
SST
GREY SHALE
RED SHALE
OUT-OF-SEQUENCE THRUST
WITH LAG GEOMETRY
EARLY THRUSTS
A
STEPPED FOOTWALL TOPOGRAPHY
B

development of a stepped footwall topography on any later thrusts. The numerous east and west dipping reverse faults in the Upper Grey shale unit most probably developed during and after the rotation of the bedding to steep angles and appear to be a general expression of continued NW-SE compression and vertical extension. The thrusts with the westward sence of overthrusting at locality 1 are interpreted to be backthrusts, that cut across earlier westward verging structures, such as the major fold pair.

In order to place the overall pattern of structural development in Study Area I in the context of probable positions in an accretionary complex, comparisons with a modern example like the Barbados Ridge are useful. In the Barbados Ridge complex around the DSDP Leg 78A & ODP Leg 110 sites (See Chapter 1, Section 1.5) the frontally accreted section has a similar thickness to that postulated for Study Area I. Usually the thrust spacing is about three times the stratigraphic thickness (see Chapter 1). Using this empirical relationship, a paleo-frontal thrust spacing of the order of 500m is arrived at for Study Area I. From the the Leg 110 studies it can be seen that the out-of-sequence thrusts may begin to develop fairly soon during the initial phase of rapid thickening of the the complex where only thin sequences are frontally accreted (i.e. within 10km or less of the deformation front). They then may continue to develop further back in the complex. The backthrusts in particular are more likely to have formed much further back in the complex, judging from where they begin to become apparent in the Barbados Ridge Accretionary Complex (Chapter 1 & 2).

The material in the fault zones appears to undergo a change in its response to continued shearing. There are a number of examples in Study Area I (eg. Loc 7) of fault zones in which the sandstones are necked and boudinaged and with poorly developed scaly clays (Plate 9, 26 & 27). Deformation appears to have been active when both the sandstones and muds were highly unconsolidated. The fault zones in which these sorts of feature are developed where observed nearly always run parallel to bedding. Features that are indicative of 'soft sediment' deformation have not been observed in the fault zones that have been interpreted to be out-of-sequence structues.

Scaly clay fabrics orientated sub-parallel to the fault zone margins appear to be the next commonly developed fabric in the argillaceous units. These are seen at most localities. The scaly clay fabric development varies between relatively mild fabrics in which the scaly clay chips are quite large (2-5mm across i.e. Plate 5.10) and intense scale clay fabrics in which the chips are very small (<1mm across, e.g. Plate 3.5 & 3.7). The included sandstone blocks appear to undergo extension along brittle shears and may have been considerably more consolidated (Plates 3.7 & 3.16). Folds may also be developed in the fault zone material, folding the main fabric. In the main fault zone at locality 3, the folds are nucleated on discrete shears that cut across the fault zone at low angles and may, therefore, be related to a later phase of movement (Plate 3.17).

The fault zone of Locality 2 best illustrates the fabrics that may develop after the scaly clays. In this case, scaly clay fabrics appear to become over-printed by a flattening or compaction fabric that would correspond to a 'S' fabric in a ductile shear zone. In places, corresponding 'C' fabrics are also developed (Plates 3.11 & 12). In addition to compaction, it may be possible that a certain amount of pressure solution and mass transfer was involved in the formation of the 'S' fabrics. Although these late forming 'ductile shear fabrics' are best developed at Locality 2, they occur sparodically in the intensely deformed and regions of a number of the faults studied ie. the back thrusts developed at Locality 1.

The variation and changes in the behaviour of the fault zone materials in response to shearing are most likely to result from changes in their state of consolidation. Continued shearing along the fault zones enhances their prospects for dewatering (Bray & Karig 1985) with soft sediment mechanisms giving way to brittle/ductile shearing and the development of scaly clay fabrics. Knipe (1986) illustrates how the deformation deformation mechanism may be controlled by the porefluid pressure, lithification and strain rate (Fig. 0.5). Soft sediment deformation features are most likely formed by independant particulate flow, which is aided by poor consolidation and high porefluid pressure. The change to scaly clay fabrics results from a change in deformation mechanism due to increasing lithification (with or without a drop in pore fluid pressure). The mechanism of deformation then largely depends on strain rate. The S/C *fabrics are interpreted to be a result of syncronous compaction and shearing in the fault zone. To form such a well developed S fabric, compaction may have been occurred quite rapidly, most probably as a consequence of a loss of fluid pressure. The most obvious indicator of high poreflid pressures within the fault zones at the time of disruption of the materials is the injection of shale into sandstone blocks, a feature seen in a number of the fault zones (Plates 3.9, 3.35). As will be discussed in greater detail in Section 3.4.4 and Chapter 4 (Section 1.7.2) these injection features require the formational pressures of the argillaceous material to be greater than those of the sandstones. The fault zones can be seen to be acting as conduits for the transmission of high fluid pressures, or a more massive transfer of overpressured argillaceous material, through deforming sequences.*

3.4.3 Frontal Accretion or Subcretion ?

Frontal accretion of this section is favoured for a number of reasons. The western regions of the complex are at sub-metamorphic grades with only the sparodic development of cleavage. Furthermore, thick sedimentary sequences are preserved in the Tertiary slope basins, just offshore of Study Area I (Bol & Hoorn 1980), and may outcrop along parts of the coastal regions near Kota Kinabalu. This would seem to imply that the nature of the deformation and sequential structural development in the Kota Kinabalu area (Study Area I) corresponds to a position near the surface of the *accretionary complex (i.e. within the upper 3km). Frontal accretion increases the chances for material to end up in a position near the surface of the complex. In addition, the presence of large slump deposits within the upper parts of the local stratigraphic section implies that they were deposited in a proximal sedimentary environment, with the axial palaeocurrent current directions indicating that this was probably in a trench. Thin turbidite sequences (i.e. the original thick stratigraphic section in Study Area I was only 140-180m thick), or the upper parts of thicker sequences, are almost always frontally accreted (See Chapters 1 & 2).*

3.4.4 Origin Of The Melanges

Broken formations and chaotic melange deposits in both Study Areas have been attributed to three different processes, tectonic disruption along fault zones, slumping and mud diapirism. Sometimes a combination of one or more of the processes may have to be invoked to explain the final form of the disrupted body.

Slumping of material into the trench or a lower slope basin, probably accounts for the original disruption of the chaotic deposits in Localites 4 and 6, and possibly 5. The slumped sequence in Locality 4 has, however, been caught up along a major thrust fault, suffering substantial modification by later tectonic shearing. The intrusive "diapiric" form to some of the features in the deposits may result from the similarities that may be expected between the interaction of mobile matrix and included blocks. The relationships are even less easy to interpret at locality 5, where it may be possible that the slumped material was reactivated diapirically after being included into the complex. That diapirs may originate from slumped material should not be unexpected, as such deposits are generally highly underconsolidated. The main reason for interpreting these particular bodies as slump deposits is the high proportion of unconsolidated sandstone in them which is generally taken to indicate the action of near surface processes. It is possible that diapirs may originate from sequences in which the sandstones had not been fully compacted or that they may intrude up into sequences where such unconsolidated sandstones occur and so incorporate them. The problems of delineating between slump and diapiric origins for these particular melanges are increased by their common association with major thrust zones and/or areas of poor surrounding exposure where their contacts with the surrounding sequences cannot be ascertained.

Mud diapir activity is thought to be the best candidate for the melanges associated with Localities 8, 9 & 10. Evidence of high porefluid pressures and great mobility of the matrix are thought to be a good indicators of potential diapiric melanges. At Locality 10, the hydro-fracturing and intrusion of argillaceous material into the sandstone blocks and their subsequent disaggregation into the distinctive block shapes are thought to be particularly indicative. Furthermore, the blocks are commonly veined with calcite and occasionally quartz and it is thought to be unlikely that such abundant veining would occur in superficial slump deposits. The *distinctive block shapes, the intermixing of a wide variety of lithologies in very large bodies of originally unfoliated argillaceous material and the association of these melange bodies with major (and often late acting) fault lines, are all taken to be suggestive of their diapiric origins.*

The formation of broken formations by shearing along fault zones, has been discussed in connection with fault zone evolution (See above). Locality 9, however, illustrates the point that these zones of disruption can be potential source regions for diapirs. The material in the fault zone may be highly overpressured and mobile. The mobility of the fault zone material may be increased from that of the original undisturbed argillaceous horizons, as a consequence of the residual strength of sheared argillaceous material being less than the peak shear strength of unfailed material (Fig. 3. 29). The relationship of the large body of the potentially very mobile melange with the major thrust zone in Locality 9, is thought to be a good model for the deeper structure of the large shale diapirs and associated major late thrust faults in the Barbados Ridge Accretionary Complex. The examples above, and others from Timor, are discussed further in Chapter 4.

3.5 CONCLUSIONS

The main conclusions form the study of the NW Borneo Subduction Complex are:

1) The western areas of the accretionary complex are most probably derived from a thin turbiditic trench fill sequence (in the order of 140-180m thick) deposited in a NE-SW trending trench.
2) The turbidites were frontally accreted and then continued to be thickened by dominantly westward (trenchward) directed out-of-sequence thrusts. Many of these out-of-sequence thrusts had lag geometries. Folding occurred at all stages in the process.
3) The fault zones with 'soft sediment' necking and boudinage of the sandstone beds and with the absence or formation of only mild scaly clay fabrics, are attributed to the earliest phases of thrusting. Prolonged movement, or development of later faults in increasingly consolidated materials, led to the superimposition of increasingly intense scaly clay fabrics and eventually S/C fabrics. Enhanced consolidation of the fault zone material, with or without fluctuations in the pore fluid pressure, is thought to be responsible for the fabric evolution. Changes in the dominant deformation mechanism occur with a progression from independant particulate flow to such mechanisms as diffusional mass transfer and cataclastic flow.
4) Conjugate reverse faults, formed in response to NW-SE compression usually postdate the folds.

5) Large eastward (or arcward) thrusts occur in the complex, they are interpreted to be back thrusts that may have developed late stages of the initial period of rapid thickening, or very much later in the development of the complex. They are commonly associated with very intense scaly clay development in the fault zones.

6) Melanges and broken formations probably of three different origins occur in the complex. Broken formations developed along major thrust faults are common throughout the areas studied. Slumps with soft sediment deformation features occur near the top of the local stratigraphic sequence in Study Area I. Mud diapirism is thought to have generated large bodies of melange in the central regions of Sabah (Study Area II), where it is associated with major late thrust and/or strike slip faults, and forms smaller bodies of melange in western regions (Study Area I).

7) The pelagic section is not imbricated with the turbidites in Study Area I. It occurs, along strike, as a dismembered sequence in melanges, along with oceanic basement material. The melanges are associated with major late fault zones, some of which at least are major strike slip faults. The Pelagic section is proposed to have been subcreted at great depths and then raised to the current structural level in shale diapirs active late in the development of the complex.

CHAPTER FOUR

MUD DIAPIRISM: A MAJOR CONVERGENT MARGIN PROCESS

4.1 *INTRODUCTION*

Mud diapirism is an important large scale mechanism by which fluids can be expelled from deep within sedimentary sequences and may result in the formation of large volumes of melange. This chapter introduces models that account for the range in morphology and genesis of mud diapirs with an emphasis on those occurring in active margin environments. Specifically, the models relate the diapir's tectonic environment and physical properties of the diapiric material to mechanisms of their emplacement and subsequent development.

Mud diapirs have been recognised in many regions of the world (Fig. 4.1) in a variety of tectonic settings:
1) Transpressive regions e.g. Trinidad (Higgins & Saunders 1964, Arnold & Macready 1956), New Zealand (Ridd 1970).
2) Passive margin or basinal environments with rapid terrigenous sedimentation e.g. the Mississippi Delta (Morgan 1968), Apsheron Peninsula (Higgins and Saunders 1973), offshore Louisiana (Musgrave & Hicks 1968).
3) Accretionary complexes where thick mud rich terrigenous sequences are being tectonised e.g. the Barbados Ridge complex (Stride et al. 1982, see Chapter 2), Sabah (Geol. Survey Dept. Memoirs), and the Makran (Higgins and Saunders 1973, Freeman 1968).

FIGURE 4.1 - Regions in which mud volcanoes and/or shale diapirs have been observed (adapted from Higgins and Saunders (1973). A large proportion of the mud diapirs are associated with active margin or petroleum producing areas. (1) Barbados Ridge Complex; (2) Trinidad & Venezuela; (3) Colombia; (4) Ecuador; (5) Mississippi Delta; (6) Offshore Louisiana; (7) Texas; (8) Franciscan; (9) Coastal ranges, Washington; (10) Aleutian accretionary complex; (11) Sakhalin; (12) Taiwan; (13) Irian Jaya; (14) New Zealand; (15) Flinders Ranges; (16) Timor; (17) Sabah; (18) Java; (19) Sumatra; (20) Burma; (21) Makran; (22) Gorgan Steppes & SE Caspian; (23) Apsheron Peninsula; (24) Taman Peninsula; (25) Roumania; (26) Italy; (27) Mediterranian Ridge; (28) Tanzania.

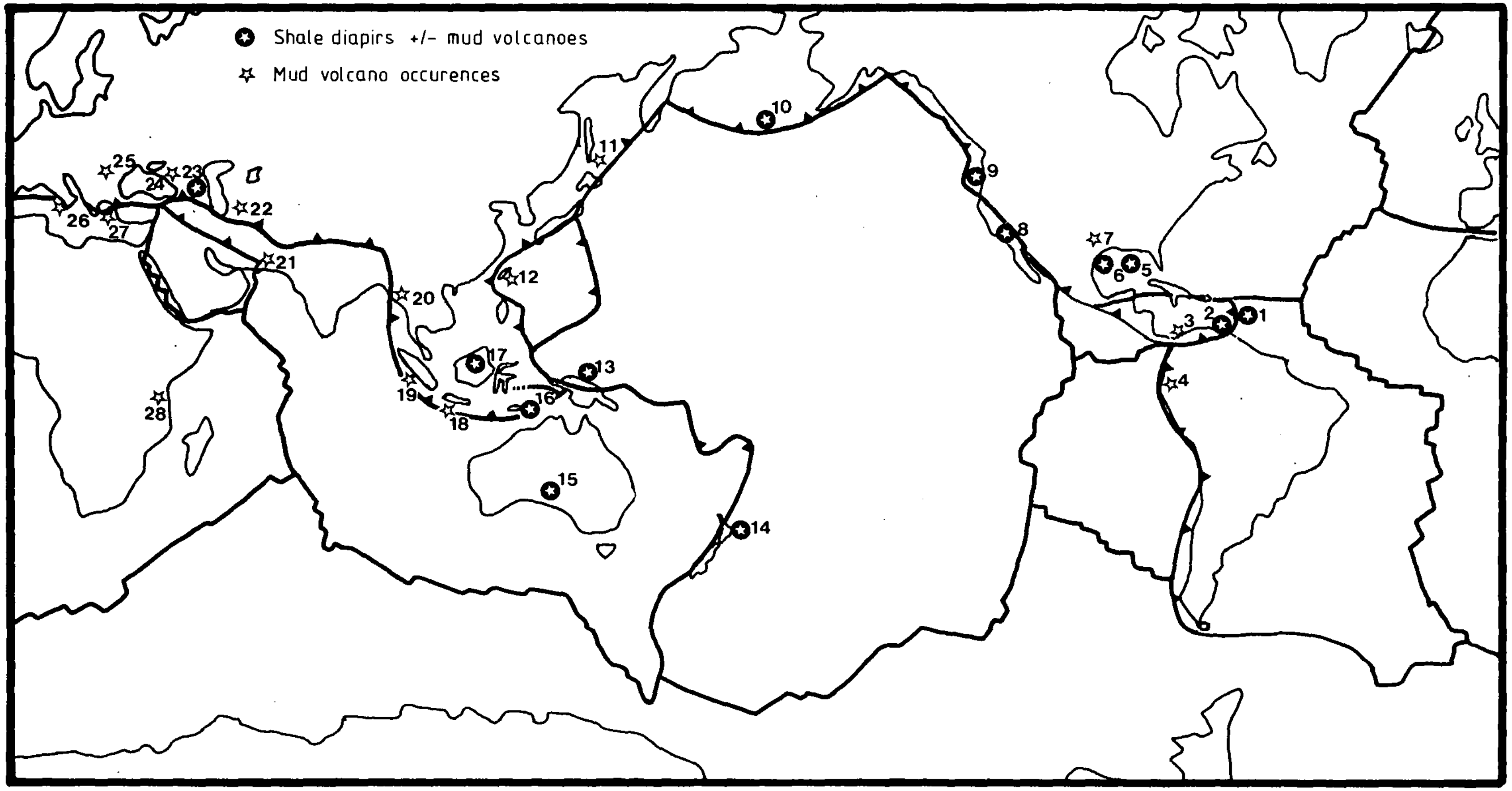

Shale diapirs +/- mud volcanoes
Mud volcano occurences
1
2
3
4
5
6
7
8
9
10
11
12
13
14
15
16
17
18
19
20
21
22
23
24
25
26
27
28

3) Collision complexes e.g. Timor (Barber et al. 1986), Italy (Higgins and Saunders 1973), Irian Jaya (William et al. 1984).

Mud diapirism is a relatively common process with many modern examples (Fig. 4.1), however, only a few ancient examples have been identified e.g. the island of Barbados (Larue and Speed 1984, Torrini et al. 1985) and the Cambria slab of the Franciscan (Becker and Cloos 1985), Timor (Barber et al. 1986). Many ancient melanges originally identified as olistostromal deposits e.g. the Franciscan (Gucwa 1975, Page 1977), the Bobonaro Scaly Clay Formation, Timor (Audley-Charles 1968), the Argille Scagliose, Italy (Page 1963, Abbate et al. 1970), and Lichi melange, Taiwan (Page 1977), may on further examination be better explained in terms of a diapiric origin. This paper is based on observations from modern and ancient mud diapir provinces, with specific reference to new data derived from W. Timor (see below) and Sabah, Borneo (see Chapter 3). It aims to provide information on the internal structure of intrusive and extrusive mud diapirs to aid in the recognition of these ancient diapiric terranes.

4.2 SUMMARY OF TECTONICS OF TIMOR

Timor is a deformation complex resulting from the imbrication of the original Banda forearc sequence and Australian continental slope sediments, with the latter being up to 6 to 7 km in thickness and ranging from Permian to

Recent in age. Continuing convergence is indicated by the development of a modern accretionary wedge in the Timor Trough. Timor is composed of a lower and an upper litho-structural unit (Barber 1977, Audley-Charles 1968, 1981) (Fig. 4.2). The lower structural unit consists of imbricated Permian to Jurassic clastics and limstones of Australian continental shelf affinities. The upper upper structural unit consists of southward directed exotic overthrust nappes interpreted as previously forming part of the Banda forearc. Audley-Charles (1965), previously interpreted the Bobonaro Scaly Clay Formation as being an unconformable olistostromal deposit on these two structural units and as being interbedded with Pliocene deep-water sediments. The Bobonaro Scaly Clay is a melange, in which blocks of the other formations of both structural units are found in a variably sheared grey, green and red argillaceous matrix. The last major tectonic event in Timor is of mid-Pliocene age (Barber et al. 1977). The Bobonaro Scaly Clay Formation is unconformably overlain by the mildly deformed Plio-pleistocene Viqueque group (Audley-Charles 1968, Carter et al. 1976).

The origin of the Bobonaro Scaly Clay has been reinterpreted as a diapiric melange (Barber et al. 1986). The Bobonaro Scaly Clay Formation is commonly found as discrete crosscutting masses intruding along major fault lines and is associated with currently active mud volcanoes. These mud volcanoes occur in 21 separate fields across W. Timor and are found in many of the adjacent islands of the outer Banda Arc (Rosidi et al. 1981, Tjrosapoetro 1978). Mud

FIGURE 4.2 - Tectono-stratigraphic map of West Timor adapted from Rosidi et al. (1981). Four divisions are emphasised; Exotic Overthrust nappes; nappes of Australian Continental material; Melanges (Bobonaro scaly clay Fm.); Slope Sediments. The location of the figures and plates discussed in this chapter and other observed mud diapirs (taken from Barber et al. in press) are marked. Quaternary sediments are left unstippled.

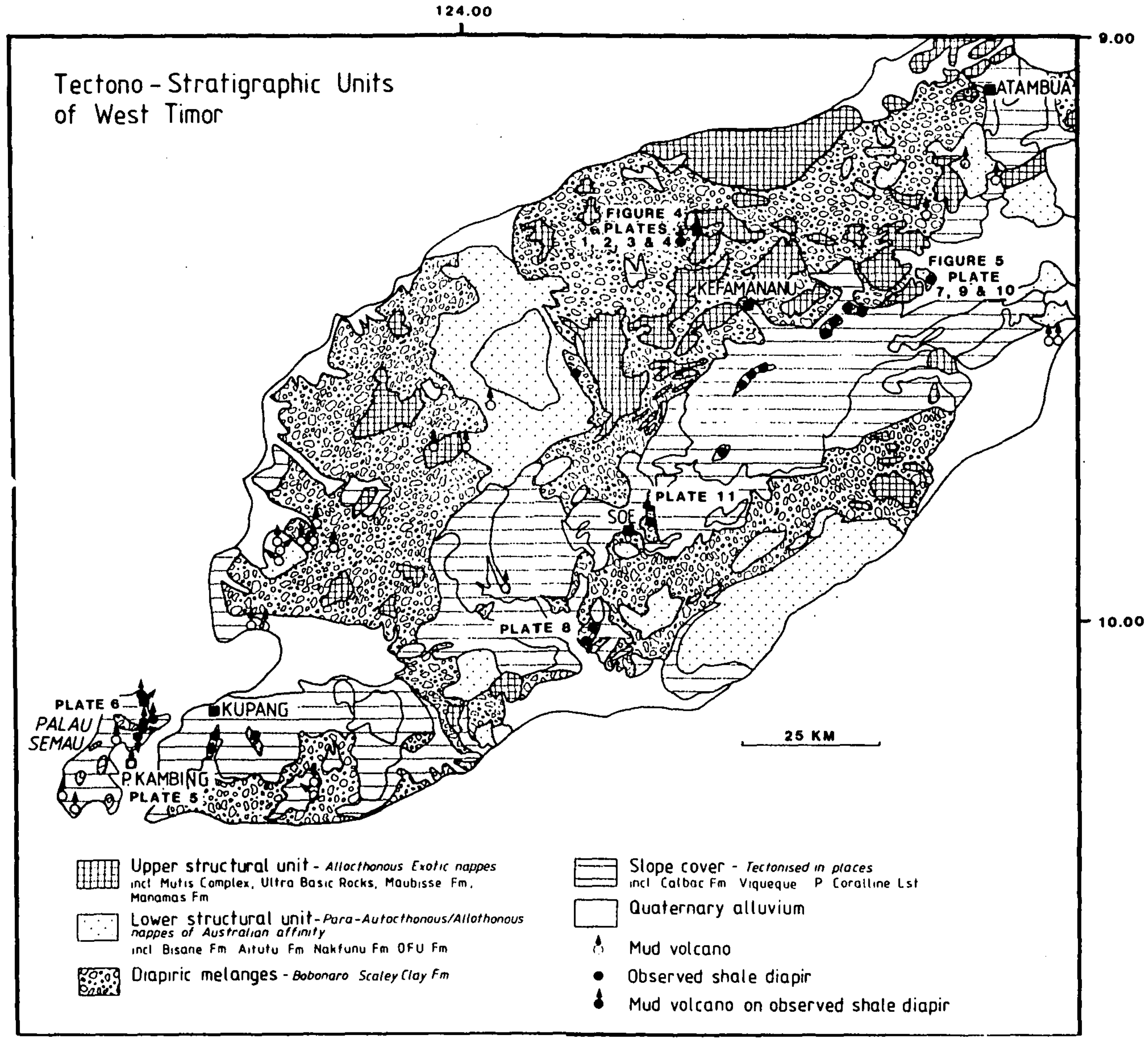

124.00
9.00
10.00
Tectono - Stratigraphic Units
of West Timor
ATAMBUA
FIGURE 4
PLATES
1, 2, 3 & 4
FIGURE 5
PLATE
7, 9 & 10
KEFAMANANU
PLATE 11
SOE
PLATE 8
PLATE 6
PALAU
SEMAU
KUPANG
P. KAMBING
PLATE 5
25 KM
Upper structural unit - Allocthonous Exotic nappes
incl Mutis Complex, Ultra Basic Rocks, Maubisse Fm, Manamas Fm
Lower structural unit - Para-Autocthonous/Allothonous nappes of Australian affinity
incl Bisane Fm Aitutu Fm Nakfunu Fm OFU Fm
Diapiric melanges - Bobonaro Scaley Clay Fm
Slope cover - Tectonised in places
incl Calbac Fm Viqueque P Coralline Lst
Quaternary alluvium
Mud volcano
Observed shale diapir
Mud volcano on observed shale diapir

diapirism appears to have occurred in Timor since Miocene times and abundant modern diapiric activity indicates that the process has continued into the present.

Barber et al. (1986) identify the Middle and Upper Triassic section as containing red, green and grey shales that are similar to the sheared shales that commonly make up the Bobonaro scaly clay matrix. The actual source regions of the diapirism are problematical as the scaly clay contains foraminifera of Mesozoic to Pliocene age (Rosidi et al. 1981). In the light of the olistostromal theory (Audley-Charles 1965), it was concluded that pre-Miocene foraminifera may have been reworked. Closer analysis of the faunal ages of the matrix of different diapirs may, however, indicate that the diapirs were sourced from several stratigraphic horizons.

4.3 *CLASSIFICATION OF MUD DIAPIRIC MANIFESTATIONS*

Variations in the genesis and subsequent behaviour of mud diapirs are related to differences in the physical properties of the diapiric matrix. The most important physical properties of the diapiric material are its viscosity and the proportion of methane within it. They are further influenced by their tectonic environment and it is a combination of both the tectonic environment and physical properties that decides their final form.

Figure 4.3 illustrates the proposed general relationship between types of mud diapir activity and the viscosity and methane content of diapirs. The field is split into three major divisions; Fluid Exhalations, Mud Volcanoes; and Shale Diapirs. These major divisions have then been subdivided into the five different types of diapiric manifestation that are refered to in the text. The fluid exhalations and mud volcanoes are surface phenemenon where as, the shale diapirs are predominantly intrusive, except for the instances where they pierce the surface (in which case they are said to form mud ridges/domes, classified as type III extrusive diapirs).

4.4 THE RANGE IN NATURE, MORPHOLOGY AND INTERNAL FEATURES OF EXTRUSIVE FORMS OF MUD DIAPIRISM

4.4.1 FLUID EXHALATIONS -(Type I)

These include gas blow-outs and hot-water vents. They are not strictly speaking diapiric manifestations and will not be discussed in detail. However, they may be considered as extreme end members of the mud diapir system, where only minor quantities of solid material are expelled along with the fluids.

Gas blow-outs (Type Ia) have methane as their predominant extrusive product. The methane may entrain some solid material and liquifies any partly consolidated material near the surface. In submarine examples the material disperses into the water column and craters tend to form (see Sweet

FIGURE 4.3 - The proposed system of classification and model illustrating the relationship between the bulk physical properties of the diapiric material and the tendency towards a particular type of diapiric manifestation. The boundaries between the different Types are transitional. Decreasing diapiric material viscosities can, as a first approximation, be equated with increasing percentage water contents (Kerr et al. 1970). Mud volcanoes may have their source regions in local fluid rich regions of both Type IV & V shale diapirs. The Type III mud ridges and domes may represent the extruded portions of either Type IV or V shale diapirs. Dewatering near the surface would tend to result in them being potentialy more consoildated than the material at depth.

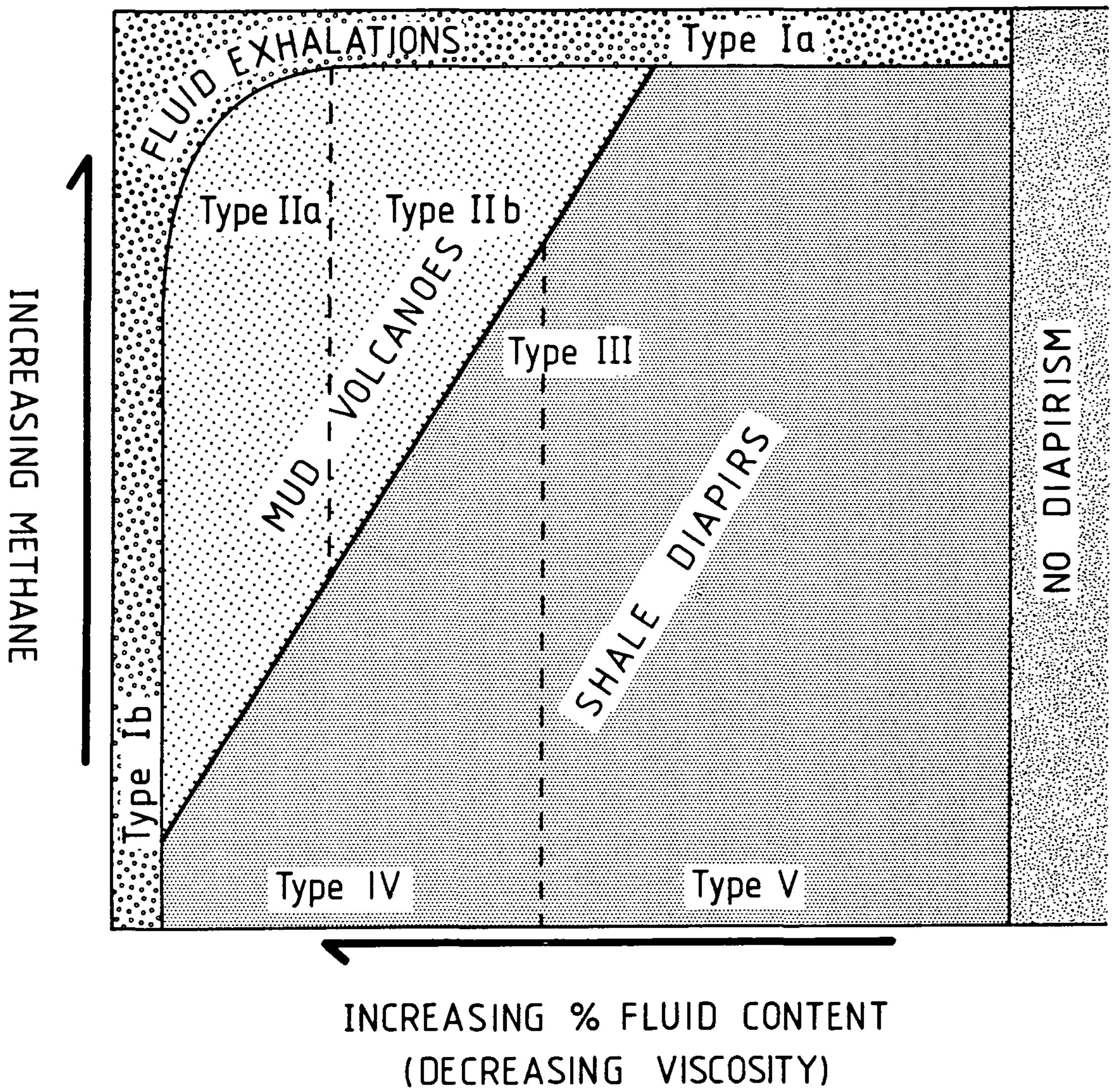

Mud diapirs and related processes can be classified into three main divisions and five subdivisions:

A) Extrusion Emmisions	Type I - gas blowouts (Type Ia) and hot water vents (Type Ib)
	Type II (a & b) - mud volcanoes
	Type III - mud ridges & domes
B) Intrusive Mud Diapirism;	Type IV - shale diapirs emplaced by stoping
	Type V - shale diapirs emplaced by forceful intrusion

1983).

Hot-water venting (Type Ib) occurs as a result of the expulsion of pore water from relatively deep within overpressured deformation complexes (Suess & Massoth 1984, Kulm et al. 1986).

4.4.2 Type II - Mud Volcanoes

These tend to develop along active fault lines, often forming linear chains. Quantities and rates of extrusion can be very high i.e. Adams (1908), estimated that the Waimata Valley mud volcano extruded 100,000 tons in an hour. Mud volcanoes show considerable variation in size, morphology and character of eruption. These variations can form the basis for classification. Shih's (1967), classification has been simplified and adapted to stress the genetic relationship between the physical properties of the diapiric material and the resulting edifice morphology (Table 4.1) and character of the eruptions. Eruptions are always associated with methane emission and its proportion relative to the other components affects the explosiveness of the emissions. The viscosity of the mud controls the angle of the edifice slopes. High viscosity muds also increase the likelihood of violent eruptions.

Type IIa mud volcanoes are characterised by gentle slopes of under 20°, resulting in broad shield-like edifices. They have potentially copious but non-violent emissions of methane

TABLE 4.1 - A classification of mud volcanoes into two types (IIa & IIb), based on their cone slope angle. The viscosites are based on studies of mud volcanoes in Tiawan by Shih (1967). Shih's classification was also based on additional factors such as crater size and has been simplified.

Shih (1967)			Reclassification Brown (1987)	
mud volcano type	cone slope angle	range of viscosity	mud volcano type	cone slope angle
A	> 20° (upto 50°)	$10^4 - 10^3$	IIb	> 20°
B	20°- 5°	$10^3 - 10^2$	IIa	< 20°
C	<5°	$< 10^2$		

and are associated with low viscosity muds (see Table 4.1). An example of this type is the small but well developed mud volcano field near Oesilo in W. Timor (Fig. 4.2). It lies in an area of low hummocky terrain formed during the erosion of the top of a shale diapir several kilometres in diameter. Recent activity has built up a mound 4-7m high and some 100-150m in width with several eruptive centres (Fig. 4.4). It is one of several mud volcano fields on the shale diapir. Its eruptive episodes are repetitive, occurring every year at the end of the dry season. The main eruptive centres are caldera-like in form with craters 5-10m wide and edifice slopes under 5° (Fig. 4.4 & Plate 4.1). Copious quantities of gas were reported to be emitted during the eruptions. Prior to, or during the eruptions, doming of the area produced tension fissures and associated fissure eruptions (Plate 4.2). The fissures developed with radial and concentric distributions round the eruptive centres (Fig. 4.4). Minor cones (less than 1-2 m in diameter) are also scattered across the area and show a wide range of cone slope angles (Plate 4.3).

Type IIb mud volcanoes are characterised by steep cone-slope angles of 20°-50° (Plate 4.4). They are potentially highly explosive and are associated with higher viscosity muds (Table 4.1). Large examples (up to 100m high and 500m in diameter) are described in the literature (cf. Ridd 1970, Freeman 1968, Kugler 1939, Snead 1964).

FIGURE 4.4 - Sketch map of mud volcano field consisting of Type IIa edifices. There has been two recent eruptions, the latest had occurred the night before our vist and the associated mud flows were still too soft to walk on. The flows had spread some 10-100m down slope as thin sheets that tapered gently towards their edges. The mud contained very few competent fragments over 1cm in diameter. Doming and subsequent collapse of areas of the field prior to or during the main eruptions led to the formation of depressions and tension fissures and associated mud extrusions (Plate 4.2). The caldera like main eruptive centres (Plate 4.1) had slopes under 5°, where as the smaller cones that occurred along with them had highly variable cone slope angles between 5-35 (Plate 4.3). (Oesilo, Occussi on the former West-East Timor border (see Fig. 4.2 for location)

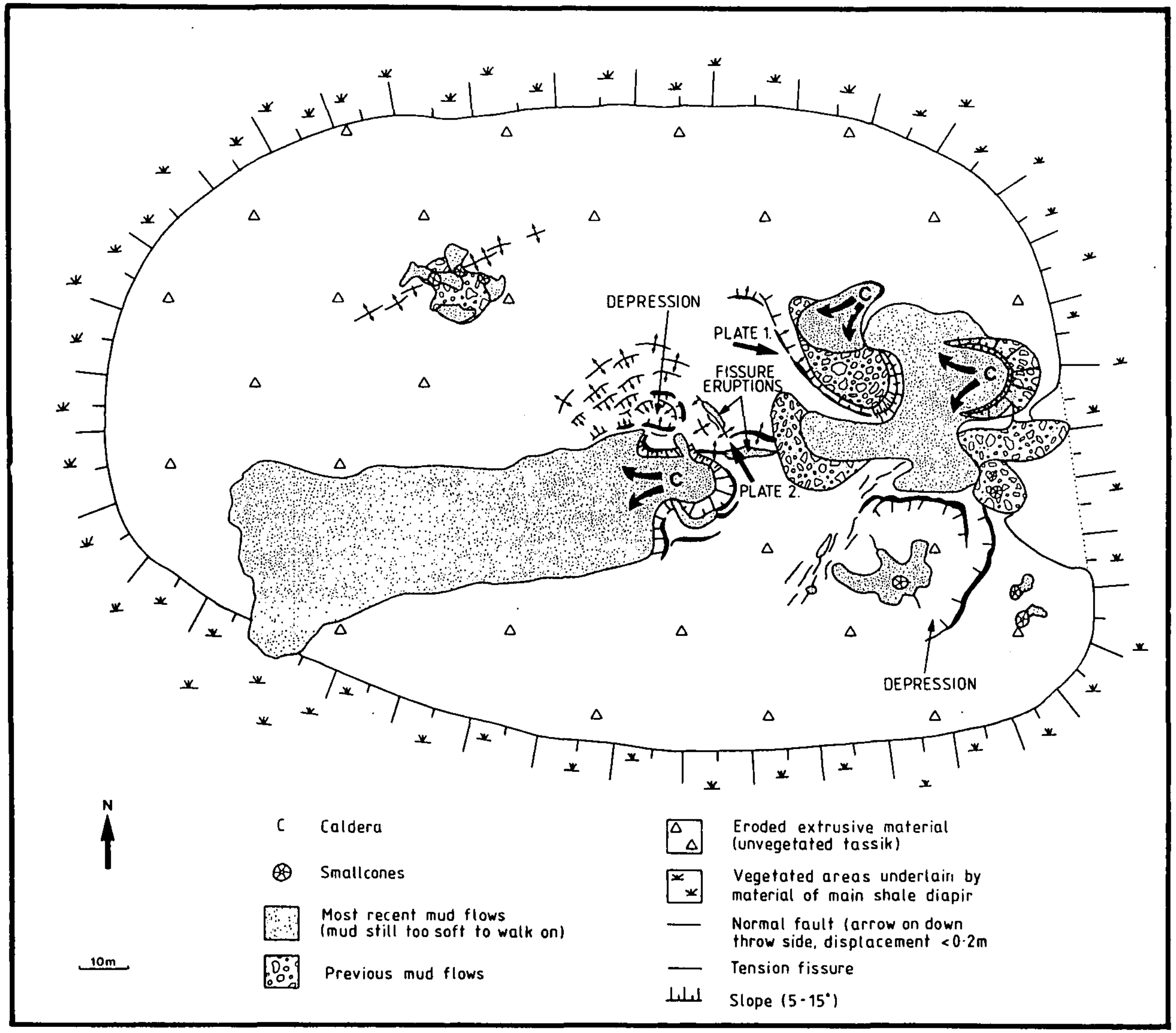

DEPRESSION
PLATE 1.
FISSURE ERUPTIONS
C
C
C
PLATE 2.
DEPRESSION
N
10m
C Caldera
Smallcones
Most recent mud flows (mud still too soft to walk on)
Previous mud flows
Eroded extrusive material (unvegetated tassik)
Vegetated areas underlain by material of main shale diapir
Normal fault (arrow on down throw side, displacement <0·2m
Tension fissure
Slope (5-15°)

PLATE 4.1 - Type IIa, caldera-like mud volcano. Note that the thin sheet like flows have an angle of repose less than 5° (see Fig. 4.4). Polygonal desiccation cracks affect the top of the flows.

PLATE 4.2 - Fissure eruptions of mud, extruded from tension features that formed during doming immediately prior to or during main eruptive episode (see Fig. 4.4).

PLATE 4.3 - A minor mud cone situated within the main mud volcano field of Figure 4.4. Slope angles of these minor mud cones are very variable. Near surface influences are thought to account for the bulk of this variation.

PLATE 4.4 - Type IIb mud volcano. This mud volcano lies on the same shale diapir, but at some distance from the mud volcano field of Fig. 4.4 and shows that the physical properties of the mud can vary widely even in a single shale diapir.

Mud volcanoes with small edifice sizes (i.e. those with diameters and heights below a few metres) can show considerable variations in their size and morphology within an individual field of mud volcanoes. This variation is thought to result from the strong modification of the diapiric material by near surface phenomenon e.g. ground water flow. In general, material erupted in copious quantities tends to be less modified by near surface processes.

The internal structure of mud volcano edifices depends on whether they have developed in a single (small number) major event or a large number of events, punctuated by periods of erosion or sedimentation.

Palau Kambing ,W. Timor (Fig. 4.2) is a Type IIa mud volcano (cone slope 10°) that forms an island 1-1.5 km wide, and which rises 100m above sea level (Plate 4.5a). At present, it has minor waneing stage activity in the form of Type IIb cones (under 10m in diameter) in its central 100m wide depression (Plate 4.5b). The internal structure of the main edifice is characterised by randomly oriented blocks of competent units (with a maximum diameter of 1.5 m) enclosed within unbedded unfoliated mud (Plate 4.5c). The lack of any bedded structure suggests that it formed in a single or very small number of major paroxisms. The Trinidad mud volcanoes of Arnold & MaCready (1956) and Higgins & Saunders (1967) are also examples of mud volcanoes with a chaotic internal structure, formed in a single catastrophic event.

PLATE 4.5 - a) Palau Kambing, a 1-1.5 km wide, 100m high mud volcano that forms an island off W. Timor (see Fig. 4.2 for position).

- b) Minor Type IIb mud volcanoes occuring as late stage waining activity in the central 100m wide caldera. Caldera wall in background.

- c) Chaotic internal structure of Palau Kambing revealed in part of the exposure along a gully cut into the flank of the mud volcano edifice. Blocks up to 1.5m in diameter are randomly oriented in a muddy matrix in which no stratification is apparent. The edifice is thought to have been erupted in a single or small number of events. (see Fig. 4.2 for location)

In contrast to Palu Kambing, there is a well developed internal fabric, recording the progressive growth of a 200m diameter, 15-20m high, mud volcano (Type IIa) near Hala on Palau Semau, W. Timor (Plate 4.6a, Fig. 4.2). The internal bedded form to the volcano results from the separation of mud flows (under 0.5m thick) by bands rich in competent fragments (generally under 0.5 cm in size)(Plate 4.6b). The fragments are thought to have been concentrated during periods of erosion between mud flows. Internally the mud flows have a faint fabric parallel to margins resulting from flow alignment of clay minerals (Plate 4.6). As the form of the volcano seems to indicate that it was formed from fluid mud, perhaps such flow aligned clay fabrics can be used to characterise low viscosity mud flows in ancient examples. In submarine occurrences the layering may result from erosion by currents, or background sedimentation between flows.

As a result of their extrusive nature the main products of mud volcanism may be interbedded with sediments in normal stratigraphic position. The extrusive products can cover very extensive areas. Single edifices up to 10 km in diameter have been identified on the Barbados Ridge accretionary complex (see Chapter 2), whilst, Williams et al. (1984) report extensive mud volcano fields in Irian Jaya, where the extrusive products cover areas up to 50 km long and 25 km wide. Ancient examples of such features tend to look like debris or mud flows of sedimentary origin. If the flows contain exotic blocks from deep within the deformation sequence they would previously have been identified as olistostromal deposits, similar to those described by Abbate

PLATE 4.6 - a) Two Mud volcanoes, the larger now inactive Type IIa edifice which is some 200m wide (to the right), is disected by the coastal cliffs.

- b) Close up of an individual mud flow exposed along the low cliff sections of the disceted mud volcano above. Bedded nature of flows picked out by fragment rich intervals. NOTE faint laminated fabric in mud subparallel to margins of the flow (and pencil).

et al. (1969) and Hoedemaeker (1973).

Smaller mud volcanoes may have enough of the edifice exposed to identify their characteristic geometry and some idea of the original viscosity of the extrusive material may be gained from the cone slope angle. However, as this is likely to be an uncommon situation, the following further features of the internal structure of the mud flows may aid in the identification of ancient examples; (1) vesicular textures (Freeman 1968); (2) concentrically foliated pellets composed of matrix material (gasoclasts) (Freeman 1968); (3) blocks with pervasive calcite veining that originated at depth within the diapir. Other features common to subaerially erupted mud flows are desiccation cracks, ropy textures and dewatering structures. In eruptions where the expeled methane has caught fire, mudflows can be fused and burnt to porcellanite (Kugler 1939). Later fluids forced up along the faults may alter or lithify the diapiric material. Freeman (1968), suggested this as the cause of the silicification of the proposed mud volcano conduits of the middle Tertiary mud diapirs.

4.4.3 *Type III - Mud Ridges and Domes*

These result from the slow extrusion of viscous muds with which there is little significant methane emission. Snead (1964), describes the occurrence of long ridges of viscous mud, in the Baluchistan area of Pakistan, that have been exuded like toothpaste from major faults. One particular ridge is 20 miles long, several hundred feet high and has *slopes of 40-70. Similar diapiric mud ridges have been identified in the offshore regions of the Barbados Ridge accretionary complex (see Chapter 2). Mud domes might be expected if the extrusion occurred only at a single point. The Chatham Island 1964 eruption appears to have had some of the characteristics of this form of extrusion (cf. Higgins & Saunders 1967).*

4.5 THE RANGE IN NATURE, MORPHOLOGY AND INTERNAL FEATURES OF INTRUSIVE FORMS OF MUD DIAPIRISM: SHALE DIAPIRS

There are a number of factors that influence the final form of shale diapirs with the tectonic environment and material properties of the diapir being the most important.

4.5.1 Effect of Tectonic Environment

The tectonic environment strongly influences the overall morphology and distribution of shale diapirs. Its effects can be summarised by examining the features of shale diapirs in areas of mild to strong tectonic activity.

In basinal environments, intrusive shale diapirs form structures similar to those of salt diapirs, with domal and piercement structures with roughly circular cross sections predominating. Their diameters rarely exceed a maximum of 16 km e.g.the Gulf of Mexico (Musgrave & Hicks 1968, Gilreath 1968, Roach 1962, Bishop 1978). Rim synclines are well *developed, controlling patterns of sedimentation. Diapirs are preferentially nucleated along regionally important faults, such as normal, transfer and strike-slip faults. Ancient exposed examples of shale diapirs that appear to have intruded up such normal faults have been described in the coastal region of Washington by Rau and Grocock (1974).*

In areas where mild lateral stresses have been imposed on the system, the shale diapir distribution becomes more closely associated with regional structural trends. Commonly a distinct pattern of broad synclines and sharp anticlines develops; the latter are often faulted and thrust at their crests. The anticlines are cored by diapiric material and mud volcanoes are developed along the fault traces. Even in these areas of mild tectonism the complexity of the interaction between diapir and thrust fault can be very great e.g.the Penal oil field, Trinidad (Bitterli 1958). In Trinidad the fold traces are roughly linear, whilst in the Apsheron peninsula, Russia (Kugler 1939), Flinders ranges, Australia (Dalgarno and Johnson 1968) and to a certain extent in New Zealand (Ridd 1970) the fold traces are variably arcuate. In general, it appears that as the degree of tectonism increases so does the linearity of the diapiric structures.

In convergent margin areas, where there has been intense tectonism with large scale thrusting of both the overburden and source regions, diapiric geometries are often very complex. Shale diapirs are most commonly observed to intrude up major regional faults. On the Barbados Ridge accretionary complex (see Chapter 2) diapiric material has intruded up large late thrust faults to form 18 km long and 1 km wide whilst, in W. Timor diapirs have intruded up strike-slip faults (Barber et al. 1986). If very large volumes of diapiric material are involved the whole complex may become chaotically disrupted in a manner similar to that in Irian Jaya (Williams et al. 1984).

4.5.2 Shale Diapirs: Physical Properties and Fabric Evolution

The common association of shale diapirs with active tectonic features means that strong post-emplacement modification of the fabrics within them is common. However, a set of fabrics that seem to to be characteristic of diapir evolution has been recognised from studies in Sabah and Timor. The fabrics have been divided into two types on the bases of the apparent state of consolidation of the diapiric matrix in which they formed.

Particulate Flow Fabrics - Early 'block in unfoliated mud' fabrics are most commonly preserved in the sheltered re-entrant angles of large competent blocks in proposed ancient diapiric melanges (see Loc. 10, Chapter 3, Plate 3.39). The absence of scaly clay fabrics implies that the matrix was behaving as a fluid and there is little evidence that it exerted shear on the blocks during this early important period of disruption. The competent blocks are randomly orientated and are not brecciated or boudinaged. Block shapes are very variable with rounded and *equant-angular shapes being common (Plates 3.43 to 3.45).*

The form of disruption is also related to the nature of the more competent material. The sandstone blocks in Plates 3.39 a, b, & c, are crosscut by an irregular net work of fractures filled with argillaceous material (Plate 3.41). These fractures are like the "web structures" described by Byrne (1984) but their close association with obvious shale injection features means that they are probably hydrofractures. In places irregular pods of argillaceous material up to 10 cm in diameter have grown within the block by injection along these fractures (Plate 3.40). The fractures are often curviplanar and some of the inclusions have subangular to sub-rounded shapes as a result (Plate 3.39). The exteriors of some of the smaller sandstone blocks have begun to disaggregate also producing rounded to irregular, wispy margins (Plate 3.39). Cowan (1985), describes similar shale injection features, especially into sandstones, as typical of his "type III" melanges.

The argillaceous material surrounding the blocks may be highly heterogeneous (Plate 3.39b), composed of a whole series of different argillaceous units, with varying degrees of competency. In the example shown in Plate 3.39b little evidence of the original heterogeneity of the matrix is still visible in the regions where it has undergone later shearing, and faunas extracted from the matrix for dating may give misleading results.

Flow fabrics may be evident, particularly if the argillaceous matrix is variegated in colour. The fabrics may also be picked out by block alignment and a very faint mild fabric (Plate 4.7). The surfaces of the partings that form the fabric in the mud are not polished or striated as in true scaly clays and perhaps formed by the alignment of clay minerals during the flowage of the mud.

Shear Fabrics - With increased consolidation the behaviour of the diapiric material goes through a transition and mild scaly clay fabrics begin to develop. It is thought that the transition arises from the change from particulate-flow to a more plastic type of deformation. The scaly clay foliation is a mesoscopic expression of displacements along closely spaced subparallel anastomosing slip surfaces, with a significant amount of strain potentially being taken up by bulk deformation in the intervening phacoids of argillaceous material as well. The long axes of the blocks are rotated into the foliation plane and a crude overall foliation tends to develop subparallel to the margin of the diapir. However, the trend of the fabric is often widely deflected round any competent block and in places may have a swirling irregular form (Plates 4.8a & b). This irregularity is thought to result from local variations of movement in the diapir, rather than the product of regional tectonic stress. As the fabric intensifies the spacing of the brittle shear surfaces decreases and the matrix increasingly exerts shear stresses on the competent blocks. Extensional fractures and shears, pinch and swell and "mullion-like" structures form, modifying earlier block shapes. The mobility of the matrix is much

PLATE 4.7 - The junction between an area of unfoliated mud (a) in which the included fragments have a random orientation and a mildly foliated region (b) in which a faint 'flow' fabric sub-parallel to the fault zone margins is developed. The nature of the fault zone is described in greater detail in respect to Figure 4.5 on which it is located. (see Fig. 4.2 for location)

PLATE 4.8 a) - River cut exposure through an area of Bobonaro Scaly Clay in which irregular swirling mild scaly clay fabrics are developed. These are thought to form during the late stages of movement of partly consolidated regions of a shale diapir

b) - Close-up of part of exposure in Plate 4.8a showing that the irregular swirling mild scaly clay fabrics are developed on all scales in this exposure. (Bentuka, W. Timor, see Fig. 4.2 for location) *reduced and the injection of scaly clay material into blocks is rarely seen. However, there are the occasional instances where scaly clays may have emplaced themselves into fissures developing in blocks (i.e. the sandstone block in Plate 3.35).*

The state of consolidation of different regions of a shale diapir can be very variable. Areas of the shale diapir that have already compacted and undergone brittle shearing may be intruded by unfoliated fluid mud potentialy originating from another region of the same diapir (Plate 4.11).

4.5.3 Type IV & V - Shale diapirs

Shale diapirs are less easily sub-divided than the surface manifestations of mud diapirism as their general intrusive geometries will also depend on the structural development of the deformation complex in which they occur, and in active margin environments will often undergo radical alteration by later tectonism (see below). In addition, their physical properties may change as a result of increasing consolidation during their active periods. However, the wide range of possible densities and viscosities gives rise to two differing potential emplacement mechanisms.

Type IV shale diapirs use stoping as an important mechanism that assists in their 'passive' emplacment. For instance, in shale diapirs exposed along the Boenoe river near Nikiniki, W. Timor (Fig. 4.2), large blocks (10's-100's *meters in diameter) of the exotic formations of the upper structural unit are encountered at the present erosion level. This is well below the structural level of the the nappes from which they come, which have since been removed by erosion. It would appear the blocks must have sunk, rather than risen, in the diapir. The foundered blocks are composed of relatively dense metamorphics, lavas, and massive limestones of the Maubisse Formation. Also within the same diapir there are blocks of the Triassic section of the lower structural unit which must have risen in the diapir. The Triassic section is composed of unmetamorphosed flysch type sediments, with (even at present) a relatively lower density than the material of the exotic formations. Foundered blocks sometimes show evidence of the surrounding melange having flowed up round them (Fig. 3.18 & 3.25).*

In contrast, Type V Shale diapirs emplace themselves by a more forceable mechanism pushing the overburden aside. The mud lumps in the Mississippi Delta (Morgan 1968), show some of the features that might be expected to relate to this form of diapir, with forceable doming of the overburden and the development of reverse faults. Stoping of the overburden is of minor importance. The general geometry of salt diapirs may be good analogies for what might be expected to occur in passive margin type environments, with the common development of normal faults in the extended portions of the of the overburden above the rising diapirs.

In general, the two mechanism differ in the amount of deformation transmitted into the overburden, the final *geometrical distribution of the blocks in the diapir in respect to their origins and the fabrics that might be expected to develop within them (see section 1.7.3).*

4.5.4 *Later Effects Of Tectonism*

Shale diapirs are often associated with active faults and suffer post-emplacement modification as a result. Many of the features of the shearing fabrics, developed during the later stages of shale diapir emplacement, are similar in form to those that may be later imposed on the diapir and they are therefore hard to separate. However, sometimes it is possible to directly relate fabrics to later tectonic activity. Figure 4.5 is a cross section through a partly tectonised shale diapir intruded into a now steeply dipping southward directed thrust in Triassic limstones near Bisnain, W. Timor (Fig. 4.2) . Near the hanging wall of the fault zone the argillaceous matrix is either unfoliated or has an irregular, faint and sometimes swirling flow foliation (Plate 4.7), in which the blocks have only have a poor alignment (Plate 4.9). The matrix becomes progressively more sheared towards the footwall with intensifying scaly clay fabrics and a greater alignment of blocks parallel to the fault margins (Plate 4.10). The lack of shear fabrics in the melange near the hanging wall suggest that it was implaced in a relatively fluid state. It was then subsequently sheared in the footwall regions by continued movement on the fault after it had dewatered. Even in the more sheared regions evidence of the early unfoliated nature of the fault zone material is

FIGURE 4.5 - Cross section through a steep fault zone cutting Triassic limestones, along which a body of melange is found. The argillaceous matrix is unfoliated at the northern margin of the fault zone and contains randomly orientated blocks. The intensity of the scaly clay fabrics increases towards the footwall of the fault zone as does the preferred orientation of the blocks. (see Fig. 4.2 for location)

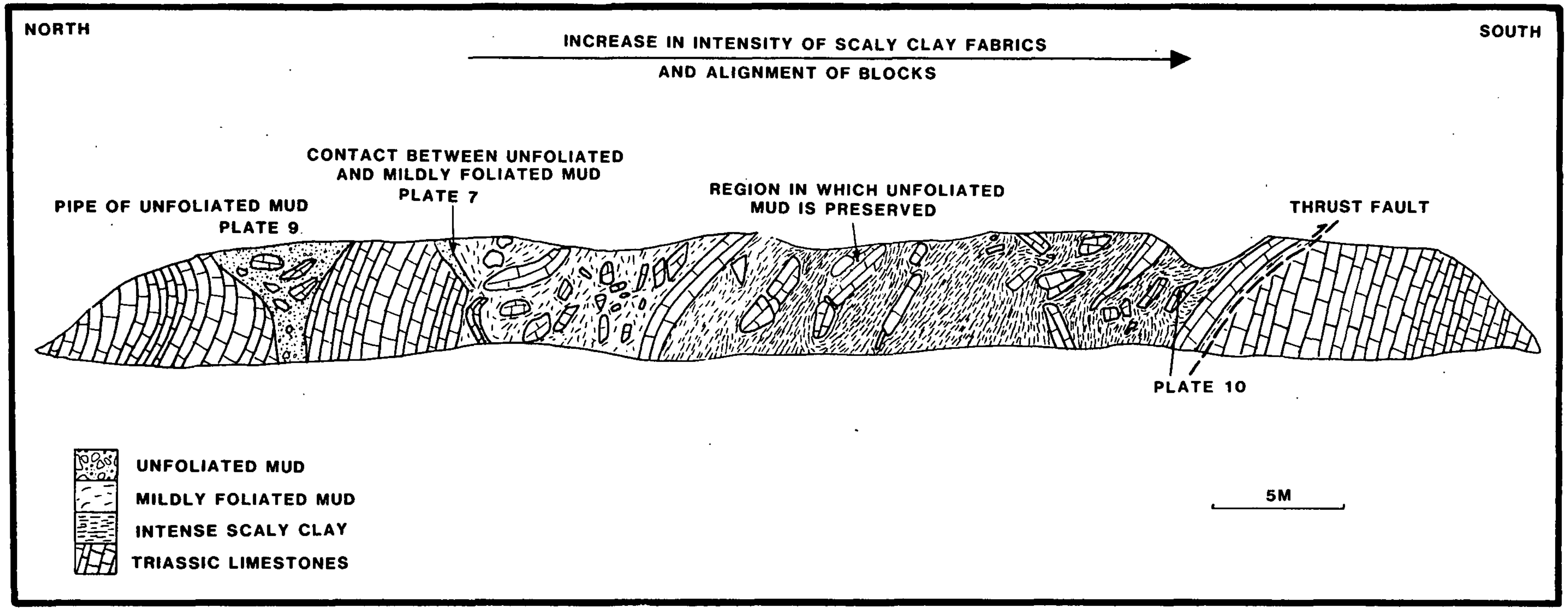
NORTH
SOUTH
INCREASE IN INTENSITY OF SCALY CLAY FABRICS
AND ALIGNMENT OF BLOCKS
CONTACT BETWEEN UNFOLIATED
AND MILDLY FOLIATED MUD
PLATE 7
PIPE OF UNFOLIATED MUD
PLATE 9
REGION IN WHICH UNFOLIATED
MUD IS PRESERVED
THRUST FAULT
PLATE 10
UNFOLIATED MUD
MILDLY FOLIATED MUD
INTENSE SCALY CLAY
TRIASSIC LIMESTONES
5M

PLATE 4.9 - Part of the plug of unfoliated mud that cut through the Triassic limestones at the northen end of the section through the fault zone illustrated in Figure 4.5. Note the chaotic block orientation. (see Fig. 4.2 for location)

PLATE 4.10 - More intensley foliated scaly clays, developed near the footwall of the fault zone illustrated in Figure 4.5. (see Fig. 4.2 for location)

preserved occasionally.

In general, later tectonism increases the intensity and uniformity of the scaly clay fabrics and the uniformity of the block shapes and their orientations, by flattening them into the foliation plane. In Timor the long axes of the blocks are predominantly aligned subparallel to the axis of the island (Rosidi et al. 1981). This is perpendicular to the main regional compressive stress and much of the scaly clay fabric in the Bobonaro Formation is thought to be the result of tectonic overprinting.

4.6 *FACTORS LEADING TO UNDERCONSOLIDATION IN SHALES*

Mud diapirism requires undercompacted argillaceous source regions. Hedberg (1974) gives a short review of many of the factors that are thought to contribute to overpressuring and undercompaction in relatively impermeable muds and shales. The significant factors in the formation of underconsolidated shale and therefore potential diapiric source regions are: (1) High rates of sedimentary loading; (2) Rapid tectonic loading; (3) Generation of oil and gas; (4) Release of bound water from expandable clays (montmorillonite or bentonite) derived from breakdown of volcanic material; (5) Development of structural barriers to fluid expulsion (i.e. faults etc).

A further important factor that may contribute to overpressuring is the lateral transmission of fluid pressures into the foreland in advance of developing thrust complexes

(Rubey & Hubbert 1959, Hubbert & Rubey 1959). Westbrook and Smith (1983), proposed that such a system was responsible for the mud diapirs in front of the Barbados Ridge accretionary complex. The laterally transmitted overpressures would have the additional effect of reducing the rates of compaction of the sedimentary section in front of the deformation complex and thus enhance the prospects for maintaining underconsolidation within it.

The relative importance of these overpressuring mechanisms varies and is dependent on the nature and composition of the source horizons (i.e. between a bentonitic source and an organic rich petroleum producing source) and the tectonic environment (i.e. between passive and active margin environments).

4.7 THE NATURE AND GENESIS OF INTRUSIVE MUD DIAPIRS

Variations in the emplacement mechanism, form and genesis of shale diapirs result from the combined influences of their tectonic environment and their physical properties.

4.7.1 Effect of Tectonic Environment On The Applicibality Of Theoretical Emplacement Models

In passive margin situations where regional tectonism has had a minimal effect on sedimentary diapirism, theoretical models have been developed to explain their diapiric behaviour. The theoretical models fall into the categories of buoyancy models and hydraulic models.

Buoyancy models have been generally applied to systems that can be treated as Newtonian fluids (Ramberg 1967, 1968a,b, Berner et al. 1972; Dixon 1975). In this type of model, diapirism results from the buoyant rise of viscous diapiric material through denser viscous sedimentary overburden. In these models it has to be assumed that fractures in the overburden do not play an important part in the emplacement process. These have most successfully been applied to simple situations in sedimentary basin environments.

Hydraulic models, developed to explain the emplacement of piercement diapirs of both salt and shale origin, assume that the overburden has cohesion (strength) rather than behaving in a purely viscous manner (Bishop 1978). Whilst, the overall driving mechanism of hydraulic and bouyancy models is similar, needing a density inversion between source and overburden, the hydraulic models involve the initiation of fractures along which the diapirs emplace themselves. The mobile substrate (mud or salt) is treated as a fluid and the diapir as a pressurised hole in a cohesive material. The model was derived to explain three mechanically distinct types of piercement emplacement (Figs. 4.6a, b, c); extrusion, vertically unconstrained intrusion and vertically constrained (forceful) intrusion. Vertically constrained diapirs must fracture and deform the overburden in order to grow, whilst vertically unconstrained diapirs do not. Vertically constrained diapirs may have their growth

FIGURE 4.6 - Models of the hydraulic emplacement of shale diapirs adapted from Bishop 1978. The diapiric material is considered to be a fluid and the diapir a pressurised hole in a cohesive overburden. Figures 6a, b & c are diapirs which are horizontally constrained in their growth by the overburden. Whilst, Figure 6d is of a shale diapir that is able to grow laterally along the fault in an unconstrained manner.

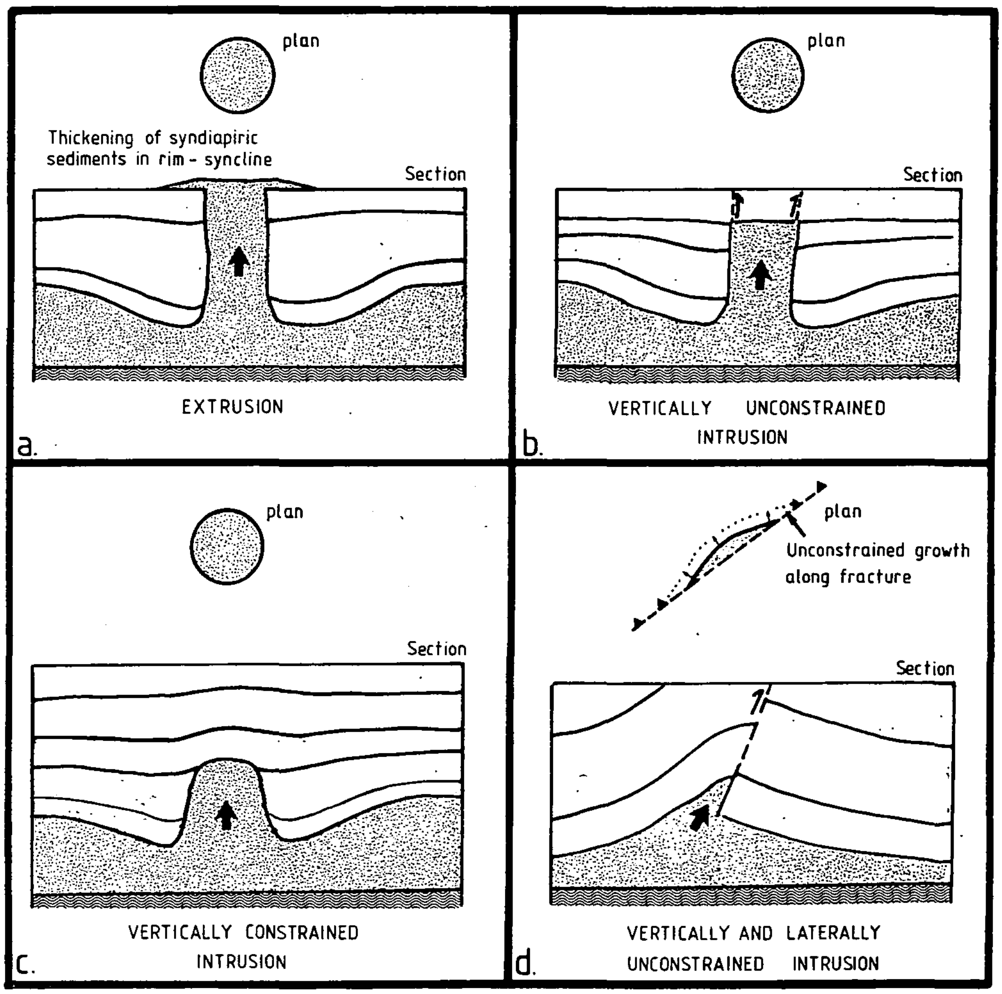
plan
Thickening of syndiapiric sediments in rim - syncline
Section
EXTRUSION
a.
plan
Section
VERTICALLY UNCONSTRAINED INTRUSION
b.
plan
Section
VERTICALLY CONSTRAINED INTRUSION
c.
plan
Unconstrained growth along fracture
Section
VERTICALLY AND LATERALLY UNCONSTRAINED INTRUSION
d.

restricted or stopped when the overburden cohesion becomes too great on the diapirs being buried deeply (i.e. when sedimentation > diapiric growth). Vertically unconstrained growth of piercement diapirs occurs if their tops remain near the sediment surface as a result of their having a growth rate that matches the rate of sedimentation. Bishops's (1978), hydraulic model assumed the diapirs were laterally constrained i.e. that they initiated their own fractures and did not intrude up pre-existing paths of weakness, like fault zones, which would allow them to develop in a completely unconstrained manner in the plane of the fault.

In active margin environments most shale diapirs are associated with fault lines. They have, therefore, grown as a vertically and laterally unconstrained hydraulic system in the plane of the fault (Fig. 4.6d). In such cases, the only limits on the size of the diapirs are the volume of the source regions and the rate at which fluids are lost from them.

In a hydraulic system, intrusion of diapiric material into the overburden will occur if the pressures in the diapiric material are greater than the sum of the least horizontal stress (i.e. geostatic plus tectonic stress) in the overburden and its tensile strength. Faults have a low or negligible tensile strength and therefore, shale diapirism in a heavily faulted and fractured thrust belt, will be controlled primarily by the horizontal stresses. Mud diapirism can be enhanced in regions where the horizontal stresses are locally reduced i.e. in pull-aparts along *strike-slip and tear faults, or along structures formed by the lateral spreading of the thrust sheets (Fig. 4.7). Shale diapirs, associated with strike-slip faults are seen in W. Timor (Barber et al. 1986). However, large diapirs have also been observed to extrude from major thrust zones where there has been no obvious reduction in horizontal stresses as in the Barbados accretionary complex (see Chapter 2).*

An important feature of a hydraulic system is that material will move from high to low pressure regions and this may be in a horizontal as well as a vertical direction. Indeed material intruding up low angle thrust faults will have travelled considerable lateral distances. If lateral expulsion of diapiric material occurs on a very large scale it could have considerable effects on regional tectonics (see below).

4.7.2 Effects of Physical Properties on Fabric Evolution Within a Shale Diapir

Thixotropic physical properties appear to be a common feature of the muds expeled from mud volcanoes. The initial proportion of fluids in the material of mud volcanoes may be higher than the average proportion in the main body of the shale diapir from which they are sourced. However, the studies do give a useful indicator as to the probable material properties of the deeper portions of shale diapirs. Kerr et al. (1970), examined the relationship between shear strength and water content of material from mud volcanoes in

FIGURE 4.7 - Regions in which the horizontal stresses may be reduced and the prospects for shale diapirism enhanced.

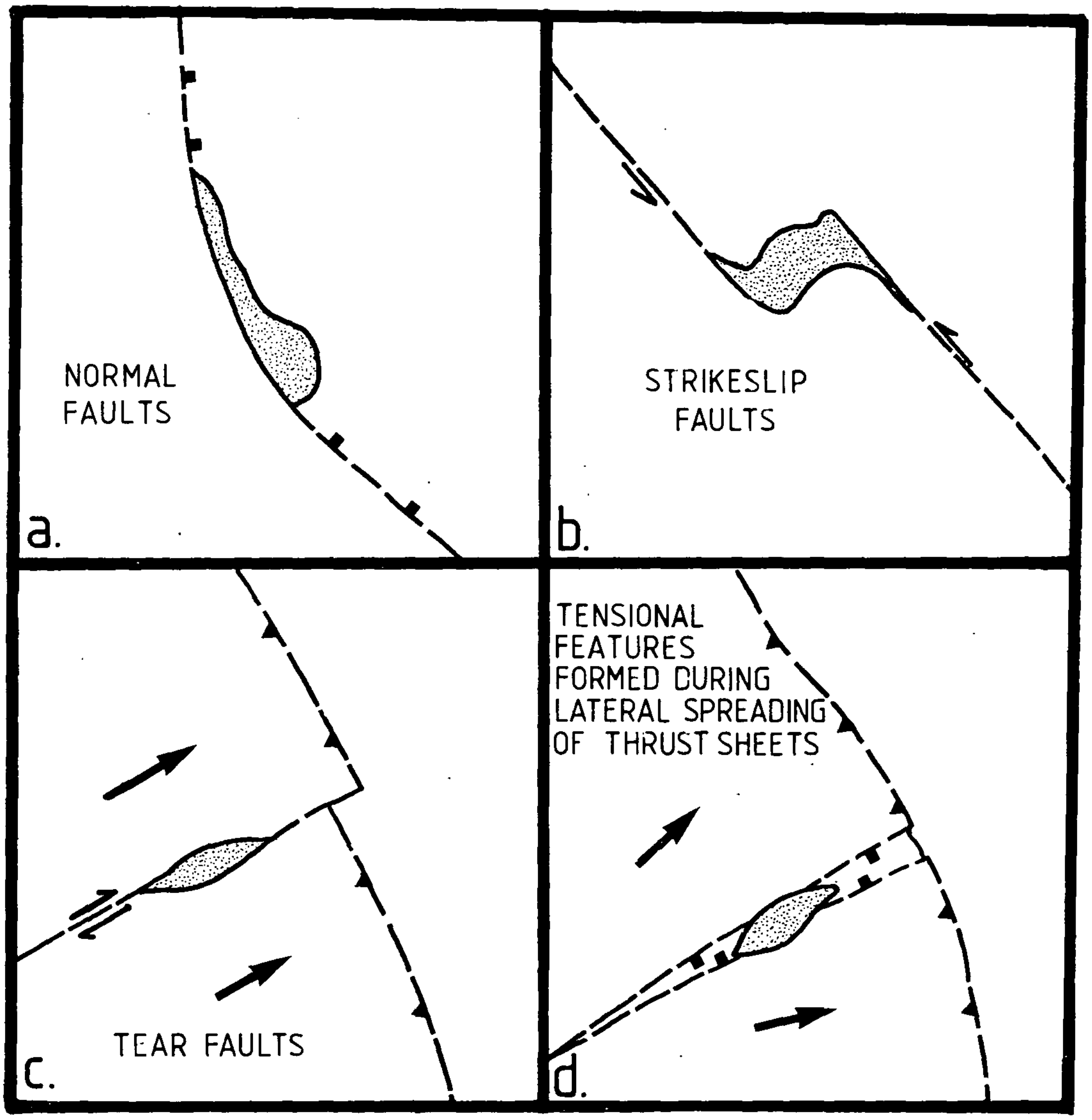
NORMAL FAULTS
a.
STRIKESLIP FAULTS
b.
TEAR FAULTS
c.
TENSIONAL FEATURES FORMED DURING LATERAL SPREADING OF THRUST SHEETS
d.

Trinidad. They found that its shear strength was noticeably low, with a water content in excess of 50-55%, rising markedly as the water content fell below 25-30%.

The early thixotropic behaviour of the diapiric material would be expected to result in the formation of the 'particulate flow fabrics', typified by unfoliated muds (i.e. Plate 3.39). The common equant angular shape to many of the sandstone blocks contained in the muds (Plate 3.44) is not likely to be a product of disruption by shearing. It is more suggestive of their having been disrupted along pre-existing fractures with the blocks acting as passive bodies. This previous fracture pattern may be unrelated to the diapiric activity. However, the block shape is a common feature of diapiric melanges studied in Sabah and Timor, suggesting that a genetic relationship exists between the block shape and the way diapirs interact with the surrounding country rock and enclosed blocks (see below). A network, or "hydrofractured-halo" will develop round a shale diapirs margins as it intrudes upwards into regions with much lower formational pore pressures if the overpressures within it exceed the cohesion and the least compressional stress in the surrounding material. When the surrounding formations are sandstones, textures in the hydrofractured-halo will be similar to those seen in the sandstone blocks illustrated in Plate 3.41. Mud is forcefuly injected into sandstone blocks and they are veined and disrupted until the the porefluid pressures in them reaches the levels of those in the diapiric matrix (Fig. 4.8). The products of the fragmentation of sandstone block tend to be equant angular (and sometimes even

FIGURE 4.8 - The development of a distinctive pattern of disruption of sandstone blocks as a result of the processes whereby the lower formational pressures in the sandstones are increased to those in the highly overpressured diapiric material. This process is accomplished by two mechanisms;

1) The migration of fluids into the block along hydrofractures (Fig. 4.8b & c), maintaining its volume. The internal regions of the sandstone block in Plates 3.39c & 3.41 is heavily hydro-fractured and these factors are thought to have formed during this process. However, as the permeability of the diapiric material is very low the diffusion of fluids out of it into the block may be a relatively slow process.

2) The compaction or implosion of the sandstone block (Fig. 4.8a) would also result in the equalisation of internal and external pressures. The volume loss is heterogenious through out the block and results in the injection of the diapiric material into it (Fig. 4.8b & c, Plates 3.39 to 3.41). Pre-existing fractures and the hydro fractures that extend into the central regions of the block would be preferential sites for intrusion. As the exterior regions of the block become disrupted, spalling off into the diapiric material, fresh surfaces would become exposed to the overpressured diapiric matrix (Figs. 4.8c & d).

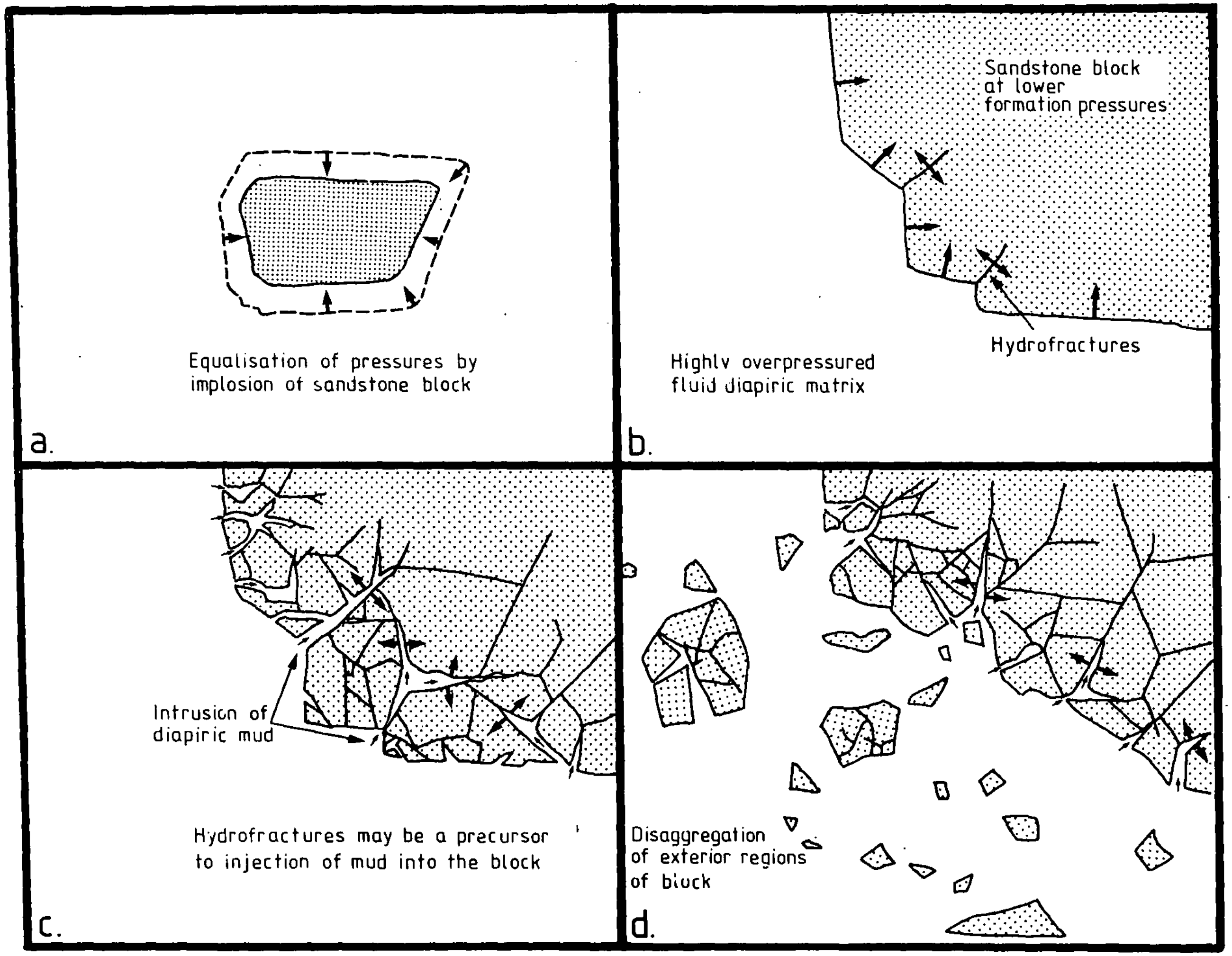

Equalisation of pressures by implosion of sandstone block
a.
Sandstone block at lower formation pressures
Hydrofractures
Highly overpressured fluid diapiric matrix
b.
Intrusion of diapiric mud
Hydrofractures may be a precursor to injection of mud into the block
c.
Disaggregation of exterior regions of block
d.

rounded) shapes, and these shapes are therefore thought to be indicative of disruption by this process. Formations in which the porosity is minimal (i.e. igneous and metamorphic rocks) will not be disrupted in quite the same way but may still be hydrofractured. This hydrofractured-halo would be one of the processes by which the diapir dewaters. Hydrofractures that may have a similar origin have been termed "vein structures" where they have been identified in mudstones units in slope deposits that sit on dewatering accretionary complexes (Ritiger 1985, Cowan 1982).

As the shale diapir dewaters to the extent where the muds can no longer behave as thixotropic fluids semi-ductile 'shear fabrics' develop with continued movement. They are likely to develop first in the upper, exterior regions of the shale diapir where the fluid losses are greatest. The early chaotic orientations of the blocks in the diapir become increasingly aligned in the foliation plane and some shearing and extension of the blocks parallel to the foliation may occur.

4.7.3 Control of Diapiric Properties and Tectonic Environment on the Emplacement Mechanisms of Intrusive Mud Diapirs

The actual mechanism of diapiric emplacement will lie somewhere in the spectrum between the passive (Type IV) and forceful (Type V) end members. Both the tectonic environment and physical properties of the diapiric material can exert an *important control.*

Type IV shale diapirs, are proposed to passively emplace themselves by stoping and need not cause wide spread disruption of the overburden material (Fig 4.9a). Stoping is far more likely to occur in situations where the diapiric material is composed of highly underconsolidated (Fig 4.3) thixotropic muds, with a potential wide spread development of particulate flow fabrics. The process of stoping requires the overburden density to exceed that of the diapiric material. The contrast must be great enough to overcome the resistence of the diapiric material to the blocks sinking through it. In this form of diapir it is possible to have lower density blocks being carried up in the diapir while others are sinking, resulting in the potential mixing of a wide variety of formations. By giving the overburden material more lateral freedom so the it can collapse into the diapiric material below extensional stresses in the overburden will assist stoping. The extensional stresses could result from exterior tectonic processes or by any doming of the overburden resulting from the more localised diapiric activity. Hydrofracturing of the country rock in the 'halo' round the margins of the diapir would also help to break up and liberate blocks into the diapir.

Type V shale diapirs emplace themselves forcefuly. They should be more consolidated than Type IV diapirs (Fig. 4.3), with greater overall viscosities and densities, behaving more in the manner of salt diapirs. Consolidation should increase towards their exterior regions from which the fluid can

FIGURE 4.9 - End member models illustrating the mechanisms by which shale diapirs may be emplaced.

A) Passive intrusion by stoping of dense overburden by diapirs with low densities and viscosities (Type IV). Hydrofracturing of the country rocks round the diapir may help in liberating blocks into the diapir (Fig. 4.9a).

B) Forceful injection of diapiric material from depth. The resulting growth and expansion of the diapir may be accomodated by the deformation of the previously consolidated outer regions of the shale diapirs (Fig. 4.9b). The diapirs growth and expansion may also accomodated by the intrusion of new diapiric material into the consolidated exterior regions without them becoming sheared (Fig. 4.9c). A combination of both mechanism is thought to operate in Type V diapirs.

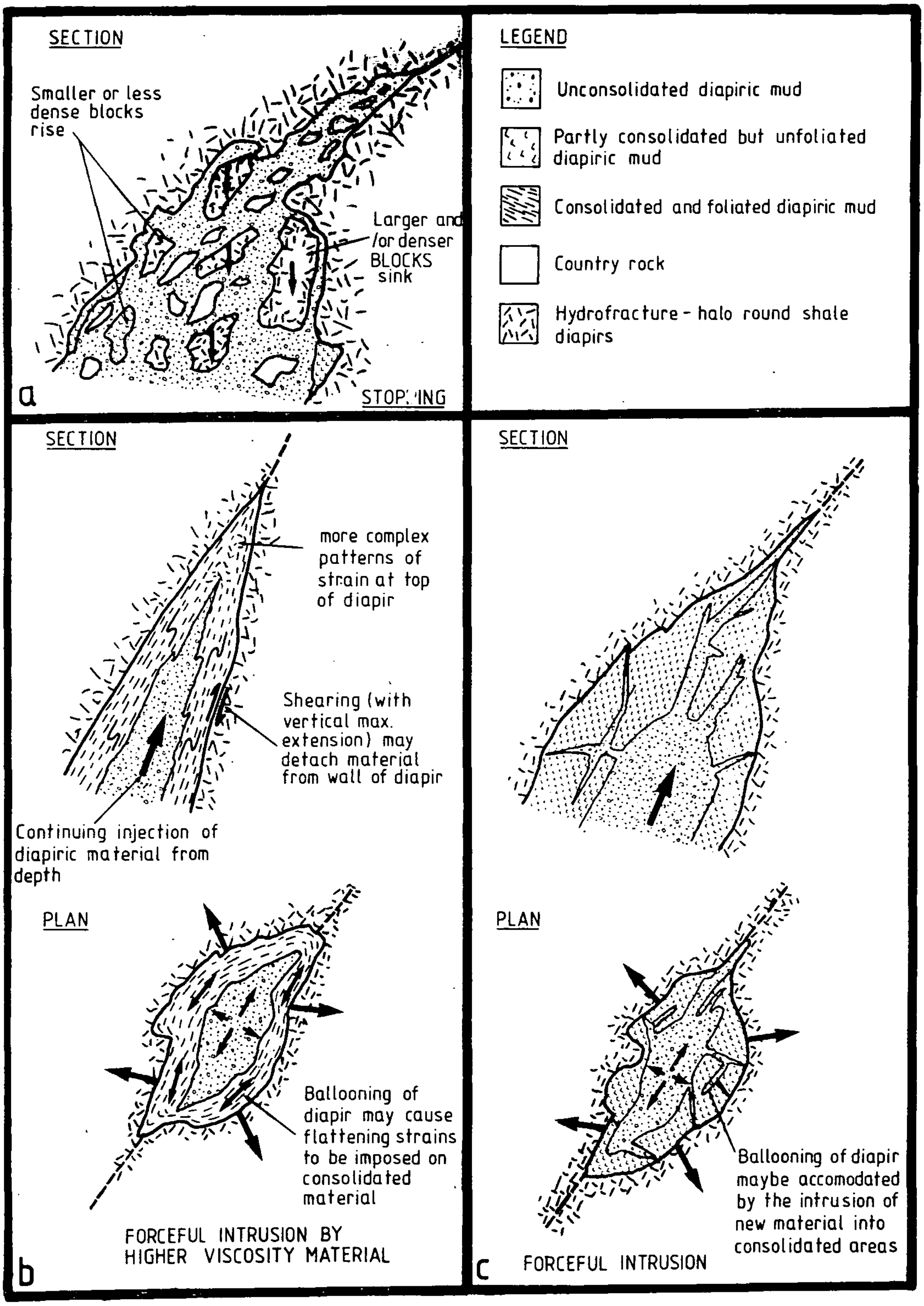

SECTION
Smaller or less dense blocks rise
Larger and /or denser BLOCKS sink
a
STOPPING
LEGEND
Unconsolidated diapiric mud
Partly consolidated but unfoliated diapiric mud
Consolidated and foliated diapiric mud
Country rock
Hydrofracture - halo round shale diapirs
SECTION
more complex patterns of strain at top of diapir
Shearing (with vertical max. extension) may detach material from wall of diapir
Continuing injection of diapiric material from depth
PLAN
Ballooning of diapir may cause flattening strains to be imposed on consolidated material
FORCEFUL INTRUSION BY HIGHER VISCOSITY MATERIAL
b
SECTION
PLAN
Ballooning of diapir maybe accomodated by the intrusion of new material into consolidated areas
c
FORCEFUL INTRUSION

escape most easily. They may develop the hydrofractured-halo round their margins but are too dense to emplace themselves by stoping and tend to entrain blocks, carrying them up towards the surface. Differential shearing within the diapiric material can mix blocks of different formations. The blocks may have originally been plucked from the walls of the diapir. In order for the diapir to grow these consolidated regions must be disrupted. This may occur by either or both of the following two mechanisims;

(1) "Ductile" shearing- The consolidated exterior regions of shale diapirs penetrated by boreholes are often found to be foliated and sheared. The foliation is usually found to be subparallel to their margins (Gilreath 1968). The shearing relates to their growth and expansion (Fig. 4.9b).

(2) The intrusion of the earlier dewatered (and possibly tectonised) diapiric material by unfoliated material (Plate 4.11 & Fig. 4.9c). This would disrupt the consolidated argillaceous regions along widely spaced fractures but would not result in them being sheared.

Relating Type IV & V mechanisms to the evolution of a diapir leads to the possibility of varying or hybrid behaviour. This will be particularly evident in situations were shale diapirs intrude up through deformation complexes in which a variety of tectonic units with widely differing densities are interleaved by thrusting. Some may be stoped by the diapir, others may not. The local structural environment and stress field encountered by the diapir may also change up through the deformation sequence. In

PLATE 4.11 - a) Contact between a plug or dyke of unfoliated mud (grey coloured mud on right) and sheared vari-coloured scaly clays of the Bobonaro Formation. (Bonoe river, W. Timor see Fig. 4.2 for location)

- b) Close up of the unfoliated grey muds in the plug or dyke. Note the angular to subrounded equidimensional shapes of the included fragments.

- c) Close up of the vari-coloured scaly clays into which the plug is intruded.

addition, as the diapir consolidates throughout its growth, an evolution from Type IV behaviour towards the Type V end member might be expected with time.

4.8 THE NATURE AND GENESIS OF EXTRUSIVE MUD DIAPIRS

The relative proportions of the two main fluid phases (water and methane) and the overall solid to fluid proportion determines which of two potentially interacting mechanisms will dominate in the extrusion of diapiric material and what the resulting surface morphology of the extrusions will be (Fig. 4.3). The mechanisms that may drive the diapiric material to the surface are;

1) Extrusion resulting from the hydraulic forces transmitted from the diapiric source regions. The diapiric ridges and domes (Type III) are thought to represent this form of extrusion. The mechanism corresponds to the extrusive end member of the hydraulic system proposed for shale diapir genesis by Bishop (1978) (Fig. 4.6a). This mechanism only requires a density inversion between diapiric source regions and overburden and a vertically unconstrained pathway to the surface. The fluids of the hot water vents (Type Ib) will also have been driven to the surface, out of the overpressured Oregon deformation complex (Suess & Massoth, 1984), by a similar hydraulic mechanism.

2) Extrusion resulting from the degassing (predominantly methane) of the diapiric source regions to form mud volcanoes and gas-blowouts (Types II & Ia). Methane is present at *depth in shale diapirs both as a separate phase, termed "trip gas" (Hedberg 1974), and in solution. With a decrease of pressure, dissolved methane comes out of solution and, as a separate phase, undergoes expansion in the conduit. The lowering of the density of the diapiric material in the conduit, due the presence of the evolving methane, enhances its prospects for reaching the surface 'en masse'. Rapid expansion of the methane near the surface gives rise to the volcanic (and sometimes explosive) nature of the extrusion. The rate of extrusion can be great, as can the volumes of methane. Kugler (1939) reports that in the Caucasus region in 1922, the Otman-Boz-Dag mud volcano exploded and caught fire with a resulting column of smoke 14 Km high whilst, in 1924, flames emitied from the Touragai Mud volcano could be seen 700 kilometers away. Mud volcanoes (Type II) form, if argillaceous material is propelled en mass to the surface. Whereas, craters form if only gas (and possibly water) is released during a gas blow-out (Type Ia, Fig. 4.3). The cone slope angle of the mud volcanoes (Types IIa & IIb) increases with increases in the viscosity (Table 4.1) or solid to fluid ratio of the mud (Kerr et al. 1970). The volume and nature of the material ejected from the shale diapir via mud volcanoes gives some indication of its fertility in the two main fluid phases. For instance, shale diapirs associated with the extrusion of large volumes of low viscosity (Type IIa) material are likely to be significantly more underconsolidated and rich in methane than diapirs that are associated with only small Type IIb or III extrusions.*

The relative importance of these two mechanisms will also vary with the depth of the diapiric material. The hydraulic mechanism will be important in the early stages of the rise of the diapiric material to the surface, even though the shale diapir may be rich in methane, because the pressures will keep much of the gas in solution. However, near the surface the transmittance of hydraulic pressure from deep within the shale will become subordinate to local buoyancy and other forces, caused by the dissolution and expansion of methane in the conduit leading up to the surface.

4.9 MECHANISMS OF FLUID MOVEMENT IN, AND EXPULSION FROM, SHALE DIAPIRS

The argillaceous material of the diapiric source regions must have been highly impermeable to the movement of fluids in order to have retained them during burial and loading. Eventually, even these low permeabilities will allow the fluids to escape, given enough time. However, on being mobilised into diapirs the prospect for losing fluids may be enhanced by a number of processes (Fig. 4.10a):

1) Methane rich regions of the shale diapir would tend to expel their fluids in the form of mud volcanoes. Mud volcanoes characteristically erupt episodically, implying that the overpressures in their source regions are regenerated over a period of time. This suggests that fluids like methane are able to migrate and concentrate within the shale diapir probably as separate phases.

2) The hydrofractured-halo round the diapir would increase

FIGURE 4.10 - Mechanisms of fluid movement through and out of shale diapirs.

- a) (1) Mud volcanoes expelling material rich in methane. (2) Hydrofractured-halo around a highly overpressured diapir enables fluids to escape from its immediate area. (3) Lateral expulsion of fluids (including hydrocarbons) into permeable formations at lower formation pressures. (4) Transmission of fluids through consolidated outer regions of diapirs may be facilitated by hydrofracturing or passage though regions that are being actively sheared (inset b & c). (5) Methane may migrate up through diapiric material as a separate phase. Further more, despite the low permeability of the diapiric material fluids would be able to migrate slowly up and out of the inner regions of the diapir.

- b) (inset) Active deformation of the outer consolidated regions of shale diapirs (4) may enhance the prospects for the movement of fluid through them by inducing local areas of reduced compressive stresses and by providing fractures which the overpressured fluids may then hold open.

-c) (inset) Shearing of semiductile-brittle exterior margins of shale diapir can reduce stresses and promote hydrofracturing with the approximate orientation shown in inset c.

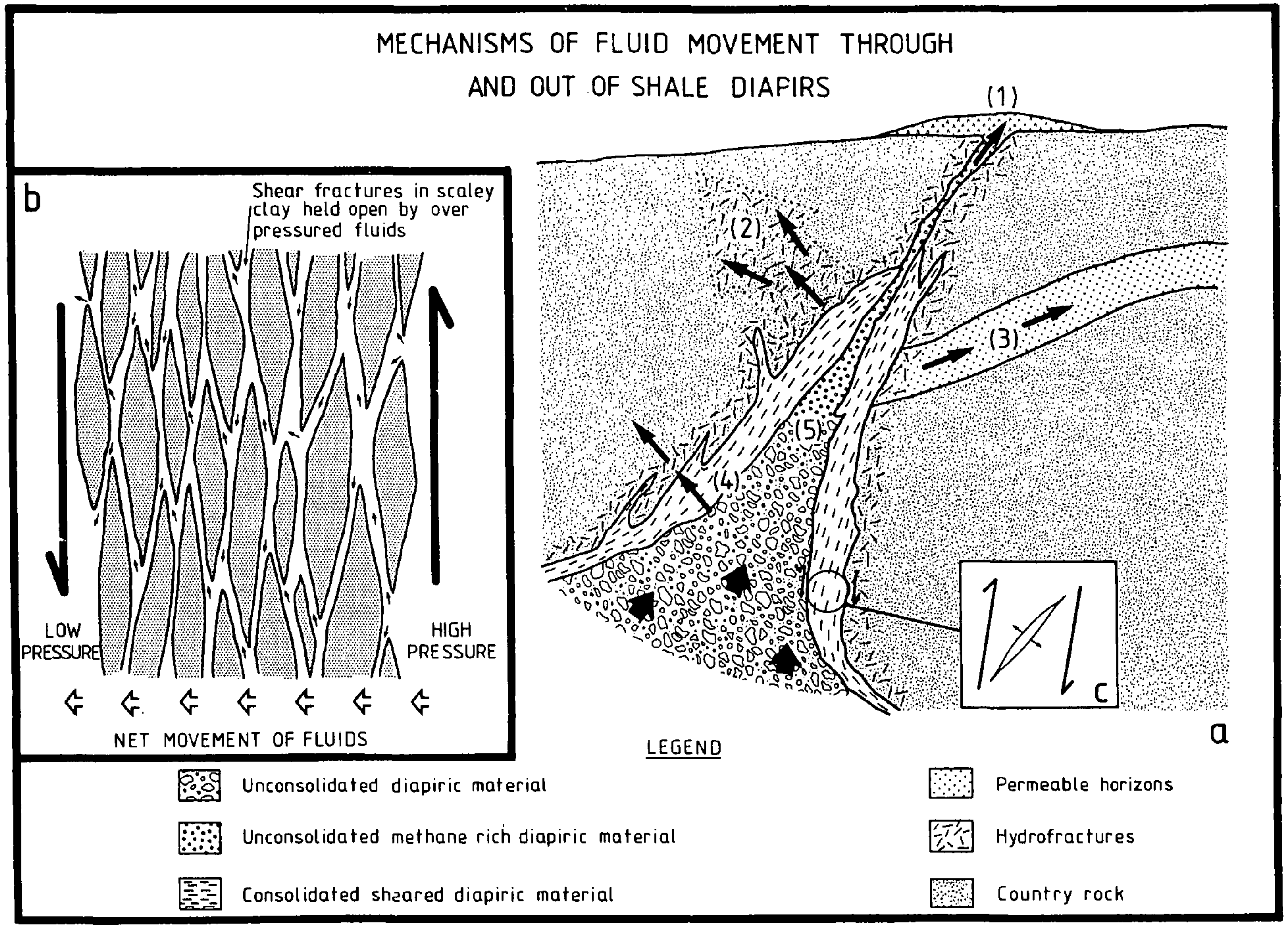
MECHANISMS OF FLUID MOVEMENT THROUGH
AND OUT OF SHALE DIAPIRS
b
Shear fractures in scaley clay held open by over pressured fluids
LOW PRESSURE
HIGH PRESSURE
NET MOVEMENT OF FLUIDS
(1)
(2)
(3)
(4)
(5)
c
a
LEGEND
Unconsolidated diapiric material
Unconsolidated methane rich diapiric material
Consolidated sheared diapiric material
Permeable horizons
Hydrofractures
Country rock

the permeability of the surrounding country rock.

3) Fluids may also escape laterally from the diapir into permeable horizons with lower formation pressures. This process may be economically important if the fluids are rich in hydrocarbons.

4) The compacted outer regions of the diapir will be disrupted as a result of the growth of the diapir or movement of the fault up which it is intruded. The microfractures thus formed would tend to be held open by the overpressured fluids expeled into them. This would increase the permeability by orders of magnitude, allowing fluids to migrate out of the diapir (Fig. 4.10b). q

4.10 IMPLICATIONS ON REGIONAL TECTONICS OF LARGE SCALE MUD DIAPIRIC PROCESSES

Mud diapirism occurs in passive margin, convergent and post convergent settings. It is quite possible that early diapiric structures developed at a passive margin may be later involved in a collisional event. In which case, the final form of a diapiric terrane may be the product of diapiric activity before, during and after convergence has taken place. The examples of Trinidad (cf Higgins and Saunders 1973, Bitterli 1958), New Zealand (Ridd 1970) and the Gulf of Mexico (Walker & Ensminger 1970), demonstrate that the stratigraphy and structure of modern basins can be greatly influenced by sedimentary diapiric activity (Fig. 4.11a). The extrusive products of mud diapirism (erupted as mud volcanoes and mud flows) may form a major component of their stratigraphic section, resembling bedded olistostromal

FIGURE 11 - Regional implications of diapiric processes.

- a) Generalised structure of diapiric provinces such as those in Trinidad and New Zealand. In both these terrains large volumes of extruded diapiric material (mud volcanoes) are interbedded with sediments in normal stratigraphic position. The areas have suffered a small degree of compression and the characteristically sharp diapiric anticlines are often thrust. The intervening broad synclinal troughs show little evidence of tectonism other than sharp lateral changes in sedimentary thicknesses.

- b) Basic model of the lateral expulsion of diapiric material due to differential loading between the interior and frontal regions of thrust belts. There is a possibility that diapiric anticlines, formed in front of an advancing deformation complex, may control the wavelength of later thrusts.

- c) Generalised model of the development of the Bobonaro Formation in Timor. The diapiric material sourced from within the imbricated Australian sequence is expelled laterally and vertically up through the thrust belt, resulting in a terrain that is essentially a diapiric melange (the Bobonaro Scaly Clay Formation). The lateral expulsion could result in stoping or extension of the overlying thrust sheets

disrupting the 'normal thrust belt development'. The process is believed to have been enhanced by the loading of the complex by the EXOTIC NAPPES which are partly composed of dense metamorphic and igneous bodies. The more local diapiric processes described in this paper form a part of this regional process.

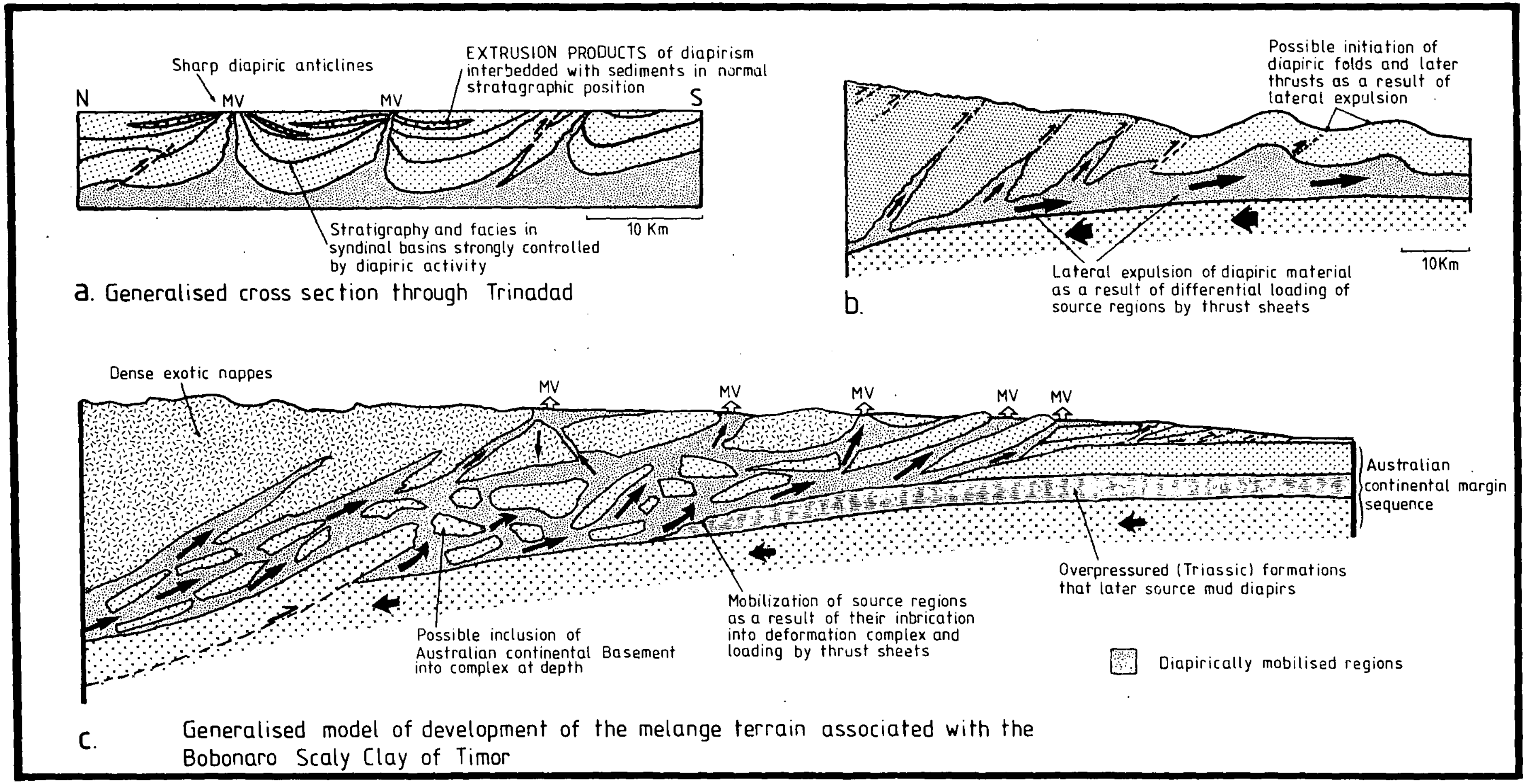

a. Generalised cross section through Trinadad

b.

c. Generalised model of development of the melange terrain associated with the Bobonaro Scaly Clay of Timor *deposits. These deposits, and the shale diapirs from which they came, will resemble those of later diapiric activity but will contain only blocks of intrabasinal formations. The diapiric anticlines in these basins are also likely to be the sites of thrust initiation in any later major compressional event and thus control the spacing of the later structures.*

The highly overpressured source regions can act as particularly effective decollement horizons and as a consequence may be thrust far beneath the frontal imbricates of a deformation complex (see Chapter 2). Either because the loading becomes sufficiently great, or because the source horizon becomes disrupted, the source regions may become mobilized as deep beneath a sequence of thrust sheets.

Diapiric material may be extruded vertically or laterally depending on the density contrasts and the pressure gradient. Such differences will arise between the frontal and more interior regions of thrust belts due to differential loading of the source regions by thrust sheets (Fig. 4.11b). This may result in diapirs being initiated in front of the deformation complex.

If the volume of diapiric material mobilised in active margin areas is very great, the lateral expulsion of diapiric material (Fig. 4.11c), and other diapiric processes mentioned previously in this paper, may control the form of the whole complex. In Irian Jaya a third of the 400km long and 100km wide deformation zone is composed of shale diapirs (Williams et al. 1984). The diapirism followed the overthrusting of *thick sedimentary sequences by dense exotic nappes (Williams et al. 1984). Blocks of the exotic nappes of all sizes are now distributed throughout the scaly clays of the diapiric melanges. A similar sequence of events to that in Irian Jaya is proposed to have occurred in Timor and the chaotic melange complex of the Bobonaro Formation is proposed to have formed in diapirs (Barber et al. 1986) in an analogous manner and not by olistostromal or gravity sliding mechanisms. The mixing of the blocks of very different metamorphic grades, ages and types would have occurred partly as a consequence of the imbrication of the strata and partly in the diapirs themselves.*

4.11 CONCLUSIONS

1) The main parameters that control the physical properties of mud diapirs are the viscosity of the mud, which at a first approximation is related to its degree of consolidation or fluid content, and the proportion of methane in the diapiric material. The great variability in the morphology and genesis of mud diapirs results from the combined effects of the wide range of possible diapiric material properties and the tectonic environment. The properties of the diapirs are further subject to a temporal evolution as a consequence of fluid losses.

2) Mud diapirs and related processes can be classified into three main divisions and five subdivisions:

A) Extrusive Emissions; Type I-gas blowouts (Type Ia) and hot water vents (Type Ib)
Type II(a &b)- mud volcanoes
Type III- mud ridges & domes

B) Intrusive Mud Diapirism; Type IV- shale diapirs emplaced by stoping
Type V- shale diapirs emplaced by forceful intrusion

3) The movement of shale diapirs stimulates the rate of loss of fluids from them by breaking up the outer consolidated rind material. Mud volcanoes remove methane, and fluids escape through the hydrofractures developed in a halo round their margins. The lateral expulsion of fluids, potentially containing hydrocarbons, into permeable horizons may be economically significant.

4) As shale diapirs consolidate there is an evolutionary progression in the nature of the fabrics, with 'particulate flow' in unfoliated thixotropic muds giving way to 'shear' (or scaly clay) fabrics.

5) Both the tectonic environment and physical properties of the diapir will control whether shale diapirs are emplaced by a passive (Type IV) or forceful mechanism.

6) The regional stress system and fault pattern exert a profound influence on the distribution of diapirism. Zones along which the horizontal stesses are reduced, such as strike-slip pull-aparts, are favoured places of diapiric intrusion but shale diapirs can also intrude up thrust

faults.

7) Melanges previously interpreted as olistostromes deposits may be better interpreted as:

A) Intrusive shale diapirs which, as they form part of a hydraulic system, may migrate in a vertical or horizontal direction depending on the pressure gradient. The lateral expulsion of diapiric material out towards the front of the complex, resulting from the loading of voluminous source regions by dense thrust sheets, can disrupt the processes of thrust tectonics, creating regionally significant diapiric melange terranes. To some extent these complexes will mimic gravity slide deposits.

B)The extrusive products of mud diapirism i.e. mud volcanoes. These can be interbedded with sediments in normal stratigraphic position. They will have the appearance of unsheared mud or debris flows and can potentially contain exotic clasts from a wide variety of stratigraphic and structural divisions. They therefore have many of the characteristics of deposits that have previously been interpreted as bedded sedimentary olistostromal deposits.

8) Mud diapirism occurs in a variety of tectonic settings. It is possible that a diapiric terrane associated with convergence may have involve the accretion of sediments in which mud diapirism had already occurred during some earlier possibly unrelated period.

CHAPTER FIVE

DISCUSSION AND SUMMARY

The relative importance of the physical processes governing the development of an accretionary complex are controlled by a number of boundary factors. An understanding of accretionary complex behaviour can, therefore, only be derived through the study of these inter-relationships. Accretionary complexes have a structural development that is, in many ways, analogous to subaerially exposed foreland thrust belts, but differ from them in two main ways. Most of the oceanic basement on which the accreted sediments were deposited is subducted and destroyed and is generally not included in the imbricate pile. The bulk of the sediments accreted at subduction zones are considerably less consolidated than those involved in foreland thrust belts. The trench-turbidites have often only been deposited just before accretion and are unlithified, and even the pelagic material deposited generally well before accretion may retain porosities above 40-50% (c.f. Moore & Biju-Duval et. al. 1984). On the other hand, the bulk of the material involved in orogenic belts is lithified or composed of crystalline basement material. The portions of the frontal thrust system involving the flysch sequences may, however, exhibit more of the features associated with accretionary complexes. A large number of different processes have been touched on in this piece of work. There are five boundary factors or overall controls affecting the genesis of an accretionary complex they are: the critical taper, the sediment input, the butress *angle, the subducting basement topography and the convergence direction. This study contributes information on three of them in particular namely; the effects of the critical taper, sediment input and basement topography. In addition, during the following discussion some of the important ramifications of the particularly important physical process of overpressuring and porefluid migration are also touched on.*

5.1 *THE INFLUENCE OF BOUNDARY CONDITIONS*

5.1.1 *Three Dimensional Systems And Critical Tapers*

The critical taper concept for the overall geometry of deformation wedges applies to both foreland thrust belts and accretionary complexes. The critical taper is a result of the interaction of several factors such as the wedges basal slope angle and surface topography (see Introduction for description of the critical taper concept). Previous mechanical models of critical taper development assume that deformation complexes are essentially cylindrical so that out-of-plane factors can be ignored (Chapple 1978, Davis et al. 1983, Stockmal 1983). However, as thrust belts and accretionary complexes have along strike terminations, are commonly arcuate and, in the case of the Barbados Ridge complex, are considerably non-cylindrical in localised regions (i.e where oceanic basement ridges like the Tiburon Rise impinge, Chapter 1, Section 1.6), simple two dimensional critical taper models cannot be applied throughout the system. Such discontinuities may also occur where the deformation belt terminates at, or contains a major *discontinuity generated by, a major strike-slip fault (or tear-fault). The necessity of maintaining a three-dimensional critical taper implies that out-of-plane forces must be taken into account. Three dimensionality in an evolving non-cylindrical system also means that material may move out of the plane-of-section parallel to the convergence vector as a natural consequence of the accretionary or mountain building process. This can have severe consequences for two dimensional balancing techniques that are commonly used in orogenic belts.*

Considering a bulldozer model in plan view in which convergence is E-W (Fig. 5.1). The wedge is laterally unconstrained in an N-S direction and would be subjected to the effects of pure shear. Extension occurring normal to the direction of maximum deviatoric stress would have the effect of extruding material out of the laterally unconstrained ends of the system (Fig. 5.2a). This would occur regardless of the effects of gravity. Tapponnier & Molnar (1976) and more recently Tapponnier et al. (1982, 1986) using the basic concept of plane-strain slip-line theory and the more visual two dimensional indentation experiments on plasticine (Fig. 5.2b), show how material may be extruded laterally from a deformation system in which there is a free lateral margin. As the deforming material is not allowed to thicken, the bulk of the deformation is taken up by strike-slip faulting and lateral extrusion, which is an exaggeration of the situation. In reality, in addition to the above possibilities a large amount of the strain will be taken up by thickening of the wedge and a consideration of the effects of gravity cannot be

FIGURE 5.1 - The bulldozer model considered in plan view. In order to maintain a critical taper in three dimensions frontal accretion must be balanced by lateral extension and changing vectors of material movement.

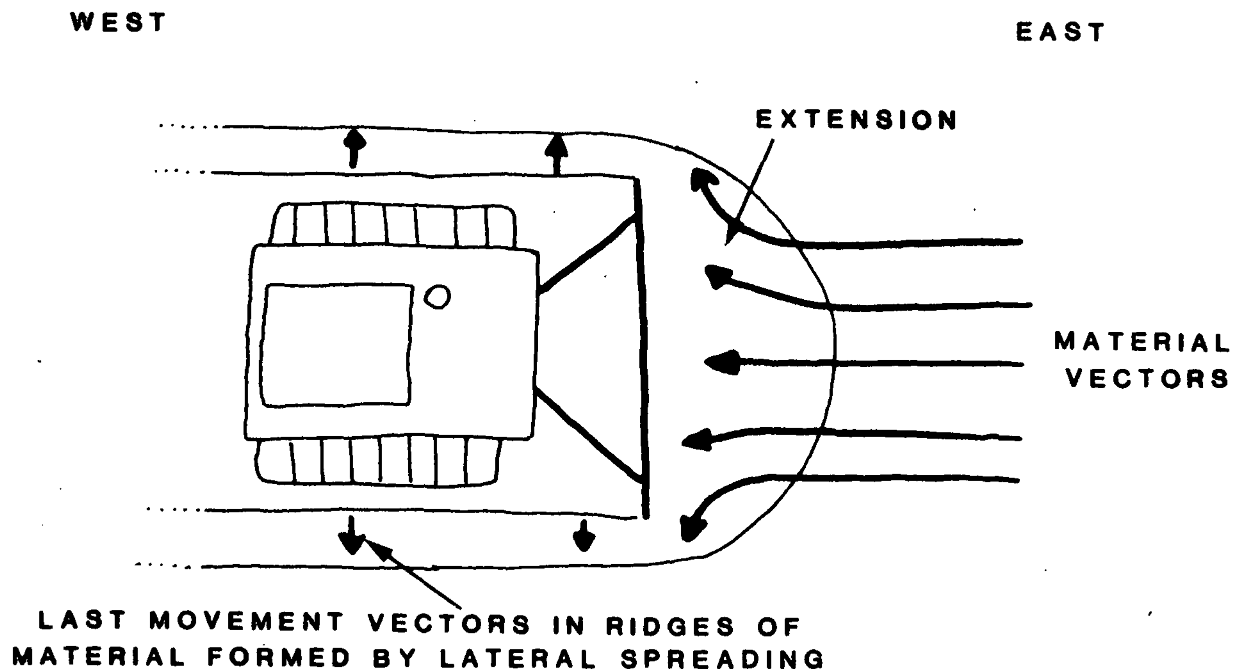

PLAN VIEW OF BULLDOZER

FIGURE 5.2 - a) A simplistic model illustrating the affects of pure shear on a body with a free lateral margin.

- b) Illustration of a plane-strain indention experiment done on plasticine (taken from P. Tapponier et al. 1986). The impinging indentor causes extrusion of material from the free boundary on the right-hand side.

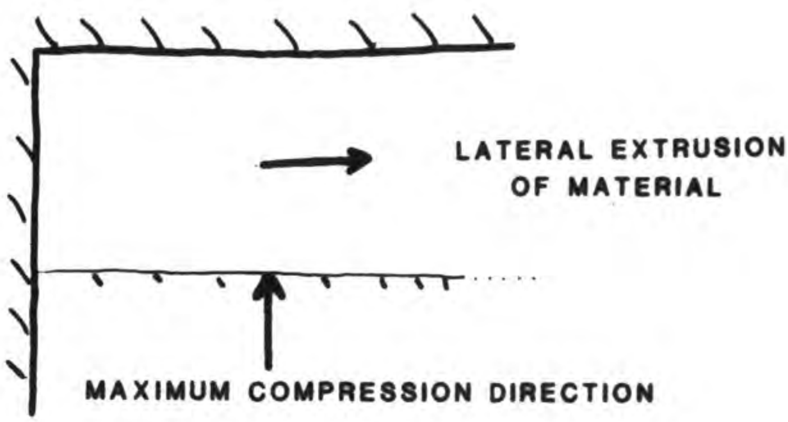

A

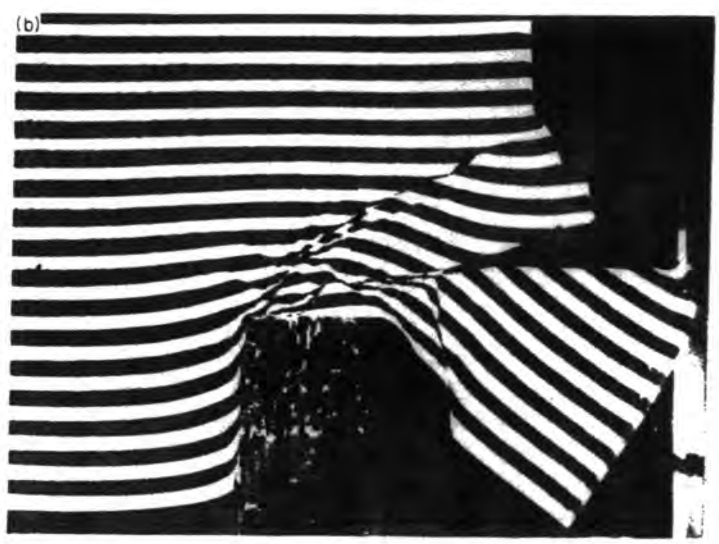

B

INDENTOR MODELS UNDER PLANE-STRAIN CONDITIONS *ignored.*

Considering the effects of gravity alone. If the material building out and thickening in responçe to E-W convergence does not collapse sideways under the influence of gravity, precipitous lateral side walls to the deformation wedge would develop. This is geologically unrealistic. Spreading of the complex laterally would occur until a stable critical taper is attained across the lateral margins of the wedge (Fig. 5.3). The gravitational spreading force (GSF) would correspond to the glacial sliding term in Eq. 1 of Figure 0.2. For the wedge to be in critical equilibrium on the verge of spreading laterally the gravitational spreading force will equal the sum of the basal shear stress (Rb) acting against it (generally taken to be independent of strain rate), the component of the gravitational body force acting down the basal decollement slope (Wb) and the wedges internal resistance to extension (Se) (See Fig. 5.3). The wedges internal resistance to extension will act against the gravitational spreading force tending to increase the critical taper for an extending complex. However, it must be borne in mind that the strength of rocks is considerably less under conditions of extension than compression, so that the term relating to the material properties of the wedge will be less important than for the compressional case.

Both pure-shear and critical taper considerations would result in extension of the interior regions of the complex, balanced by an additional component of accretion to the frontal regions of the oblique margin. If, however, the pure

FIGURE 5.3 - A simple model illustrating the general configuration of forces acting on a non-cylindrical system undergoing gravity spreading in responçe to E-W convergence. The forces acting on accretionary complexes are; the basal shear stress (Rb), the body force acting down the slope of the basal decollement (Wb), the strength of the wedge (S- compression, Se- extension) and the gravitational force resulting from and acting down the topographic slope of the complex (GSF).

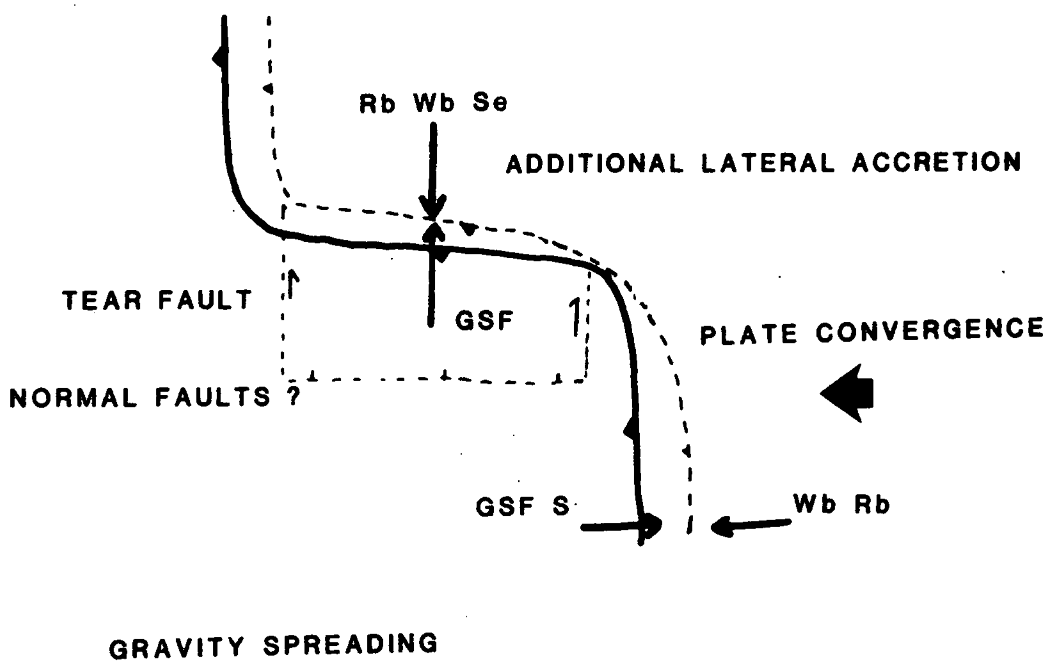
Rb Wb Se
ADDITIONAL LATERAL ACCRETION
TEAR FAULT
GSF
PLATE CONVERGENCE
NORMAL FAULTS ?
GSF S
Wb Rb
GRAVITY SPREADING

shear component in the lateral system is dominant, the whole system will remain in compression as it develops and there will not be any gravity spreading. Conversely, if the pure shear component is minimal, gravity spreading will predominate. The relative balance between the two processes will depend on whether the rate of thickening of the complex in response to E-W compression and accretion is greater than the increasing pure shear component due to changes in the deviatoric stress system.

The lateral removal of material by pure shear and/or gravity spreading will interfere with the critical taper required to balance the E-W compressional forces ("the compressional critical taper"). As material is displaced laterally out of the system, increasing amounts of intra-wedge thickening by out-of-sequence faults must occur to counteract the loss and maintain the E-W critical taper. This results in a slower rate of advancement around the arcuate portion of the accretionary front necessitating the encroachment of the extensional regime into originally unaffected areas as accretion proceeds. The following series of models try to address the problem in a more geologically realistic manner.

MODEL 1 accommodates extension resulting from gravity spreading using a series of tear faults with a large extensional component on them (Fig. 5.4). The addition of the displacement rates across each extensional tear fault ramp will cause the displacement vector, on the basal decollement beneath each screen of deformation complex, to

FIGURE 5.4 - MODEL 1 in which the progressive growth and consequent lateral gravitational spreading may be accomodated by a series of tear faults across which there is a significant extensional component. The relative displacement between points within the complex, and the relative movement between complex and underthrust plate need not be the same. Section A-B illustrates how the extension within the complex may be transfered to additional frontal accretion on the margins of the complex. Additional material will also be accreted to the lateral margin as a result of convergence. During the growth of the wedge the geometry of the system will change leading to complexities.

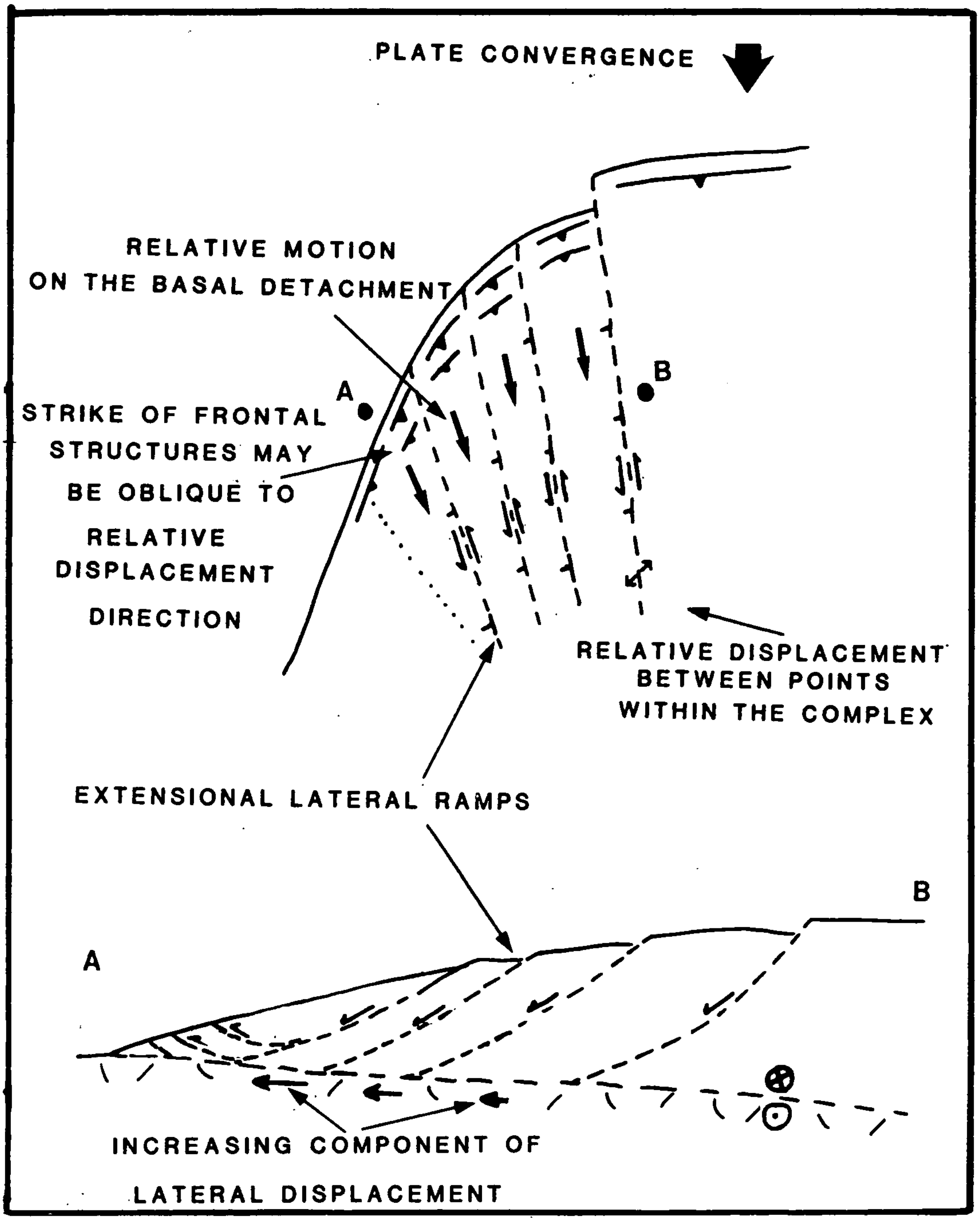
PLATE CONVERGENCE
RELATIVE MOTION
ON THE BASAL DETACHMENT
A
B
STRIKE OF FRONTAL
STRUCTURES MAY
BE OBLIQUE TO
RELATIVE
DISPLACEMENT
DIRECTION
RELATIVE DISPLACEMENT
BETWEEN POINTS
WITHIN THE COMPLEX
EXTENSIONAL LATERAL RAMPS
A
B
INCREASING COMPONENT OF
LATERAL DISPLACEMENT

swing away from the convergence vector. The cross section illustrates how the lateral normal displacement may be transfered to additional thrust faulting at the accretionary front.

MODEL 2 is essentially a variation of the Tapponier (Fig. 5.2b) plane-strain model with development of an imbricate wedge along the leading edge of the extruded segment which will be controlled by a critical taper (Fig. 5.5). The segment is bounded on its rear edge by strike-slip or oblique slip faults (which potentially will have compressional components to them).

MODEL 3 constrains the wedge by having very much steeper basal decollement dip beneath its oblique margin, corresponding to a lateral ramp or strike-slip fault (Fig. 5.6). This model obviates the necessity for lateral extension within the complex. Changes in the slope of the basal decollement on this lateral margin may cause additional lateral compression in the wedge if it becomes steeper, and extension if it becomes shallower.

Some of the models outlined above can be illustrated using examples drawn from the Barbados Ridge complex. Two regions in particular will be looked at, namely its southern termination and the region of Tiburon Rise impingement at latitude 15 N.

The SW termination of the complex is being contained by its abutment against the S. American continental margin (see

FIGURE 5.5 - MODEL 2 in which the unbounded lateral edge of the complex migrates outwards as a result of pure-shear within the wedge. Additional frontal accretion occurs on the lateral edge with the maintainance of a stable critical taper. The out of plane-movement may initiate out-of-sequence thrusting in order to maintain a stable E-W critical taper.

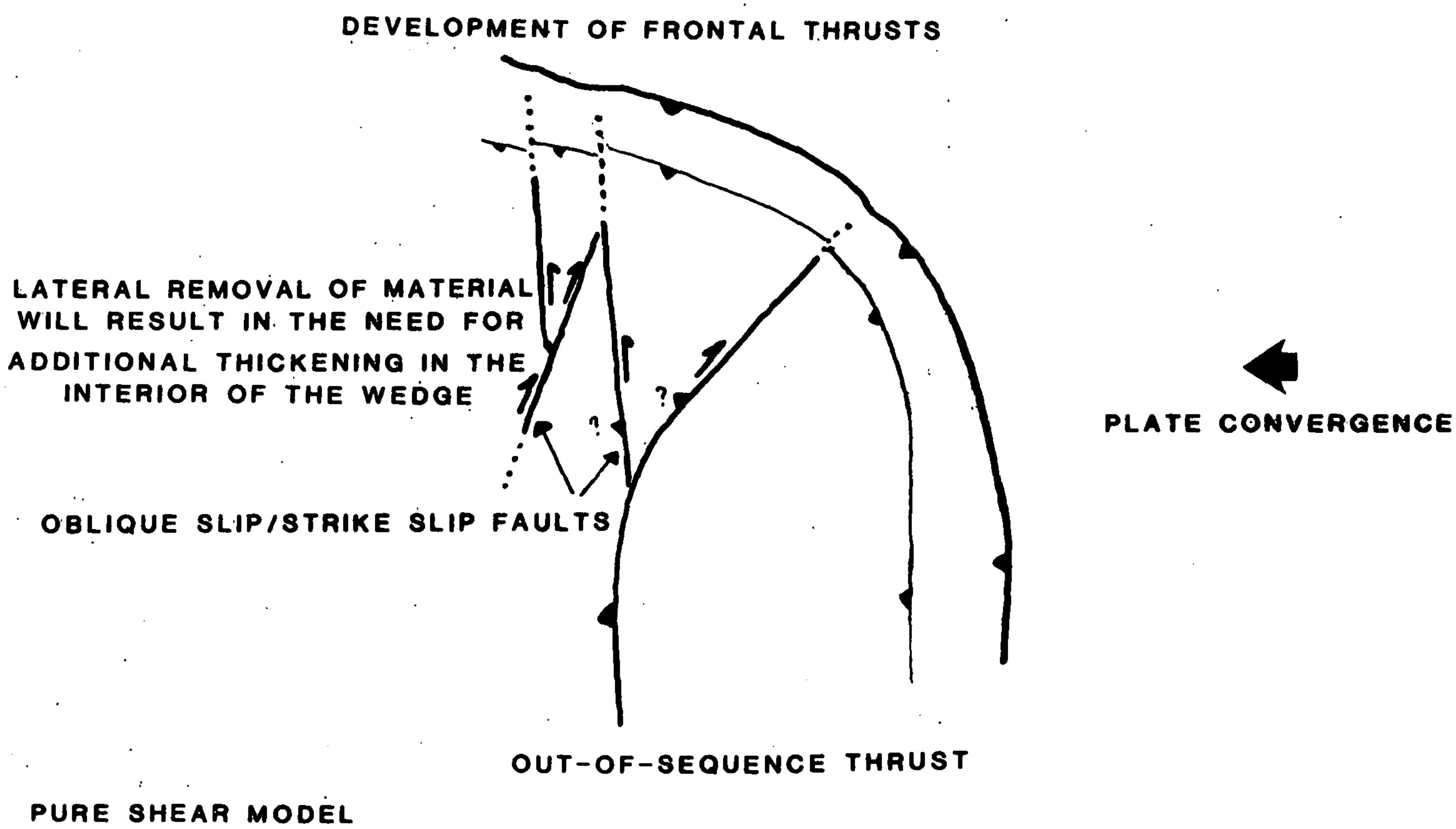
DEVELOPMENT OF FRONTAL THRUSTS
LATERAL REMOVAL OF MATERIAL WILL RESULT IN THE NEED FOR ADDITIONAL THICKENING IN THE INTERIOR OF THE WEDGE
?
?
OBLIQUE SLIP/STRIKE SLIP FAULTS
PLATE CONVERGENCE
OUT-OF-SEQUENCE THRUST
PURE SHEAR MODEL

FIGURE 5.6 - MODEL 3 in which the discontinuity is held in equlibrium by steepening the basal decollement on the lateral margin. If the lateral margins decollement became shallower extension would occur within the complex (going from section 1 to 2). Conversally if the basal decollement steepened lateral compression would occur in the wedge (going from section 2 to 1).

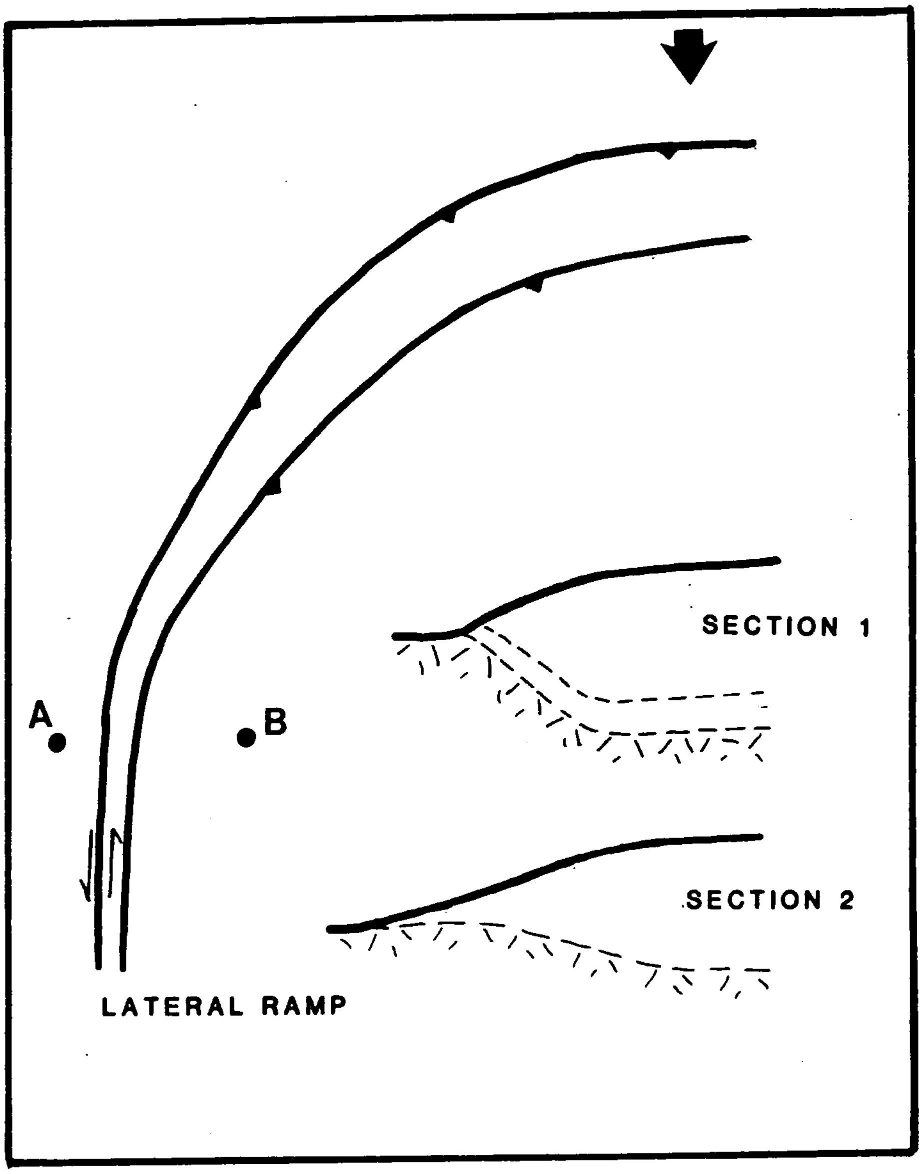
SECTION 1
A
B
SECTION 2
LATERAL RAMP

Appendix A and Speed & Westbrook et al. 1984). The basal decollement beneath this portion of the complex may have relatively steep northward dips as a result (cf. model 3 Fig. 5.6). The the E-W trending zone of complexity (see Chapter 1, section 1.4) is interpreted to correspond to a series of lateral ramps. The occurrence of sigificant amounts of reverse faulting in association with the lateral ramps indicates that they are compressive features and little if any extension is occurring across this region of the complex.

The Tiburon Rise system at latitude 15 N (Fig. 5.7a & b , See Appendix A), is slightly different. A rapid change in strike of the complex occurs in the vicinity of the Tiburon Rise due to the differences in the thickness of sediment accreted to the complex on either side, with roughly ten times the thickness of sediments being accreted on the southern side. As a result, the complex to the south of the ridge is building out at a much faster rate than the complex to the north. The dominant structural trend and the accretionary front swing to a roughly E-W to ESE-WNW orientation across the southern flank of the Tiburon Rise, which is highly oblique to the roughly E-W convergence vector (Fig. 5.7a). Only a small amount of accretion to this north facing margin can directly result from E-W convergence and problems with maintaining a stable critical taper across this oblique margin might be expected.

A number of faults strike at N-S to NE-SW, at high angles to the accretionary front. These cross-faults have been interpreted to be tear faults. Their orientation suggests

FIGURE 5.7- (A) Enlargement of the structural and lineament map in Appendix A that illustrates the disposition of the main structural elements of the Tiburon Rise System. The orientation of the tear faults within the obliquly trending seqment of the complex appear to indicate that the relative displacement of material points within the complex in this region of the complex is in a N-S to NE-SW direction.

(B) Oceanic basement topography (depth below sealevel in km) and bathymetry (in meters) around the Tiburon Rise system. The line of section of Fig. 5.9 is marked.

that the direction of material movement in portions of the complex may be strongly discordant to the convergence direction. This may occur as the stress distribution within the wedge depends on a series of different forces that do not act in the same plane as the convergence direction. In the Tiburon Rise system both the basal decollement dip (and therefore the down dip component of the wedges body force, which will effect the orientation of the principal compressive stress) and the topographic slope (and therefore the force associated with glacial term of EQ 1, Fig 0.2) are in different directions to each other, and the convergence direction (Fig. 5.7b). The resulting principal stress direction should, therefore have an orientation other than in the plane of the convergence direction.

Considering the various forces acting on the system in turn different solutions can be arrived at. The divergence of movement suggested by the tear faults could result from the lateral gravitational collapse of the topographic ridge developed in the complex, as the tear faults do appear to fan round its northern end (Fig. 5.8, Cf. Model 1, Fig. 5.4). However, the tear faults distribution is also similar to the strike slip faults formed in the plasticine models illustrated in figure 5.2b and may therefore be attributed to the lateral extrusion resulting from the effects of pure shear (Model 2 Fig. 5.5). Conversely, the Tiburon Rise, as it is being thrust obliquely under the complex, may be preventing lateral extension altogether putting the wedge into increased compression in the regions over the Rises southern flank as a result of the steep southward dip imposed

FIGURE 5.8 - The system of late thrusts and tear faults around the Tiburon Rise region maybe related to the presence of a topographic ridge in the complex. This ridge has formed in response to the accretion of thick sequences of material in the trough area, south of the Tiburon rise, a process that is still continuing. In addition ramping up of the complex on to the flanks of the Tiburon Rise may be responsable for the northern part of the ridge.

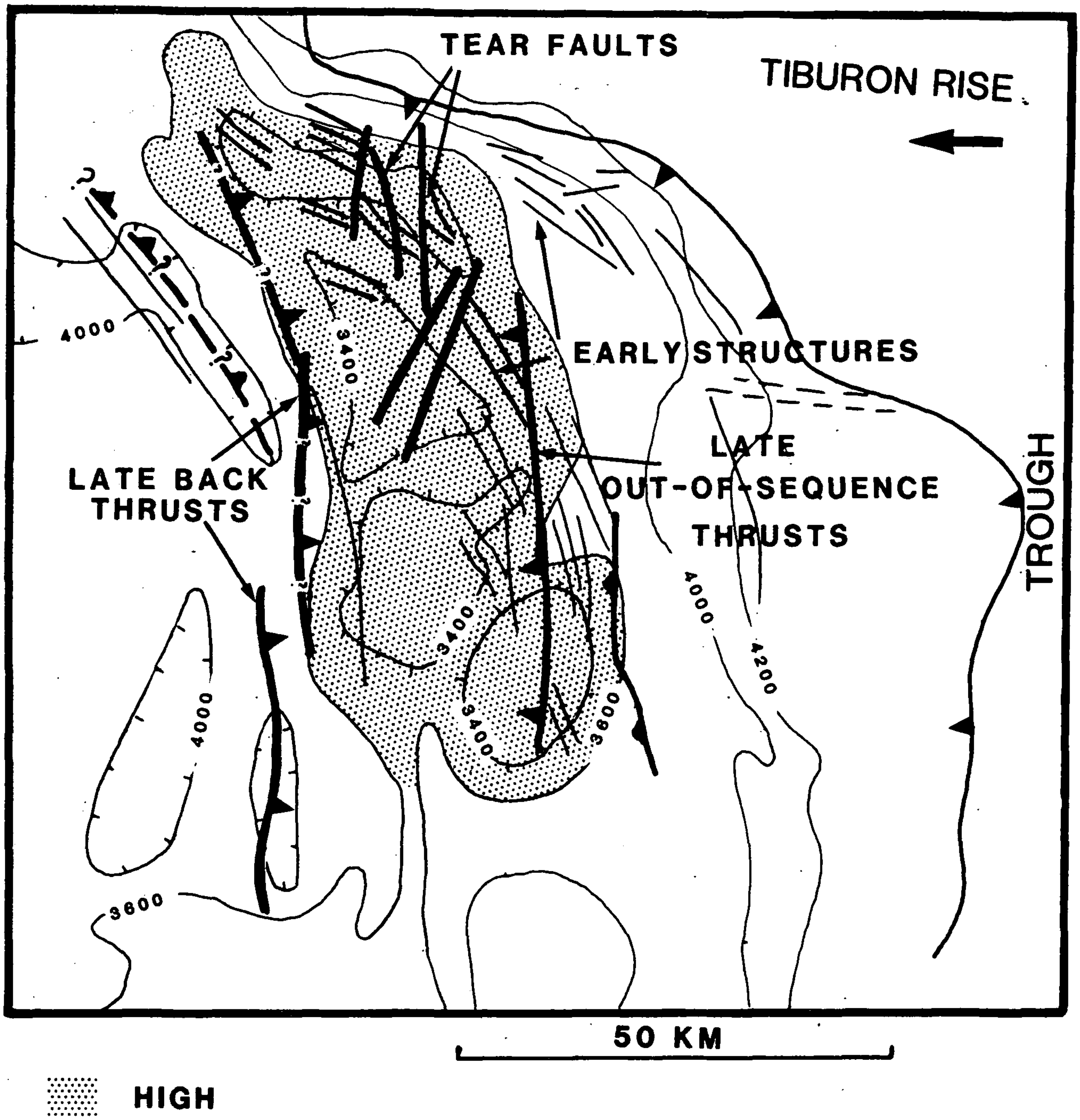

TEAR FAULTS
TIBURON RISE
EARLY STRUCTURES
LATE
OUT-OF-SEQUENCE
THRUSTS
LATE BACK
THRUSTS
TROUGH
4000
3400
3400
3400
3600
4000
4200
4000
3600
50 KM
HIGH

on the basal decollement (Fig. 5.7b & 5.9, cf. Model 3 Fig. 5.6). A step in basement topography occurs beneath some of the postulated tear faults. A laterally introduced low angled step (Fig. 5.9) may have caused the complex to extend above it in order to maintain the critical taper. This extending portion of the complex would be partitioned from the rest of the complex by the tear faults (Fig. 5.10).

At the present time the interplay between the effects of the various different forces is not sufficiently understood to come to a firm decision in favour of any particular model. However, it is hoped the above analysis goes someway towards illustrating the more geologically realsitic possibilities. Aseismic ridges, volcanic plateaus and fracture zones are relatively common features of the present day oceanic basins. Discontinuities such as those developed in the Barbados Ridge Complex may occur in many other modern and ancient accretionary complexes.

5.1.2 The Sediment Input

The sediment input is probably the single most important variable controlling the form of the accretionary complex. The sediment input can vary in a number of interrelated ways i.e. in type, thickness, state of consolidation and organic content.

Taking the Barbados Ridge accretionary complex as an example (See Chapters 1 & 2), the structural development differs markedly between the southern and northern parts of

FIGURE 5.9 - Line drawing of a seismic reflection line that runs across part of the obilque margin of the Tiburon Rise system. (Postion of this Figure is marked on Figure 5.7)

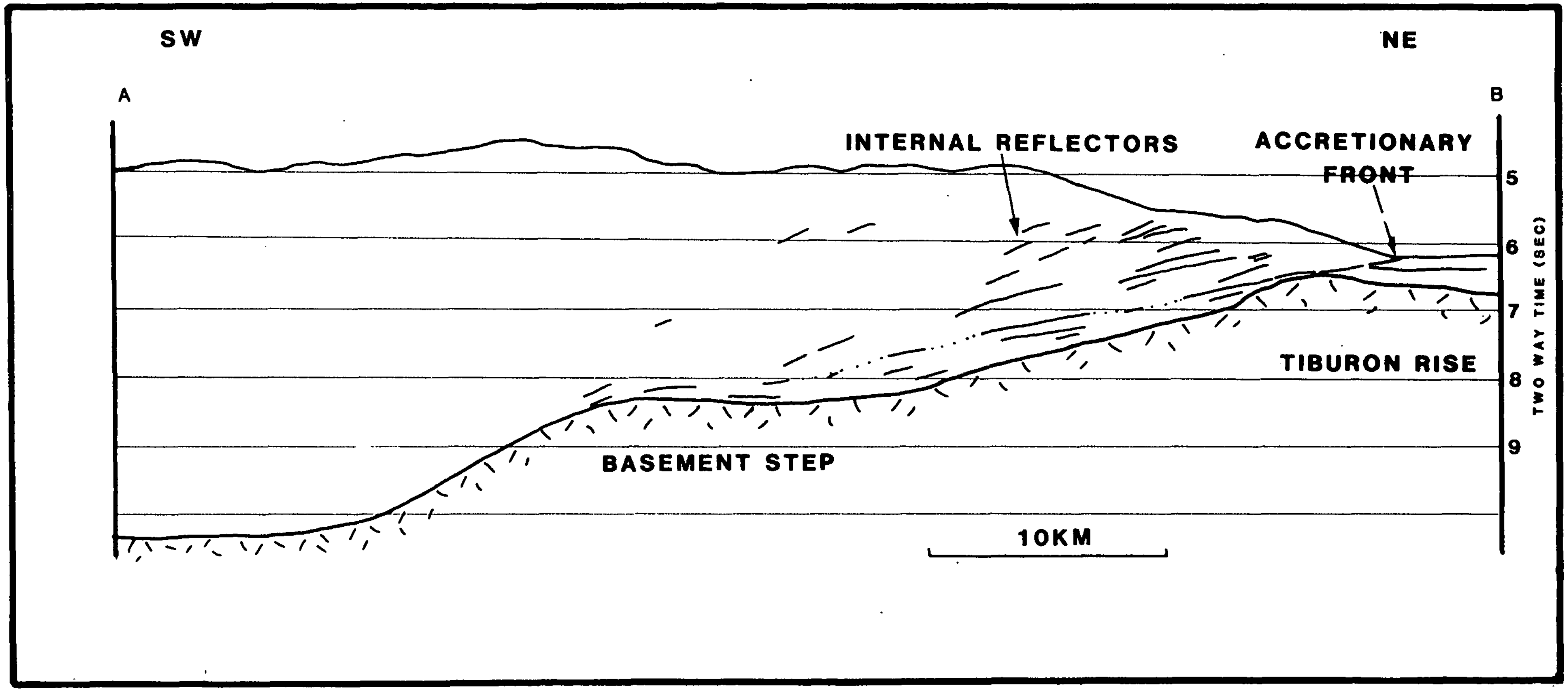
SW
NE
A
B
INTERNAL REFLECTORS
ACCRETIONARY FRONT
5
6
7
8
9
TWO WAY TIME (SEC)
TIBURON RISE
BASEMENT STEP
10KM

FIGURE 5.10- Development of some of the northerly trending tear faults may related to the lateral underthrusting of a basement step. Changes in basal decollement angles will necessatate either extension in the overriding complex if the angle is lower, or further thickening if the angle is steeper. The tear faults partition the individual regions. As the step is introduced laterally, a series of tear faults will develop.

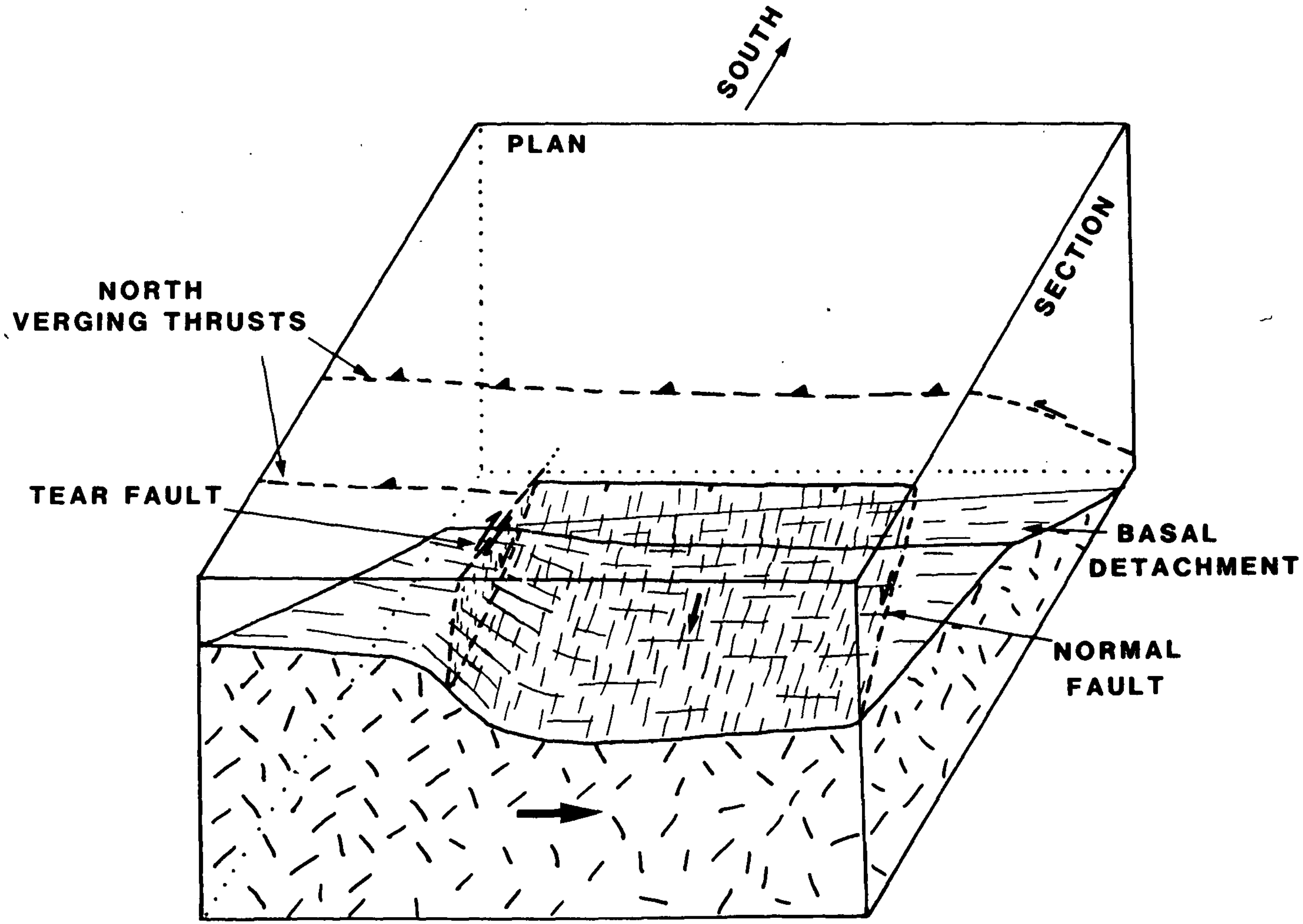

SOUTH
PLAN
SECTION
NORTH VERGING THRUSTS
TEAR FAULT
BASAL DETACHMENT
NORMAL FAULT

the complex (see sctions 1.4 & 1.5). It can be seen that the intensity of the deformation and the spacing of both the frontal thrusts and later out-of-sequence structures are inversely proportional to the initial thickness of the accreted sequence. In the south, thick sequences of underconsolidated, organic rich Orinoco fan turbidites are accreted. Whilst in the northern areas (i.e. around the DSDP Leg 78a and ODP Leg 110 sites) only thin sequences of better consolidated, organic poor hemipelagics and pelagics are accreted. In the south, thick sequences of turbidites allow the accretion of packets up to 1-2 km in thickness resulting in wide thrust spacings, similarly large packets are accreted in other super-replete complexes like the Makran (White & Louden 1982). The simple form of the frontal structures is preserved. Back rotation and some tightening of the large open folds occurs, bedding dips in the near surface regions remain largely below 20°-30°. In general, the frontally accreted section remains as a structurally "simple" near surface "rind" to the complex. As thrust spacings are large (in the order of 3-6 km) even small amounts of back rotation and folding can account for a large amount of the thickening of the complex. Widely spaced out-of-sequence thrusts (i.e. with spacings of 100's m to several kilometers) begin to occur well back in the complex (i.e. 18km or more, west of the deformation front, see Appendix B).

In the north, frontal imbricates on the flanks of the Tiburon rise are only in the order of 300 m thick (Biju-Duval & Moore et al. 1984). Seismic reflection profiles and the DSDP and recent ODP Leg 110 holes (Moore and Mascle et al.

1987, in press.) show that, in the initial stages of frontal accretion the section suffers a high degree of deformation. Within 12-14 km of the accretionary front, the accretionary complex is intensely deformed with much of it being composed of steeply dipping beds (i.e. above 50°), with the occurrence of tight to isoclinal folds (i.e. developed by the time Leg 110 Site 673 is reached, see Fig. 5.11). Out-of-sequence thrusts begin to develop and are particularly well developed at site 674 (derived from work in progress of the results of ODP Leg 110). They often have lag geometries, appearing to cut down section possibly through previous folds, steeply dipping beds and earlier thrusts (Fig. 5.11). The out-of-sequence structures may originate even nearer the front but are hard to pick out on seismic reflection sections due to the intensity of the deformation. Much the same thickness of stratigraphic section is accreted in the area studied in Sabah (Chapter 3) and this ancient accretionary complex appears to have had a fairly analogous structural development. In Sabah, a thin sequence of Crocker Fm. turbidites, rather than hemipelagics, is accreted, but the initial thickness of the section appears to have exerted an important control on its early structural evolution.

The nucleation of the basal decollement will be controlled by such factors as differences in shear strengths of the incoming sections i.e. in Sabah the basal detachment predominantly occurred between the Sandstone and Basal Grey Shale Unit. Factors that are thought to considerably influence the shear strength of particular horizons are their initial state of consolidation and the effects of the lateral

FIGURE 5.11 - A schematic cross section through the sites of DSDP Leg 78A and ODP Leg 110 just north of the Tiburon Rise. The section is based on a depth converted seismic reflection section. The more westerly portions of the cross section is increasingly interpretive, based on the style of structures documented at Sites 673 & 674. The development of the large folds may be a response to the diffculty of moving material up increasingly steep ramp angles and/or they may be associated with the development of out-of-sequence thrusts.

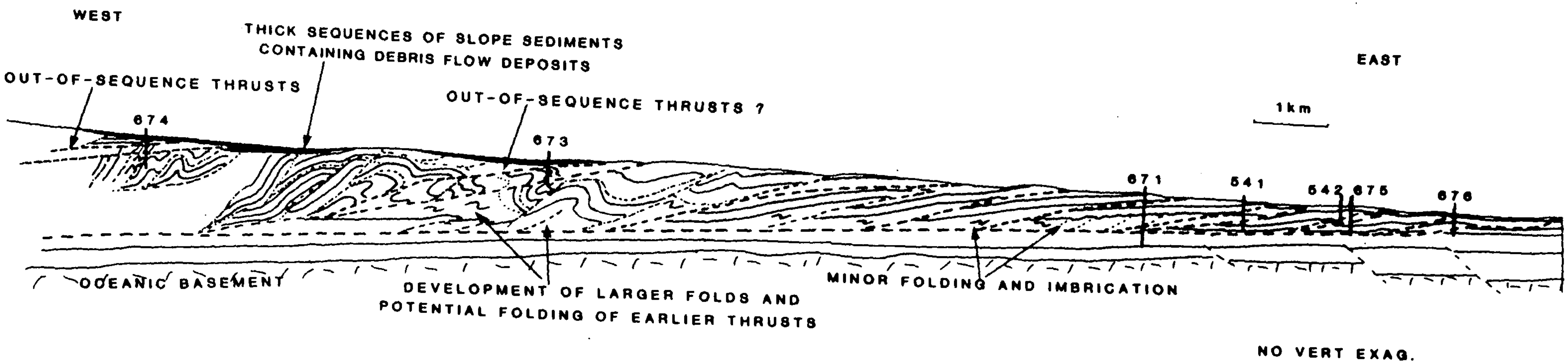
WEST
THICK SEQUENCES OF SLOPE SEDIMENTS
CONTAINING DEBRIS FLOW DEPOSITS
EAST
OUT-OF-SEQUENCE THRUSTS
674
OUT-OF-SEQUENCE THRUSTS ?
1km
673
671
541
542
675
676
OCEANIC BASEMENT
DEVELOPMENT OF LARGER FOLDS AND
POTENTIAL FOLDING OF EARLIER THRUSTS
MINOR FOLDING AND IMBRICATION
NO VERT EXAG.

transmission of high pressure porefluids from deeper with the complex (Westbrook & Smith 1983). A rapidly deposited thick argillaceous section is already likely to be overpressured as a result of its depositional history and low permeability. In addition, laterally transmitted high porefluid pressures may help maintain underconsolidation within the sedimentary section in front of the complex. As has been indicated in Chapter 2, such overpressured underconsolidated horizons tend to be subcreted. In the south, where they are particularly thick and rich in fluids and organic material, they source mud diapirism further back in the complex.

If the general distribution of turbiditic and pelagic rock types, and the nature of their disruption, is examined in a number of ancient subaerially exposed complexes, distinct patterns are found. One general relationship is for example seen in the Southern Uplands. In the Southern Uplands pelagics and spilites occur in the northern belt along thrust faults (McKerrow et al. 1977, Leggett & Casey 1982). Apparently parts of the pelagics and upper section of the oceanic basement have been accreted as tectonic slices along with the turbidites. The pelagics, however, only occur in the regions of the complex at higher metamorpmic grade. These would correspond to the hotter, deeper parts of the complex. The second general relationship is the common association of the pelagic section, along with parts of the oceanic basement, with melanges. Such melanges could have formed by any one of a number of processes i.e. in olistostromes, mud diapirs, or as a result of tectonic shearing (Cowan 1985). The melanges in the Shimanto Belt of

Japan contain a variety of rock type including a dismembered pelagic section and pillow basalts set in a younger sheared argillaceous matrix. The melanges are surrounded by fairly coherent turbidite sequences that are generally younger than the included blocks (Hada & Suzuki 1983, Suzuki 1986). The Uyak melange complex, SW Alaska, contains a pelagic section along with ultramaphics, gabbros and pillow basalts (Suzuki 1986). The Oyo complex in Nias Island contains a dismembered pelagic section along with oceanic basement and parts of a turbidite section (Moore & Karig 1980). The pelagic section in the NW. Borneo subduction complex in Sabah and Sarawack only occurs as a disrupted sequence in the Lubok Atu melange and other potentially intrusive melanges (Tan 1982 , See Chapter 3). In the accretionary melange described in New Zealand by Nelson (1982), there is an interleaving on a scale of a few kilometres between broken formations derived form a turbidite section and melanges containing pelagic and oceanic basement blocks. The consistency in the common association between the pelagic section and melanges and-or the deeper parts of accretionary complexes suggests a uniformity of processes that is controlled, at least in part, by sediment type.

Frontal accretion and subcretion,or underplating, are proposed as the processes that confer a pattern to the distribution of rock types within accretionary complexes. The process of accretion and subsequent position of the material within the complex will in turn affect the style of deformation they suffer. If the original sedimentary section is composed of an upper seqence of turbidites and a lower *sequence of pelagics, the turbidites are generally offscraped either as frontal imbricates, or relatively soon after during subcretion. However, the pelagics are often thrust deep beneath the accretionary complex i.e greater than 80 km in parts of the Barbados Ridge accretionary complex (Westbrook et al. 1982, Westbrook and Smith 1983). They are, therefore, likely to be associated with the deeper regions of accretionary complexes and therefore to be accreted under different conditions. They are also likely to remain nearer the basal shear zone for longer, as generally oceanic basement material is not subcreted in any quantities beneath them. This is one major difference between accretionary complexes and orogenic belts. Subduction zones are steady state systems in which crustal material is predominantly lost to the mantle. Crustal thickening involving ophiolite formation occurs, but generally forms only a volumetrically minor component of well developed accretionary complexes. Conversely, in orogenic belts there is commonly a considerable amount of basement involvment and crustal thickening. In accretionary complexes, as the pelagic material can remain in the "high strain zone" for a long period of time the prospects for their suffering intense shearing and tectonic dismemberment are enhanced. This is perhaps one reason why melanges are often associated with subduction zones. Fault brading may include of slivers of oceanic basement and tubidites and so interleave melanges with differing proportions of constituents. Preservation of sediments in ponds amongst rough oceanic basement topography may allow more recently input formations to get down into the deeper regions of the complex (Cf. McCarthy & Scholl 1985).*

The pelagic material may remain at depth, to be observed in the uplifted & deeply eroded metamorphic cores of ancient complexes as may be the case in New Zealand (Nelson 1982). Or the disrupted pelagics may find themselves emplaced into the upper regions of the complex along major out-of-sequence thrusts, either as tectonic slices, or as xenoliths in deep seated mud diapirs. The diapirs may have been sourced from later subcreted underconsolidated horizons.

The ultimate control of sedimentation on accretionary processes is that the nature of the incoming sedimentary section will determine whether the accretionary complex is largely formed through coherent processes, such as thrusting and folding, or incoherent processes like mud diapirism and bulk shearing. The N. Borneo (Sabah) & Barbados Ridge accretionary complexes (See Chapters 2 & 3) can be taken as examples of predominantly coherent and intermedate cases, whilst, Timor is the incoherent end member of the spectum (See Chapter 4). It is proposed that the main factor determining the overall coherency or incoherency of a complex is the state of underconsolidation of the accreted section. In the case of Barbados only the deeper parts of the turbidite section appear to source mud volcanoes and the complex appears to have remained largely coherent. Diapirism continues to be active well back in the older regions of the complex with the suface manifestations of mud diapirism being abundant despite high slope sedimentation rates that would lead to their rapid burial. The older parts of the accretionary complex should therefore be full of crosscutting diapiric bodies emplaced at a variety of times and in a *variety of settings during the complexes development. The extrusive diapiric products (mud volcanoes) will be present at different stratigraphic levels within the slope sediments, perhaps even being incorporated into the deformed complex themselves as a result of out-of-sequence thrusting. In Timor, a large proportion of the accreted Australian margin section appears to have been mobilised, to the extent that the general process of thrust tectonics appear to have been overwhelmed by diapiric processes. In Timor, this [illegible]ss mobilization could have been enhanced by the rapid [illegible]ing of the underconsolidated complex by the overthrust dense e[illegible]ic nappe sheets. Diapiric activity can be relatively long lived, with diapiric activity in Timor probably beginning in Miocene times and continuing up to the present day.*

A discussion of some of the characteristic forms and processes operating within mud diapirs has been presented in Chapter 4 and will not be belaboured further here . Much more work will be needed to accesses whether a large number of the other melange terranes, previously interpreted to be of olistostromal or gravity slide origin, may in fact be better interpreted in terms of diapirism. If this is the case then marked changes in our appreciation of the possible range of mountain belt and accretionary complex processes will be needed.

5.1.3 *Subducting Basement Topography*

The basement topography of the subducting oceanic plate can affect the development of accretionary complexes like the Barbados Ridge in a number of ways (see Chapters 1 & 2). The ridges induce variations in the type and thickness of accreted sediments. The effects of sediments on accretionary processes has been discussed above (see Section 5.1.2). The variation in the volume of sediment accreted to either side of the Tiburon Rise (see Chapter 1) leads to the non-cylindrical development of the complex and the consequent structural complexities that have been discussed in section 5.1.1.

The ridges influence accretionary development more directly by causing variations in the basal decollement angle which again affects the critical taper (see section 5.1.1). This will result in extension of the complex if the basal angle is lowered, or increased compressive deformation if the angle increases. As basement ridges may have orientations that are oblique to the convergence direction, cycles of increased compression and relative extension may occur leading to a complex history of minor fault development. Oceanic basement ridges are common in the modern oceans and there is no reason to believe that they were any less so in the ancient oceans with which old accretionary terranes were associated.

5.2 *OVERPRESSURING & FLUID MIGRATION: IMPORTANT PHYSICAL PROCESSES IN ACCRETIONARY COMPLEX DEVELOPMENT*

High porefluid pressures affect the development of the accretionary complexes in a number of important ways. High porefluid pressures are thought to result in the development of very low critical taper angles by reducing the effective stress on the base of the accretionary complex (Chapple 1978, Davis et al. 1983). Overpressuring also results in regions within accretionary complexes remaining sufficiently underconsolidated for mud diapirism to occur long after the initial accretion of the material i.e. mud diapirs are still abundant 180 km westwards of the accretionary front in the Barbados Ridge complex (see Chapter 2). However, the fluids must eventually escape from the complexes as low porosities are generally observed in ancient subaerially exposed examples.

The fluid pressure will influence the mechanisms by which the rocks deform. This thesis study has predominantly concentrated on the unmetamorphosed upper regions of accretionary complexes, where small-scale deformation process will be dominated by the mechanisms of independent particulate flow, diffusion mass transfer, crystal plasticity and cataclastic flow (Knipe 1986, see Introduction). The main factors that control how the accreted sediments deform are the strain rate, porefluid pressure and state of lithification. This thesis has shown that mud diapirism, indicative of high pore fluid pressures and poor consolidation, can occur well back in the older regions of accretionary complexes. Therefore, deformation mechanisms operating in partly consolidated sediments may be important for long periods of time during the development of large regions within accretionary complexes. Fabrics developed in some of the fault zones (particularly the shale injection features) display many of the characteristics of the fabrics developed in the proposed deep seated mud diapirs and it is thought that the physical processes operating in them are largely similar.

Pore fluid pressures may also exert a considerable control on the initial development of structures at the accretionary front. This is interrelated with the effects of sediment type, discussed above. Overpressure developed preferentially along certain stratigraphic horizons enhances the chances for the basal decollement to initiate along them. There are three interrelated factors that control the position of these key horizons. Primarily, rapid burial and deposition of a particularly thick low permeability argillaceous unit would result in it being initially overpressured anyway. Further to this, tectonically induced stresses may induce a further degree of overpressuring within sediments in front of deformation complexes. The lateral expulsion of fluids from deep beneath the accretionary complex along certain key horizons has been proposed as an explanation for the development of mud volcanoes in front of the Barbados Ridge (Westbrook & Smith 1983). The recent ODP Leg 110 initial results (Moore & Mascle et al. 1987, in press.) show that thermogenic methane generated in the hotter deeper parts of the complex is expeled along the basal decollement and *continues out into the undeformed sediment pile along the proto-decollement horizon (Fig. 1,17b). Thus, the basal decollement horizon does appear to be predetermined by fluid migration paths. The fluids are expelled despite the low permeability of the section. In order to be present in the sediments in front of the complex, the laterally expelled fluids must migrate at a velocity faster than the rate of advancement of the deformation front (in the order of a few cm a year). This would seem to indicate the presence of some sort of horizontal fracture permeability within the argillaceous section. Such fluid filled fractures would make an ideal locus for later shearing and basal decollement development.*

The absence of mud diapirs associated with the frontal accretion of turbidites in the southern regions of the Barbados Ridge Complex has been proposed to result from the higher permeabilites of the the upper parts of the turbidite section (See section 2.5). High permeabilities may result from a low degree of compaction in the upper sequences, accretion induced fracture permeability, and the presence of interconected permeable sand horizons. These allow a sufficient rate of fluid loss to inhibit the generation of excessively high pore fluid pressures and diapiric activity i.e. porefluid pressure with values below the minimum deviatoric stress will not be able to form vertical hydrofractures to initiate diapirism. However, seismic velocities do show that the turbidites are to some extent undercompacted in the frontal regions of the complex. It is proposed that the above observations must be considered when *examining the results of porosity studies like the one done, using seismic velocities, on the Makran accretionary complex by Fowler et al. (1985). They study the top 4 km of the 6-7 km thick incoming section and the even thicker accretionary complex and find that the sedimentary section has a normal compaction curve with depth and that the accreted sediments becomes rapidly overcompacted, presumably as a result of increased tectonic stresses. These observations appear to belie the existence of overpressuring and underconsolidation within the complex. However, as with the Barbados Ridge system mud diapirs do occur further back within the interior regions of the Makran (Snead 1964). The presence of more abundant interconected permeable sands in the upper parts of the turbidite sequence in the Makran may explain the apparent contradiction. These would allow the bleeding off of fluids laterally so that compaction in the frontal imbricates could proceed at normal or high rates. Undercompacted material must, however be present at depth in order for their to be mud diapirism further back in the complex.*

Leg 110 (Moore et al. in press) found that fluids were expeled along discrete fault zones further back in the accretionary complex (Fig. 1.7). The increased fracture permeability in the argillaceous units caught up in the fault zones is thought responsible for this localisation. Sufficient fluids are being expeled to maintain an high geothermal gradient.

Another consequence of the expulsion of fluids from the complexes is the development of "vein structures" in slope sediments deposited on top of the complexes (Cf. Carson & von Huene 1982, Ritiger 1985). Fluids, presumably expelled along fractures in the underlying deformed accretionary complex, collect in the basal regions of the sediment drape causing abnormally high fluid pressures and in places intense hydrofracturing and "vein structure" development in the sediments. The consequent effective stress reduction is also thought to trigger down-slope creep of the slope sediment which may lead to slumping.

5.3 SUMMARY

A structural map (Appendix A) of the offshore regions of the Barbados Ridge complex has been constructed as part of the work included in this thesis (Chapter 1). It draws together all the available geophysical data on the region. During the course of developing this map an appreciation of the consistency and possible variability of the processes operating within different regions of the accretionary complex was arrived at. In particular, mud diapirs can be seen to be important features of the development of the southern regions of the complex. The presence of mud diapirs was found to relate to the accretion of thick sequences of turbidites whilst, the actual distribution in the complex was influenced by where subcretion of underconsolidated material to the base of the complex occurred and the activity of later faults (Chapter 2). Mud diapirism is one of the more visible signs of the importance fluids within deformation systems. The decollement horizon of at least the frontal imbricates appears to be predetermined by variations in the physical properties of the incoming section and fluid migration paths. Also well illustrated in the map is the basement topography's control of the thickness of sediments and distribution of turbidites on the subducting oceanic plate and the affect this has on the structural development of the complex. Changes in sedimentary thickness affected the wavelength of frontal imbricate structures and the later out-of-sequence thrusts. The changes in sedimentary thickness also produced variations in the amount of material accreted to the complex, with the development of marked changes of thickness and strike of the complex. These variations in strike and the influence of the basement ridges on the basal decollement orientation require a new evaluation of the consequences of critical taper and plane-strain affects in non-cylindrical regions of deformation complexes. This leads to the conclusion that extension may occur in the deformation wedge, with material moving out of the plane of convergence as a natural consequence of the wedge building process.

Fieldwork in Timor and Sabah concentrated mainly on attempting to understand and classify the various forms of mud diapir activity first seen only by geophysical means in the Barbados Ridge. In addition, an initial interpretation of the geology of the Kota Kinabalu area of the Crocker Range has been made, with the conclusion that its structural development was very similar to that of the DSDP Leg 78A and ODP Leg 110 sites in the Barbados Ridge Complex (Chapter 3). The similarites resulted from the comparable thickness of sediment accreted in both areas (around 200m) with the differences in lithology only producing relatively minor *variations between the two systems. The potential range of mud diapir forms and behaviour, as summarised in Chapter 4, is very large. There is the possibility that intrusive shale diapirs may stope material from their roof and walls as well as entrain blocks within them. Mud volcanoes, gas blow outs and hot water vents can be associated with the expulsion of large quantities of methane and pore fluids from deep within overpressured deformation systems. A mud diapir classification is proposed, based in part on their physical properties and in part on their behaviour. It is presented as a first step towards a more complete understanding of this melange generating phenomenon. Walking across a landscape out of which mud oozes via fissures and cracks leads to an immediate appreciation of their potential significance.*

5.3.1 Acknowledgements

I am indebted to G.K Westbrook for his interest, help and many constructive critisims during the course of this research. Special thanks go to J.F Dewey, S. Hook, M. Helman, G. Karner and C.H. Emeleus for reviewing parts of this thesis. The construction of the map of the offshore regions of the Barbados Ridge Complex would not have been possible but for the Gloria data collected during the Cruises 109 of RRS Discovery (1980) and M.T. Farnella (1982). This material was kindly donated by A.H. Stride, R.H. Belderson and N.H. Kenyon of the Institute of Oceanographic Sciences. Copies of multichannel seismic reflection sections obtained the Comite d'Etudes Petrolieres Marines were provided by B. Biju-Duval and A. Mascle of the Institute Francais du

Petrole, and P. Valery of the Societe Nationale Elf Aquitaine. M.J. Smith carried out most of the processing of the multichannel seismic data collected on Discovery Cruise 109. Seabeam bathymetry from Cruise RC2603 of the Robert D. Conrad is included with permission of M.G. Langseth. C. Burness drafted the final version of the map.

I would also like to thank T. Barber for encouragement and help during fieldwork in Borneo and Timor and to F. Tongkul, S. Barker, P. Bird and T. Hasan for company and help in the field. I would also like to acknowledge the invaluable logistical and administrative assistance of the Dept. of Geology at the Sabah Kampus of the Universiti Kebangsaan Malaysia, and M. Untung, director of the Geological Research and development Centre, Bandung, Indonesia.

Lastly but not least, I have much appreciated my time in Durham, made especially memorable by the kindness and good humor of the people I have worked with at the Dept. of Geological Sciences, people like Colin Bradshaw, Sid Lake, Steve (but I did the washing up last month) Jolley, Tony Dixon, Chris Jones, D.H. (The Don) Hutton, Ken McCaffery, Rob Butler, Ian (wild man) Alsop and T.J. (lend me ten pence) Munday. I would also like to thank Dave Asbery, Gerry Dresser, Alan Carr, Carol Blair and Kate Gittings for helping me so much on the logistical side of compiling this thesis and Grace Whale for many a verbal ear bashing and good cup of tea during the last three years.

I am grateful for the support of NERC during this research studentship.

REFERENCES CITED

Aalto, K.R., Multistage melange formation in the Franciscan complex northern most California: Geology, v. 9, p. 602-607, 1981.

Abbate, E., M. Sagri, The eugeosynclinal sequences. In: G. Sestini (ed), Develompent of the northern Apennines Geosyncline: Sediment Geol., v. 4, p. 251-340, 1970.

Abbate, E., v. Bortolotti, P. Passerini, Olistostromes and olistoliths: In: G. Sestini (ed), Develompent of the northern Apennines Geosyncline.: Sediment Geol., v. 4, p. 251-340, 1970.

Adams, J.H., The eruption of the Waimata mud spring: New Zealand mines record, v. 12, p. 97-101, 1908.

Arnold, R., G. A. MacCready, Island forming Mud volcano in Trinidad, British West Indies: Am. Ass. Pet. Geol, 2748-2758, 1956.

Audley-Charles, M.G., A Miocene Gravity Slide Deposit from Eastern Timor: Geol. Mag. v. 102, n.3, p. 267-276, 1965.

Audley-Charles, M.G., The geology of Portuguese Timor. Mem. Geol. Soc. Lond., v. 4, pp. 76, 1968.

Audley-Charles, M.G., Geometrical problems and implications of large scale overthrusting in the Banda Arc-Australian margin collision zone. in Mc Clay, K.R., N.J. Price, Thrust and Nappe Tectonics: Geol. Soc Lond. Spec. Pub., No. 9, p. 407-416, 1981.

Barber, A.J, S. Tjokrosapoeto, T.R. Charlton, Mud volcanoes, shale diapirs, wrench faults and melanges in accretionary complexes, Eastern Indonesia: Bull. Am. Ass. Petrol. Geol., v. 70, p. 1729-1741, 1985

Barber, A.J., Structural interpretations of the

Island of Timor, Eastern Indonesia: SEAPEX Proceedings, v. 9, p. 9-21, 1977.

Baadsgaard, P.H., Barbados exploration results, 1950-1958: Proc. XXI International Geol. Congress, Copenhagen, Part XVII, p. 21-27, 1960.

Baldwin, S.L., T.M. Harrison, K. Burke, Fission track evidence for the source of accreted sandstones, Barbados: Tectonics, v. 5, No. 3, p. 457-468, 1986.

Beck, M.E., On the mechanism of tectonic transport in zones of oblique subduction: Tectonophysics, v. 93, p. 1-11, 1983.

Becker, D.G., M. Cloos, Melange diapirs into the Cambria slab: A Fransiscan trench slope basin near Cambria, California, J. Geol., v. 93, n.2, p.101-110, 1985.

Belderson, R.H., N.H. Kenyon, A.H. Stride, Morphologh and structural trends of the Barbados Ridge complex in the vicinity of Deep Sea Drilling Project Sites 541, 542, and 543 as revealed by Gloria long-range side-scan sonar: Initial Rep. Deep Sea Drill. Proj., 78A, (U.S. Goverment Printing Office) 1984.

Bender, M.L., R.G. Fairbanks, F.W. Taylor, R.K. Matthews, J.G. Goddard, W.S. Broecker, Uranium-series dating of the Pleistocene reef tracts of Barbados, West Indies: Geol. Soc. Am. Bull. Part 1, v. 90, p. 577-594, 1979.

Berner, H., H. Ramberg, O. Stephansson, 1972, Diapirism in theory and experiment: Tectonophysics, v. 15, p. 197-218, 1972.

Biju-Duval,B., A. Mascle, L. Montadert, and J. Wanneson, Seismic investigations in the Colombia, Venezuela and Grenada basins, and on the Barbados Ridge for future IOPD Diilling: Geologie en Mijnbouw, v.57. p.105-116, 1978.

Biju-Duval,B., P.Le Quellec. A. Mascle,

V. Renard, P. Valery, Multibeam Bathymetric survey and high Resolution seismic investigation on the Barbados Ridge Complex (- Eastern Caribbean): A key to the Knowlage and interpretation of an accretionary wedge: Tectonophysics, v. 86, p. 275-304, 1982.

Bishop, R.S., Mechansim for emplacement of pierecement diapirs: Am Ass. Pet. Geol. Bull., v. 62, No. 9, p. 1561-1583, 1978.

Bitterli, K.M., Herrera subsurface structure of the Penal Field, Trinidad: Am. Assoc. Petrol. Geol. Bull., v. 42, p. 145-158, 1965.

Bol, A.J., B. van Hoorn, Structural styles in western Sabah offshore: Geol. Soc. Malaysia Bull., v. 12, p.1-16, 1980.

Bouma. A.H., Sedimentology of some flysh deposits. Elsevier, Amsterdam, 168p., 1962.

Bowen, J.M., J.A., Geology of the Crocker Range and ajoining areas. In: Geology of Sarawack, Brunei and northwest Sabah, (ed) P. Leichti, Brit. Terr. Borneo Geol. Survey Dept., 3, 1957.

Boyer, S.E., D. Elliott, Thrust systems: Am. Ass. of Pet. Geol. Bull. v. 66 p. 1196-1230, 1982.

Bray, J.C., D.E. Karig, Porosity of sediments in accretionary prisms and some implications for dewatering processes, J. Geophys. Res., v.90, p. 768-778, 1985.

Breen, N.A., E.A. Silver, D.M. Hussong, structural styles of an accretionary wedge south of the Island of Sumba, Indonesia, revealed by Seamarc II Side Scan Sonar: Geol. Soc. Am. Bull. in press.

Butler, R.W.H, M.P. Coward, Geological constraints, structural evolution and deep geology of the northwest

Caledonides: Tectonics, v. 3, p. 347-365, 1984.

Byrne, T., Eocene underplating along the Kodiak Shelf, Alaska: implications and regional correlations: Tectonics, v. 5, no. 3 p. 403-421, 1986.

Carson, B., R. von Huene, M.A. Authur, Small scale deformation structures and physical properties related to convergence in the Japan Trench slope: Tectonics, V.1, p. 277-302, 1982.

Carter, D.J., M.G. Audley-Charles, and A.J. Barber, Stratigraphic analysis of island acr-continental margin collision in eastern Indonesia: Jour. Geol. Soc. Lond., v. 132, p. 179-198, 1976.

Chapple, W.M.,Mechanics of thin-skinned fold-and-thrust belts Geol. Soc. Am. Bull, v.89, p.1189-1198, 1978.

Chase, R.L. and E.T. Bunce, Underthrusting of the eastern margin of the Antillies by the floor of the western North Atlantic Ocean, and the origin of the Barbados Ridge: J. Geophys. Res., V.74, p.1413-1420, 1969.

Cloos, M., Flow Melanges: Numerical modeling and geoligical constraints on their origin in the Franciscan subduction complex, California: Geol. Soc. Am. Bull., v.93, p.330-345, 1982.

Cloos, M., Lanndward dipping reflectors in accretionary wedges: Active dewatering conduits?: Geology, v.12, p. 519-522, 1984.

Cloos, M., Flow Melanges: Numerical modeling and geoligical constraints on their origin in the Franciscan subduction complex, California: Disscussion and reply: Geol. Soc. Am. Bull., v.94, p.1241-1244, 1983.

Coleman, R.G., Ophiolites, ancient oceanic lithospheric ?: Spingernerlag, Berlin, Heidelberg, New York, P. 229, 1977.

Collenette, P., The geology and mineral resources of the Jesselton-Kinabalu area, North Borneo: Brit. Borneo Geol. Survey Dept, Mem. 6, p.194, 1958.

Cowan, D.S., R.M. Silling, A dynamic scaled model of accretion in trenches and its implications for the tectonic evolution of subduction complexes: J. Geophys. Res., v. 83, p. 5389-5396, 1978.

Cowan, D.S, Origin of "vein structure" in slope sediments on the inner slope of the middle America Trench off Guatemala: in J. Aubouin, R. von Huene, and others, (eds.), Intital Reports of the Deep Sea Drilling Project: D.C., U.S. Goverment Printing Office, v. 67, p. 645-650, 1982.

Cowan, D.S., J.C. Moore, S.M. Roeske, N. Lundberg, S.E. Lucas, Structural features at the deformation front of the Barbados ridge complex, Deep Sea Drilling project Leg 78A: Initial Rep. Deep Sea Drill. Proj. Leg 78A, (U.S. Goverment Printing Office) p. 535-545, 1985.

Cowan D. S., Structural styles in Mesozoic and Cenozoic melanges in the western Cordillera of North America: Geol.Soc. Am.Bull., 96, 451-462, 1985.

Craig, R.F., Soil mechanics: 3rd edition, Van Nostrand Reinold Ltd, 1983.

Dalgarno C.R., J.E. Johnson, Parachilna sheet H 54-13: Map Preperation By Catographic section, Dept. Mines. Australia, 1966.

Davis, D., J.Suppe, F.A. Fahlen, Mechanics of fold-and-thrust belts and accretionary wedges; J. Geophys. Res., v.88, 1153-1172, 1983.

Davis, D.M., The compressive mechanics of accretionary wedges applied to the Leg 78A study area near Barbados Initial rep. Deep Sea Drill. Proj. Leg 78A,(U.S. Goverment Printing Office)

p. 559-569, 1984.

Davis, D.M., D.M. Hussong, Geothermal observations during Deep Sea Drilling Project Leg 78A: Initial rep. Deep Sea Drill. Proj. Leg 78A, (U.S. Goverment Printing Office) p. 593-598, 1984.

Dahlen, F.A., J. Suppe, D. Davis, Mechanics of fold-and-thrust belts and accretionary wedges: cohesive Coulomb theory: J. Geophys. Res., v. 89, p.10087-10101, 1984.

Dixon, J.M., Finite strain and progressive deformation in models of diapriric structures: Tectonophysics v. 28, P.89-124, 1975.

Dickinson, W.R., Seely D.R, Structure and stratigraphy of Forearc Regions: Am. Ass. Petrol. Geol. Bull., v. 63, p. 2-31 1979.

Duque-Caro, H. Structural style,diapirism, and accretionary episodes of the Sinu-San terrane, southwestern Carribbean border-land: Geol. Soc. Am. Memoir 162, p.303-316, 1983.

Fitch, T.J., Plate convergence, transcurrent faults, and internal deformation adjacent to Southeast asia and western Pacific: Jour. Geophysical Res., v. 77, p, 4432-4461, 1972.

Freeman, P.S., Exposed middle tertiary mud diapirs and related features in south Texas: Am. Assoc. Pet. Geol., Memoir 8, p. 162-182, 1967.

Gilreath, J.A., Electic-log characteristics of diapiric shale, Diapirism and Diapirs: Am. Assoc. Petrol. Geol. Mem. v. 8, p. 137-144, 1928.

Guewa, P.R., Middle to late Cretaceous sedimentary melange , Franciscan Complex, northern California: Geology, v. 3, p. 105-108, 1975.

Hada, S., T. Suzuki, Tectonic environments and crustal section of the Outer Zone of Southwest Japan: Accretion Tectonics in the Circum-Pacific Regions, M. Hashimoto & Uyeda (eds), Terra Sci. Pub. Co., Tokyo, P. 207-218, 1983.

Hamilton, W., tectonics of the Indonesian region: U.S. Geological Survey, Professional paper 1078, 1979.

Hedberg, H.D., Relation of methane Generation to undercompacted shales, shale diapirs and mud volcanoes, Am. Assoc. Pet. Geol. Bull., v. 58, n.4, p.661-673, 1974.

Hill, A.J., The evolution of the forearc basins on and behind the Barbados Ridge Complex: Unpublished Msc. Thesis, Durham University Dept. Geological Sciences, 1983.

Higgins, G.E., J.B. Saunders, Report on 1964 Chatham mud island, Erin Bay, West Indies: Am. Assoc. Pet. Geol. Bull., v. 51, p.183-189, 1967.

Higgins, G.E., J.B. Saunders, Mud Volcanoes-their nature and origin: Contributions to the Geology and Paleobiology of the Caribbean and Ajacent Areas: Verhandl. Naturf. ges. Basel, Band 84, Nr.1, 1973.

Hoedemaeker, P.J., Olistostromes and other delapsional deposits, and their occurrence in the region of Moratalla (province of Murcia, Spain): Scriptia Geologica 19, p. 207, 1973.

Hovland, M.G. A.G. Judd, L.H. King, Characteristic features of pockmarks on the North Ses Floor and Scotian Shelf: Sedimentology, v. 31, p. 471-480 1984.

Hubbert, M.K., and W.W. Rubey, Role of fluid pressure in mechanics of overthrust faulting;1. Mechanics of fluid filled porous solids and its application to overthrust faulting: Geol. Soc. Am. Bull., v. 70, p. 115-166, 1959.

von Huene, R., H. Lee, The possible

significance of pore fluid pressures in subduction zones Am. Ass. Pet. Geol. memoir 34, p.781-791, 1982.

von Huene, R., Structural diversity along modern convergent margins and the role of overpressured pore fluids in subduction zones: Bull. Soc. Geol. France, v. 26, no. 2, p. 207-219. 1984.

von Huene, R., Direct measurement of pore fluid pressure, Leg 84, Guatemala and Costa Rica: in Von Huene, R., J. Aubouin, et al., Initial Rep. Deep Sea Drill. Proj., Leg 84, 1985.

Hutchinson, G., Tectonic evolution of Sundaland: Bull. Geol. Soc. Malaysia, v. 6, p. 61-86, 1973.

Hutchinson, G., Ophiolite in South Asia: Geol. Soc. of AM. Bull., v. 86, No. 6, p. 797-806, 1975.

McIver, R.D., Role of naturally occuring gas hydrates in sediment transport: Am. Assoc. Pet. Geol. Bull., V.66, P.789-792, 1982.

McIver, R.D., Role of naturaly occuring gas hydrates in sediment transport:Reply: Am. Assoc. Pet. Geol. Bull., v. 67, p.877, 1983.

Jacobson, G., Gunung Kinabalu area, Sabah, Malaysia,: Malaysian Geol. Survey Rep., No. 8, 1970.

Karig, D.E., Sharman G.F., Subduction and Accretion in Trenches: Geol. Soc. Am. Bull., v. 86, p.377-389, 1975.

Kasper, D.C., D.K. Larue, Paleogeographic and tectonic implications of Quartzose sandstones of Barbados: Tectonics, v. 5, p. 837-854, 1986.

Khain, V.E., L.E. Levin, Tectonic Types of marginal and inner seas; their place in the development of the crust:

Tectonophysics, v. 70, p. 237-260, 1980.

Kerr, P.F., I.M. Drew, S.D. Richardson, Mud volcano clay, Trinidad: Am. Assoc. Petrol. Geol. Bull., v. 54, p. 2101-2110, 1970.

Knipe, R.J., Deformation mechanism path diagrams for sediments undergiong lithification: Geol. Soc. Am. Memoir 166, in press. (1986).

Kvenvolden, K.A., Comparison of marine gas hydrates in sediments of active and passive continental margin: Marine and Pet. Geol., v.2, p. 65-71, 1985.

Kvenvolden, K.A. 2.A. McMenamin, Hydrates of natural gas; a review of their geologic occurance: U.S. Geological Survey Circular 825, 11p. 1980.

Kugler, H.G., Visit to Russian oil districts: J. Inst. Petrol., v. 25/184, p. 68-88, 1939.p

Kulm, L.D., E. Suess, J.C. Moore, B. Carson, B.T. Lewis, S.D. Ritiger, D.C. Kaolko, T.M. Thornburg, R.W. Embley, W.D. Rugh, C.J. Massoth, M.G. Langseth, G.R. Cochrane, R.L. Scamman, Oregon subduction zone: Venting, fauna and carbonates: Science, v. 231, p. 561-566, 1986.

Ladd, J.W., Seismic Section G-G' in Speed, R.C. G.K. Westbrook and others (eds), Lesser Antillies arc and adjacent terranes, Atlas series: Marine Science International, Woods Hole, MA, Sheets 19-22, 1984.

Ladd, J.W., Bathymetry, in: Speed, R.C. G.K. Westbrook and others (eds), Lesser Antillies arc and adjacent terranes, Atlas series: Marine Science International, Woods Hole, MA, Sheets 19-22, 1984.

Larue, D.K, R.C. Speed, Quartzose turbidites of the accretionary complex of Barbados I: Chalky Mount Sucession: Jour. Sed. Pet., v. 53, No. 4, p. 1337-1352, 1983.

Larue, D.K., J. Schoonmaker, R. Torrini,

J. Lucas-Clark, M. Clark, R. Schneider, Barbados: Maturation, source rock potential and burial history within a Cenozoic accretionary complex: Jour. Marine Pet. Geol., v. 4, 1984.

Larue, D.K., R.C. Speed, Structure of the accretionary complex of Barbados, II: Bissex Hill, Geol. Soc. Am. Bull., v. 95, p. 1360-1372, 1985.

Laughton, A.S., The first decade of Gloria: J. Geophys. Res., V.86, p. 11,511-11,534, 1981.

Lee, D.C.T., Regional of Sabah: Geol. Survey Malaysia, Ann Rep., p. 119-131, 1979.

Lee, D.C.T., Application of Landsat to regional geologic studies, with reference to the geology of central and west coast Sabah and adjacent areas: Geol. Survey. Malaysia Geol. Papers v. 3, p. 126-133, 1980.

Leggett, J.K., Oceanic sediments from the Ordovician of the Southern Uplands, in The Caledonides of the British Isles-reviewed: Geol. Soc. of London Spec. Pub. 8, p. 495-498, 1979.

Leggett, J.K., The sedimentological evolution of a lower Palaeozoic accretionary fore-arc in the Southern Uplands of Scotland: Sedimentology, v. 27, P.401-417, 1980.

Leggett, J.K., W.S. McKerrow, D.M. Casey, The anatomy of a lower Palaeozoic accretionary forearc: The Southern Uplands of Scotland: Trench-Forearc geology, Ed. J.K. Leggett, Geol. Soc. Lond. Spec. Pub. No. 10, P. 494-520, 1982.

Leggett, J.K., D.M. Casey, The Southern Uplands accretionary prism: Implications for controls on structural development of subduction complexes: Contential Margin Geology, AAPG Memoir 34, p. 377-393, 1984.

Leggett, J.K., Y. Aoki, T. Toba, Transition from frontal accretion to underplating in part of the Nankai Trough accretionary complex off Shikoku (SW Japan) and extensional features on the lower trench slope: Marine and Pet. Geol., V.35, 1984.

Liechti, P., F.W. Roe, N.S. Haile, The geology of Sarawak, Brunei and the western part of Borneo: Bull. Brit. Borneo Geol. Survey, No. 3, 1960.

Lu, R.S., J.K. McMillen, Multichannel seismic survey of the Colombia Basin and adjacent margins: AAPG Memoir 34, P. 395-410, 1983.

Marlow, M.S., L.E. Garrison, R.G. Martin, G.V.A. Trumbull and A.K. Cooper, Tectonic transition zone in the northeastern Carribbean: U.S. Geol. Survey J. Res., v. 2 p. 289-302, 1974.

Marlow, M.S., H.J. Lee, A.W. Wright, Physical properties of sediment from the Lesser Antillies margin along the Barbados Ridge: Results from Deep Sea Drilling Project Leg 78A: Initial Rep. Deep Sea Drill. Proj. Leg 78A, P. 549-558, 1984.

McCarthy, J., D.W. Scholl, Mechanisms of subduction alond the central Aleutian trench: Geol. Soc. Am. Bull., v. 96, p. 691-701, 1985.

McKerrow, W.S., J.K. Leggett, M.H. Eales, Imbricate thrust model of the Southern Uplands of Scotland: Nature London, v. 267, p. 237-239, 1977.

McManus, J., R,B. Tate, Volcanic control of structures in north and west Borneo: SEAPEX Program paper 5, 1951.

Minster, J.B., T.H. Jordan, Present-day plate motions: J. Geophys. Res. v.83, p 5331-5354, 1978.

Morgan, J.P., J.M. Coleman, S.M. Gaglino, Mudlumps: Diapiric structures in Mississippi delta sediments: Am.

Assoc. Pet. Geol. Memoir 8, p.145-161, 1965.

Moore, G.F., Karig, D.E. Structural geology of Nias Island, Indonesia: Implications for subduction zone tectonics: Am. J. Sci., v.280, p. 193-223, 1980.

Moore, J.C, J.S. Watkins, T.H. Shipley, K.J. McMillen, S.B. Bachman, N. Lundberg, Geology and tectonic evolution of a juvenile accretionary terrane along a truncated convergent margin: Synthesis of results from Leg 66 of the Deep Sea Drilling Project, southern Mexico: Geol. Soc. Am. Bulletin, v. 93, p. 847-861, 1982.

Moore, J.C., N. Lundberg, Variations in forearc ductility: Consequences for the stratigraphic record (abs): Eos, Am. Geophys. Union Trans., v. 64, p. 828, 1983.

Moore, J.C., B. Biju-Duval, Tectonic synthesis, deep sea drilling project leg 78A: Structural evolution of offscraped and underthrust sediment, northern Barbados Ridge Complex: Initial Rep. Deep Sea Drill. proj., 78A, (U.S. Goverment Printing Office),1984.

Moore, J.C., D.S. Cowan, D.E Karig, Structural styles and deformation fabrics of accretionary complexes: Penrose conference report, Geology, v. 13, p. 77-79, 1985.

Moore, J.C., Mascle and shipboard party of Leg 110; Accretionary complex penetrated, defined: Geotimes, p. 13-16, January, 1987.

Moore, J.C., A. Mascle, and others, Structural and hydrological framework of the northern Barbados Ridge Complex: results of Leg 110: nature in press. 1987.

Moseley, F.A, A tectonic history of northwest England: Jour. Geol. Soc. London, v. 128,

p. 561-598, 1972.

Murphy, J.M., K.R. Aalto, Flow Melanges: Numerical modeling and geoligical constraints on their origin in the Franciscan subduction complex, California: Disscussion and reply: Geol. Soc. Am. Bull., v.94, p.1241-1244, 1983.

Musgrave, A.W., Hicks, W.G., Outlining shale masses by geophysical methods: Diapirism and diapirs: Am. Ass. Pet. Geol., Mem. v. 8, p122-136, 1968.

Nelson, K.D., A suggestion for the origin of megascopic fabric in accretionary melange, based ofsfeatures observed in the Chrystalls Beach Complex, South Island, New Zealand: Geol. Soc. Am. Bull., v. 93, p. 625-634.

Page, B.M., Gravity tectonics near Passo Della Cisa, Northern Apennines, Italy: Geol. Soc. Am. Bull., v. 74, N.1 p.655-672, 1963.

Page, B.M., Fransiscan melanges compaired with olistostromes of Taiwan and Italy, Tectonophysics, v.47 p. 223-246, 1978.

Park, M,J.M., Numerical analysis of deformation in the upper parts of subduction zones: Phd thesis, Unvi. Durham, 1981.

Peter, G., G.K. Westbrook, Tectonics of southwestern North Atlantic and Barbados Ridge Complex: Am. Ass. Pet. Geol. Bull., v. 60, p.1065-1077, 1976.

Platt, J.P., Secondary cleavages in ductile shear zones: Jour. of Structural Geol., v. 6, No. 4, p. 439-442, 1984.

Platt, J.P., J.K. Leggett, J. Young, H. Raza, S. Alam, Large-scale sediment underplating in the Makran accretionary prism, southwest Pakistan: v. 13, p. 507-511, 1985.

Platt, J.P., Dynamics of orogenic wedges and the *uplift of high-pressure metamorphic rocks: Geol. Soc. Am. Bull., v. 97, p. 1037-1053, 1986.*

Ponce De Leon, M.J., P. Choukroune, shear Zones in the Iberian arc: J. Struct. Geol., v. 2, p. 63-68, 1980.

Ramberg, H., Gravity, deformation and the earth's crust: New York, Academic Press., p. 214, 1967.

Ramberg, H., Fluid dynamics of layered systems in the field of gravity, a theoretical basis for certain global structures and their isostatic adjustment: Physics Earth and Planetary Interiors, v. 1, p. 63-87, 1968a.

Ramberg, H., Instability of layered systems in the field of gravity, I and II: Physics Earth and Planetary Interiors, v. 1, p. 427- 474, 1968b.

Rau, W.W., G.R. Grocock, Piercement structure outcrops along the Washington coast: Washington Divisions of Mines a d Geology, Information Circular, n.51, 7p, 1974.

Ridd, M.F., Mud volcanoes in New Zealand: Am. Assoc. Pet. Geol. Bull., v. 54, n. 4, 1970.

Ritger, S.D., Origin of vein structures in slope deposits of modern accretionary prisms: Geology, June, p. 437-439, 1985.

Roach, C.B, Intrusive shale dome in south Thornwell Field, Jefferson Davis and Cameron Parishes, Louisana: Bul.Am. Ass. Pet. Geol., v. 46, No. 12, 1962.

Rosidi, H.M.D., K. Suwitodirdjo, S. Tjokroosapoetro, Geological map of the Kupang-Atambua Quadrangles, Timor: Geol. Res. and Development Centre, Bandung, 1981.

Rubey, W.W., and M.K. Hubbert, Role of fluid pressure in mechanics of overthrust faulting; 2. Over-

thrust belt in geosynclinal area of western Wyoming in light of fluid pressure hypothesis: Geol. Soc. Am. Bull. v. 70, p.167- 205, 1959.

Sample, J.C., D.M. Fisher, Duplex accretion and underplating in an ancient accretionary complex, kodiak Islands, Alaska: Geology, v. 14, p.160-163, 1986.

Sanderson, D.J., D. Marchini, Transpression, Jour. Struct. Geol., v. 6, p. 449-459, 1984.

Sanderson, D.J., J.R. Andrews, W.E.A. Phillips and D.H.W. Hutton, Deformation studies in the Irish Caledonides: Jour. Geol. Soc. London, v. 137, p. 289-302, 1980.

Senn, A., Paleogene of Barbados and its bearing on the history and structure of the Antillean-Carribean region: Am. Ass. Pet. Geol. Bull., v. 24, P. 1548-1610, 1940.

Shouldice, D.H., Geology of the Western Canadian continental shelf: Bull. of Canadian Pet. Geol., v.19, n.2 p. 405-436, 1971.

Shih, T.T, A survey of the active mud volcanoes in Taiwan and a study of their Types and the Character of the mud: Petrol. Geol. Taiwan, v. 5, P.259-311, 1967.

Shipley, T.H., J.W.Ladd, R.T. Buffler, J.S.Watkins Tectonic processes along the Middle America Trench inner slope: Trench Forearc Geology, Ed by S.K. Legget, Geol. Soc. Spec. Pub., No. 10, 1982.

Silver, E.A., J.M. Ellis, N.A Breen, T.H. Shipley, Comments on the Growth of Accretionary Wedges: Geology, v. 13, P. 6-9, 1985.

Smith G.N., elements of soil mechanics for civil and mining engineers: 4th edition, Granada Pub., 1975.

Snavely, P.D., J.E. Pearl, and D.L. Lander, Interm report on petroleum resources *potential and geological hazards in the outer continental shelf, Oregon and Washington Tertiary Province: U.S. Geol. Survey, Open-file report 77-282, 63p. 1977.*

Snead, R.E., Active Mud volcanoes of Baluchistan, West Pakistan: The Geographical Review, v. 14 no. 4, p. 546-560, 1964.

Soper, N.J., D.H.W. Hutton, Late Caledonian sinistral displacements in Britian: Implications for a three-plate collision model: Tectonics, v. 3, No. 7, p.781-794, 1984.

Speed, R.C., Barbados: Architecture and implications for accretion: Jour. Geophys. Res., v. 87, p. 3633-3643, 1982.

Speed, R.C., Structure of the accretionary complex, I: Chalky Mount: Geol. Soc. Am. Bull. v. 94, p. 92-116, 1983. Lesser Antillies Arc and adjacent terraines: Ocean Margin Drilling Program: Regional Atlas Series, Atlas 10, 1984.

Speed, R.C., G.K. Westbrook, and others, Lesser Antillies arc and adjacent terranes, Atlas 10 Ocean Margin Drilling Program, Regional Atlas series: Marine Science International, Woods Hole, MA, 27 sheets. 1984

Speed, R.C., Cenozoic Collision of the Lesser antillies arc and contential South America and the origin of the El Pilar fault: Tectonics, v. 4, No. 1, p. 41-69, 1985.

Stauffer, P.H., Unravelling the mosaic of Palaeozoic crustal blocks in S.E. Asia: Geologische Rundschau, v. 72, No. 3, p. 1061-1081, 1983.

Stauffer, P.H., Studies in the Crocker Formation Sabah: Borneo Region Malaysia Geol. Survey Bull., v. 8, p. 1-13, 1967.

Stockmal, G.S. Modeling of large-scale accretionary wedge deformation: Jour. Geophys. Res., v. 88, p.8271-8287, 1983.

Stride, A.H., R.H. Belderson, N.H. Kenyon Evolving miogeanticlines of the east Mediterranean (Hellenic, Calabrian and Cyprus Outer Ridges): A. Mathematical and Physical Sciences, v. 284, p. 255-285, 1977.

Stride, A.H., R.H. Beldeson, and N.H. Kenyon, Structural grain, mud volcanoes and other features on the Barbados Ridge Complex revealed by GLORIA long range side-scan sonar: Marine Geol., v.49, p. 187-196., 1982.

Striniger, P., J.E. Treagus, Non-axial Planar S1 clevage in the Hawick Rocks of the Galloway area, Southern Uplands, Scotland: Jour. Struct. Geol. v. 2, p. 317-331, 1980.

Suess, E., GJ. Massoth, Evidence for the venting of porewaters from subducted sediments of the Oregon continental margin, EOS Trans: Am. Geophys. Union, v. 65, p.1089, 1984.

Suppe, J., J.H. Wittke, Abnormal pore-fluid pressures in relation to stratigraphy and structure in the active fold-and-thrust belt of Taiwan: Pet. Geol. Taiwan, No. 14, P. 11-24, 1977.

Suzuki, T., Melange problem of convergent plate margins in the Circum-Pacific regions: Memoirs faculty of Science, Kochi University, Series E, 1986.

Sweet, W.E., Role of naturally occuring gas hydrates in sediment transport: Discussion: Am. Ass. Pet. Geol., v. 67, No. 5, p.876, 1983.

Sykes,R.,W.R. McCann, A.L.Kafka Motions of Caribbean plate during last 7 million years and implications for earlier Cenozoic movements: J. Geophys. Res., V.87, p 10656-10676, 1982.

Tan, D.N.K., Siliceous depostis (chert) of Malaysia: Geol. Survey Malaysia, v. 3 p. 100-114, 1980.

Tan, D.N.K., The Lubok Antu Melange, Lupar valley, west Sarawak: A Lower Tertiary subduction complex: Geol. Soc. Malaysia Bull., v. 15, p. 31-46, 1982.

Tapponnier, P., P. Molnar, Slip line field theory and large-scale continental tectoincs: Nature, Lond, v.264, p. 319-324, 1976.

Tappoonier, P., G. Peltzer, A.Y. Le Dain, R. Armijo, P. Cobbold, Propogating extrusion tectonics in Asia: New insights from simple experiments with plasticine: Geology, v. 10, p. 611-616, 1982.

Tapponnier, P., G. Peltzer, R. Armijo, On the mechanics of the collision between India and Asia: in Collision Tectonics, ED. Coward & Ries: Geol. Soc. Spec. Pub., no. 19, p.115-157, 1986.

Tija, H.D. Sence of tectonic transport in intensely deformed Trusmadi and Crocker Sediments, Ranu-Tenompok area, Sabah: Sains Malaysiana, v. 3, p. 171-188 1974.

Tissot, B., B. Durand, J. Espitalie, A. Combaz, Influence of nature and diagenisis of organic matter in formation of petroleum: Am. Assoc. Pet. Geol., v. 58, n. 3, P. 499-506, 1974.

Tokuyama, A., S. Yoshida, Kinabalu Fault, a large strike-slip fault in Sabah, East Malaysia: Geol. and Pal. of southeast Asia, v. 14, p.171-188, 1974.

Tongkul F., Geology of the Crocker Formation, Kota Kinabalu area, Western Sabah, Malaysia: unpublished Msc. thesis Chelsea College, 1985.

Torrini, R., R.C. Speed, G.S. Mattioli, Tectonic relationships between forearc-basin strata and the accretionary complex at Bath, Barbados: Geol. Soc. Am. Bull., v 96, p. 861-874, 1985.

Tjokroosapoetro, S., Holocene tectonics on Timor island, Indonesia: Bulletin of the Geological Research and Development Centre, v. 4, p. 48-63, 1978.

Valery, P., G. Nely, A. Mascle, B. Biju-Duval, P. Le Quellec, J.L. Berthon, Structure et croissance D'un prisme D'accretion tectonique proche d'un continent: la Ride de la Barbade an sud de l'arc Antilais: Geodymamic des Caraibes, Symposium Paris, Editions Technip, 1985.

Walker, R., H.R. Ensminger, Effect of diapirism on sedimentation in Gulf of Mexico: Am. Assoc. Pet. Geol. Bull., v. 54, No. 11, 1970.

Westbrook, G.K, 1975, The structure of the crust and upper mantle in the region of Barbados and the Lesser Antillies: Royal Astr. Soc. Geophy. Jour., v. 43, P. 201-242, 1975.

Westbrook, G.K., The Barbados Ridge Complex: Tectonics of a mature forearc system, in Legget, J.K. Legget,ed., Trench and forearc geology: Sedimentation and tectonics in ancient and modern active plate margins: Geol. Soc. London Special pub.10 p. 275-290, 1982.

Westbrook, G.K., M.J. Smith, J.H. Peacock and M.J. Poulter, Extensive Underthrusting of undeformed sediment beneath the accrretionary complex of the Lesser Antillies Subduction Zone: Nature, v. 300, p. 625-628, 1982.

Westbrook, G.K., M.J. Smith, Long decoll-

ements and mud volcanoes: Evidence from the Barbados Ridge complex for the role of high pore-fluid pressure in the development of an accretionary complex. Geology v. 11 p. 279-283, 1983.

Westbrook, G.K., A. Mascale and Biju-Duval, Geophysics and the structure of the Lesser Antillies Forearc, in Biju-Duval,B., J.C. Moore., et. al. Initial reports of the Deep Sea Drilling Project, v. 78A,(U.S. Goverment Printing Office) 1984.

White, R.S., Louden, The Makran Contential Margin: Structure of a Thickly Sedimented Convergent Plate Boundary: AAPG Memoir 34, p.499-518, 1982.

Williams, P.R., C.J. Pigram, D.B. Dow Melange production and the importance of shale diapirism in accretionary terrains, Nature v.309 p. 145-146, 1984.

Wilford, G.E., Geological map of Sabah, east Malaysia: 2 nd edition, Geol. Survey Borneo Region, Malaysia, 1967.

Wilson, R.A.M., N.P.Y. Wong, The geology and mineral resources of the Labuan and Padas valley area, Sabah, east Malaysia: Geol. Survey Mem., v. 17 p. 150, 1964.

Wright, A., Sediment distribution and depositional processes operating in the Lesser Antillies Intra-oceanic Island arc, Eastern Caribbean. Initial Rep. Deep Sea Drill. Proj., 78A, 1984.

Zhao, W.L., D.M. Davis, F.A. Dahlen, J. Suppe, Origin of convex accretionary wedges: Evidence from Barbados: J. Geophys. Res., v. 91, p. 10246-10258, 1986.

Locality 1

Locality 1, is the most western of the localities studied (Fig. 3.5). Exposed, during excavations associated with the building of a school, is a section through a major trenchward verging fold pair that has been imbricated by a series of arcward verging thrusts (Fig. 3.6). The structures involve mainly the Red Mudstone and Sandstone Units, with the red mudstones providing an important repeated marker horizon. The repetition of the Red Mudstone Unit enables the division of the structures into a series of thrust Packets (1-10) seperated by thrust faults (1-9).

Proceeding from west to east along Section 1 (Fig. 3.6) Packet 1 (0-25m) is part of the eastern margin of the most seaward sandstone ridge on the local geological map of the Kota Kinabalu area (Fig. 3.5). The sandstones further to the west of Section 1 are predominantly steeply dipping (‹60°) and homoclinally bedded, younging to the east. A depositional contact between the Sandstone Unit and Red Mudstone unit is exposed at about 25m. The red muds are about 10m thick and contain occasional thin sandstone beds within them. In two horizons, these sandstone beds are contorted and disrupted by slumping. The deformation occurred before they were consolidated, with the development of sandstone dykes (Plate 3.4), irregular bulbous folds and sandstone blocks with wispy terminations. The sandstones appear to have provided conduits for reducing fluids, as green reduction halos are developed around them (Plate 3.4). The undeformed parts of red homogeneous mudstones exhibit a blocky conchoidal

The tectonic fabric of the Barbados Ridge accretionary complex

K.M. Brown
Department of Geological Sciences, University of Durham, Science Laboratories, South Road, Durham DH1 3LE, UK
and G.K. Westbrook
Department of Geological Sciences, The University of Birmingham, PO Box 363, Birmingham B15 2TT, UK
Received 6 September 1986

A map showing near-surface structure and other surficial geological features on the Barbados Ridge accretionary complex has been constructed from GLORIA long-range side-scan sonographs, detailed bathymetric surveys using Seabeam, and single and multichannel seismic reflection sections. The map shows major variations in the size, orientation and style of structures across the accretionary complex that are principally related to the increasing thickness of the complex and the sediment drape upon it, and variations along the complex that derive from the northward thinning of sediment accreted from the ocean floor and the effects of ridges in the oceanic basement. The development of crossfaulting is mainly associated with basement ridges. Mud diapirism is abundant in the southern part of the complex and is characteristic of that part of the complex into which turbidites from the Orinoco submarine fan are accreted. Slumping on a variety of scales is another feature of the complex.

The map is presented at a scale of 1:1063415 (4 inches per degree of longitude) and also shows bathymetry at 200 m contour intervals.

Keywords: Accretionary complex; Structure; Side-scan sonar; Seismic reflection sections

Introduction

The Barbados Ridge Complex lies to the east of the Lesser Antilles island arc at the eastern margin of the Caribbean plate, where the Atlantic oceanic crust is subducted beneath it westwards or slightly south west at a rate of 20 km/m.y. (Minster and Jordan, 1978) to 37 km/m.y. (Sykes, *et al.*, 1983) (*Figure 1*). It is an example of a subduction accretion complex that is extensively developed. A map (*Figure 2*) of the shallow structure of accretionary complex and related morphological and sedimentary features has been compiled from GLORIA long-range side-scan sonar images, Seabeam bathymetry and seismic reflection profiles. The map shows that within the accretionary complex there are great variations in the style of deformation. These variations arise principally from radial variation in stress regime of the accretionary complex and its history along strike variations in sedimentation both onto and in front of the complex, and effects of ridges associated with transform faults in the oceanic crust beneath the complex.

The Barbados Ridge accretionary complex has been broadly subdivided into four zones (*Figure 1*) (Westbrook *et al.*, 1984) that reflect radial changes in the structure of the complex:

(1) *Zone of Initial Accretion*, where rapid thickening of the complex occurs by frontal imbricate thrusting and further back by subcretion and large-scale reimbrication. It is dominated by trenchward facing slopes.

(2) *Zone of Stabilization* where the rate of thickening of the complex is small. A dynamic equilibrium exists between the gravitational body forces that would cause the complex to spread and the compressional forces that seek to thicken it. The increased strength of this older part of the complex, resulting from compaction and lithification reduces the rate of shortening.

(3) *Zone of Supracomplex Sedimentary Basins.* Well developed south of latitude 13°N, this is a zone where thicknesses of up to 3 km of undeformed sediments lie on top of the accretionary complex in basins that are created by the relative uplift of the parts of the complex that forms their margins. The Barbados Trough is the largest of these basins.

(4) *Barbados Ridge Uplift* lies at the western margin of the accretionary complex. The uplift is related to the complex being thrust westwards, up onto the forearc basement. The uplift has recently been most active in the central region and dies out to the south and north. Forearc sediments of the Tobago Basin and the other forearc basins are being deformed and accreted to the complex along the inner deformation front, which form the western boundary of the complex.

Basement ridges in the Atlantic oceanic crust that are associated with fracture zones trend at high angles to the strike of the deformation front. The basement ridges ponded turbidites from the Orinoco Fan in the south, restricting their northward flow. There are pppronounced variations in the thickness of sediments between ridges and trough (Speed, Westbrook and others, 1984) which are reflected in the wavelengths of the frontal accretionary structures. Structures are also induced in the complex directly by the tectonic influence of the ridges, which produce compressional features on their southern flanks.

0264–8172/87/01078–11 (plus Fig. 2 fold-out) $03.00

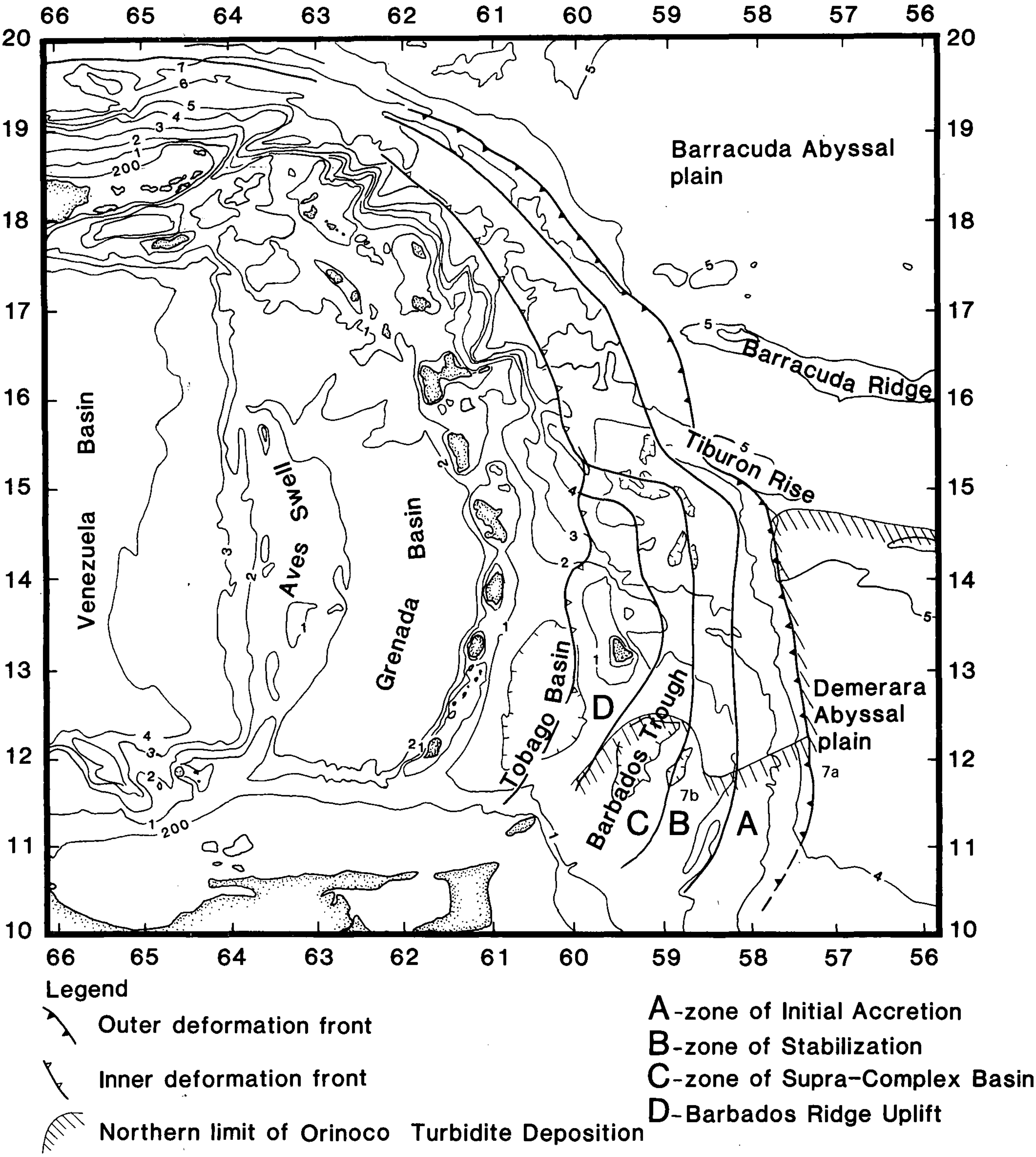

Figure 1 The location of the Barbados Ridge Complex east of the Lesser Antilles island arc, with its four main lateral subdivisions. Bathymetric contours are at 1 km intervals. The locations of two seismic sections of *Figure 7* are shown, 7a and 7b

Data sources and map construction

The following data sources were used in the compilation of the structural map (*Figure 3*) of the offshore regions of the Barbados accretionary complex:

(1) A regional, long-range side-scan (GLORIA) survey from cruise 109 of RRS Discovery in 1980 (Stride *et al.*, 1982), plus some additional coverage from a cruise of M.T. Farnella in 1982.

(2) Multichannel seismic reflection lines from RRS Discovery Cruise 109 (Westbrook and Smith, 1984), from sites surveys and the Carven project conducted by IFP and CEPM (Biju-Duval *et al.*, 1978, 1982, Valery *et al.*, 1985), from Lamont-Doherty Geological Observatory (Ladd, 1984, Maufrett *et al.*, 1984), and from Shell International. Single-channel seismic profiles, principally from cruises by Lamont-Doherty Geological Observatory and Woods Hole Oceanographic Institute were also found to be of use in some areas.

(3) Seabeam bathymetric surveys undertaken in the Carven project were of great value in the limited areas surveyed (Biju-Duval *et al.*, 1982, Valery *et al.*, 1985).

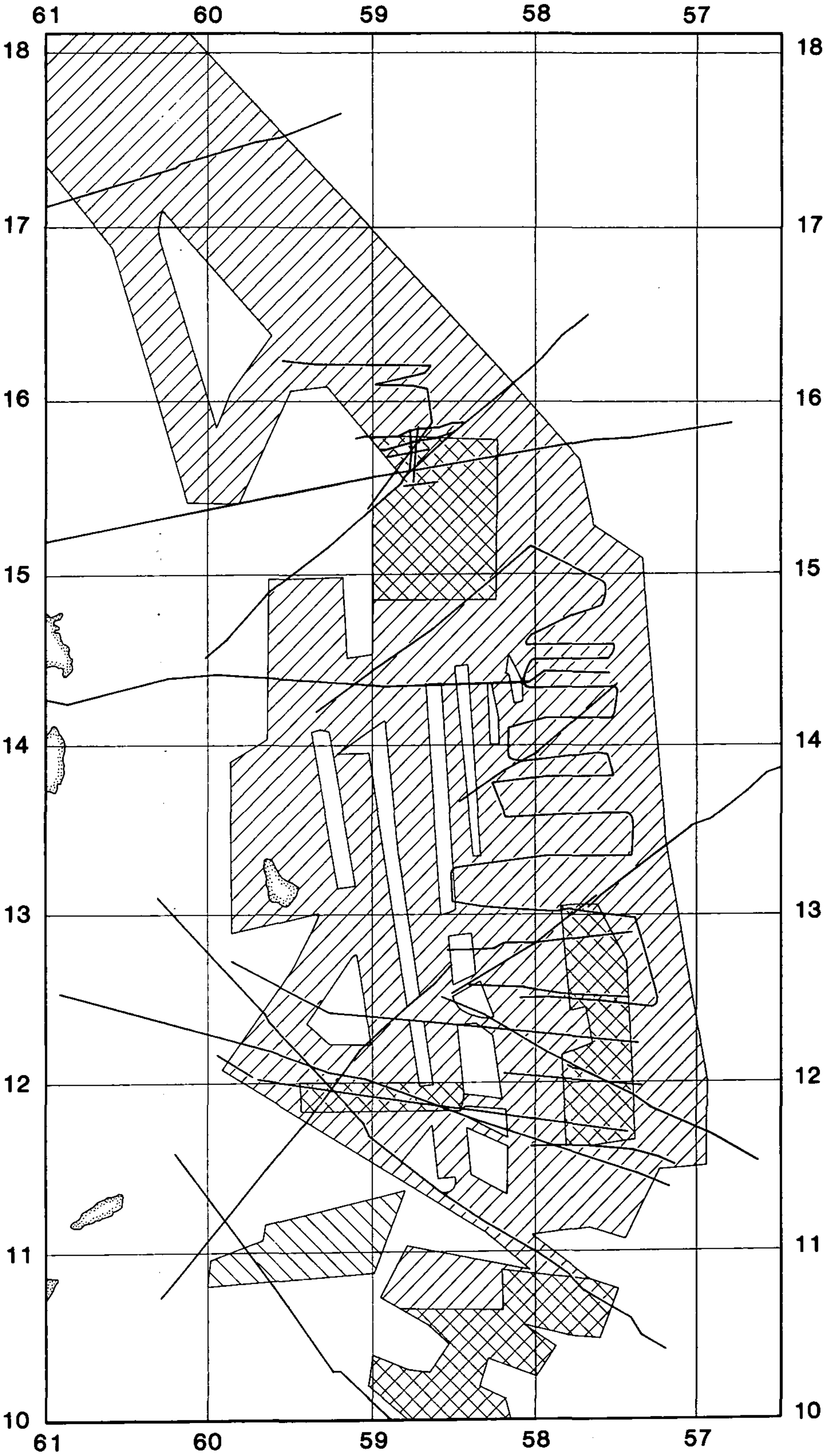

Legend

Multi-channel seismic reflection lines

Gloria side scan sonar coverage

Sea beam coverage

Figure 3 Map showing the coverage of GLORIA and Seabeam data and multichannel seismic reflection sections used in the compilation of the structural map of *Figure 2*

A preliminary stage in the production of the structural map was the construction of a lineament map from the GLORIA data. GLORIA records the intensity of backscattered sound waves from features on the sea floor against the time taken for sound to return to the transducer. The backscatter intensity is enhanced if the sea floor slopes towards the transducer or if it has a small scale surface roughness that may be of a tectonic or sedimentary origin. GLORIA images features that strike roughly parallel to the ship's track more readily than those that are highly oblique to it, and the most detailed information comes from regions of the map where the ship's tracks form a grid pattern. Features appear on the sonographs at a distance from the centre line that is proportional to the travel time of the reflected sound waves, not true distance (*Figure 4*). Features were marked on the sonographs and then their positions were corrected for slant range before transcription onto the lineament map. (These data were recorded in analogue form, and sonographs digitally corrected for slant range were not available.)

The lineament map was interpreted using the structural information gained from the seismic reflection data. Although less able to define smaller structural features, the Seabeam bathymetric data was useful in assessing the true magnitudes of the features imaged by the GLORIA. It was also used in its own right to map more major features. In the southern regions of the map where the wavelengths of the structures are large, individual structures can be traced along strike for great distances and the seismic coverage is sufficient for correlation. Further north, where the structures are less continuous along strike, direct correlation of surface features lying between tracklines with seismic sections is not always possible. Certain features of the sea floor, however, have characteristic forms on the GLORIA sonographs. Ridges, that are commonly formed by anticlines developed on the hanging wall of thrusts, show up as alternating brighter and darker bands on the sonograph (*Figure 5*) as the intensity of backscattering changes with the changes of slope across the images. Sinuous channels in the submarine fan at the foot of the complex (Belderson *et al.*, 1984) can have a similar appearance although their relief is much smaller, presumably because of changes in bottom roughness related to variations in sedimentation, so quantitative measurements of bathymetry, even if only along profiles, are important to the correct interpretation of some features on the sonographs. If there is disruption of the seafloor along fault traces, they may show up as narrow bright bands. Mud volcanoes on the seafloor form very 'bright' features because of the backscattering from the rough surface of erupted material.

Effect of variations in sediment thickness on the subducting Atlantic crust upon the general morphology of complex

The Barbados Ridge complex varies in width (300–80 km) and maximum thickness (20–10 km) from south to north, reflecting the overall northward thinning sediment on the Atlantic oceanic floor. Sediment thickness on the incoming Atlantic oceanic crust decreases from about 7 to 5 km between latitudes 11°N and 12° 20'N (Speed, Westbrook *et al.*, 1984) due to a northward thinning of the turbidites of the submarine fan of the Orinoco. At the base of the sediment sequence a group of horizons of consistent character with high lateral continuity of horizons, interpreted as pelagics, maintain a thickness of approximately 1 km throughout these southern regions. North of 12° 20'N, the oceanic basement ridges have dammed the northerly flowing turbidites causing a reduction in the sedimentary thickness across them. This results in reductions in the rates of accretion across the ridges and pronounced indentations of the outer deformation front. The largest indentation is produced by the Tiburon Rise. North of the Tiburon Rise there are only a few turbidites in the sedimentary sequences.

The overall northward decrease in the elevation of the complex is not uniform. There are a series of northward facing steps in the topography of the complex that lie above the westward extensions of the oceanic basement ridges beneath the complex. These features appear to result from two effects of the ridges (Westbrook, 1982). Due to the indentation of the accretionary front, the complex begins to rise at a position further to the east on the south side of a ridge. Therefore, if the eastward slope of the complex remains constant, for a given longitudinal transect the complex has a higher elevation to the south of a ridge. In addition, the obliquity of convergence of the WNW–ESE trending ridges produces an extra southward directed component of compressional stress that steepens the slope of the complex above the southern flank of the ridges.

The complex undergoes its most pronounced lateral change across the Tiburon Rise (*Figure 2*), both in its topography and width and also in the type of sediments that are accreted to it. For the ease of description of its structural features, the complex can be divided into two regions south and north of the Tiburon Rise.

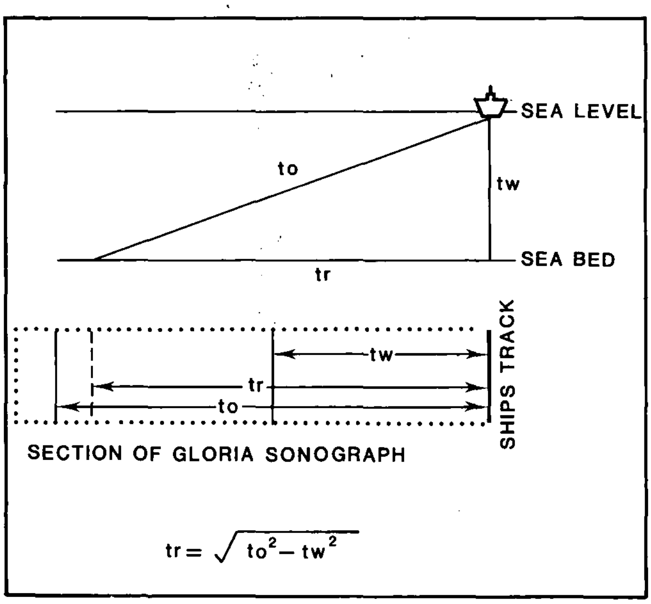

Figure 4 An illustration of the slant-range distortion produced in GLORIA sonographs by the depth of the sea beneath the transducer. This gives a finite offset on the sonograph of the seabed reflection beneath the ship's track. Before plotting, corrections need to be made to features on the sonographs, to give their true range from the ship's track. The simple correction does not take into account the depth of the imaged feature; only depths beneath the ship's track have been used

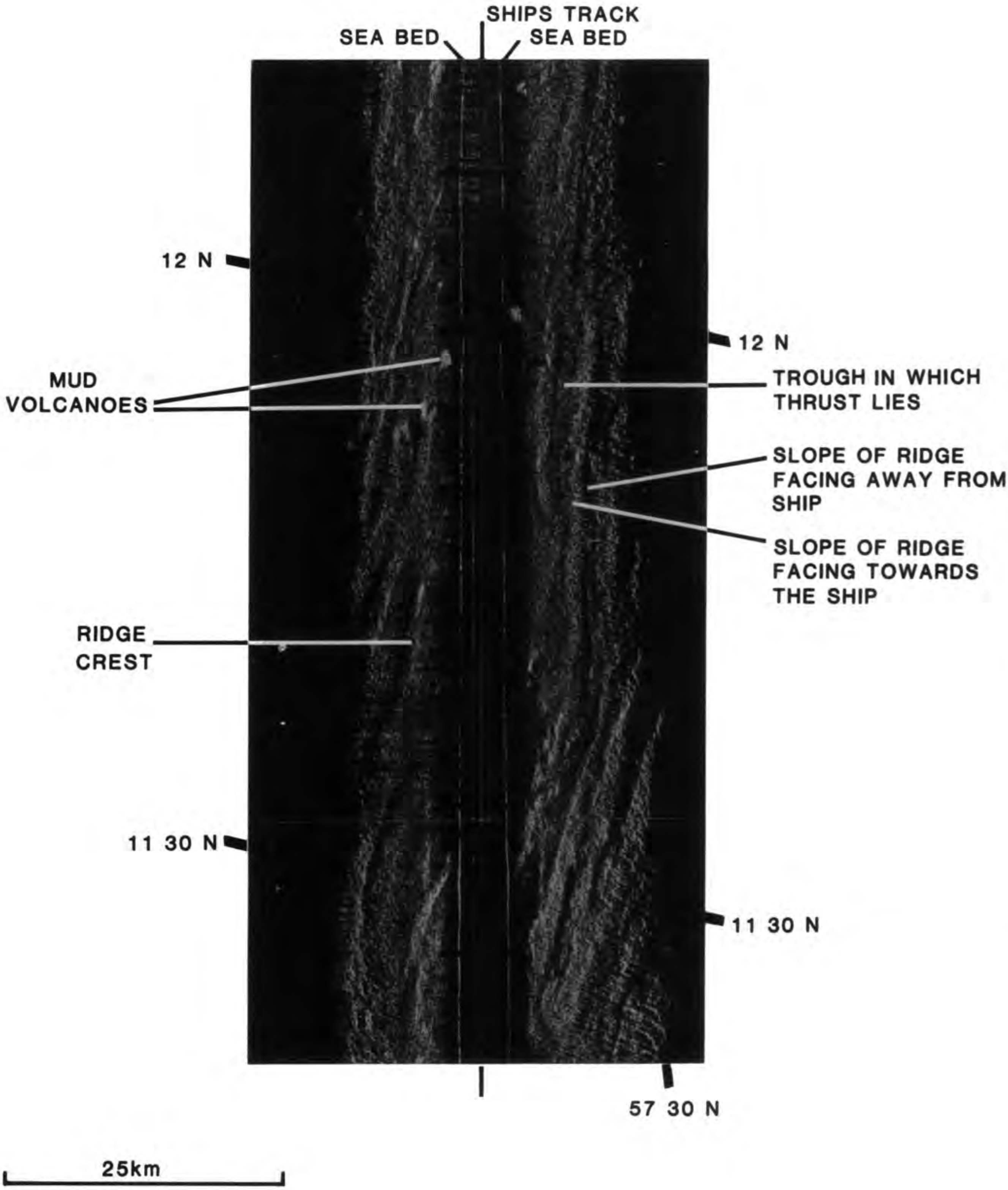

Figure 5 An example of a GLORIA sonograph. The ship's track lies along the centre of the Figure. Either side of it, bilaterally symmetric, the first bright line is the reflection of the seabed beneath the ship's track from the transducers on each side of the towed sonar vehicle. The sonograph was displayed with automatic gain control to equalise the strength of image from weakly and strongly reflecting areas. This process can produce false shadows in front of brightly reflecting features. Features shown on the sonograph include anticlinal ridges, fault traces and mud volcanoes

Variations in structural style of the regions south of the Tiburon Rise

South of latitude 10° 20′N the accretionary complex merges with the undeformed Orinoco Fan sequence that extends across the Southern American continental margin and out onto the Altantic floor (*Figures 1* and *2*). The southern margin of the complex, which lies along the eastward extensions of the dextral transpressive margin (Speed, 1985) between the South American and Caribbean plates, is one of broad transition. It is subject to a component of dextral shear but the tectonics of the region are complicated by the accretionary complex being partly decoupled from both plates. Extensive mud diapirism adds to this complication.

Two large canyons of the Orinoco submarine fan cut across the accretionary complex in this southernmost area. They wind their way down to the front accretionary complex deflected by the ridges formed by the frontal imbricates.

Zone of Initial Accretion

The style of deformation in this zone (*Figures 1* and *2*), south of latitude 12° 20′N, is relatively unaffected by the basement topography of the subducting Atlantic oceanic crust (*Figure 6*), which is covered by thick sediments. The structures of the frontally imbricated section are in the form of gently asymmetric folds with amplitudes of ~ 0.5 km and wavelengths of between 4 and 5 km (*Figure 7a*). The folds, with an eastward vergence, are developed above thrusts which dip westwards at 20° (Westbrook, 1982), rooting into a decollement that lies 1.2–1.7 km beneath the sea floor at the toe of the complex. The relatively long wavelength of the frontal structures is a consequence of the thickness of the deformed layer. The folds form bathymetric ridges, some of which can be traced for over 120 km along strike using GLORIA side-scan sonar (*Figure 5*) and Seabeam bathymetric survey data. Fold amplitudes vary gently along strike. A further feature of the Zone of Initial Accretion in this southern region is the development of slumps resulting from the failure of portions of the steeper, eastward facing slopes of a small number of the ridges formed by the thrust related folds (*Figures 2* and *7a*). These slump deposits form mounds about 1 km wide and 20–50 km long parallel to the foot of the slope.

North of latitude 12° 20′N, the oceanic basement has greater topographic relief with amplitudes of 3–4 km between basement ridge crest and adjacent trough (Westbrook *et al.*, 1984) (*Figure 6*). This produces the following additional features in the frontal regions of the complex; (1) Marked variations in the strike and wavelength of structures occur across the ridges. Thrusts and folds tend to develop very nearly parallel to the deformation front, so the trends of older folds preserve a record of past orientations of the deformation front. (2) Wavelengths of structures vary in proportion to the thickness of the thrust slice. The spacing of the thrusts is usually three times the thickness. Consequently, thrusts are widely spaced opposite troughs, where the sediment is thicker and the level of decollement is usually deeper, and closely spaced opposite ridges. (3) The number of oblique or crossfaults greatly increases in the region of the basement ridges. They form discontinuities that have westerly to northwesterly trends across the frontal region of the complex where they are present in large numbers. Many are probably oblique-slip transpressional faults resulting from the continued deformation of the complex by the basement ridges. (4) Several slumps, or debris flows, occur in the area of impinging ridges. The slump occurring off the northward facing slope of the accretionary complex, where the Tiburon Rise impinges on the complex, covers an area of some 100 km. The slope of the complex here is at its steepest. Further south at latitude 14° 20′N, another debris flow appears to be associated with a mud volcano. The large area of sea floor with hummocky topography in front of the complex at latitude 13°N appears to be a slump that has been subsequently obscured by later sedimentation. Seismic sections show that it is ~ 160 m thick at the foot of the slope of the complex.

In the south, the decollement beneath the frontal imbricate structure initially lies within the turbidites sequence so that the lower part of the turbidite and all the pelagic section passes, undeformed, beneath the leading edge of the accretionary complex. Further to the north around latitudes 13°–14°N, where sediments are thinner, subcretion of turbidites beneath the frontal imbricate section can be seen to occur by means of the formation of duplexes (Westbrook and Smith, 1983; Westbrook and Smith, 1984; Brown and Westbrook, 1986).

There are considerable numbers of mud diapirs in the Barbados Ridge accretionary complex (Stride *et al.*, 1982). It is proposed that the mud volcanism has its source in the subcreted section and is one of the processes that allow these regions to dewater.

Zone of Stabilization

This lies to the West of the Zone of Initial Accretion and is characterised by an undulating plateau region (*Figures 1* and *2*). In the south, its earlier structural fabric is masked by slope-sediment cover that increases in thickness westwards (*Figure 6*). The slope-sediments overlie the accreted sediments and are not so strongly deformed. They are deformed by widely-spaced faults and folds, and sedimentation has accompanied deformation so that sequences commonly change thickness across faults and show progressive local thickening in synclinal troughs with offlap and subsequent overstep on the flanks of growing anticlines. In the north, the slope sediments are thin and many of the deformational features associated with accretion are still visible. The style of the recent phase of deformation of the Zone of Stabilization is most clearly displayed in the south where it deforms the slope sediments. Similar deformational features may occur in the north, but it is hard to distinguish them from earlier features.

Mud volcanoes are amongst the most prominent features observed on GLORIA sonographs in the Zone of Stabilization. They form brightly reflecting patches on the seafloor. The brightness derives from bottom roughness that, by analogy with mud islands near Trinidad (Higgins and Saunders, 1967), is caused by blocks extruded from the volcano. The mud volcanoes are concentrated in the areas where the current phase

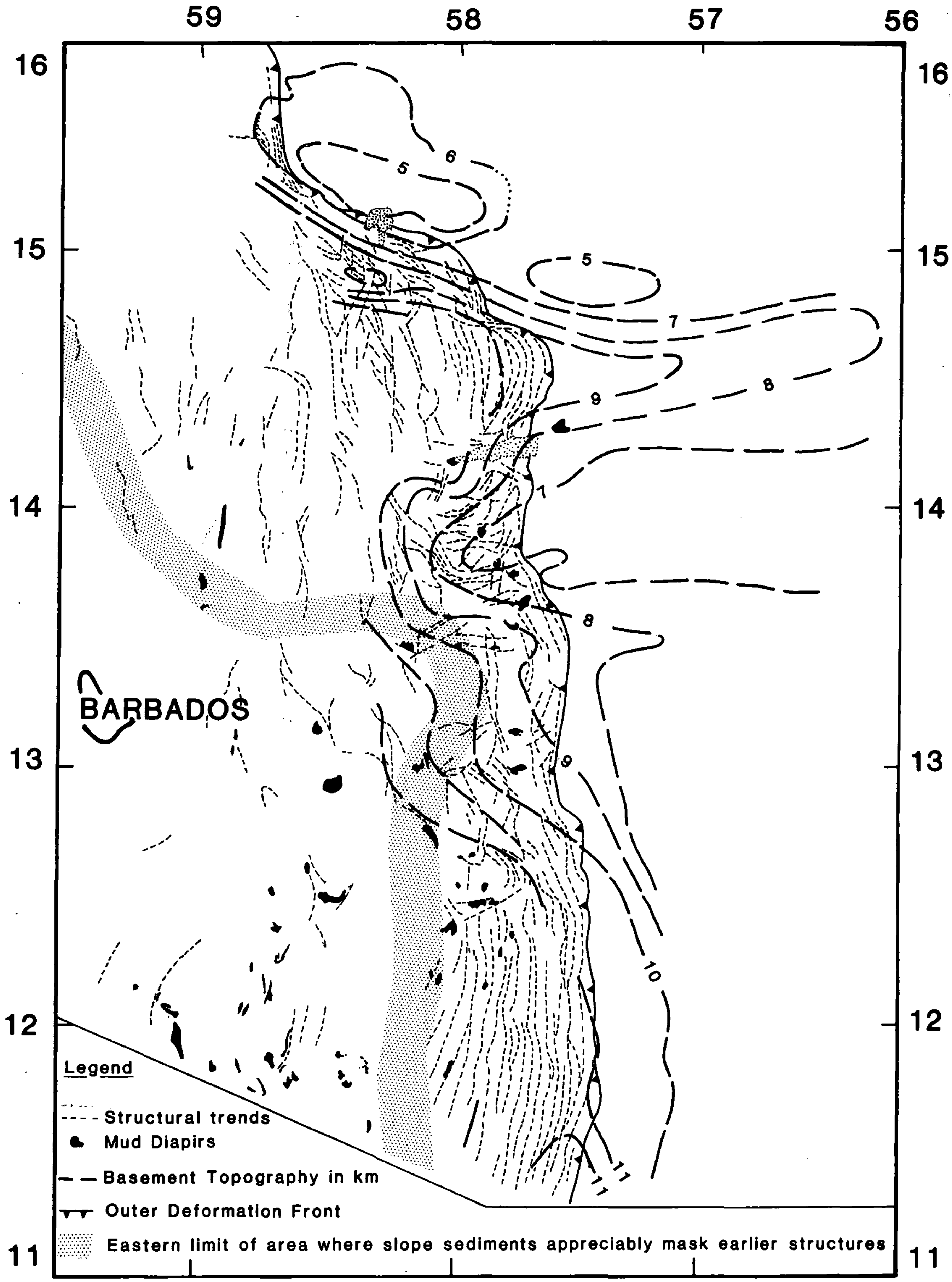

Figure 6 Map showing the relationship between the principal structural trends of the accretionary complex and the topography of the oceanic igneous basement beneath the complex. (The basement topography is from Westbrook *et al.*, 1984). Also shown is the diffuse boundary of the region where the slope sediments obscure the structures formed during the accretion of sediment

of deformation is most intense and some are interpreted, on seismic evidence, as having intruded up reverse faults (*Figure 5b*) (Biju-Duval *et al.*, 1982). The recent phase of deformation is thought to have begun in Pliocene times (Hill, 1983) and is characterized by reverse faults and associated folds that verge both to the east and west, deforming the slope sediments quite strongly in places (*Figure 7b*). The deformation becomes locally more intense westwards, towards the Zone of Supra-complex Basins. The reverse faults have similar trends to the frontal imbricate faults. Two sets of oblique structures with NW–SE and NE–SW orientations are also developed (*Figure 2*). Biju-Duval *et al.*, 1982) mapped one NW–SE trending feature using Seabeam and proposed that it was a transcurrent fault on finding that reverse faults terminated at it. These oblique faults also have mud diapirs situated on them.

Zone of Supra-complex Basins

This zone lies to the west of the Zone of Stabilization. It appears that before the present phase of deformation, the southern regions of the complex were dominated by a single very large basin which subsided relative to the Zone of Stabilization and Barbados Ridge Uplift (*Figure 1*), but which is now divided into sub-basins by the tectonic uplift and deformation of sediments to form intervening ridges. At present, it is filled with ~ 2–3 km of sediment (Speed, Westbrook and others, 1984). The Barbados Trough is its largest sub-basin. The eastern margin of the earlier basin is currently being deformed by predominantly westward verging thrusts. The thrusts have a horizontal spacing of approximately 10–15 km (*Figure 2*) and their associated folds form ridges that rise 500–600 m above the troughs. Some of the troughs are synclines that are tightening as the present phase of deformation proceeds. They contain a syntectonic sedimentary infilling of turbidites and slump deposits, the latter having originated from their over-steepened margins (Biju-Duval *et al.*, 1982; Valery *et al.*, 1985).

Considerable numbers of mud diapirs are concentrated along the ridge crests and thrust faults. GLORIA sonographs show that some of the shale diapirs are up to 17 km long and 1 km wide. From the number and size of the diapirs associated with the ridges, it would appear that large portions of some of them may be of diapiric material.

Barbados Ridge Uplift

This is the most westerly structural zone of the Barbados Ridge accretionary complex (*Figure 1*). The central part of the ridge has been uplifted by at least 3 km relative to the Tobago Trough which lies on its western margin (Westbrook *et al.*, 1984). The uplift is currently greatest in its central regions and dies away to the north and south. The inner deformation front is the western limit of the accretionary complex, which has accreted forearc basin sediments through a series of westward vergent thrust and folds and is currently deforming the sediments of the Tobago forearc basin, except in the area south of 12°N.

The Barbados Ridge Uplift rises above sea level to form the island of Barbados, on which the accreted terrigenous sediments of the complex are exposed as the Eocene Scotland Formation. This is tectonically overlain by the Eocene to Miocene pelagic rocks of the Oceanic Formation, Bissex Hill Formation and Consett Marl, which have been interpreted to be part of the forearc basin or slope cover sequence (Speed and Larue, 1982). Larue and Speed (1984) suggest that the basal complex was probably accreted in uppermost Eocene times and that in late Oligocene times the Oceanic Formation underwent eastward transport as thrust nappes to be juxtaposed in its present position.

The ridge crest is generally covered by Plio-Pleistocene sediments except in areas where these have been eroded. These areas of outcropping older terrigenous or pelagic rocks correspond, in general, to areas of rough brightly reflecting seafloor on GLORIA sonographs.

Few mud diapirs have been positively identified on the Barbados Ridge Uplift except on its eastern flank. However, mud diapirs have been identified on the island of Barbados, as intrusions into the Basal Complex and Oceanic Formation (Larue and Speed, 1984; Torrini *et al.*, 1985). To the north of 12° 20′N a number of canyons and slumps occur on the eastern side of the uplift.

Variations in structural style of the regions north of the Tiburon Rise

North of the Tiburon Rise, very little turbiditic deposition has occurred on the Atlantic ocean floor and the Zone of Supra-complex Basins and the Barbados Ridge Uplift die out. There is also little or no mud diapirism in the complex. Near the crest of the Tiburon Rise, where DSDP sites 541 and 542 were drilled into the leading edge of the complex, an approximately 200 m thick veneer of predominantly hemipelagic section is frontally accreted (Moore and Biju-Duval, 1984). The wavelength of accretionary structures as revealed on GLORIA is correspondingly short, being between 0.5 and 1 km (*Figure 2*). Individual ridges can be followed along strike for up to 12 km and are approximately 10 m high within the vicinity of the DSDP site (Belderson *et al.*, 1984). Seismic reflection sections reveal that the pelagic section is under thrust horizontally without being stripped from the oceanic basement, at least 70 km beneath the accretionary complex in the region between the Tiburon and Barracuda ridges (Westbrook *et al.*, 1982).

Further westwards and to the North of latitude 16° 20′N, the structural grain increases in wavelength to ~ 2 km, reflecting an increase in the thickness of section offscraped in the frontal imbricates (*Figure 2*). The wavelengths of structures vary only a small amount on either side of the basement ridges. Apparently there are only slight variations in the thickness of the frontally accreted layer either side of the ridges in this northern area. The ridges, however, do cause variations in the strike of the structural grain of the complex. The Barracuda Ridge impinges on the accretionary complex at latitude 17°N and results in the imposition of a major discontinuity on the complex. The discontinuity is mostly inactive west of the Zone of

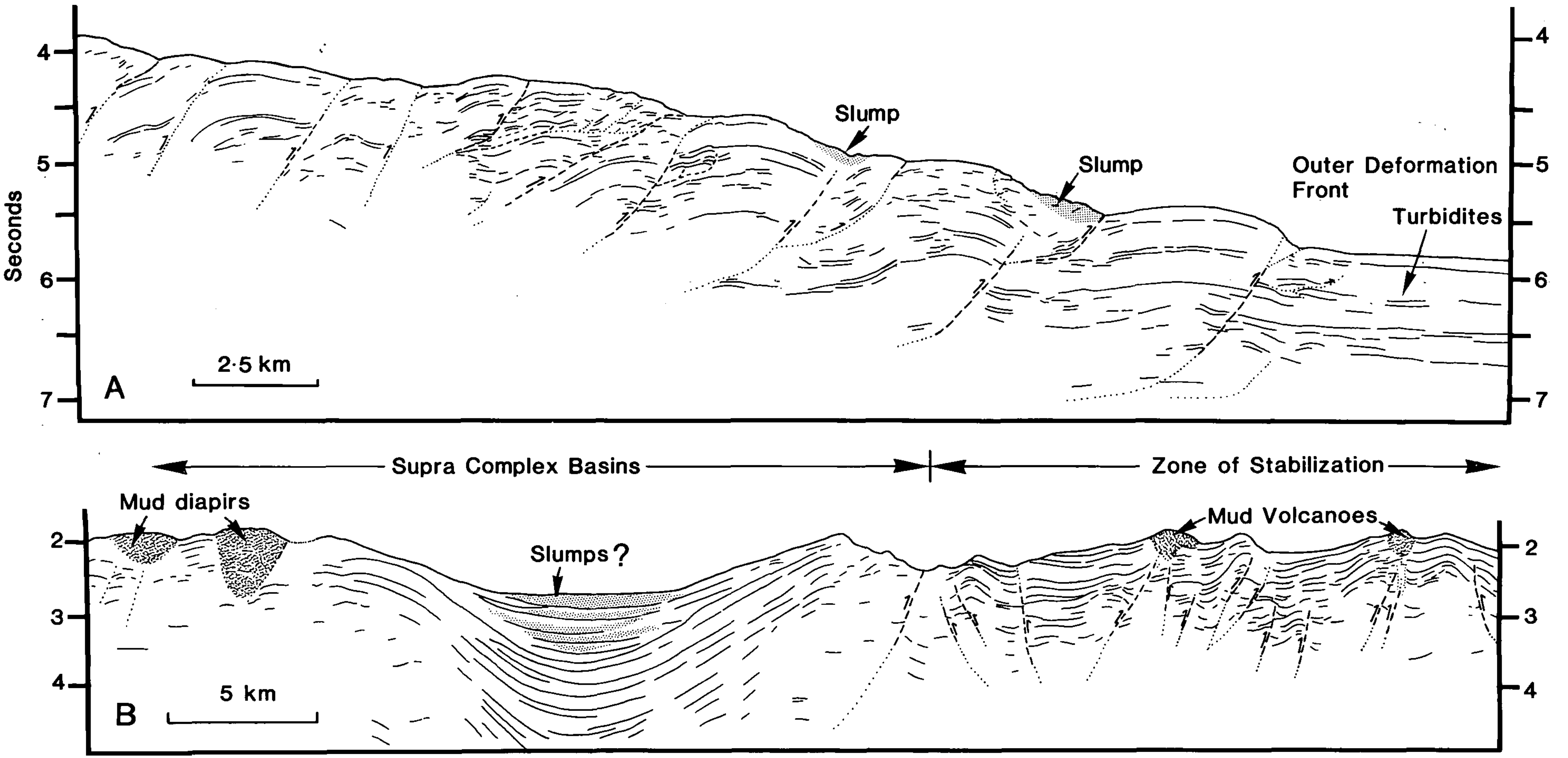

Figure 7 Line drawings of two seismic sections illustrating some of the characteristic features of the southern part of the complex. The positions of the two sections are shown in *Figure 1*. They come from a multichannel seismic reflection line shown in Biju-Duval *et al.* (1982)

Section A shows the front of the complex with its seaward verging thrusts and associated ridge-forming anticlines. The steeper seaward slopes of some of the anticlinal ridges has become unstable slumping into the troughs below.

Section B shows the transitional region between the Zone of Stabilization and the Zone of Supra-complex Basins, where the slope cover has been deformed during sedimentation. Some landward verging structures are present and mud diapirism is prevalent.

Initial Accretion. The trend of the deformation front and resulting structures progressively swings to NW–SE orientation, becoming more oblique to the convergence direction as the Puerto Rico Trench is approached.

Summary

The map of the Barbados Ridge accretionary complex represents a large body of geological and geophysical data in a condensed format. In the overview presented by the map, several major aspects of the structure are apparent, of which the following appear to be the most significant:

(1) There is an east–west change in the dominant direction of vergence of currently active structures across the southern areas of the complex. Thrust vergence changes from being to the east at the outer deformation front, to being both to the east and to the west in central regions of the complex and then finally to the west in the western regions of the complex. Through time in the development of the complex a body of material may move from one region to another.

(2) As a result of the interaction of basement ridges associated with fracture zones and the pattern of sedimentation, the complex undergoes marked north to south changes in strike, type of sediment accreted and style of structures developed at its front. In the south, where the oceanic basement is deeper, structures are broader and show much greater continuity along strike. In particular, a series of E–W to NW–SE trending discontinuities are imposed on the complex by the ridges.

(3) Mud diapirism only occurs, in the regions of the complex south of the Tiburon Rise, where rapidly sedimented terrigenous sediments have been accreted. The abundance of mud volcanoes and diapirs increases towards the south in concert with the increasing thickness of the Orinoco submarine fan.

(4) There are a number of slumps developed in different parts of the complex. In the south they are mostly associated with the failure of the steep slopes of the folds associated with the frontal thrusts and with the oversteepening of the margins of the slope basins, although one large slide has slipped from the frontal slope of the complex onto the ocean floor. In the north slumps have tended to occur in areas affected by the impinging ridges. Where discernible, thicknesses of slumps are less than two hundred metres.

Acknowledgements

Most of the GLORIA data and some of the multichannel data were collected on Cruise 109 of RRS Discovery in 1980 for which A.H. Stride was principal scientist. R.H. Belderson and N.H. Kenyon of the Institute of Oceanographic Sciences gave valuable assistance in discussion of the initial interpretation of the GLORIA sonographs and in providing preliminary plots of the data made during the cruise. They also provided sonographs collected from a cruise of the M.T. Farnella, 1982, in the south of Barbados Ridge Complex. Copies of multichannel seismic reflection sections obtained by the Comité d'Études Petrolières Marines were provided by B. Biju-Duval and A. Mascle of the Institut Français du Petrole, and P. Valery of the Societé Nationale Elf Aquitaine. Some of these sections were part of the data set used in compiling seismic maps for the Ocean Margin Drilling Project Atlas 10 (Speed, Westbrook and others, 1984). Copies of seismic sections from Shell International also used in that compilation, were kindly made available by P. Lehner. M.J. Smith carried out most of the processing of the multichannel seismic data collected on Discovery Cruise 109. An earlier version of part of the map in the region of Barbados was originally compiled by A.J. Hill (1983). Seabeam bathymetry from Cruise RC2603 of the Robert D. Conrad, which is incorporated in the bathymetry of *Figure 2*, is included with permission of M.G. Langseth. C. Burness drafted the final version of the map.

Data collection and seismic processing was supported by NERC research grant GR3/3551. K.M. Brown is grateful for the support of a NERC research studentship.

References

Belderson, R.H., Kenyon, N.H. and Stride, A.H. (1984) Morphology and structural trends of the Barbados Ridge complex in the vicinity of Deep Sea Drilling Project Sites 541, 542 and 543 as revealed by GLORIA long-range side-scan sonar, in: Biju-Duval, B., Moore, J.C., *et al.*, *Initial Rep. Deep Sea Drill. Proj.* **78A**: Washington (U.S. Government Printing Office)

Belderson, R.H., Kenyon, N.H., Stride, A.H. and Pelton, C.D. (1984) A 'braided' distributary system on the Orinoco deep sea fan, *Marine Geology* **56**, 195–206

Biju-Duval, B., Le Quellec, P., Mascle, A., Renard, V. and Valery, P. (1982) Multibeam bathymetric survey and high resolution seismic investigation of the Barbados Ridge Complex (Eastern Caribbean): A key to the knowledge and interpretation of an accretionary wedge, *Tectonophysics* **86**, 275–304

Higgins, G.E. and Saunders, J.B. (1976) Report on the 1964 Chatham Mud Island, Erin Bay, Trinidad, West Indies, *Bull. Am. Assoc. Petrol. Geol.* **58**, 55–64

Hill, A.J. (1983) *The evolution of forearc basins on and behind the Barbados accretionary complex:* MSc unpublished

Ladd, J.W. (1984a) Seismic Section G–G, in: (Eds. Speed, R.C., Westbrook, G. K. *et al.*) *Lesser Antilles arc and adjacent terranes*, Atlas 10, Ocean Margin Drilling Program, Regional Atlas Series: Marine Science International, Woods Hole MA, Sheets 19–22

Ladd, J.W. (1984b) Bathymetry, in: (Eds. Speed, R.C., Westbrook, G.K. *et al.*) *Lesser Antilles arc and adjacent terranes*, Atlas 10, Ocean Margin Drilling Program, Regional Atlas Series: Marine Science International, Woods Hole, MA, Sheet 1

Larue, D.K. and Speed, R.C. (1984) Structure of the accretionary complex of Barbados, II *Geol. Soc. Am. Bull.* **95**, 1360-1372

Laughton, A.S. (1981) The first decade of GLORIA. *J. Geophys. Res.* **86**, 11511–11534

Minster, J.B. and Jordan, T.H. (1978) Present-day plate motions. *J. Geophys. Res.* **83**, 5331–5354

Moore, J.C. and Biju-Duval, B. (1984) Tectonic synthesis, Deep Sea Drilling Project leg 78A: Structural evolution of offscraped and underthrust sediment, northern Barbados Ridge Complex, in: Biju-Duval, B., Moore, J.C., *et al.*, *Initial Rep. Deep Sea Drill. Proj.* 78A: Washington (U.S. Government Printing Office)

Speed, R.C. and Larue, D.K. (1982) Barbados: Architecture and implications for accretion *J. Geophys. Res.* **87**, 3633–3643

Speed, R.C., Westbrook, G.K., *et al.* (1984) *Lesser Antilles Arc and adjacent terranes,* Atlas 10, Ocean Margin Drilling Program, Regional Atlas Series: Marine Science International, Woods Hole, MA, 27 sheets

Stride, A.H., Belderson, R.H. and Kenyon, N.H. (1982) Structural grain, mud volcanoes and other features on the Barbados Ridge Complex revealed by GLORIA long-range side-scan sonar. *Marine Geol.* **49**, 187–196

Sykes, R., McCann, W.R. and Kafka, A.L. (1982) Motions of Caribbean plate during last 7 million years and implications for earlier Cenozoic movements. *J. Geophys. Res.* **87**, 10656–10676

Torrini, R., Speed, R.C. and Mattioli, G.S. (1985) Tectonic relationships between forearc-basin strata and the accretionary complex at Bath, Barbados. *Geol. Soc. Am. Bull.* **96**, 861–874

Valery, P., Nely, G., Mascle, A., Biju-Duval, B., Le Quellec, P. and Berthon, J.L. (1985) Structure et croissance d'une prisme d'accretion tectonique proche d'un continent: la Ride de la Barbade au sud de l'arc Antillais, in: *Geodynamique des Caraibes.* Symposium Paris 5–8 Fevrier 1985. (Ed. Mascle, A.) Editions Technip, 27 Rue Ginoux, 75015 Paris, p. 173–186

Westbrook, G.K. (1982) The Barbados Ridge Complex: Tectonics of a mature forearc system, in: (Ed. Legget, J.K.) *Trench and forearc geology: Sedimentation and tectonics in ancient and modern active plate margins.* Geol. Soc. London Special Pub. 10, p. 275–290

Westbrook, G.K., Smith, M.J., Peacock, J.H. and Poulter, M.J. (1982) Extensive underthrusting of undeformed sediment beneath the accretionary complex of the Lesser Antilles Subduction Zone *Nature* **300**, 625–628

Westbrook, G.K. and Smith, M.J. (1983) Long decollements and mud volcanoes: evidence from the Barbados Ridge Complex for the role of high porewater pressures in the development of an accretionary complex, *Geology* **11**, 279–283

Westbrook, G.K. and Smith, M.J. (1984) Migrated seismic sections across edge of accretionary complex, in: (Eds. Speed, R.C., Westbrook, G.K., *et al.*) *Lesser Antilles arc and adjacent terranes*, Atlas 10, Ocean Margin Drilling Program, Regional Atlas Series. Marine Science International, Woods Hole, MA, USA

Westbrook, G.K., Mascle, A. and Biju-Duval, B. (1984) Geophysics and the structure of the Lesser Antilles Forearc, in: Biju-Duval, B., Moore, J.C., *et al.* Initial Reports of the Deep Sea Drilling Project **78A**: Washington (U.S. Government Printing Office)

Mineralogical analysis and the evaluation of the petrophysical parameter V_{shale} for reservoir description

Andrew Hurst
Statoil, Forus, Postboks 300, 4001 Stavanger, Norway
Received 6 September 1986

Water saturation in otherwise hydrocarbon-saturated sandstones is closely related to the sandstone's clay mineralogy. Laboratory analysis of the clay mineralogy of three sandstones, containing kaolinite, chlorite and illite, is used to provide the basis for deciding which logs are most suitable for evaluating clay mineral content and distribution (V_{shale}). The gamma log, which is held traditionally to be a reliable 'shale' log, proves to be a poor indicator of shaliness (i.e. clay mineral content) in all three examples. Microresistivity (MSFL) logs, and in some instances neutron porosity logs, give the most realistic correlations with the actual clay mineralogy. Standard values for clay mineral properties which are often used in the petrophysical characterization of sandstones are thought to be unreliable especially when not used in conjunction with textural data from petrographic studies.

Keywords: Water saturation; Clay mineralogy; Wireline logs

Introduction

Discovery of large hydrocarbon accumulations in geographically remote areas, or deep offshore waters, and also in reservoirs with low permeabilities and high water saturations, has made necessary the investment of considerable resources for description of reservoir characteristics prior to the start of production. These resources often include extensive coring and the running of large (relative to many onshore operations) suites of wireline logs. Geologists working on the characterization of sandstone reservoirs are required to produce sedimentological and mineralogical data which are used to define reservoir zones (Johnson and Stewart 1985; Hurst and Archer 1986 a) and to enhance petrophysical evaluations (Hurst and Archer 1986 b). Despite the increasing range of measurements possible with wireline logs, none of the fundamental reservoir characteristics, porosity (ϕ), permeability (K) or water saturation (S_w), can be measured directly.

Deep resistivity measurements made with wireline logs in the uninvaded volumes of hydrocarbon-saturated reservoirs are affected by the presence of conductive pore fluids associated with mineral surfaces. Evaluation of the water saturation (S_w) of the uninvaded reservoir may be accomplished by estimating the volume of 'shale' (V_{shale}) present, where a general relationship is often implied between the clay mineralogy and the water saturation (S_w) (Juhasz 1979, Frost and Fertl 1981).

Evaluation of water saturation (S_w) is vital to volume calculations as:

$$\phi_t = (S_{HC} + S_w)\,\phi_t$$

where ϕ_t = total porosity and S_{HC} = hydrocarbon saturation. Equally important is the role of water saturation with respect to the physical properties of sandstone reservoirs, for example, with respect to framework stability when water, or other fluids, are injected. Overestimation of V_{shale} results in an underestimation of S_{HC}.

0264–8172/87/01068–10 $03.00

Water saturation and V_{shale}

Although water saturation of core samples can be measured in the laboratory, such measurements are problematic. The retrieval of samples from the subsurface and preparation of those samples for analysis inevitably changes their physical properties. Different analytical methods invariably give different results for the same formation, and the same method of analysis is often imprecise (Burck 1983). Additionally, laboratory conditions rarely approach the *in situ* reservoir conditions. In a recent review, Worthington (1985) concluded that in general, saturation profiles currently must be evaluated from wireline logs which, at least, are measurements made of reservoir characteristics in the sub-surface.

Water remains bound to the surfaces of some, or all grains in otherwise hydrocarbon saturated sandstones. Clay minerals have high surface area:mass ratios (*Table 1*) and are commonly the main water-binding components of sandstones. Surface-bound water has electrolytic properties inherited from the formation water displaced during hydrocarbon emplacement, and modified by chemical equilibration with the grains with which it is in contact.

Traditionally, geologists have distinguished between sandstones and shales using the gamma log, which has been demonstrated to be a reliable indicator of grain size variation and useful for sub-surface facies analysis (Selley 1976). Because of the simplistic relationships — low gamma ray response interpreted as sandstone, high gamma ray response interpreted as shale — the gamma log has been routinely employed to evaluate the 'shale' content of sandstones (*Figure 1*). Implicit in this use of the gamma log is that the shale present in sandstones has the same natural gamma radioactivity, and thus the same clay mineralogy, as the true shale lithology chosen to represent the value of 100% shale. In the Norwegian North Sea it is not common practise to apply any single log to evaluate V_{shale} but rather, to use a variety of logs (e.g. Frost and Fertl 1980), usually


A


B


C

a b

A

B

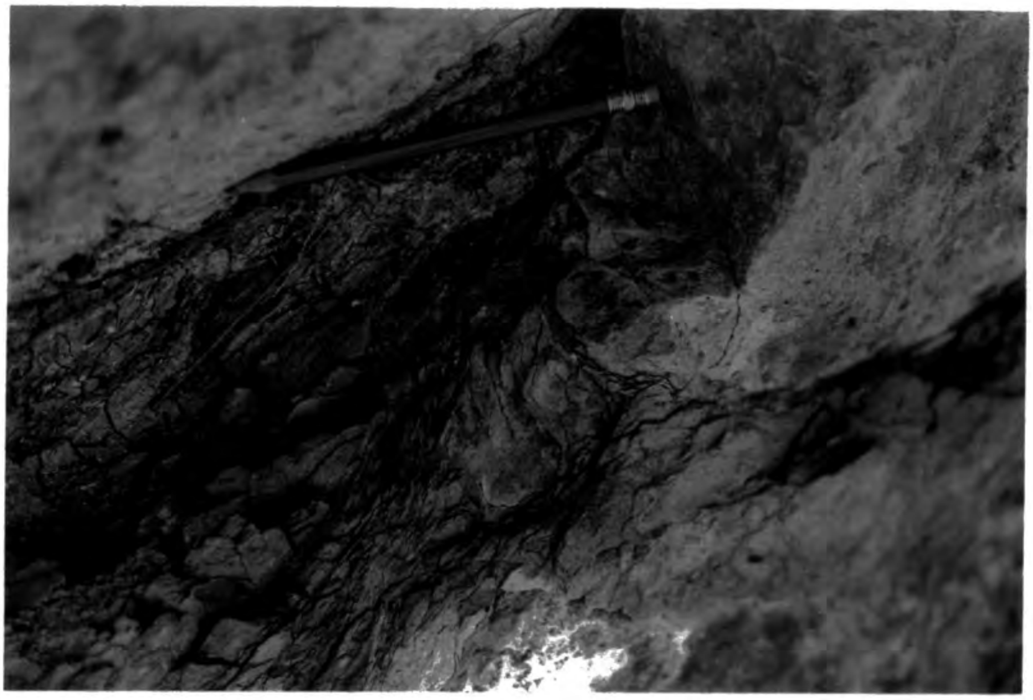

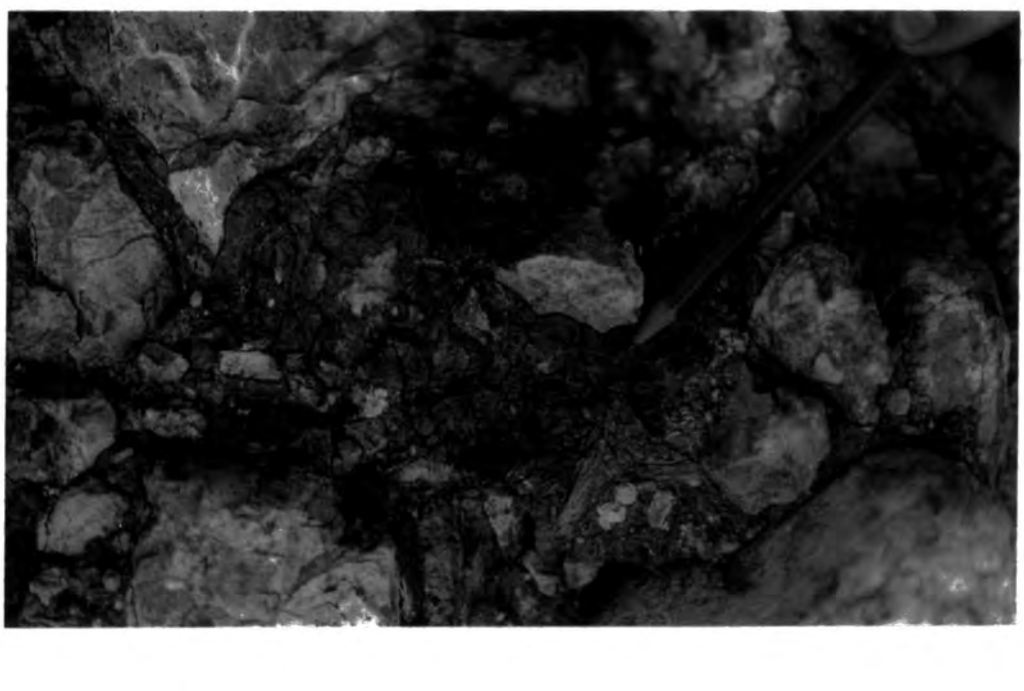

A

B

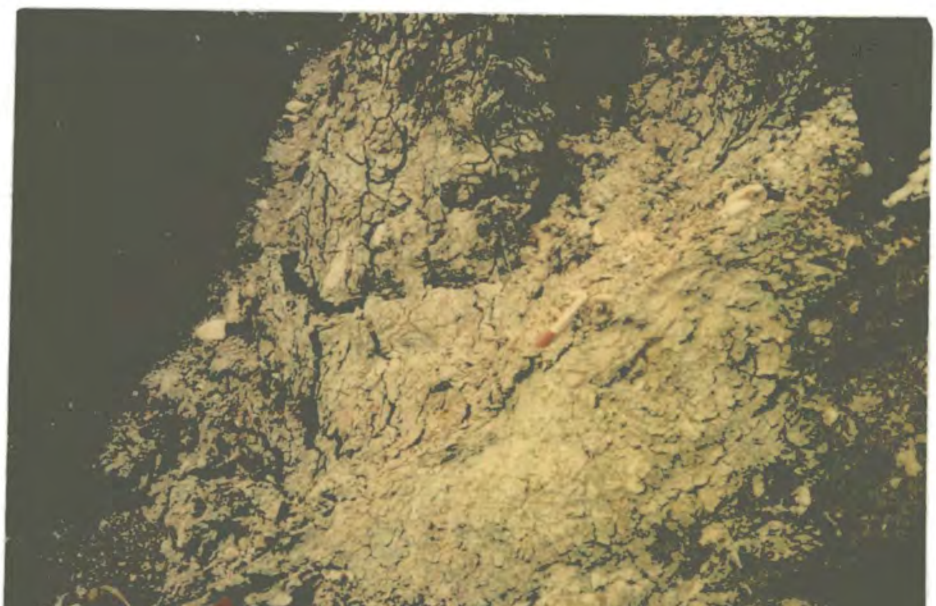

C

A

B

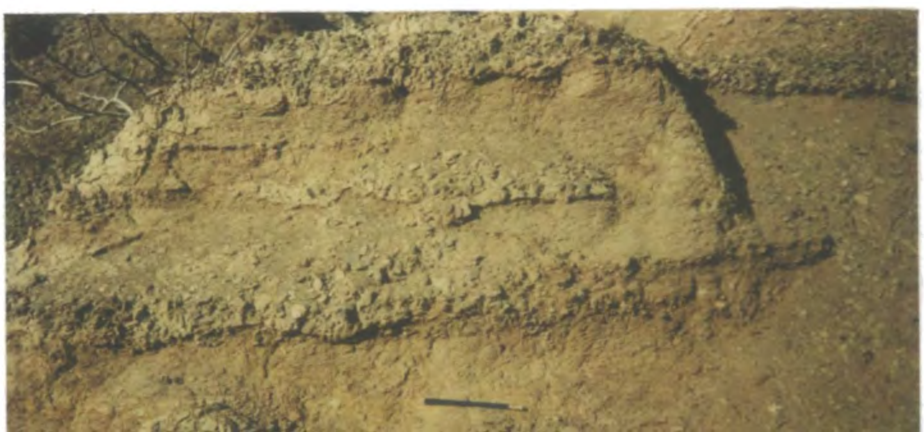

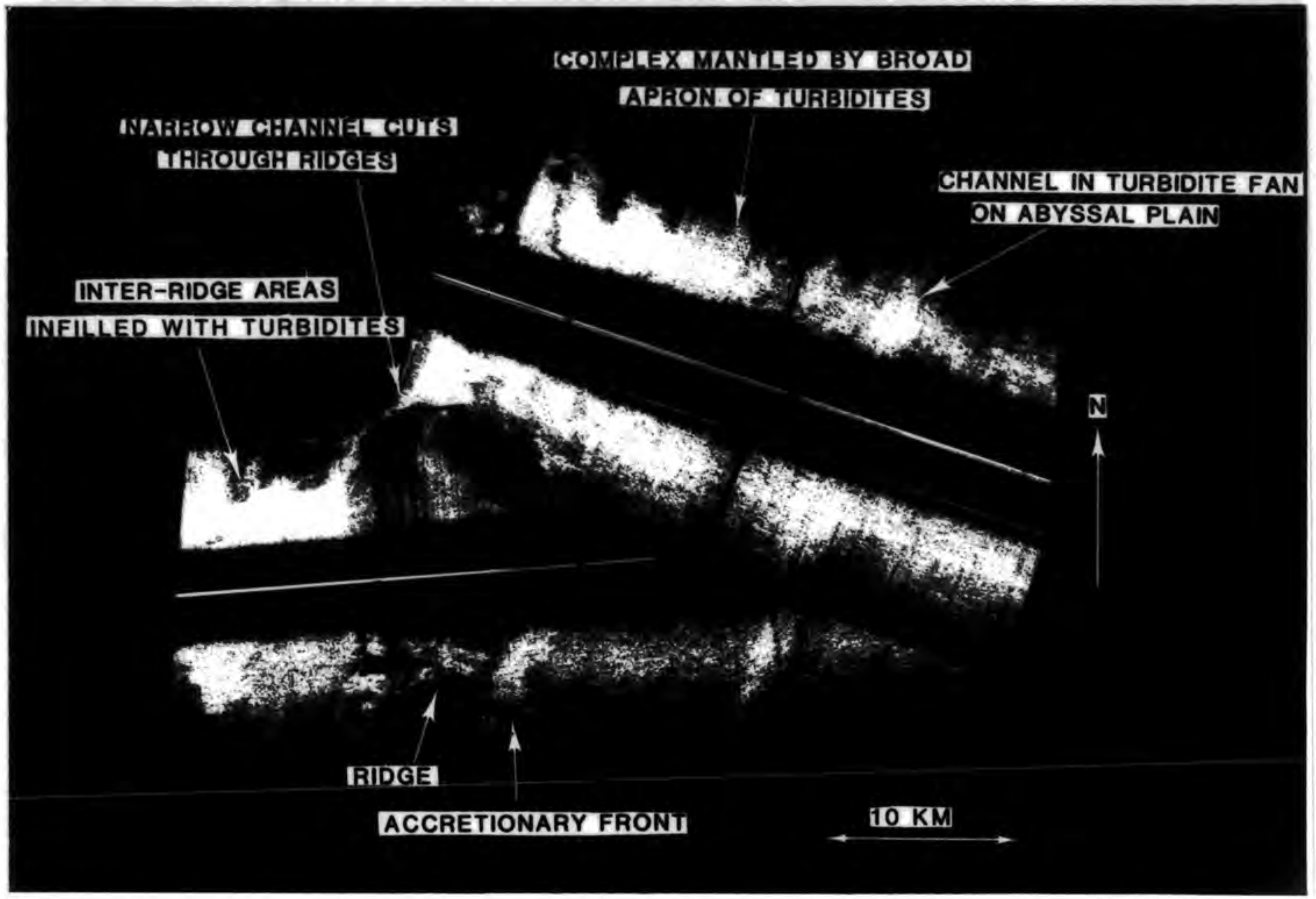
COMPLEX MANTLED BY BROAD
APRON OF TURBIDITES
NARROW CHANNEL CUTS
THROUGH RIDGES
CHANNEL IN TURBIDITE FAN
ON ABYSSAL PLAIN
INTER-RIDGE AREAS
INFILLED WITH TURBIDITES
N
RIDGE
ACCRETIONARY FRONT
10 KM

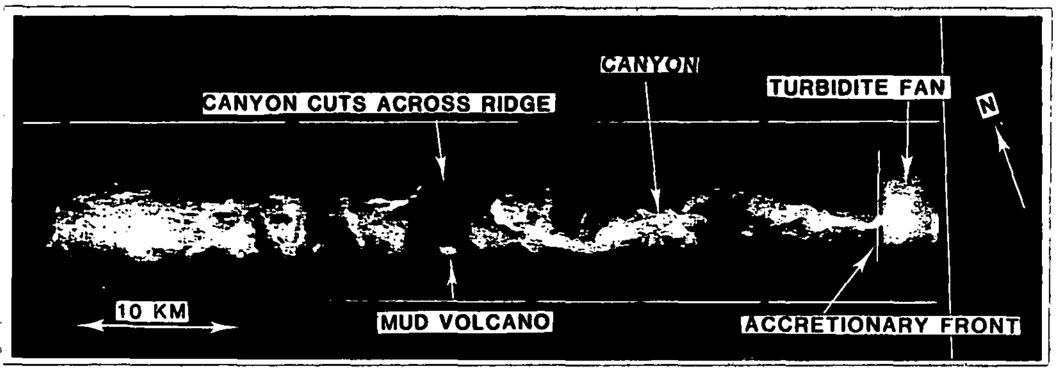
CANYON
TURBIDITE FAN
CANYON CUTS ACROSS RIDGE
N
10 KM
MUD VOLCANO
ACCRETIONARY FRONT

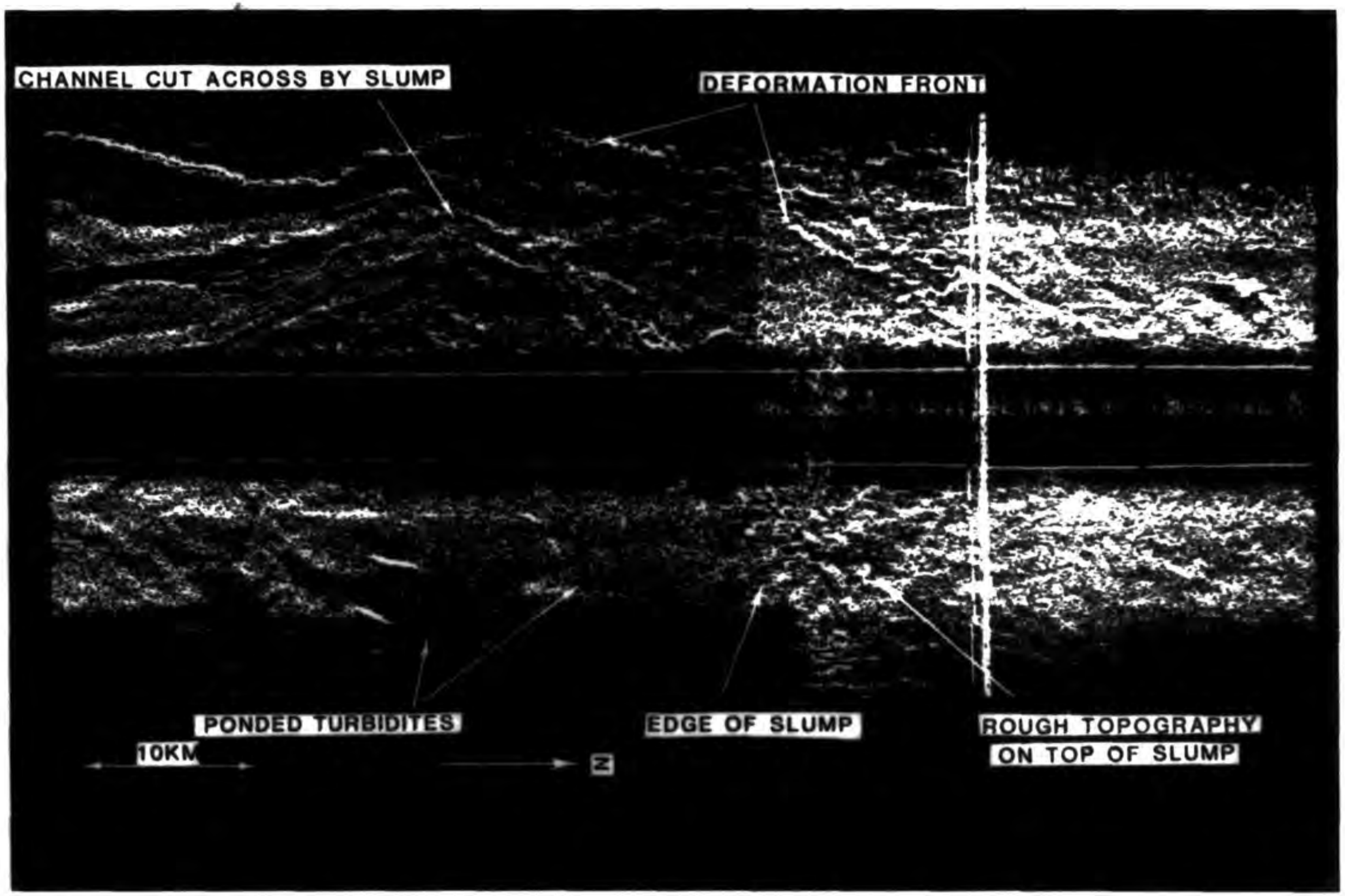
CHANNEL CUT ACROSS BY SLUMP
DEFORMATION FRONT
PONDED TURBIDITES
EDGE OF SLUMP
ROUGH TOPOGRAPHY
ON TOP OF SLUMP
10KM
N

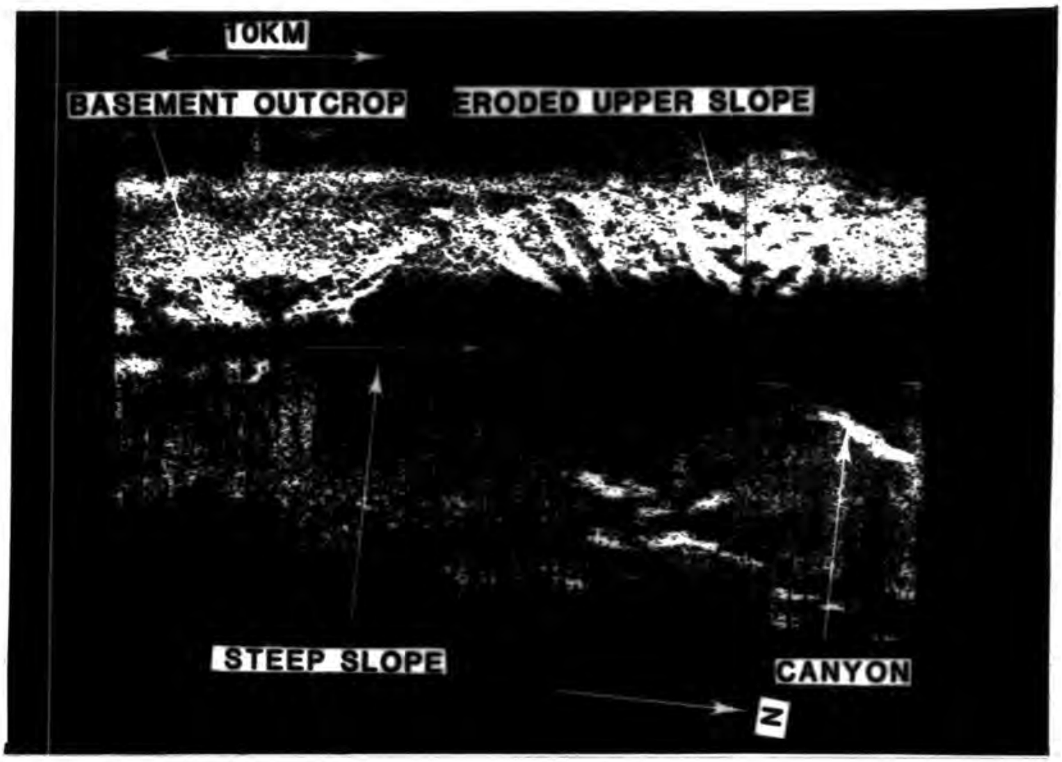
10KM
BASEMENT OUTCROP
ERODED UPPER SLOPE
STEEP SLOPE
CANYON
N

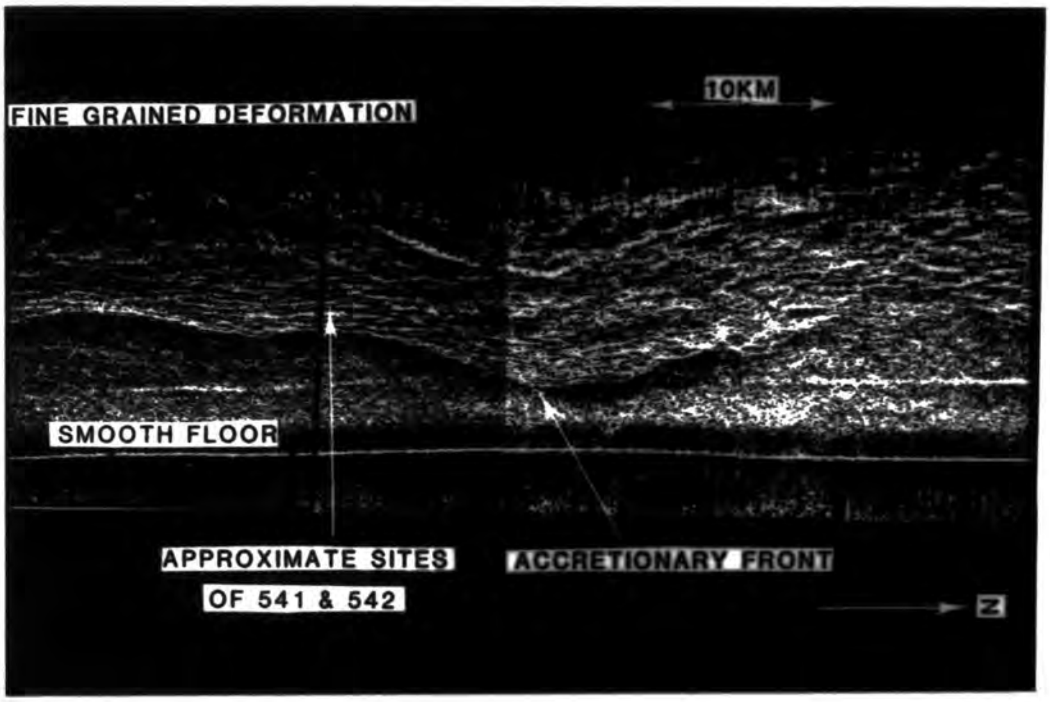

10KM
FINE GRAINED DEFORMATION
SMOOTH FLOOR
APPROXIMATE SITES
OF 541 & 542
ACCRETIONARY FRONT
N

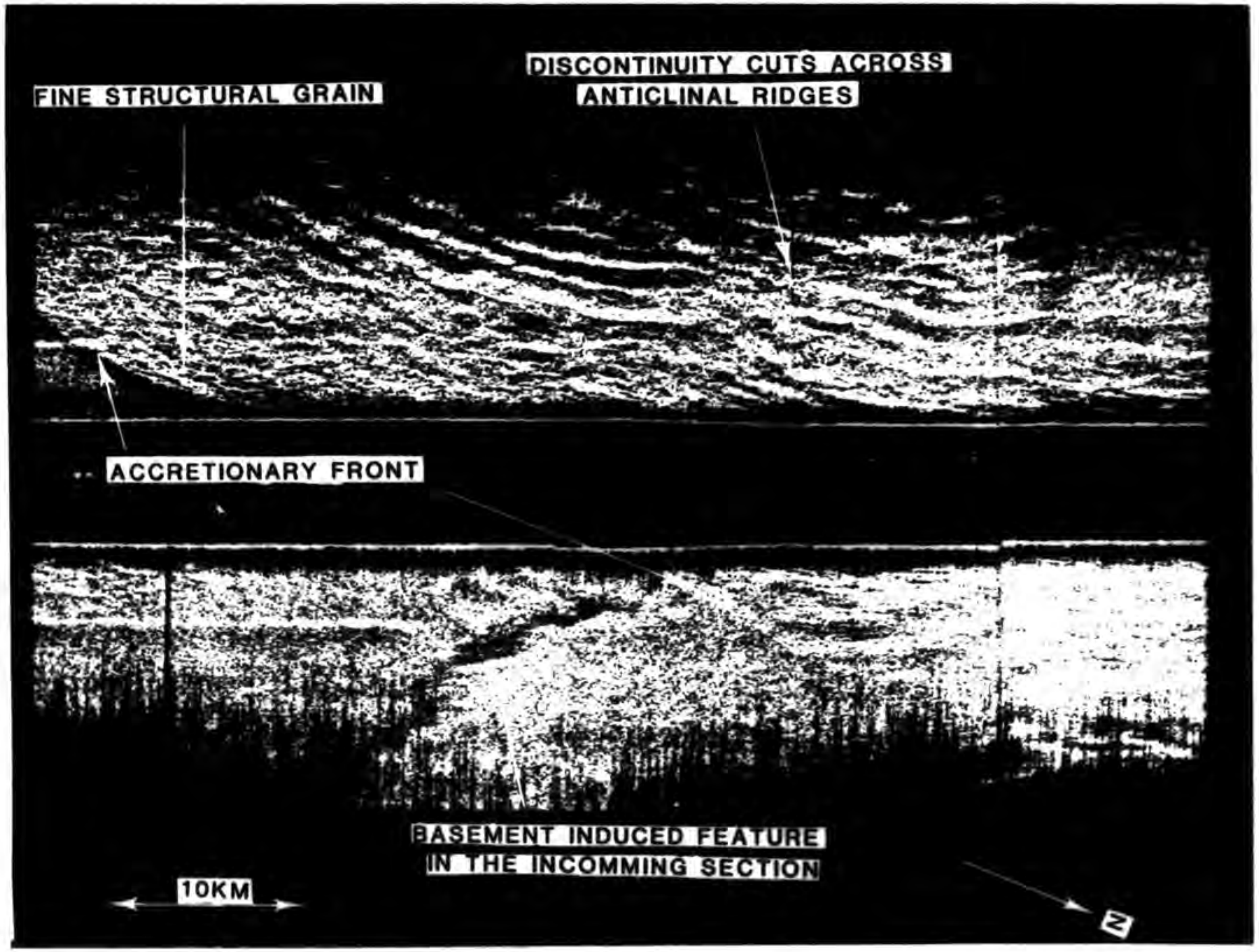
FINE STRUCTURAL GRAIN
DISCONTINUITY CUTS ACROSS
ANTICLINAL RIDGES
ACCRETIONARY FRONT
BASEMENT INDUCED FEATURE
IN THE INCOMMING SECTION
10KM
N



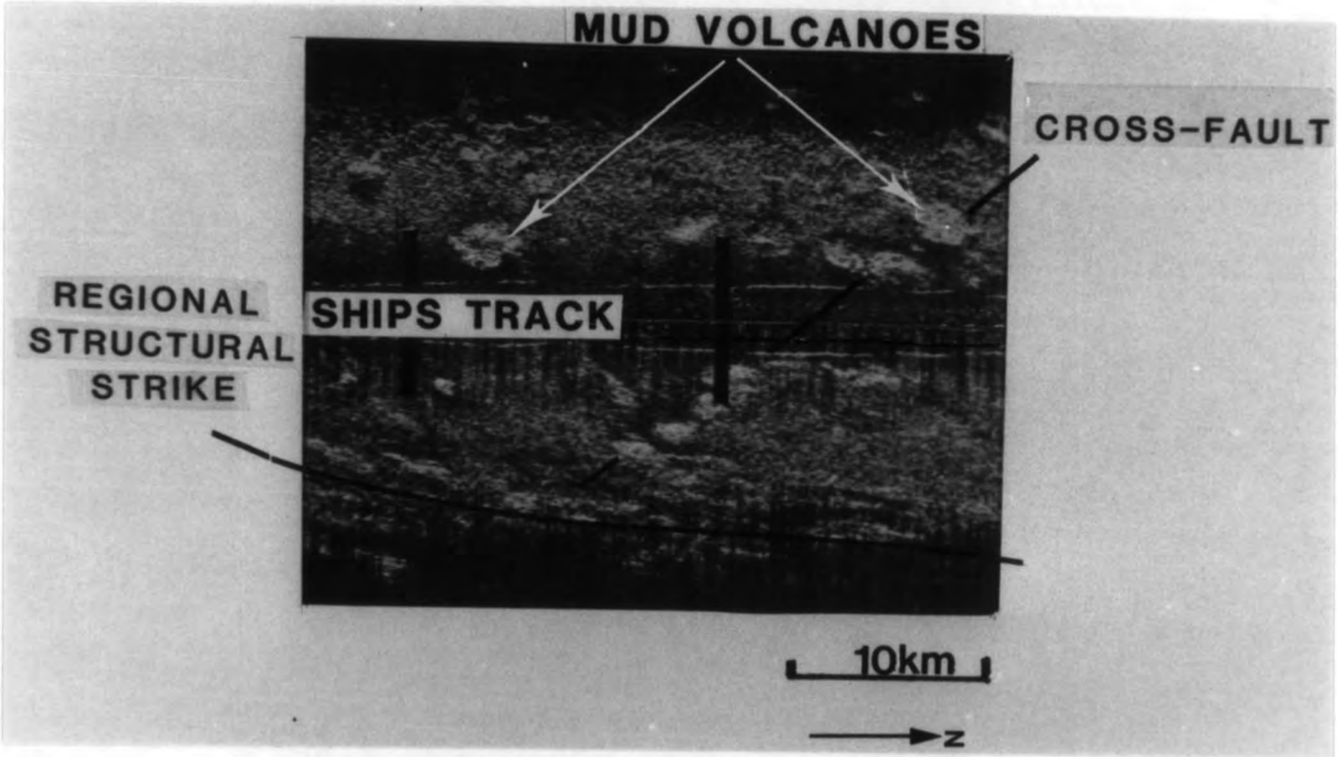
MUD VOLCANOES
CROSS-FAULT
REGIONAL STRUCTURAL STRIKE
SHIPS TRACK
10km
N

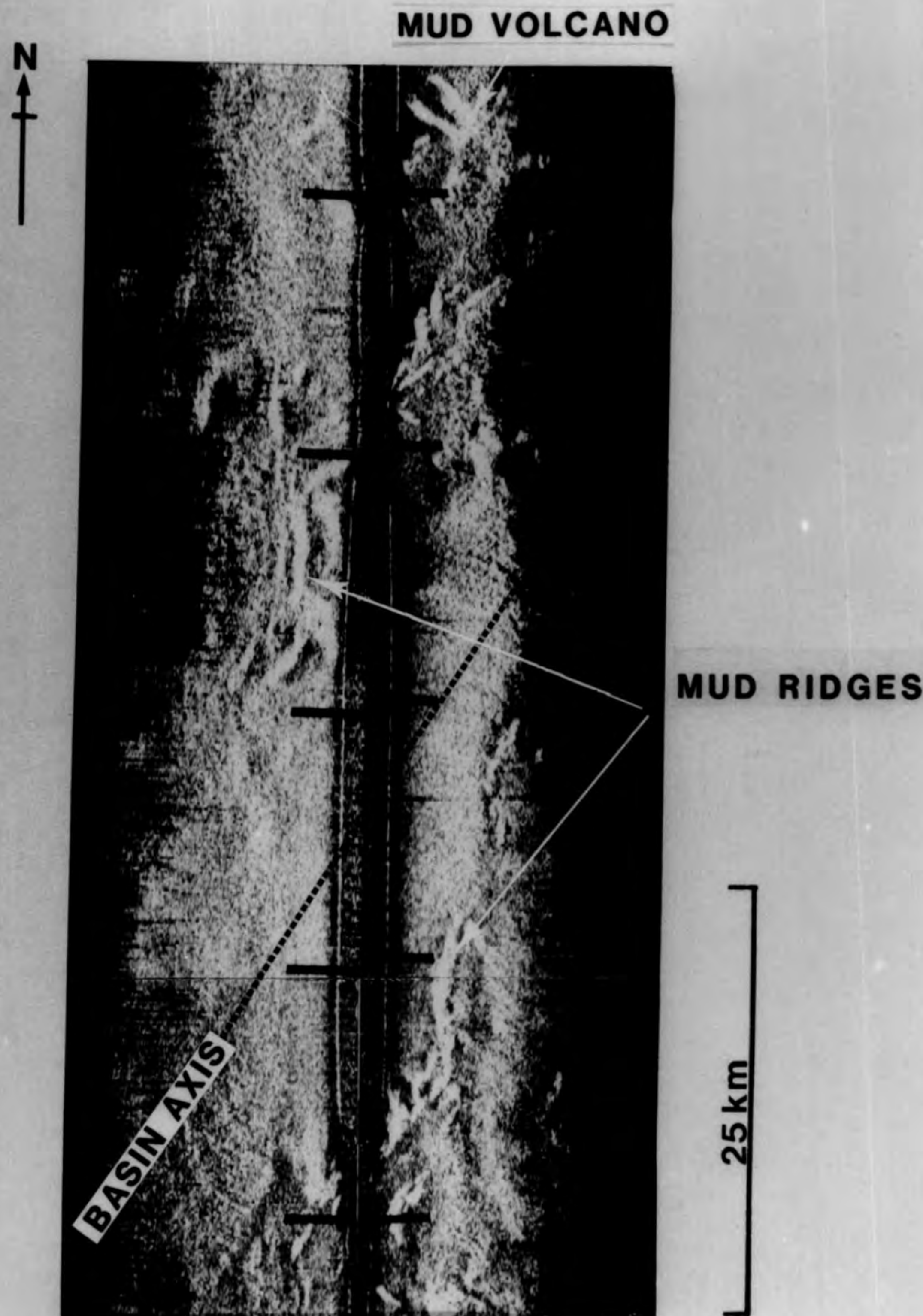
MUD VOLCANO
N
MUD RIDGES
BASIN AXIS
25 km

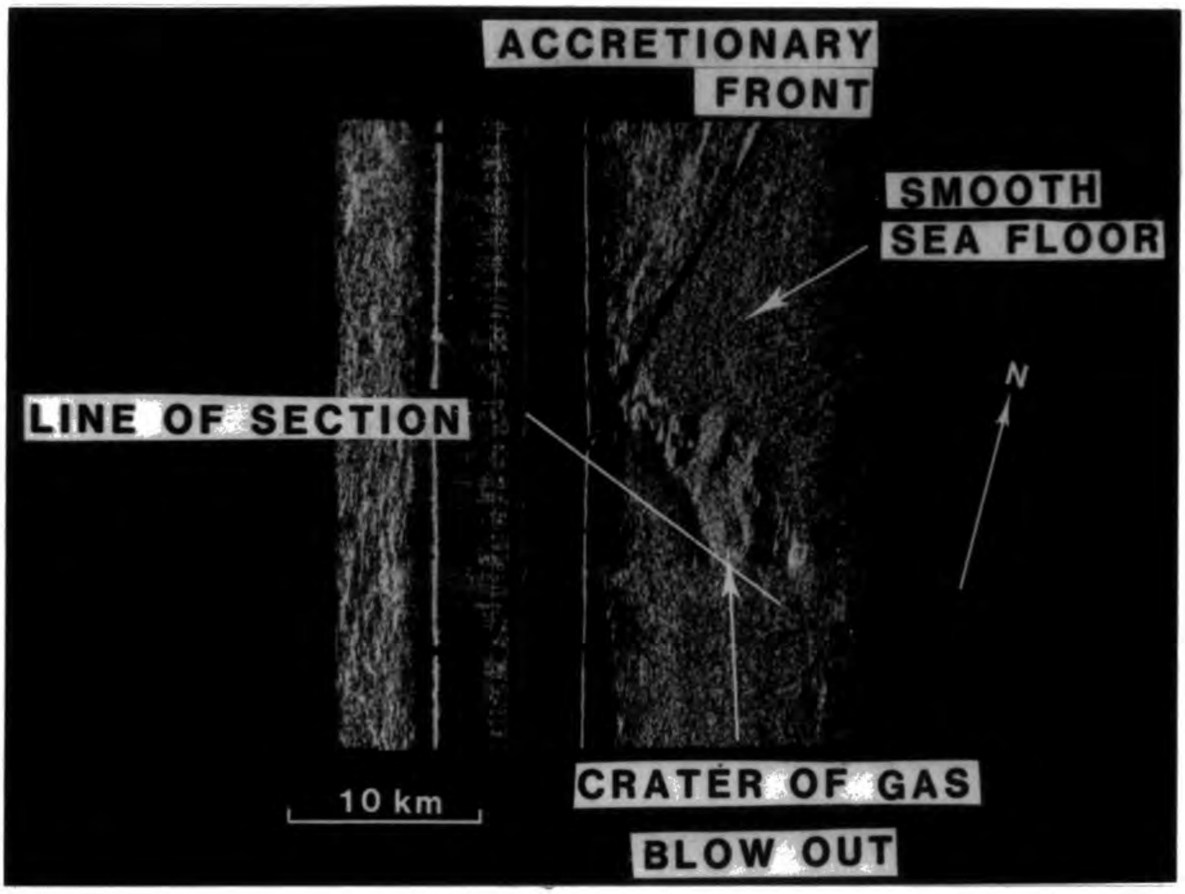
ACCRETIONARY
FRONT
SMOOTH
SEA FLOOR
N
LINE OF SECTION
10 km
CRATER OF GAS
BLOW OUT

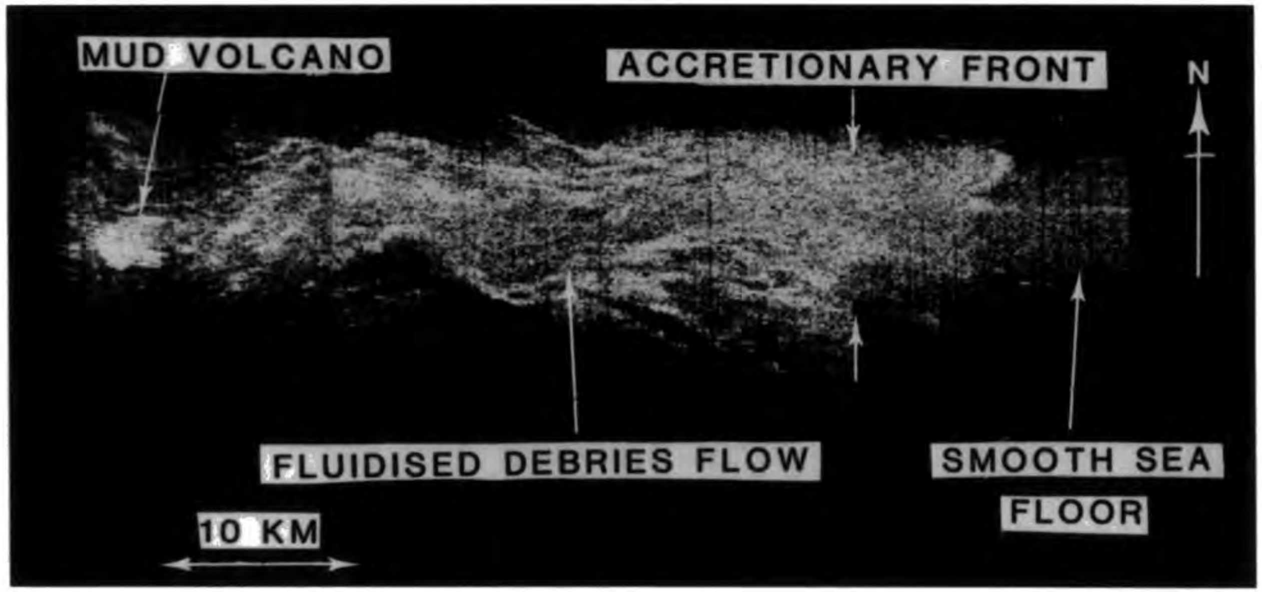
MUD VOLCANO
ACCRETIONARY FRONT
N
FLUIDISED DEBRIES FLOW
SMOOTH SEA
FLOOR
10 KM

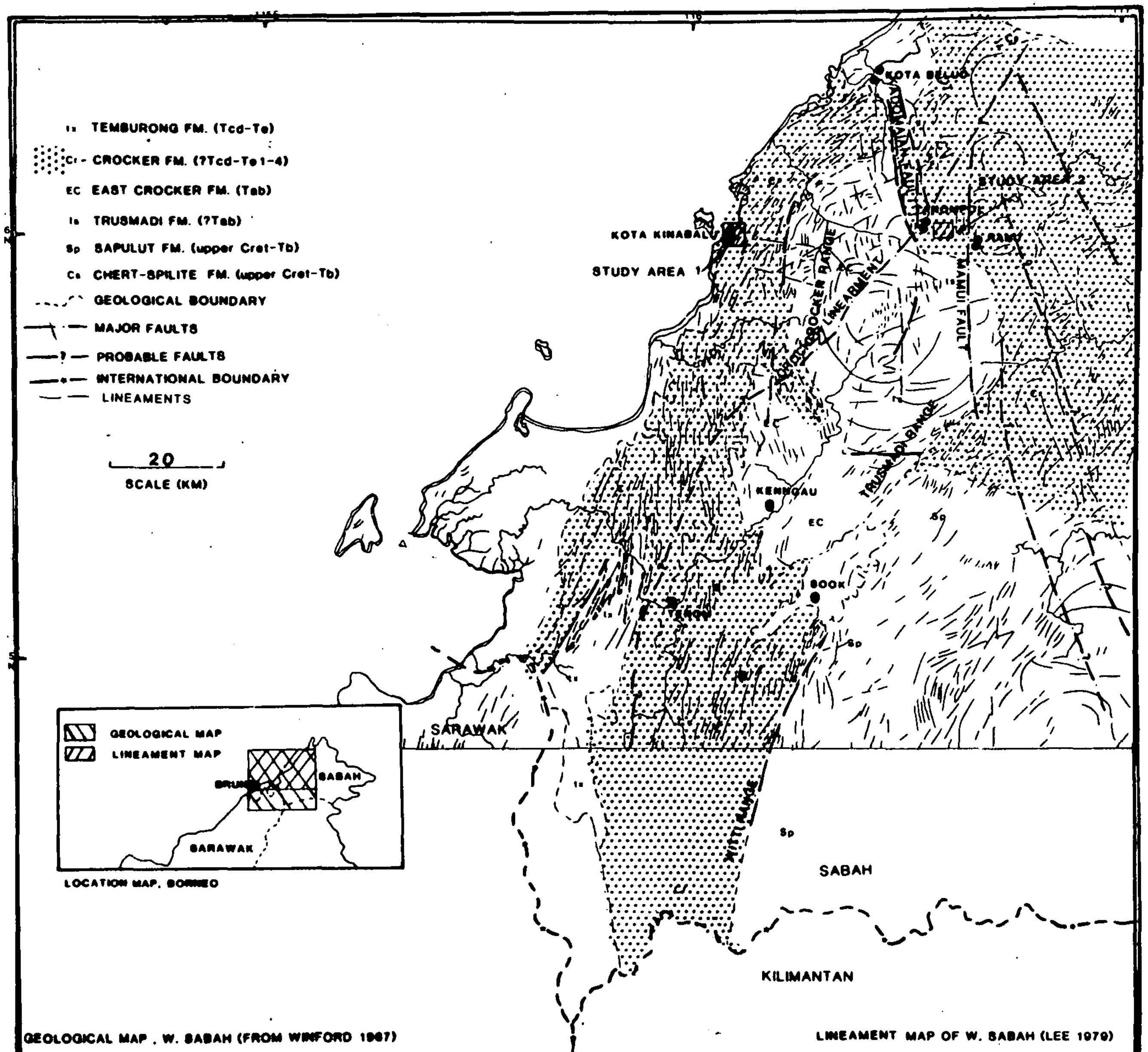
TEMBURONG FM. (Tcd-Te)
CROCKER FM. (?Tcd-Te1-4)
EAST CROCKER FM. (Tab)
TRUSMADI FM. (?Tab)
SAPULUT FM. (upper Cret-Tb)
CHERT-SPILITE FM. (upper Cret-Tb)
GEOLOGICAL BOUNDARY
MAJOR FAULTS
PROBABLE FAULTS
INTERNATIONAL BOUNDARY
LINEAMENTS
20
SCALE (KM)
KOTA BELUD
STUDY AREA 2
KOTA KINABALU
STUDY AREA 1
CROCKER RANGE
MANSUI FAULT
TRUSMADI RANGE
KENINGAU
EC
Sp
SOOK
TENOM
SARAWAK
SABAH
KILIMANTAN
GEOLOGICAL MAP
LINEAMENT MAP
BRUNEI
SARAWAK
LOCATION MAP, BORNEO
GEOLOGICAL MAP, W. SABAH (FROM WINFORD 1967)
LINEAMENT MAP OF W. SABAH (LEE 1979)

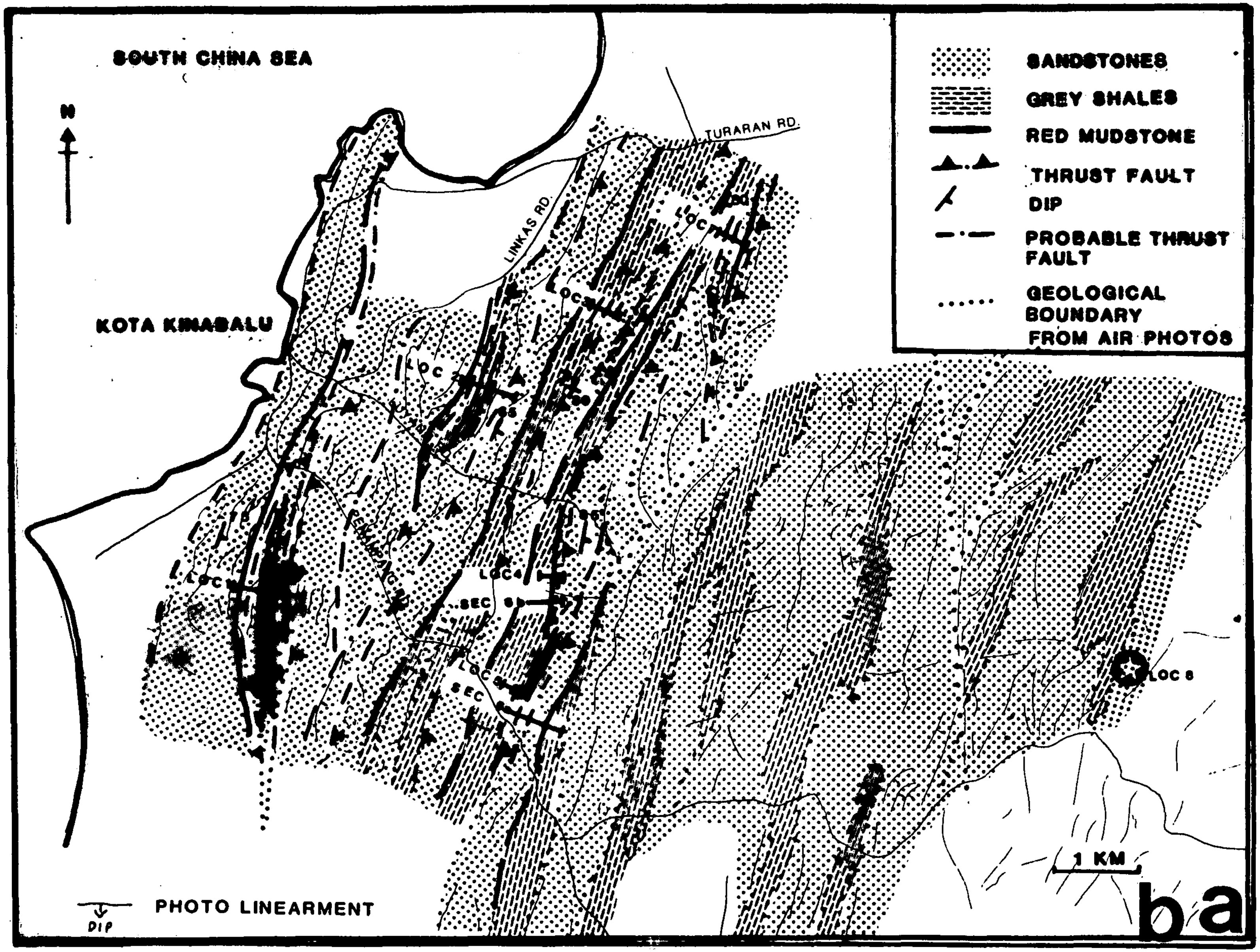

SOUTH CHINA SEA
N
KOTA KINABALU
TURARAN RD.
LINKAS RD.
SANDSTONES
GREY SHALES
RED MUDSTONE
THRUST FAULT
DIP
PROBABLE THRUST FAULT
GEOLOGICAL BOUNDARY FROM AIR PHOTOS
LOC 4
LOC 8
1 KM
PHOTO LINEARMENT
DIP
b a

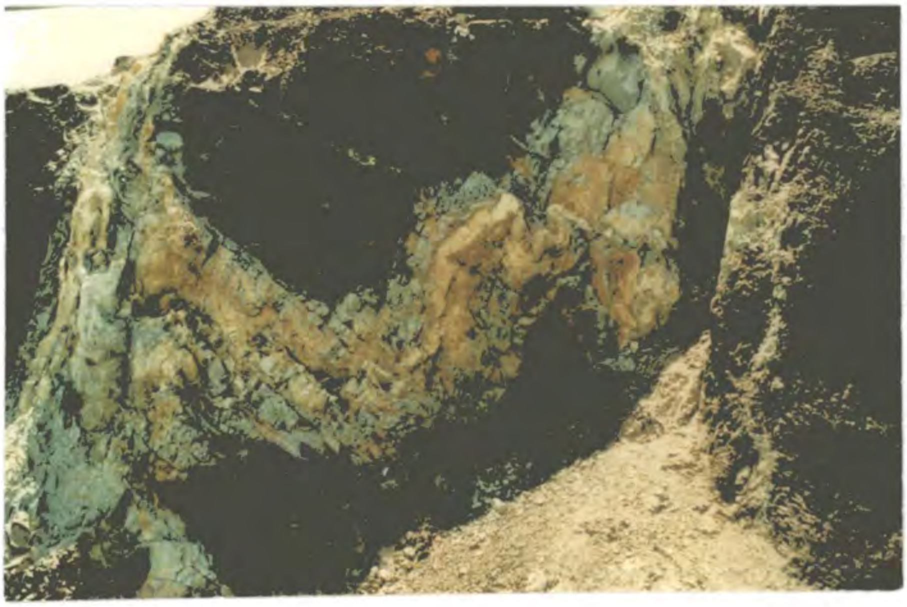

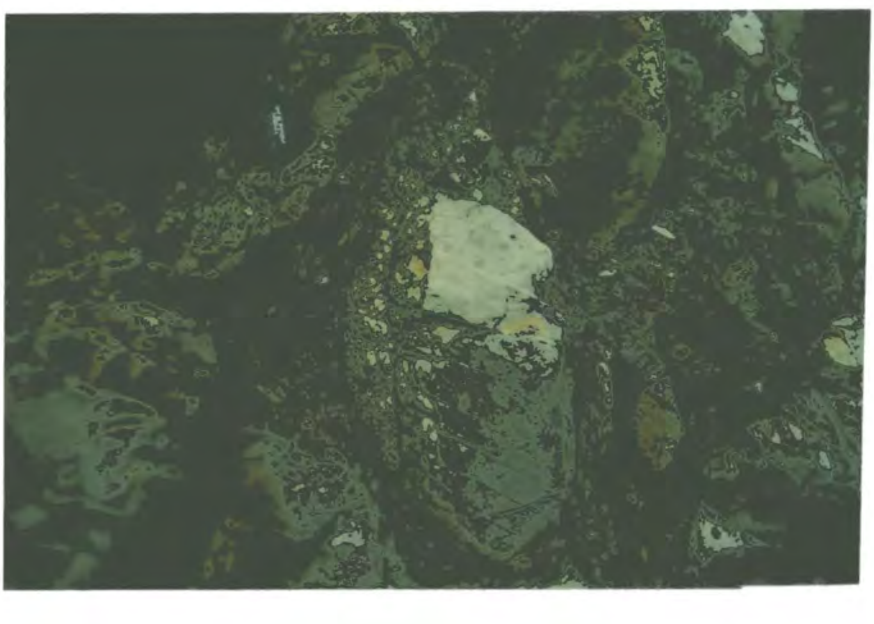

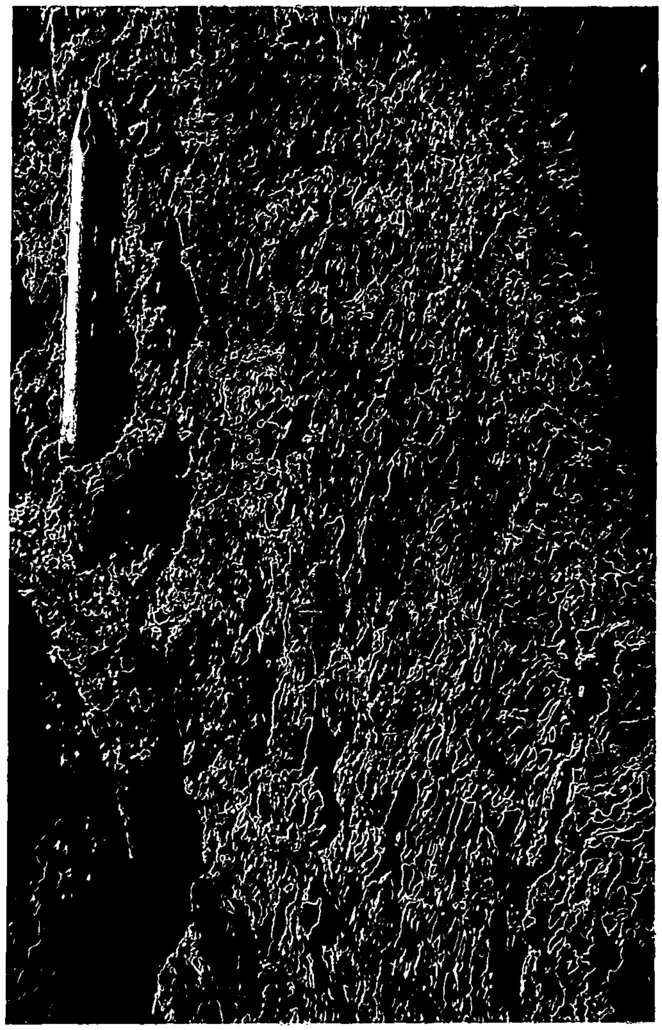

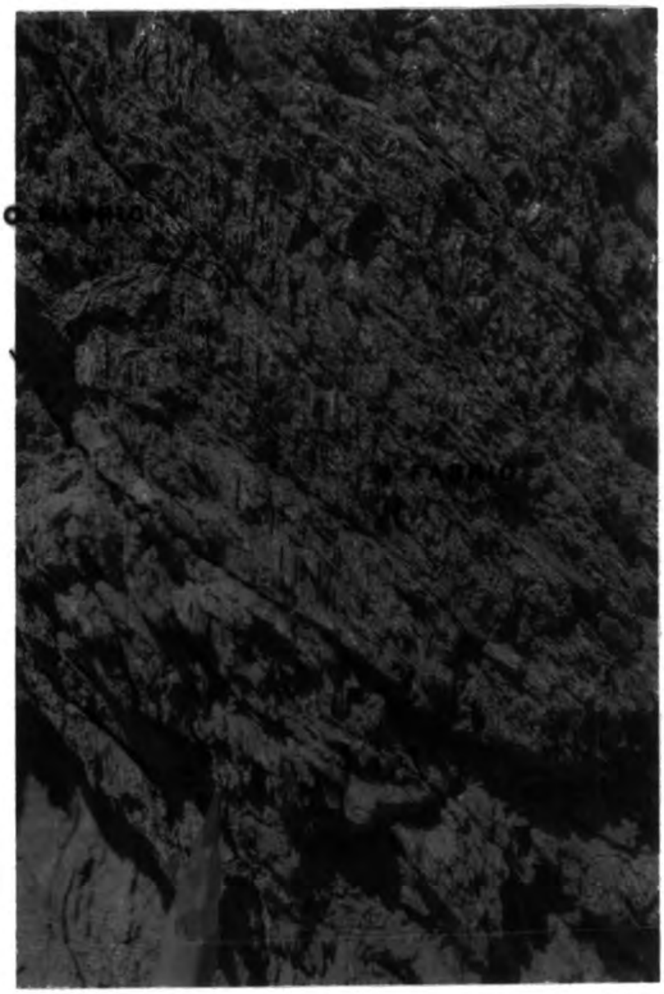

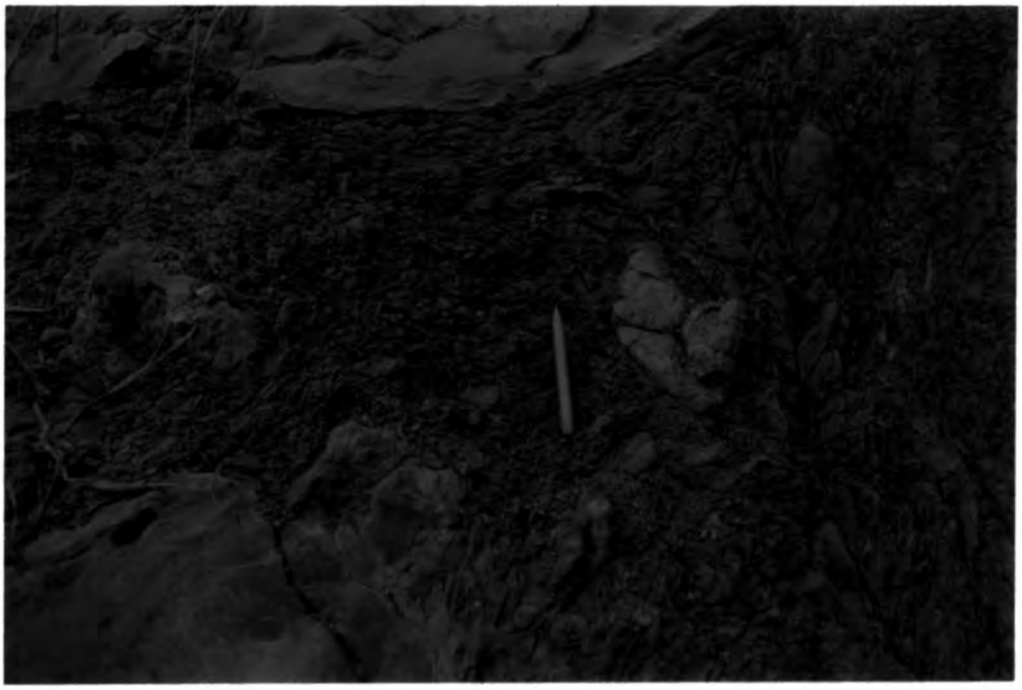


BLOCK
MELANGE
RELATIVELY
UNDISTURBED
SECTION


SST BLOCK

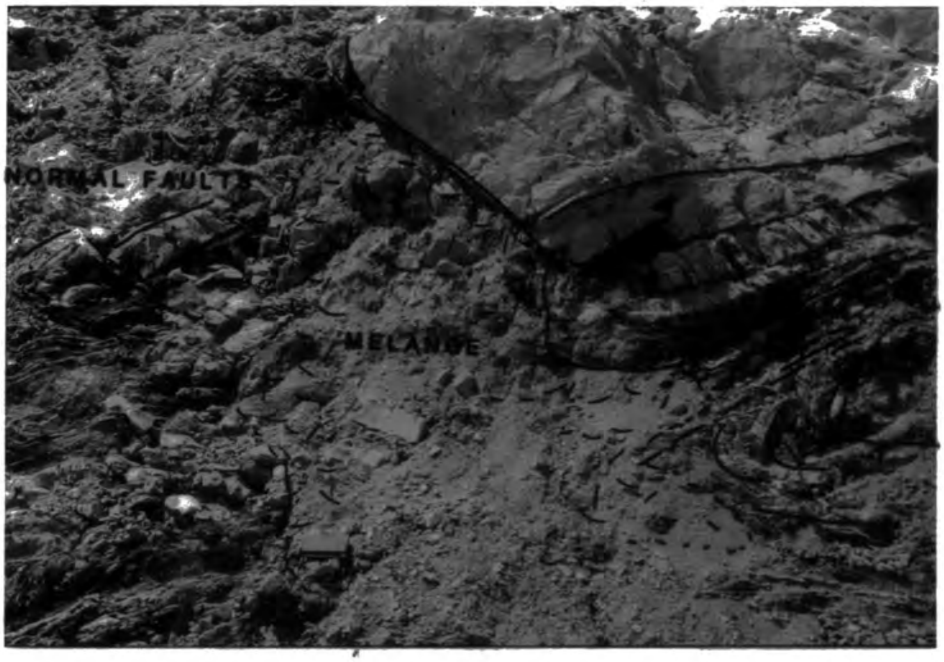
NORMAL FAULTS
MELANGE

A

B

C

A

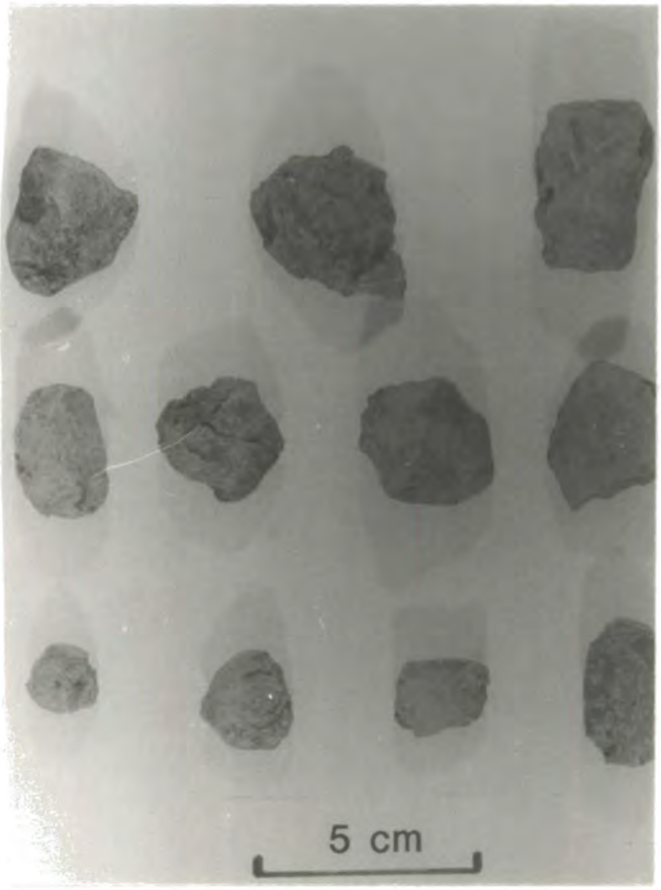

B


5 cm

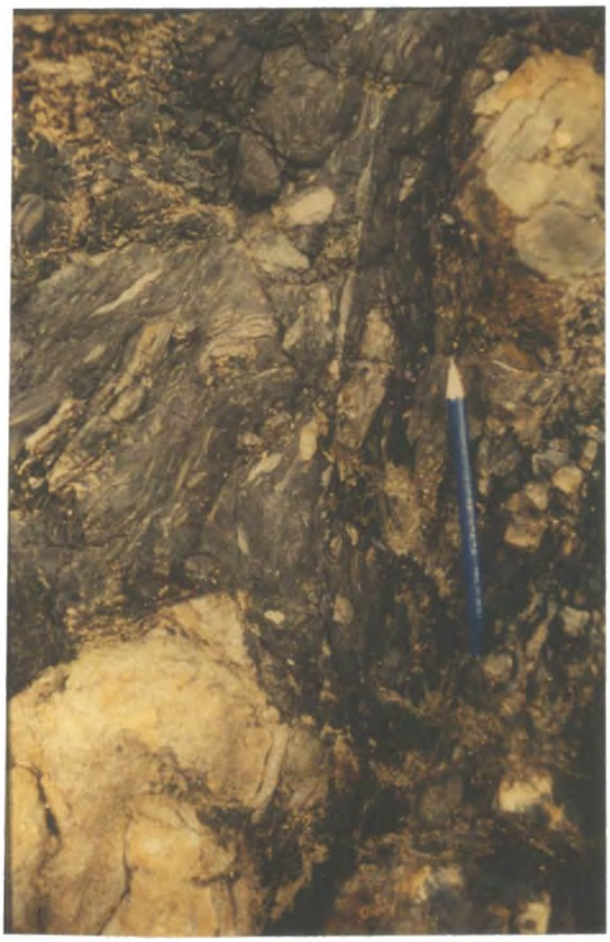

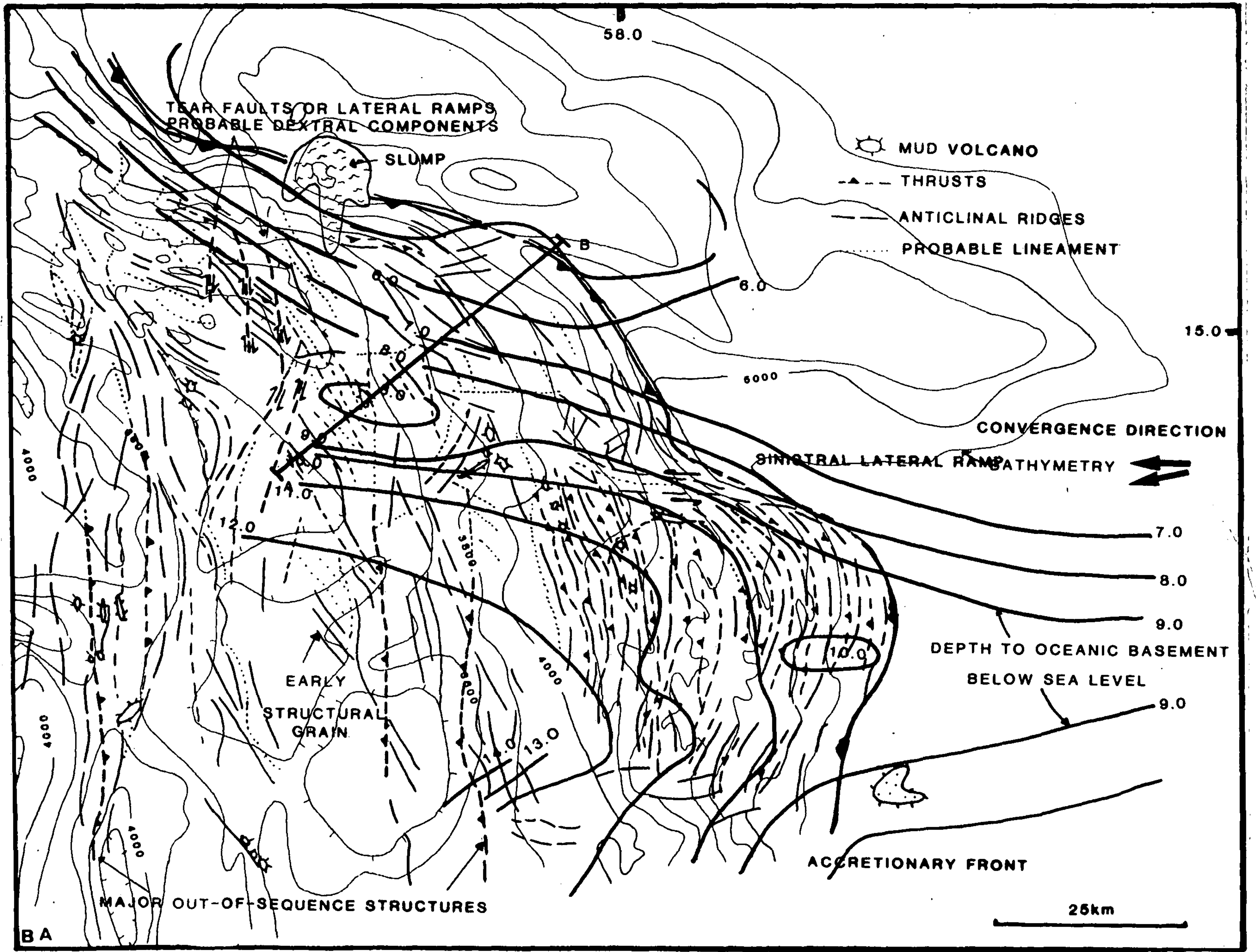
58.0
TEAR FAULTS OR LATERAL RAMPS
PROBABLE DEXTRAL COMPONENTS
SLUMP
MUD VOLCANO
THRUSTS
ANTICLINAL RIDGES
PROBABLE LINEAMENT
B
6.0
6.0
7.0
8.0
15.0
6000
CONVERGENCE DIRECTION
SINISTRAL LATERAL RAMP
BATHYMETRY
9
10.0
11.0
12.0
4000
7.0
8.0
9.0
DEPTH TO OCEANIC BASEMENT
BELOW SEA LEVEL
9.0
10.0
EARLY
STRUCTURAL
GRAIN
4000
13.0
ACCRETIONARY FRONT
MAJOR OUT-OF-SEQUENCE STRUCTURES
25km
B A

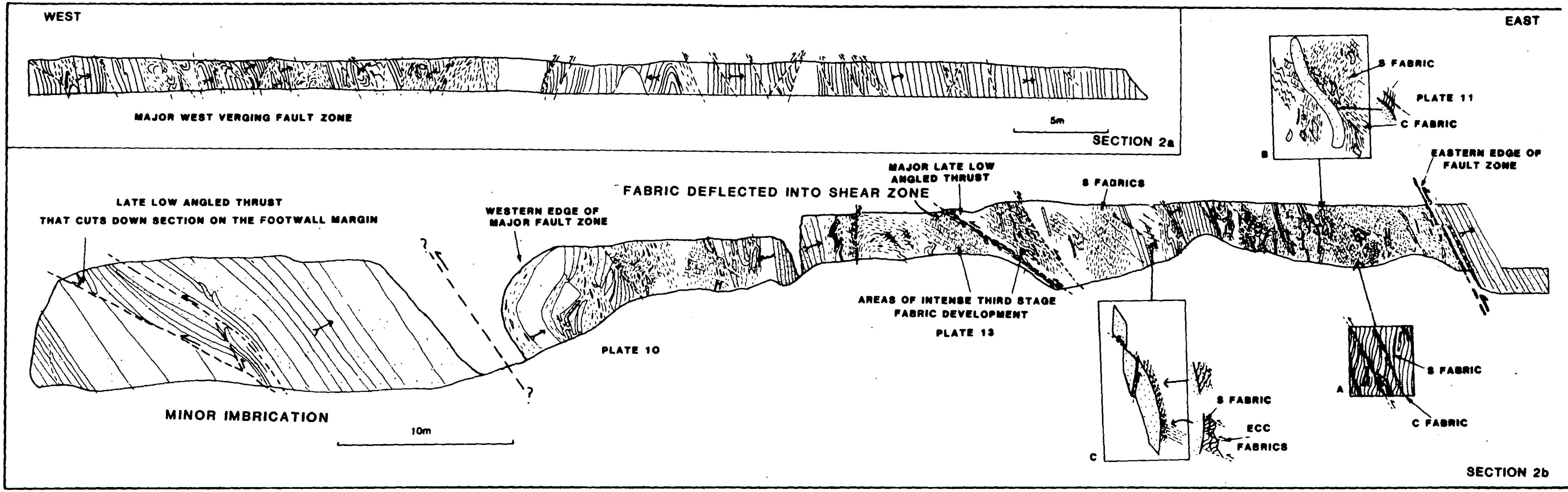

WEST
EAST
MAJOR WEST VERGING FAULT ZONE
5m
SECTION 2a
S FABRIC
PLATE 11
C FABRIC
B
EASTERN EDGE OF
FAULT ZONE
MAJOR LATE LOW
ANGLED THRUST
S FABRICS
FABRIC DEFLECTED INTO SHEAR ZONE
LATE LOW ANGLED THRUST
THAT CUTS DOWN SECTION ON THE FOOTWALL MARGIN
WESTERN EDGE OF
MAJOR FAULT ZONE
AREAS OF INTENSE THIRD STAGE
FABRIC DEVELOPMENT
PLATE 13
PLATE 10
S FABRIC
A
C FABRIC
S FABRIC
ECC
FABRICS
C
MINOR IMBRICATION
10m
SECTION 2b

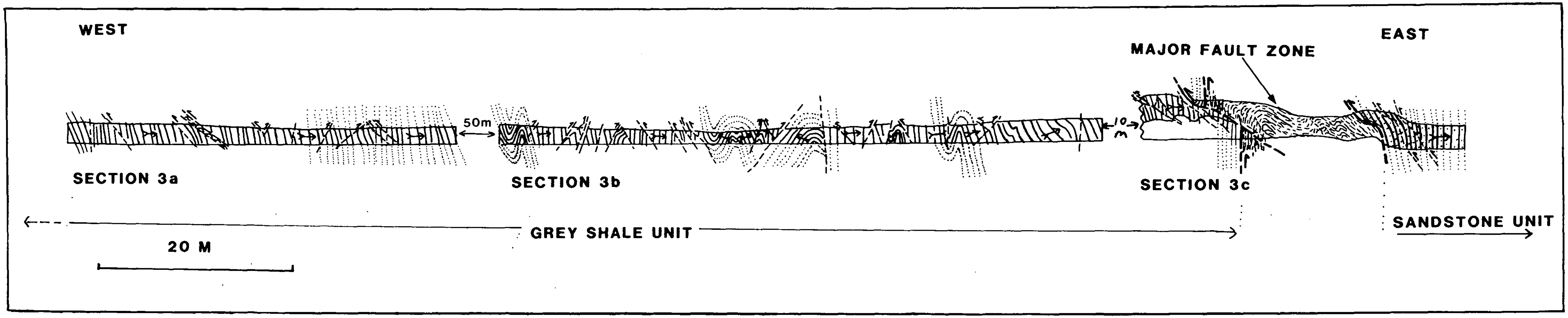
WEST
EAST
MAJOR FAULT ZONE
50m
10 m
SECTION 3a
SECTION 3b
SECTION 3c
GREY SHALE UNIT
SANDSTONE UNIT
20 M

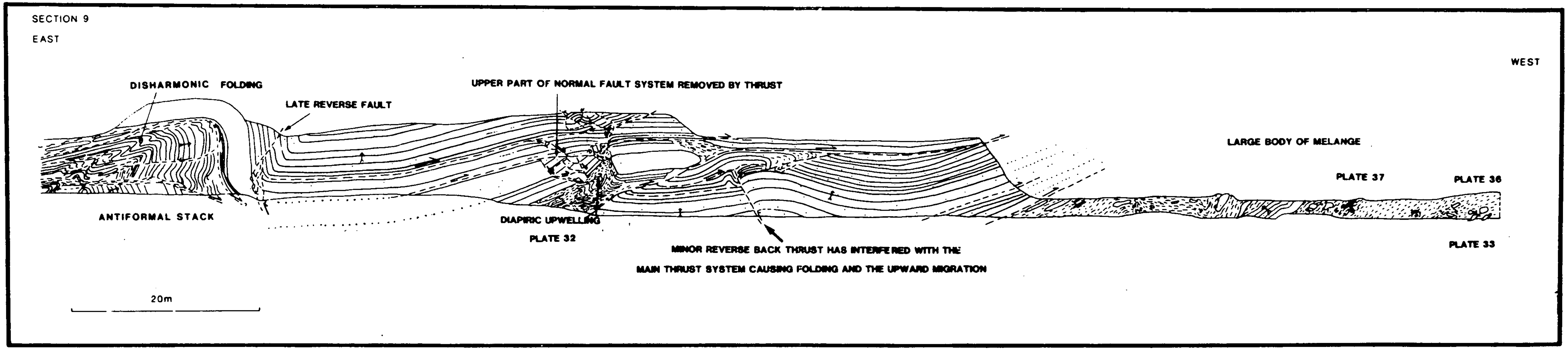
SECTION 9
EAST
WEST
DISHARMONIC FOLDING
LATE REVERSE FAULT
UPPER PART OF NORMAL FAULT SYSTEM REMOVED BY THRUST
LARGE BODY OF MELANGE
PLATE 37
PLATE 36
ANTIFORMAL STACK
DIAPIRIC UPWELLING
PLATE 32
PLATE 33
MINOR REVERSE BACK THRUST HAS INTERFERED WITH THE
MAIN THRUST SYSTEM CAUSING FOLDING AND THE UPWARD MIGRATION
20m

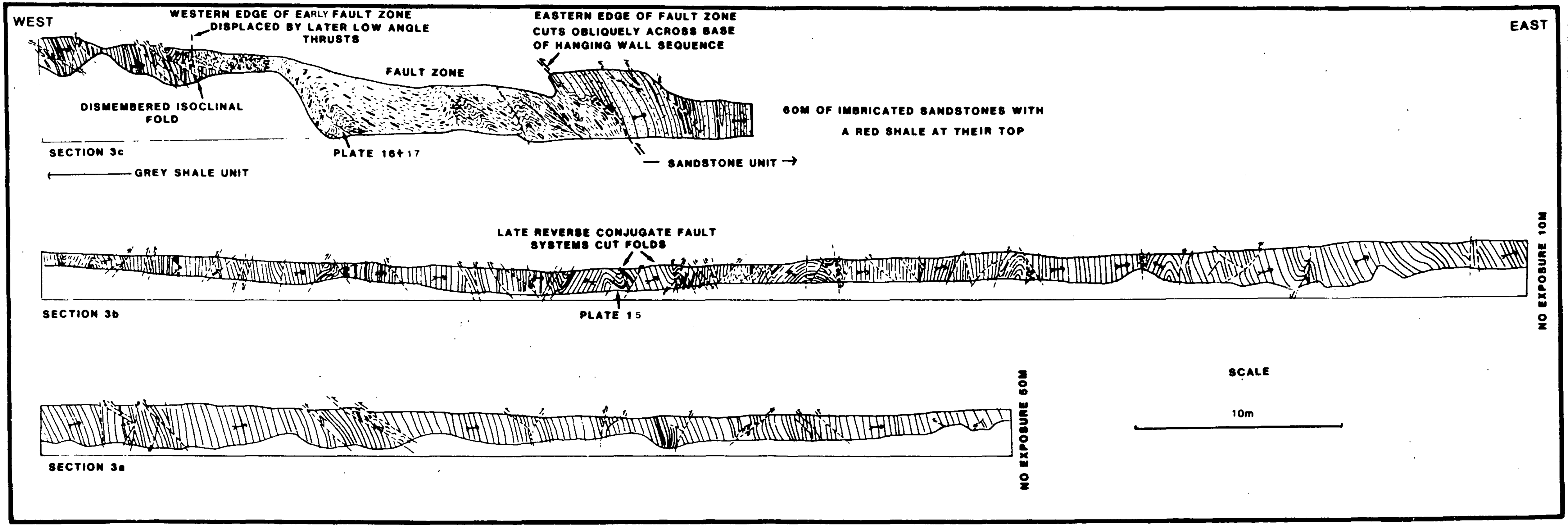
WEST
WESTERN EDGE OF EARLY FAULT ZONE
DISPLACED BY LATER LOW ANGLE
THRUSTS
EASTERN EDGE OF FAULT ZONE
CUTS OBLIQUELY ACROSS BASE
OF HANGING WALL SEQUENCE
EAST
FAULT ZONE
DISMEMBERED ISOCLINAL
FOLD
60M OF IMBRICATED SANDSTONES WITH
A RED SHALE AT THEIR TOP
SECTION 3c
PLATE 16+17
SANDSTONE UNIT
GREY SHALE UNIT
LATE REVERSE CONJUGATE FAULT
SYSTEMS CUT FOLDS
SECTION 3b
PLATE 15
NO EXPOSURE 10M
NO EXPOSURE 50M
SCALE
10m
SECTION 3a

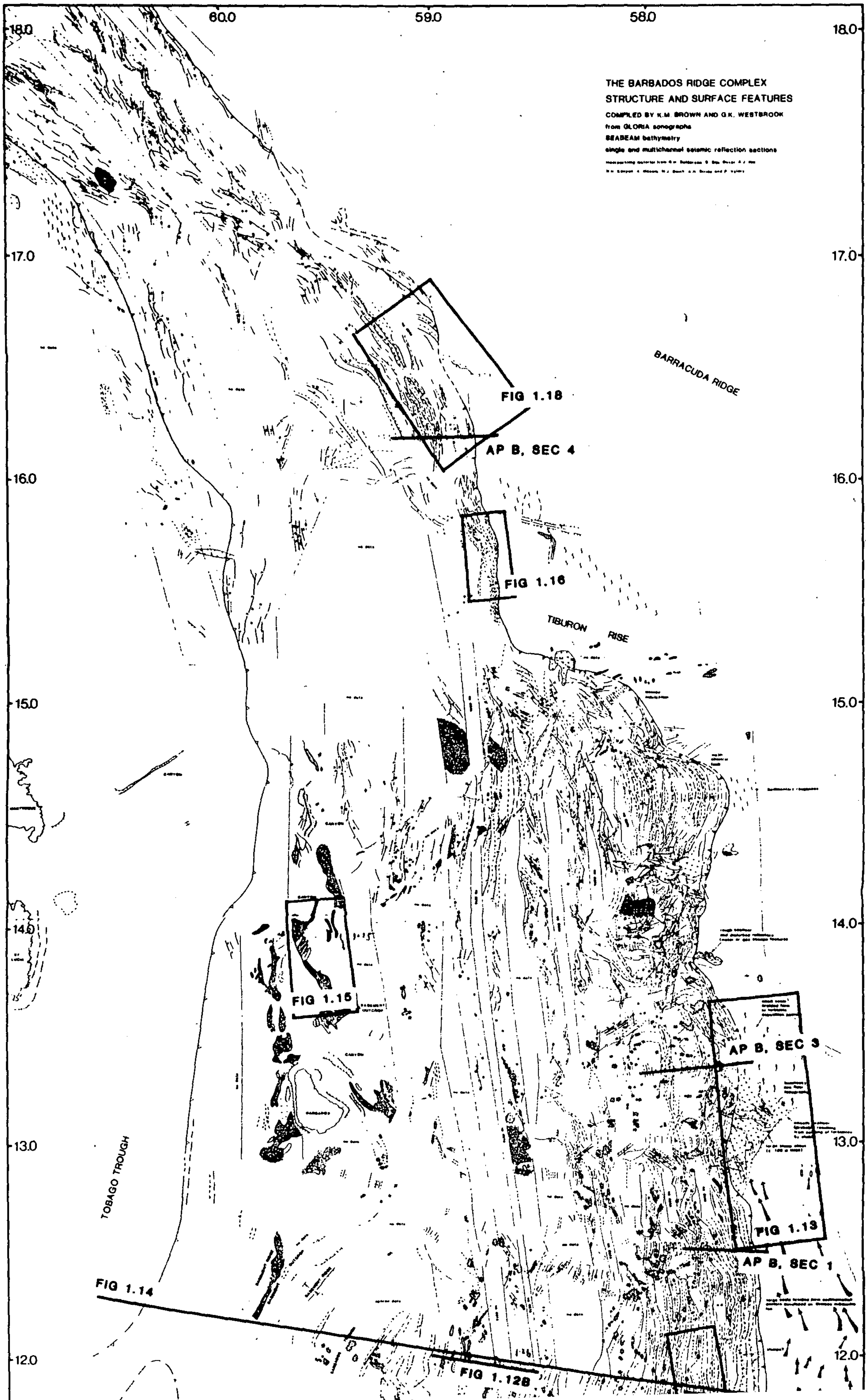

THE BARBADOS RIDGE COMPLEX
STRUCTURE AND SURFACE FEATURES
COMPILED BY K.M. BROWN AND G.K. WESTBROOK
from GLORIA sonographs
SEABEAM bathymetry
single and multichannel seismic reflection sections
60.0
59.0
58.0
18.0
17.0
16.0
15.0
14.0
13.0
12.0
FIG 1.18
AP B, SEC 4
FIG 1.16
BARRACUDA RIDGE
TIBURON RISE
FIG 1.15
AP B, SEC 3
FIG 1.13
AP B, SEC 1
FIG 1.14
FIG 1.12B
TOBAGO TROUGH

LINE DRAWING ACROSS THE BARBADOS RIDGE ACCRETIONARY COMPLEX

APPENDIX B

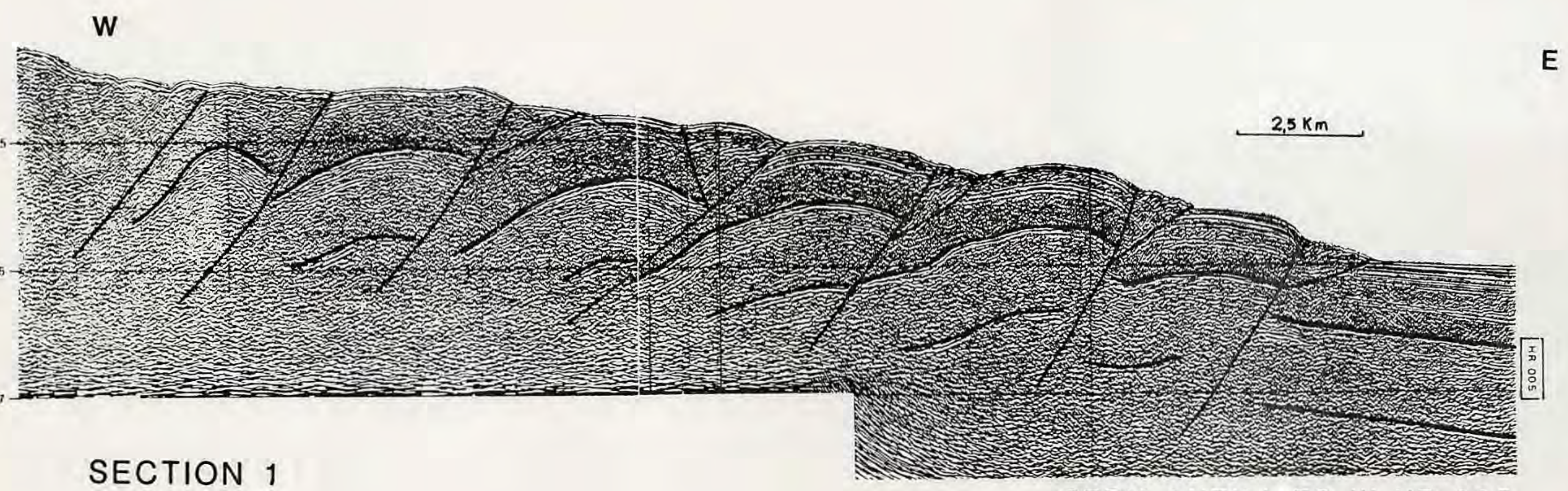

SECTION 1

CEPM ANTILL ES III HR 005

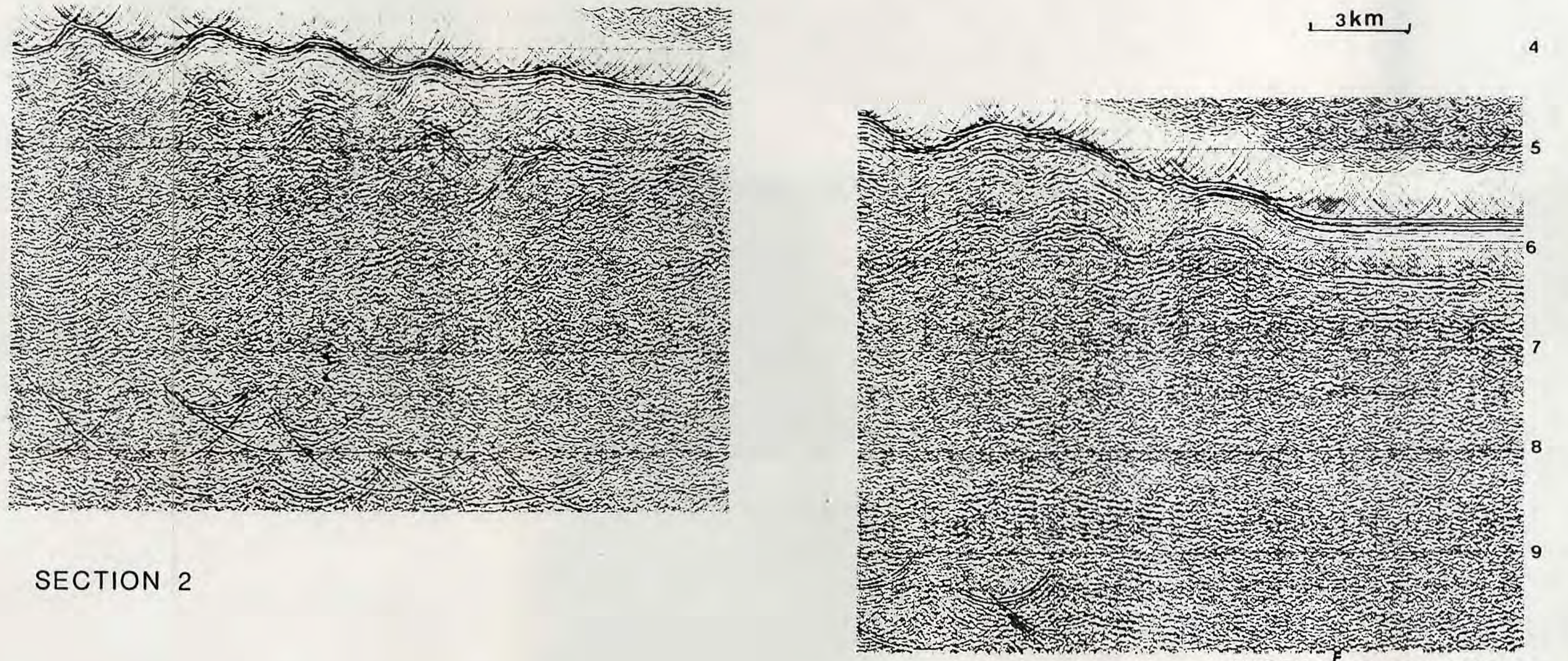

SECTION 2

DISCOVRY 109 LINE 1

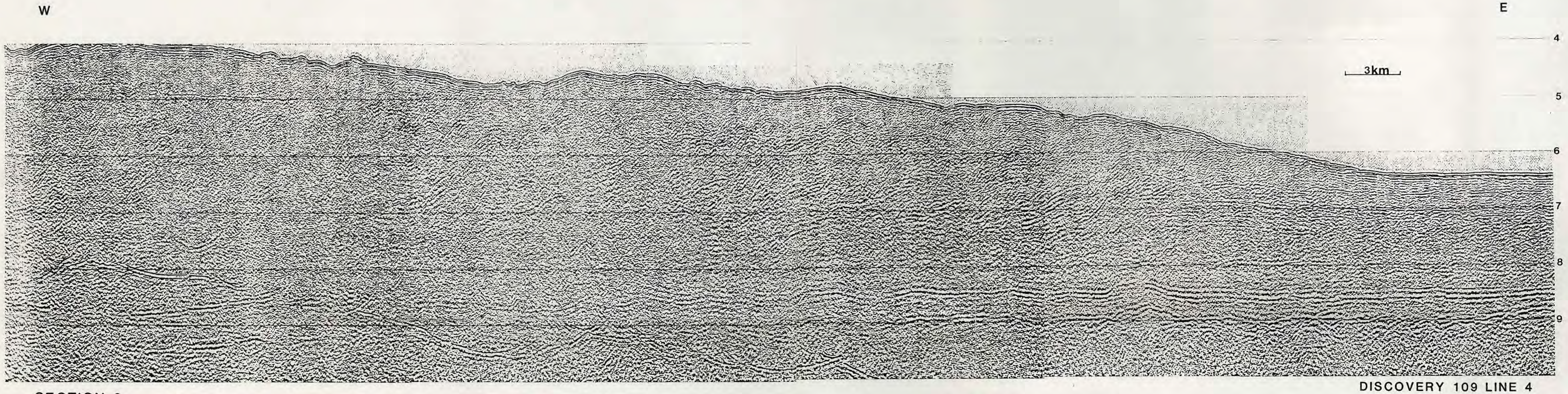

SECTION 3

DISCOVERY 109 LINE 4

SECTION 4

DISCOVERY 109 LINE 17

Figure 2 Map of structure and surface features at a scale of 1:1063415 (4 inches per degree of longitude). Bathymetric contours at 200 m intervals, shown in pale blue, are taken from Ladd (1984) except where Seabeam-derived bathymetry has been incorporated

APPENDIX B

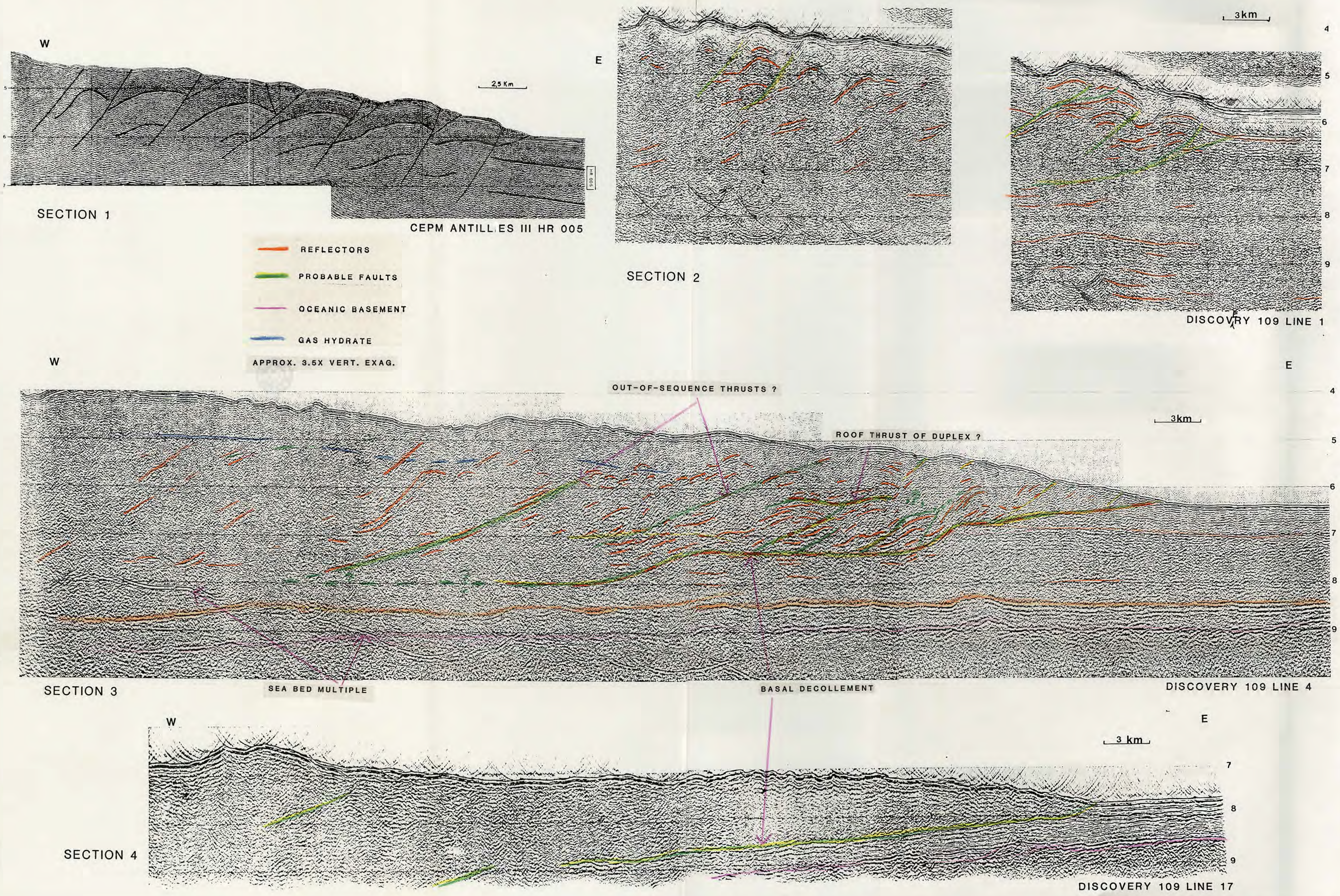

SECTION 1
W
E
2.5 Km
CEPM ANTILLES III HR 005
SECTION 2
3km
DISCOVERY 109 LINE 1
REFLECTORS
PROBABLE FAULTS
OCEANIC BASEMENT
GAS HYDRATE
APPROX. 3.5X VERT. EXAG.
OUT-OF-SEQUENCE THRUSTS ?
ROOF THRUST OF DUPLEX ?
SECTION 3
SEA BED MULTIPLE
BASAL DECOLLEMENT
DISCOVERY 109 LINE 4
SECTION 4
3 km
DISCOVERY 109 LINE 17